CHARACTERIZATION OF THE ACTIVATION MECHANISM OF BAX

CHARACTERIZATION OF THE ACTIVATION MECHANISM OF BAX

By

JUSTIN HAYWARD KALE, B.Sc.

A Thesis Submitted to the

School of Graduate Studies in Partial Fulfilments

of the Requirements for the Degree

Doctor of Philosophy

DOCTOR OF PHILOSOPHY (2017) McMaster University

(Biochemistry and Biomedical Sciences) Hamilton, Ontario

TITLE: Characterization of the activation mechanism of Bax

AUTHOR: Justin Hayward Kale, B.Sc. (University of Windsor)

SUPERVISOR: Dr. David W. Andrews

NUMBER OF PAGES: xviii, 218

Lay abstract

Every day the human body creates billions of cells replacing damaged or unwanted cells. The death of these cells is tightly controlled and can result in disease when misregulated. Cancers arise when there is too little cell death and neurodegenerative diseases, such as Alzheimer's, arise from too much cell death. Much research, including this thesis, is focused on understanding how cells die because once understood, cell death can be manipulated to treat disease. Cell death ironically occurs at the mitochondria, a cellular organ normally responsible for creating the energy required for the cell to live. When cell death is initiated, the mitochondria get holes poked into them, releasing pro-death factors that irreversibly commit the cell to dying. The work presented here uncovers new information about the regulation of the hole poking process, how it is blocked in breast cancer and how the process may be modulated to treat cancers.

Abstract

Mitochondrial outer membrane permeabilization (MOMP) is regulated by protein-protein and protein-membrane interactions between Bcl-2 family proteins. These interactions are governed by the concentrations and relative binding affinities of the proteins for each other. These affinities are altered by conformation changes of Bcl-2 family proteins resulting from interactions with each other and with membranes. How Bcl-2 proteins transition into and out of the conformations that controls their functions, and ultimately the fate of the cell, is not well understood. Here, kinetic analysis of the pore-forming Bcl-2 family member, Bax, revealed that Bax undergoes a conformational rearrangement through at least one structurally distinct intermediate that is a necessary precursor to pore formation. We discover that four cancer-associated Bax point mutants are trapped in the intermediate state, suggesting that transitions into and out of this intermediate can be modulated independently with consequences for the execution of apoptosis. Furthermore we report that the conformation changes Bax undergoes can be regulated by phosphorylation of Bax on residue S184 by the pro-survival kinase, Akt. Phosphorylation converts Bax into an anti-apoptotic protein that functions in a dominant-negative fashion. Bioinformatics revealed that in human cancers, higher levels of Bax are positively associated with high levels of PI3K/AKT pathway genes representing an added mechanism for cancer cells to evade apoptosis. Additionally we studied the interactions between Bax, the anti-apoptotic protein Bcl-XL, the sensitizer BH3 protein Bad and the BH3 activator protein Bid. We uncover a new mechanism of apoptosis regulation whereby Bad binds to one monomer of a Bcl-XL dimer eliciting an activating conformation change in a tBid bound to the other monomer of the Bcl-XL dimer. This allows Bad to function as a non-competitive inhibitor of Bcl-XL, and represents a novel mechanism that significantly enhances the potency of Bad to elicit apoptosis.

Acknowledgements

To Dr. David Andrews and Dr. Brian Leber thank you for mentoring me – it has truly been an honour and a privilege. You have both kept me enthusiastic about research and have provided unending guidance and support throughout my graduate studies. David, thank you for all of the opportunities you have given to me in order to enhance my training as a researcher specifically being able to go to conferences (one in Brazil!), write invited reviews and your setting up of fruitful collaborations for my projects. To Dr. Cecile Fradin thank you for all of your help with anything that required math and your helpful and important insights into my research. Lastly, to Dr. Yingfu Li for your support during committee meetings.

I would like to thank my collaborators Dr. Ozgur Kutuk, Dr. Anthony Letai, Dr. John Bachman, Dr. Peter Sorger and Dr. Christian Bogner for actively supporting these long standing collaborations. I am truly lucky to have worked with such great scientists. To John, it was always a pleasure to discuss the intricacies of our research and Bcl-2 family biochemistry during conferences or our numerous Skype meetings. To Dr. Christian Bogner, thank you for allowing me to be a part of your paper (it will be published I promise!) and for the many enjoyable moments in and outside of lab – Prost!

Thank you to the many past and present members of the DWA lab, you have all helped me in one way or another and have made the lab a fun work environment. A very special thank you to the Andrews lab members: Dr. Hetal Brahmbhatt, Dr. Xiaoke Chi, Dr. Aisha Shamas-Din, Dr. Christian Bogner, Dr. Wiebke Schormann, Sanjee Shivakumar, Frank Chan, Dr. Fei Geng, Dr. Qian Liu, Elizabeth Osterlund, Nehad Hirmiz James Pemberton, Justin Pogmore and Dr. Laura Canty for all of your helpful insights and discussions inside and outside of the lab. Moreover to Hetal, Xiaoke, Aisha, Christian you all made the whole PhD journey a very fun time and have helped me the most with the research presented here. Thank you to Mina Falcone and Weija Zhu who taught me the ropes of the DWA lab at McMaster, you were the best techs anyone could ever ask for. To everyone who worked on the other side of the lab aka the HIICA office (Sunnybrook) aka the porch (McMaster) I have always enjoyed making the trek to discuss life and science and to get a healthy dose of ever important coffee. Specifically I would like to thank Santosh Hariharan and Jarkko Ylanko (TWD and GoT episode breakdowns were always

something I looked forward to Monday morning) for countless hours of joking around and in-depth discussions on anything ranging from science to adapting a lab journal article into a story about bRad and Maxine pulverizing mattresses (ask me for a copy).

To my brothers and sisters from many different mothers and misters - Kevin Virk, Steve Phounpadith, Vlad Latiu, Brad Yared, Sylvester Asiedu, Klementina Stojanovska and Jenny DaDalt thank you for being the best friends anyone could ask for, although you didn't contribute intellectually to this thesis the support throughout the years and the many nights of fun times really allowed me to stay sane during this whole process.

To my parents, Terry and Cheryl Kale, I literally could not have done this without your tremendous support, encouragement and love of which I could never repay you. To my brother and sister, Jordan and Samantha Kale you guys are the absolute best thank you for always making me laugh.

I would like to dedicate my dissertation to my wife Alison and newborn son, Oliver. Alison, you are the love of my life. You started this journey with me 7 years ago and I couldn't picture anyone else standing beside me when this is all over. You have had the most patience and understanding out of anyone and without that this thesis would not be possible. To Oliver, maybe someday you will read this, maybe not but I'd like you to know that you gave me the final push to get this thesis finished and for that I will be forever grateful.

Table of Contents

List of Main Figures

List of Supplementary Figures

List of Tables

List of Abbreviations

ANT	Adenine nucleotide translocase
ANTS	8-Aminonaphthalene-1,3,6-Trisulfonic Acid
Bak	Bcl-2 antagonist/killer
Bax	Bcl-2 associated X protein
Bcl-2	B-cell CLL/lymphoma 2
Bcl-XL	B-cell lymphoma extra long
BH	Bcl-2 homology
Bid	BH3 interacting domain death agonist
cBid	Cleaved Bid
CL	Cardiolipin
CNA	Copy Number Alterations
DAC	N-(7-Dimethylamine-4-Methylcoumarin-3-yl)
DACM	N-(7-Dimethylamine-4-Methylcoumarin-3-yl) Maleimide
DPA	Dipicolinic acid
DPX	p-Xylene-Bis-Pyridinium Bromide
DTT	Dithiothreitol
ER	Endoplasmic reticulum
FCS	Fluorescence correlation spectroscopy
FRET	Förster resonance energy transfer
GFP	Green fluorescent protein
Kd	Dissociation constant
kDa	kiloDalton
IB	Immunoblot
IMPACT	Intein Mediated Purification with an Affinity Chitin-binding Tag
IMS	Intermembrane space
IAP	Inhibitor of Apoptosis Protein
IP3	Inositol 1,4,5 triphosphate
IPTG	Isopropyl β-D-1-thiogalactopyranoside
LUV	Large unilamellar vesicle
MAC	Mitochondria apoptosis-induced channel

mC3	mCerulean 3
MCMC	Markov chain Monte Carlo
MIM	Mitochondrial inner membrane
MOM	Mitochondrial outer membrane
MOMP	Mitochondrial outer membrane permeabilization
NBD	N,N'-Dimethyl-N-(Iodoacetyl)-N'-(7-Nitrobenz-2-Oxa-1,3-Diazol-4-yl) Ethylenediamine
NMR	Nuclear magnetic resonance
OMM	Outer mitochondria membrane
OMV	Outer Membrane Vesicles
PC	Phosphatidylcholine
PCD	Programmed Cell Death
PE	Phosphatidylethanolamine
PG	Phosphatidylglycerol
PI	Phosphatidylinositol
PI3K	Phosphatidylinositol-4,5-bisphosphate 3-kinase
PS	Phosphatidylserine
PTEN	Phosphatase and tensin homolog deleted on chromosome 10
PTM	Post-translational modifications
PTP	Permeability transition pore
SEM	Standard error of mean
S.D.	Standard Deviation
Tb	Terbium III
tBid	Truncated Bid
TCGA	The Cancer Genome Atlas
TNF	Tumour necrosis factor
VDAC	Voltage dependent anion channel
WT	Wild-type

1
Introduction

1.1. Programmed Cell Death and Caspases

Sixty-billion cells per day are generated as a result of cell division in the average adult human, replacing an equal number of cells that died due to programmed cell death (PCD). PCD is important for the development of multicellular organisms, tissue homeostasis and removal of damaged, potentially harmful cells. PCD helps shape complex structures of the body, such as our fingers and toes or folds in our brain, it leads to the destruction of infected cells, self-identifying cells in the immune system and rapidly dividing cells that could lead to cancer. For many years cell death was described as a choice between apoptosis (a morphologically defined form of PCD) and necrosis; the former being a controlled, non-inflammatory, genetically defined intracellular death pathway, and the latter being accidental and highly inflammatory resulting from cellular trauma (Kerr et al., 1972). Discovery of other PCD mechanisms changed this paradigm: in contrast to apoptosis, necroptosis (a programmed form of necrosis) and pyroptosis are highly inflammatory, allowing efficient detection and removal of intracellular pathogens and infected cells by the immune system (Oberst, 2016). Thus dysregulation of inflammatory forms of PCD have important implications in host immunity and due to considerable cross-talk between inflammatory forms of PCD and apoptosis dysregulation of the inflammatory signaling within cells has been linked to carcinogenesis (Philpott et al., 2014). With that said, the majority cell death occurring in the body is via apoptosis and when dysregulated, apoptosis is implicated in many human diseases. Evasion of apoptosis allows cancerous cells to escape death causing the formation of both solid tumours and hematopoietic malignancies (Look, 1997; Green and Evan, 2002). Conversely, unnecessary activation of apoptosis in neurons, seen in patients afflicted with stroke or neurodegenerative diseases, causes permanent loss of brain function (Friedlander,

2003). Determining the mechanisms underlying apoptosis regulation is critically important for understanding how these diseases develop and how therapies can be created to treat them.

The activation status of intracellular caspases (cysteine-dependent aspartate specific proteases) links the different forms of PCD together. In humans there are 11 caspases divided into three groups: inflammatory (caspase 1, 4 and 5), initiator (caspase 2, 8, 9 and 10) and executioner (caspase 3, 6 and 7) (McIlwain et al., 2015). During pyroptosis activated inflammatory caspases process pro-inflammatory cytokines and cleave Gasdermin D which forms pores in the plasma membrane, resulting in the secretion of these cytokines provoking an immune response (Liu et al., 2016; Yuan et al., 2016). Activation of initiator caspases that cleave and activate the executioner caspases triggers apoptosis. A single executioner caspase can activate other executioner caspases and so on creating a caspase cascade that accelerates apoptosis. In contrast, necroptosis is caspase-independent and appears to serve as a backup mechanism of PCD when viral infection prevents apoptosis via viral protein inhibition of caspases (Li and Beg, 2000; Oberst, 2016). During apoptosis caspases cleave hundreds of proteins vital for proper cellular function and homeostasis including those required for cell adhesion and structure, DNA synthesis and repair, and transcription and translation all culminating in the typical biochemical and morphological features of apoptosis - DNA fragmentation, nuclear condensation, membrane blebbing, and condensing and packaging of the cell for non-inflammatory phagocytic clearance (Fischer et al., 2003; McIlwain et al., 2015). Well known examples of caspase action include the activation of CAD (Caspase Activated DNAse) by ICAD (Inhibitor of Caspase Activated DNAse) cleavage resulting in DNA fragmentation, PARP (poly (ADP-ribose) Polymerase) cleavage preventing DNA repair, and the cleavage and inactivation of flippases ATP11A and ATP11C, which are responsible for keeping

phosphatidylserine in the cytoplasmic leaflet of the plasma membrane, resulting in the exposure of phosphatidylserine in the outer leaflet - the 'eat-me' signal for phagocytes (Tewari et al., 1995; Enari et al., 1998; Nagata et al., 2016).

1.2. Initiating Apoptosis: The Intrinsic and Extrinsic Pathways

In vertebrates apoptosis triggered by intrinsic or extrinsic pathways results in the activation of the executioner caspases (Tait and Green, 2010). The intrinsic pathway is initiated by a multitude of intracellular stressors (DNA damage, premature mitotic arrest, the unfolded protein response, etc.) that ultimately leads to mitochondria outer membrane permeabilization (MOMP) which is controlled by the Bcl-2 family of proteins. The process by which Bcl-2 family proteins regulate MOMP is the main subject of this thesis and is introduced in detail in Chapter 2 and then addressed experimentally in subsequent chapters. MOMP releases pro-apoptogenic factors (cytochrome *c*, SMAC/DIABLO, OMI/HTRA2 and Endonuclease G) from the intermembrane space (IMS) of mitochondria. Cytochrome *c* released into the cytosol complexes with, and causes oligomerization of Apaf-1 (Apoptotic protease activating factor 1) exposing a caspase-recruitment domain (CARD) on each Apaf-1 subunit. The CARD domain of procaspase-9 binds the CARD domain in Apaf-1 facilitating dimerization induced activation of caspase-9 which cleaves and activates the executioner caspases (Bratton and Salvesen, 2010). SMAC/DIABLO & OMI/HTRA2 inhibit caspase-inhibiting IAPs (inhibitor of apoptosis proteins) allowing caspase activation and Endonuclease G migrates to the nucleus and degrades DNA (Du et al., 2000; Verhagen et al., 2000; Li et al., 2001; Suzuki et al., 2001).

The extrinsic pathway is activated by extracellular death ligands, like FASL, TRAIL or TNF binding their cognate death receptors. For example, FASL binds the FAS receptor forming

the death-inducing signaling complex (DISC) that recruits and activates procaspase-8 by proximity induced dimerization (Parrish et al., 2013). Caspase-8 cleaves and activates executioner caspases as well as the Bcl-2 family protein Bid triggering the intrinsic pathway, initiating MOMP and greatly accelerating apoptosis. The intrinsic apoptosis pathway can differ depending on the cell (Type I or II). Type I cells only require the direct activation of executioner caspases by caspase-8 whereas type II cells require the activation of Bid by caspase-8 and subsequently MOMP (Scaffidi et al., 1998). The difference is due to the levels of caspase-inhibiting IAPs (inhibitor of apoptosis proteins) in the two cell types. Type II cells have increased levels of IAPs compared to Type I cells thus Type II cells require MOMP to release IMS proteins that inhibit the IAPs (e.g SMAC/DIABLO and OMI/HTRA2) to result in executioner caspase activation (Jost et al., 2009). Since most vertebrate cells are Type II, MOMP is essential for both intrinsic and extrinsic activation of apoptosis (Tait and Green, 2010). MOMP is rapid and complete, once it occurs, most cytochrome c is released (<5 minutes), followed by complete executioner caspase activation resulting in the inevitable death of the cell (<=15 minutes) (Goldstein et al., 2000; Rehm et al., 2002). Furthermore, the capacity of a cell to trigger MOMP predicts clinical response to anti-cancer chemotherapy, underpinning the importance in understanding MOMP regulation (Chonghaile et al., 2011).

1.3. Modeling the 'embedded together' Bcl-2 family

The discovery of the *bcl-2* gene, which encodes a protein that prevents MOMP, led to an explosion of research on the molecular mechanisms governing MOMP (Tsujimoto and Croce, 1986; Delbridge et al., 2016). These traditional experimental approaches have helped shape our understanding of apoptosis and specifically MOMP regulation by the Bcl-2 family of proteins.

As with many fields, such intense research led to various competing models (explained in detail in chapter 2) of Bcl-2 family regulation concerning which Bcl-2 family members interact with each other to control MOMP (Shamas-Din et al., 2013). The 'embedded together' model developed by our lab synthesized features from two competing models, while putting an emphasis on the role of the membrane as the 'locus of action' for most Bcl-2 family proteins (Leber et al., 2007). The model explained briefly, but in detail in subsequent chapters, is as follows: the Bcl-2 family of proteins that regulate MOMP are divided into anti- and pro-apoptotic groups (Chi et al., 2014). The pro-apoptotic proteins are subdivided into the membrane-permeabilizing proteins (Bax, Bak, Bok), activator BH3-proteins (Bid, Bim, Puma) and sensitizer BH3 proteins (Bad, Noxa). The anti-apoptotic proteins (Bcl-2, Bcl-XL, Bcl-w, Mcl-1) bind to and inhibit both the membrane-permeabilizing proteins and all of the BH3 proteins. The activator BH3 proteins also bind to and activate the membrane permeabilizing proteins which then insert into the MOM and oligomerize to form pores in the outer mitochondrial membrane. Sensitizer BH3 proteins are believed to inhibit the anti-apoptotic proteins by displacing bound activator BH3-proteins and pore-formers from anti-apoptotic proteins by competing for the same binding sites. The membrane plays an active role in facilitating distinct changes in conformations of Bcl-2 family proteins that govern the interactions between the family members and thus whether or not MOMP occurs.

Discriminating between competing models is sometime difficult, especially with complex biological processes like apoptosis, which are even more difficult to predict. Quantitative modeling is a tool that in combination with experimental data can be used to explain, predict and understand the behavior of complex biological processes while validating and discriminating competing models. Our collaborators (Dr. Peter Sorger Lab) have successfully used quantitative

modeling to explain the substantial cell-to-cell variability in death kinetics upon induction of extrinsic apoptosis that is attributed to the time it takes each cell to trigger MOMP, which can be many hours. The interactions of the Bcl-2 family regulating Bax pore formation and subsequent SMAC/DIABLO release due to MOMP were critical to controlling the all-or-none phenotype of MOMP and executioner caspase activation thus effectively modeling TYPE II cells (Albeck et al., 2008). A similar approach using Bayesian statistics was used to discriminate between the competing models of Bcl-2 family interactions finding that the 'embedded together' model reproduces MOMP dynamics observed in single-cells (Lopez et al., 2013). In Chapter 5 of this thesis, we collaborated with Dr. Peter Sorgers lab and combined computational modeling, Bayesian statistics and experimental data of Bax conformation change to create a Bax activation kinetic model. This new kinetic model aided in identifying a novel Bax intermediate conformation associated with activator BH3:Bax binding that occurs before Bax insertion into membranes, Bax oligomerization and membrane permeabilization. In Chapter 7, I quantitatively model the binding interactions between the sensitizer BH3 protein Bad and the anti-apoptotic protein Bcl-XL to discover a novel function of the BH3 sensitizer protein Bad.

The aforementioned quantitative models allowed for important insights into the complex regulation of the Bcl-2 family proteins that likely would have been missed when examined only qualitatively. Furthermore, given the relatively large number of Bcl-2 family proteins and subtle differences in their binding affinities and mechanisms of action (described in detail in Chapter 2), and that dysregulation of the Bcl-2 family proteins has wide-ranging implications in human disease, quantitatively modeling apoptosis will provide a deeper understanding of how cell fate is controlled, how it can become dysregulated, and how it can be modulated to treat human disease, and in particular cancer.

1.4. Pharmacological Manipulation of Bcl-2 Family Proteins for the Treatment of Cancer

Normal cells become cancerous due to mutations that cause defects in pathways controlling cell proliferation and homeostasis resulting in uncontrolled cell growth and genomic instability (Hanahan and Weinberg, 2011). Normal cells trigger apoptosis to counteract both of these facets of transformation therefore, for a tumour to develop, transformed cells must block apoptosis. The initial observation that the *bcl-2* gene did not function as a standard oncogene by increasing cellular proliferation but that preventing death of normal lymphocytes was sufficient for the gene to function as an oncogene, underpinned the importance of regulation of apoptosis by Bcl-2 family proteins in carcinogenesis (McDonnell et al., 1989).

Cancerous cells can and do undergo apoptosis. For a tumour to develop, apoptosis has to be sufficiently inhibited that growth outstrips death. For this to occur apoptosis is often blocked at the point of MOMP due to overexpression of one or more anti-apoptotic Bcl-2 family proteins (Deng et al., 2007). Simply put, life outweighs death; active anti-apoptotic proteins bind to and inhibit all of the active pro-apoptotic proteins in cancerous cells. As a result these cancer cells are 'addicted' to the expression of anti-apoptotic Bcl-2 family proteins because in their absence the cells die faster than they grow. Such cells are described as 'primed for death' only requiring a 'push' in the right direction to trigger MOMP and subsequent apoptosis (Certo et al., 2006). Inactivating the anti-apoptotic Bcl-2 family proteins with small molecules is one potential 'push' as displacing the active but sequestered pro-apoptotic proteins results in MOMP (Leber et al., 2010; Del Gaizo Moore and Letai, 2013; Shamas-Din et al., 2013).

Selective inhibition of anti-apoptotic Bcl-2 family proteins is an emerging cancer treatment strategy that contrasts with the broad toxicity of classic chemotherapy that kills dividing cells regardless if they are cancerous or normal (Czabotar et al., 2014). In contrast to cancer cells, normal cells do not have upregulated apoptotic signaling and are not 'primed' for death. Thus, normal cells can withstand inhibition of anti-apoptotic Bcl-2 family, whereas cancerous cells cannot. The first truly selective drug using this strategy was ABT-263 (Navitoclax) which inhibits Bcl-2, Bcl-XL and Bcl-w. Navitoclax showed promise for treating hematological malignancies in clinical trials, however patients had dose-limiting thrombocytopenia (low platelet counts); an on-target effect resulting from the inhibition of Bcl-XL in platelets (Mason et al., 2007; Tse et al., 2008; Vogler et al., 2011). ABT-199 (venetoclax), which targets only Bcl-2 and does not cause thrombocytopenia, was developed and in April 2016 was approved for treatment of relapsed CLL (Souers et al., 2013; Roberts et al., 2016). Navitoclax and venetoclax are in dozens of clinical trials as use as single agents or in combination with other therapies (Delbridge et al., 2016) and show promise for cancers that are addicted to Bcl-2, Bcl-XL or Bcl-w. However, certain cancers depend on Mcl-1 for survival (Xiang et al., 2010; Zhang et al., 2011; Grabow et al., 2014) and cancers may acquire resistance to drugs that target Bcl-2/Bcl-XL/Bcl-w by upregulating Mcl-1 (Yecies et al., 2010).

At present there is only one small molecule Mcl-1 inhibitor, S63845 that shows promise as a therapeutic. S63845 was efficacious in killing multiple cancer derived cell lines *in vitro* and pre-clinical mouse models of hematological malignancies *in vivo* while sparing normal tissues. The future of pharmacological manipulation of Bcl-2 family members is promising. While it will be exciting to see how these drugs function as single agents and synergistically with other therapeutics in future clinical trials, a more complete understanding of the molecular

mechanisms by which the Bcl-2 family regulates MOMP is essential to not only understand how their dysregulation contributes to human disease but to also identify and validate other potential therapeutic targets.

1.5. Thesis synopsis

In this thesis I begin to fill some of the gaps in understanding the regulation of Bcl-2 family proteins. The thesis starts with three chapters (2, 3 and 4) that were previously published and together they provide a detailed summary of the functions of Bcl-2 family proteins (Chapter 2), the rationale for the use of fluorescence techniques to study Bcl-2 family protein interactions and function (Chapter 3), and the detailed methods used to study these proteins in this thesis (Chapter 4)(Kale et al., 2012; Shamas-Din et al., 2013; Kale et al., 2014). My experimental contributions to the field are described in Chapters 5, 6 and 7.

In Chapter 5, I use kinetic analysis of a reconstituted protein-membrane system to characterize the dynamics of the structural rearrangements of Bax as it undergoes activation by either cBid or Bim, followed by insertion into the membrane and pore formation. The environment change of 19 different residues was tracked contemporaneously with activator BH3: Bax binding and liposome permeabilization. With our collaborators, we used quantitative modeling paired with Bayesian statistics to fit the environment change dynamics of each residue to create a novel kinetic model for Bax conformation changes. I find that Bax undergoes a fast rearrangement through a structurally distinct intermediate, associated with activator BH3 binding, followed by the rate-limiting insertion of Bax into the membrane, as we have previously observed for Bax (Lovell et al., 2008), transitioning into the final inserted state. Furthermore, point mutations of Bax found in human cancer and human cancer cell lines block Bax at this

intermediate conformation suggesting that transitions into and out of this intermediate can be modulated independently with consequences for the execution of apoptosis.

In chapter 6, I discover that phosphorylation of Bax at residue S184 by the pro-survival kinase AKT traps Bax in the intermediate conformation converting Bax into an anti-apoptotic protein. A phosphomimetic mutant of Bax (Bax S184E) functions as a dominant-negative preventing liposome permeabilization of WT Bax by sequestering activator BH3 proteins and protecting cells from a variety of apoptotic stimuli. Analysis of The Cancer Genome Atlas (TCGA) database revealed that in human cancers, increasing the expression of Bax, and therefore phosphorylated anti-apoptotic Bax in cells with hyper-active AKT represents an additional mechanism for cancer cells to prevent apoptosis. In these cells the mitochondria are 'unprimed' by Bax phosphorylation and our data suggests that a combination of AKT inhibitors and BH3 mimetics could represent a viable treatment strategy.

Finally in Chapter 7, I uncover a novel function of the sensitizer BH3 protein Bad - it modulates the activity of tBid indirectly through Bcl-XL dimers. Under physiological concentrations of Bcl-2 family proteins (<100 nM), Bad should not be able to displace cBid from Bcl-XL since Bad has a 10-fold lower affinity to Bcl-XL compared to cBid. By using a quantitative model for Bad displacement of cBid from Bcl-XL I find that Bad binding to a Bcl-XL:tBid complex acts as an allosteric switch converting the antiapoptotic tBid:Bcl-XL dimer complex to a proapoptotic one thus representing a novel mechanism that enhances the pro-apoptotic potency of Bad. As a whole, this thesis contributes to the vast body of work devoted to understanding how the Bcl-2 family regulates MOMP and in particular uncovers novel

mechanisms for the activation of Bax, inhibition of Bax by AKT, and the pro-apoptotic activity of Bad.

1.6. References

Albeck, J.G., Burke, J.M., Spencer, S.L., Lauffenburger, D.A., and Sorger, P.K. (2008). Modeling a snap-action, variable-delay switch controlling extrinsic cell death. PLoS biology *6*, 2831-2852.

Bratton, S.B., and Salvesen, G.S. (2010). Regulation of the Apaf-1-caspase-9 apoptosome. J Cell Sci *123*, 3209-3214.

Certo, M., Del Gaizo Moore, V., Nishino, M., Wei, G., Korsmeyer, S., Armstrong, S.A., and Letai, A. (2006). Mitochondria primed by death signals determine cellular addiction to antiapoptotic BCL-2 family members. Cancer Cell *9*, 351-365.

Chi, X., Kale, J., Leber, B., and Andrews, D.W. (2014). Regulating cell death at, on, and in membranes. Biochimica et biophysica acta *1843*, 2100-2113.

Chonghaile, T.N., Sarosiek, K.A., Vo, T.T., Ryan, J.A., Tammareddi, A., Moore, V.D., Deng, J., Anderson, K.C., Richardson, P., Tai, Y.T., *et al.* (2011). Pretreatment Mitochondrial Priming Correlates with Clinical Response to Cytotoxic Chemotherapy. Science *334*, 1129-1133.

Czabotar, P.E., Lessene, G., Strasser, A., and Adams, J.M. (2014). Control of apoptosis by the BCL-2 protein family: implications for physiology and therapy. Nature reviews Molecular cell biology *15*, 49-63.

Del Gaizo Moore, V., and Letai, A. (2013). BH3 profiling--measuring integrated function of the mitochondrial apoptotic pathway to predict cell fate decisions. Cancer letters *332*, 202-205.

Delbridge, A.R., Grabow, S., Strasser, A., and Vaux, D.L. (2016). Thirty years of BCL-2: translating cell death discoveries into novel cancer therapies. Nature reviews Cancer *16*, 99-109.

Deng, J., Carlson, N., Takeyama, K., Dal Cin, P., Shipp, M., and Letai, A. (2007). BH3 profiling identifies three distinct classes of apoptotic blocks to predict response to ABT-737 and conventional chemotherapeutic agents. Cancer Cell *12*, 171-185.

Du, C., Fang, M., Li, Y., Li, L., and Wang, X. (2000). Smac, a mitochondrial protein that promotes cytochrome c-dependent caspase activation by eliminating IAP inhibition. Cell *102*, 33-42.

Enari, M., Sakahira, H., Yokoyama, H., Okawa, K., Iwamatsu, A., and Nagata, S. (1998). A caspase-activated DNase that degrades DNA during apoptosis, and its inhibitor ICAD. Nature *391*, 43-50.

Fischer, U., Janicke, R.U., and Schulze-Osthoff, K. (2003). Many cuts to ruin: a comprehensive update of caspase substrates. Cell death and differentiation *10*, 76-100.

Friedlander, R.M. (2003). Apoptosis and caspases in neurodegenerative diseases. N Engl J Med *348*, 1365-1375.

Goldstein, J.C., Waterhouse, N.J., Juin, P., Evan, G.I., and Green, D.R. (2000). The coordinate release of cytochrome c during apoptosis is rapid, complete and kinetically invariant. Nature cell biology *2*, 156-162.

Grabow, S., Delbridge, A.R., Valente, L.J., and Strasser, A. (2014). MCL-1 but not BCL-XL is critical for the development and sustained expansion of thymic lymphoma in p53-deficient mice. Blood *124*, 3939-3946.

Green, D.R., and Evan, G.I. (2002). A matter of life and death. Cancer Cell *1*, 19-30.

Hanahan, D., and Weinberg, R.A. (2011). Hallmarks of cancer: the next generation. Cell *144*, 646-674.

Jost, P.J., Grabow, S., Gray, D., McKenzie, M.D., Nachbur, U., Huang, D.C., Bouillet, P., Thomas, H.E., Borner, C., Silke, J., *et al.* (2009). XIAP discriminates between type I and type II FAS-induced apoptosis. Nature *460*, 1035-1039.

Kale, J., Chi, X., Leber, B., and Andrews, D. (2014). Examining the molecular mechanism of bcl-2 family proteins at membranes by fluorescence spectroscopy. Methods in enzymology *544*, 1-23.

Kale, J., Liu, Q., Leber, B., and Andrews, D.W. (2012). Shedding light on apoptosis at subcellular membranes. Cell *151*, 1179-1184.

Kerr, J.F., Wyllie, A.H., and Currie, A.R. (1972). Apoptosis: a basic biological phenomenon with wide-ranging implications in tissue kinetics. British journal of cancer *26*, 239-257.

Leber, B., Lin, J., and Andrews, D.W. (2007). Embedded together: The life and death consequences of interaction of the Bcl-2 family with membranes. Apoptosis : an international journal on programmed cell death *12*, 897-911.

Leber, B., Lin, J., and Andrews, D.W. (2010). Still embedded together binding to membranes regulates Bcl-2 protein interactions. Oncogene *29*, 5221-5230.

Li, L.Y., Luo, X., and Wang, X. (2001). Endonuclease G is an apoptotic DNase when released from mitochondria. Nature *412*, 95-99.

Li, M., and Beg, A.A. (2000). Induction of necrotic-like cell death by tumor necrosis factor alpha and caspase inhibitors: novel mechanism for killing virus-infected cells. Journal of virology *74*, 7470-7477.

Liu, X., Zhang, Z., Ruan, J., Pan, Y., Magupalli, V.G., Wu, H., and Lieberman, J. (2016). Inflammasome-activated gasdermin D causes pyroptosis by forming membrane pores. Nature *535*, 153-158.

Look, A.T. (1997). Oncogenic transcription factors in the human acute leukemias. Science *278*, 1059-1064.

Lopez, C.F., Muhlich, J.L., Bachman, J.A., and Sorger, P.K. (2013). Programming biological models in Python using PySB. Molecular systems biology *9*, 646.

Lovell, J.F., Billen, L.P., Bindner, S., Shamas-Din, A., Fradin, C., Leber, B., and Andrews, D.W. (2008). Membrane binding by tBid initiates an ordered series of events culminating in membrane permeabilization by Bax. Cell *135*, 1074-1084.

Mason, K.D., Carpinelli, M.R., Fletcher, J.I., Collinge, J.E., Hilton, A.A., Ellis, S., Kelly, P.N., Ekert, P.G., Metcalf, D., Roberts, A.W., *et al.* (2007). Programmed anuclear cell death delimits platelet life span. Cell *128*, 1173-1186.

McDonnell, T.J., Deane, N., Platt, F.M., Nunez, G., Jaeger, U., McKearn, J.P., and Korsmeyer, S.J. (1989). bcl-2-immunoglobulin transgenic mice demonstrate extended B cell survival and follicular lymphoproliferation. Cell *57*, 79-88.

McIlwain, D.R., Berger, T., and Mak, T.W. (2015). Caspase functions in cell death and disease. Cold Spring Harbor perspectives in biology *7*.

Nagata, S., Suzuki, J., Segawa, K., and Fujii, T. (2016). Exposure of phosphatidylserine on the cell surface. Cell death and differentiation *23*, 952-961.

Oberst, A. (2016). Death in the fast lane: what's next for necroptosis? The FEBS journal *283*, 2616-2625.

Parrish, A.B., Freel, C.D., and Kornbluth, S. (2013). Cellular mechanisms controlling caspase activation and function. Cold Spring Harbor perspectives in biology *5*.

Philpott, D.J., Sorbara, M.T., Robertson, S.J., Croitoru, K., and Girardin, S.E. (2014). NOD proteins: regulators of inflammation in health and disease. Nature reviews Immunology *14*, 9-23.

Rehm, M., Dussmann, H., Janicke, R.U., Tavare, J.M., Kogel, D., and Prehn, J.H. (2002). Single-cell fluorescence resonance energy transfer analysis demonstrates that caspase activation during apoptosis is a rapid process. Role of caspase-3. The Journal of biological chemistry *277*, 24506-24514.

Roberts, A.W., Davids, M.S., Pagel, J.M., Kahl, B.S., Puvvada, S.D., Gerecitano, J.F., Kipps, T.J., Anderson, M.A., Brown, J.R., Gressick, L., *et al.* (2016). Targeting BCL2 with Venetoclax in Relapsed Chronic Lymphocytic Leukemia. N Engl J Med *374*, 311-322.

Scaffidi, C., Fulda, S., Srinivasan, A., Friesen, C., Li, F., Tomaselli, K.J., Debatin, K.M., Krammer, P.H., and Peter, M.E. (1998). Two CD95 (APO-1/Fas) signaling pathways. The EMBO journal *17*, 1675-1687.

Shamas-Din, A., Kale, J., Leber, B., and Andrews, D.W. (2013). Mechanisms of action of Bcl-2 family proteins. Cold Spring Harbor perspectives in biology *5*, a008714.

Souers, A.J., Leverson, J.D., Boghaert, E.R., Ackler, S.L., Catron, N.D., Chen, J., Dayton, B.D., Ding, H., Enschede, S.H., Fairbrother, W.J., *et al.* (2013). ABT-199, a potent and selective BCL-2 inhibitor, achieves antitumor activity while sparing platelets. Nature medicine *19*, 202-208.

Suzuki, Y., Imai, Y., Nakayama, H., Takahashi, K., Takio, K., and Takahashi, R. (2001). A serine protease, HtrA2, is released from the mitochondria and interacts with XIAP, inducing cell death. Molecular cell *8*, 613-621.

Tait, S.W., and Green, D.R. (2010). Mitochondria and cell death: outer membrane permeabilization and beyond. Nature reviews Molecular cell biology *11*, 621-632.

Tewari, M., Quan, L.T., O'Rourke, K., Desnoyers, S., Zeng, Z., Beidler, D.R., Poirier, G.G., Salvesen, G.S., and Dixit, V.M. (1995). Yama/CPP32 beta, a mammalian homolog of CED-3, is a CrmA-inhibitable protease that cleaves the death substrate poly(ADP-ribose) polymerase. Cell *81*, 801-809.

Tse, C., Shoemaker, A.R., Adickes, J., Anderson, M.G., Chen, J., Jin, S., Johnson, E.F., Marsh, K.C., Mitten, M.J., Nimmer, P., *et al.* (2008). ABT-263: a potent and orally bioavailable Bcl-2 family inhibitor. Cancer research *68*, 3421-3428.

Tsujimoto, Y., and Croce, C.M. (1986). Analysis of the structure, transcripts, and protein products of bcl-2, the gene involved in human follicular lymphoma. Proceedings of the National Academy of Sciences of the United States of America *83*, 5214-5218.

Verhagen, A.M., Ekert, P.G., Pakusch, M., Silke, J., Connolly, L.M., Reid, G.E., Moritz, R.L., Simpson, R.J., and Vaux, D.L. (2000). Identification of DIABLO, a mammalian protein that promotes apoptosis by binding to and antagonizing IAP proteins. Cell *102*, 43-53.

Vogler, M., Hamali, H.A., Sun, X.M., Bampton, E.T., Dinsdale, D., Snowden, R.T., Dyer, M.J., Goodall, A.H., and Cohen, G.M. (2011). BCL2/BCL-X(L) inhibition induces apoptosis, disrupts cellular calcium homeostasis, and prevents platelet activation. Blood *117*, 7145-7154.

Xiang, Z., Luo, H., Payton, J.E., Cain, J., Ley, T.J., Opferman, J.T., and Tomasson, M.H. (2010). Mcl1 haploinsufficiency protects mice from Myc-induced acute myeloid leukemia. The Journal of clinical investigation *120*, 2109-2118.

Yecies, D., Carlson, N.E., Deng, J., and Letai, A. (2010). Acquired resistance to ABT-737 in lymphoma cells that up-regulate MCL-1 and BFL-1. Blood *115*, 3304-3313.

Yuan, J., Najafov, A., and Py, B.F. (2016). Roles of Caspases in Necrotic Cell Death. Cell *167*, 1693-1704.

Zhang, H., Guttikonda, S., Roberts, L., Uziel, T., Semizarov, D., Elmore, S.W., Leverson, J.D., and Lam, L.T. (2011). Mcl-1 is critical for survival in a subgroup of non-small-cell lung cancer cell lines. Oncogene *30*, 1963-1968.

2

Mechanisms of Action of Bcl-2 Family proteins

2.1. Preface

This chapter has been previously published as a book chapter in:

Shamas-Din, A., Kale, J., Leber, B., and Andrews, D.W. (2013) Mechanisms of Action of Bcl-2 Family Proteins. Cold Spring Harb Perspect Biol. 5(4):a008714.

The publisher has granted permission for the work to be reproduced here

Author Contribution:

Shamas-Din, A wrote the sections on the models and on 'BH3 members'. Kale, J wrote the section 'Multi-domain pro-apoptotic members'. Leber, B wrote the section on 'anti-apoptotic members' and the conclusion. Figures 1 & 2 were prepared by Shamas-Din, A. Figure 3 was prepared by Kale, J. Andrews, DW edited the manuscript and directed the layout of the book chapter.

Objective:

To detail the molecular mechanisms governing the regulation of the Bcl-2 family of proteins

Highlights:

- The Bcl-2 family of proteins regulates the commitment step to apoptosis – mitochondrial outer membrane permeabilization (MOMP)
- There are 3 classes of Bcl-2 Family proteins
    - Pore-forming multiregion proapoptotic proteins that permeabilize the mitochondrial outer membrane (MOM)
    - BH3-only proteins that directly or indirectly activate the pore-forming members
    - Anti-apoptotic multiregion proteins that inhibit both the pore-formers and the BH3-only proteins
- The Bcl-2 family proteins undergo significant conformation changes when targeting to the MOM which changes their binding interactions to one another
- The fate of the cell is determined by the interactions between the Bcl-2 family members within the cytosol or MOM which are governed by the differences in concentrations and relative binding affinities of the proteins

2.2. Introduction

Apoptosis was formally described and named in 1972 as a unique morphologic response to many different kinds of cell stress that was distinct from necrosis. However, despite the novelty and utility of the concept, little experimental work was done over the following twenty years because no tools existed to manipulate the process. In the early 1990s two seminal observations changed the landscape. First, as the complete developmental sequence of the nematode *Caenorhabditis elegans* was painstakingly elucidated at the single cell level, it was noted that a fixed, predictable number of "intermediate" cells were destined to die, and that this process was positively and negatively regulated by specific genes. Second, a novel gene called B-cell CLL/Lymphoma 2 (Bcl-2; encoded by *BCL2*) that was discovered as a partner in a reciprocal chromosomal translocation in a human tumor, turned out to function not as a classic oncogene by driving cell division, but rather by preventing apoptosis. When it was discovered that the mammalian *BCL2* could substitute for *CED-9*, the *C. elegans* gene that inhibits cell death, the generality of the process was recognized and the scientific literature exploded with now well over 10^5 publications on apoptosis. However, it is ironic to note that after a further 20 years of intensive investigation, it is clear that the mechanism of action of Bcl-2 is quite distinct from Ced-9 that sequesters the activator of the caspase protease that is the ultimate effector of apoptosis. By contrast, Bcl-2 works primarily by binding to other related proteins that regulate permeabilization of the mitochondrial outer membrane (MOM).

This review will examine how apoptosis is regulated by the members of the (now very large) Bcl-2 family comprised of three groups related by structure and function (illustrated in Figure 1): (1) the BH3 proteins that sense cellular stress and activate (either directly or indirectly) (2) the executioner proteins Bax or Bak that oligomerize in and permeabilize the MOM thereby releasing components of the intermembrane space that activate the final, effector caspases of apoptosis, and (3) the anti-apoptotic members like Bcl-2 that impede the overall process by inhibiting both the BH3 and the executioner proteins. To understand the consequence of the interactions between the three subgroups, several models have been proposed (Direct Activation, Displacement, Embedded Together, and Unified Model illustrated in Figure 2) that are briefly described here before a more detailed discussion of the Bcl-2 families.

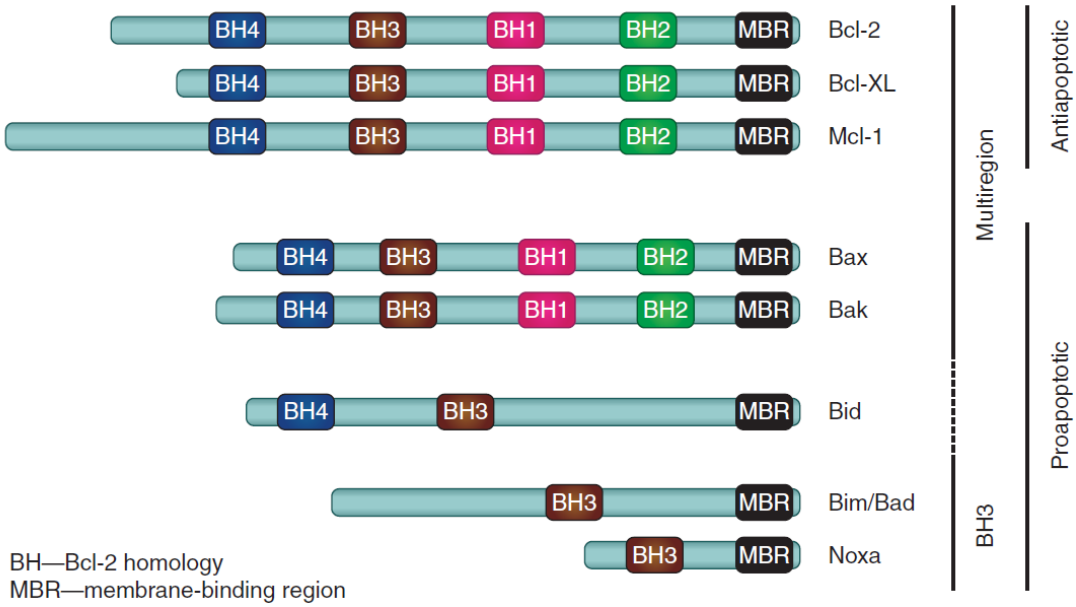

Figure 2.1- Schematic overview of the Bcl-2 Family of proteins.

The family is divided into two subgroups containing proteins that either inhibit apoptosis, or promote apoptosis. The pro-apoptotic proteins are further sub-divided functionally into those that oligomerize and permeabilize the MOM, such as Bax and Bak; or those that promote apoptosis through either activating Bax or Bak or inhibiting the anti-apoptotic proteins, such as tBid, Bim, Bad, Noxa. Proteins are included in the Bcl-2 family based on sequence homology to the founding member, Bcl-2 in one of the four Bcl-2 homology (BH) regions. All the anti-apoptotic proteins, as well as Bax, Bak and Bid, have multiple BH regions, are evolutionary-related and share a three-dimensional structural fold. The BH3 proteins contain only the BH3 region, are evolutionary distant from the multi-region proteins and are intrinsically unstructured. Most members of the Bcl-2 family proteins contain a membrane-binding region (MBR) on their carboxyl-terminal in a form of a tail-anchor, mitochondrial-targeting sequence or as a hydrophobic amino-acid sequence that facilitates binding and localization of these proteins to the MOM or ER membrane.

2.2.1. Direct Activation model

The distinctive feature of the direct activation model is that a BH3 protein is required to directly bind and activate the Bcl-2 multi-homology region pro-apoptotic proteins, Bax and Bak. The direct activation model classifies BH3 proteins as activators or sensitizers based on their affinities for binding to Bcl-2 multi-region proteins (Letai et al. 2002) (See Table 1). The activator BH3 proteins, tBid, Bim and Puma bind to both the pro-apoptotic and the anti-apoptotic Bcl-2 multi-region proteins (Kim et al. 2006). The sensitizer BH3 proteins, Bad, Noxa, Bik,

Bmf, Hrk, Bnip3 bind to the anti-apoptotic proteins, thereby liberating activator BH3 proteins to promote mitochondrial outer membrane permeabilization (MOMP) (Letai et al. 2002; Kuwana et al. 2005; Certo et al. 2006). The anti-apoptotic proteins bind to both the activator and the sensitizer BH3 proteins, but are unable to complex with Bax and Bak (Kim et al. 2006). Therefore, for a cell to evade apoptosis, anti-apoptotic proteins must sequester the BH3 proteins to prevent Bax/Bak activation and apoptosis.

Table 2.1 - Binding profiles within Bcl-2 family members

	Antiapoptotic protein binds to		
		BH3 proteins	
Antiapoptotic protein	Bax/ Bak/Bid	Activator	Sensitizer
Bcl-2	Bax, Bid	Bim, Puma	Bmf, Bad
Bcl-XL	Bax, Bak, Bid	Bim, Puma	Bmf, Bad, Bik, Hrk
Bcl-w	Bax, Bak, Bid	Bim, Puma	Bmf, Bad, Bik, Hrk
Mcl-1	Bak, Bid	Bim, Puma	Noxa, Hrk
A1	Bak, Bid	Bim, Puma	Noxa, Bik, Hrk

Letai et al. (2002); Chen et al. (2005).

2.2.2. Displacement model

In the displacement model, BH3 proteins do not directly bind to Bax and Bak to cause their activation. Rather Bax and Bak are constitutively active and therefore must be inhibited by the anti-apoptotic proteins for the cell to survive. To initiate apoptosis, BH3 proteins displace Bax and Bak from the anti-apoptotic proteins to promote Bax or Bak mediated MOMP. Since BH3 proteins selectively interact with a limited spectrum of anti-apoptotic proteins, a combination of BH3 proteins is required to induce apoptosis in cells expressing multiple anti-apoptotic Bcl-2 family members (Chen et al. 2005) (See Table 1). In support for this model, hetero-dimers of Bak with Mcl-1 and Bcl-XL are present in dividing cells and over-expression of Noxa displaces Bak-Mcl-1 heterodimers releasing Bak and forming Noxa-Mcl-1 complexes. In

these cells, a combination of Bad and Noxa is required to neutralize the effects of both Bcl-XL and Mcl-1 in order to finally induce apoptosis (Willis et al. 2005).

2.2.3. Embedded Together model

The 'Embedded Together' model incorporates the role of the membrane as the 'locus of action' for most Bcl-2 family proteins since MOMP does not occur until Bax and Bak achieve their final active conformation in the membrane. The interactions with membranes result in distinct changes in conformations of the Bcl-2 family proteins that govern their affinity for the relative local concentrations of the binding partners (Leber et al. 2007; Garcia-Saez et al. 2009; Leber et al. 2010). For example, the cytoplasmic multi-region proteins Bax and Bcl-XL undergo large but reversible conformational changes after interacting with MOM (Edlich et al. 2011), that increase the affinity for binding to a BH3 protein causing a further conformational change and allowing insertion in the membrane.

In this model, sensitizer BH3 proteins bind only to anti-apoptotic proteins. However, the consequences of this interaction incorporate the features of both the displacement and direct activation models, as the sensitizer BH3 proteins neutralize the dual function of the anti-apoptotic proteins by displacing *both* the activator BH3 proteins and Bax or Bak from the membrane embedded conformers of the anti-apoptotic proteins (Billen et al. 2008; Lovell et al. 2008). Because it is the activated forms of Bax and Bak that are bound to the membrane embedded anti-apoptotic proteins, sensitizer proteins release Bax and Bak conformers competent to oligomerize and permeabilize membranes.

Another distinguishing feature of this model is the dual role assigned to activator BH3 proteins, which directly activate pro-apoptotic proteins and also bind to anti-apoptotic proteins. When activator BH3 proteins interact with Bax and Bak, they promote insertion into the membrane whereupon Bax and Bak oligomerize and permeabilize cellular membranes. Similarly, interaction of activator BH3 proteins with anti-apoptotic proteins promotes their insertion into membranes. However, in this case the BH3 protein functions like a sensitizer, since the bound anti-apoptotic protein is unable to bind Bax or Bak. However, sequestration goes both ways and by binding the BH3 protein the anti-apoptotic protein inhibits it at the membrane.

Moreover, as the interaction of the activator BH3 proteins with both the pro- and the anti-apoptotic Bcl-2 family proteins is reversible, it is therefore possible for a single BH3 protein to interact with both pro- and anti- apoptotic proteins (depending on their relative expression levels) thereby changing their conformation at the membranes. Recently many of the interactions proposed by this model have been measured directly in living cells (Aranovich et al. 2012).

2.2.4. Unified model

The unified model of Bcl-2 family function builds upon the 'embedded together' model (Llambi et al. 2011). This model distinguishes the known interactions of anti-apoptotic Bcl-2 proteins to sequester the activator BH3 proteins as mode 1, and to sequester the active forms of Bax and Bak as mode 2 (Figure 2D). Although in cells both modes of inhibition take place simultaneously, in the unified model inhibition of apoptosis through mode 1 is less efficient and is easier to overcome by BH3 sensitizers to promote MOMP than inhibition through mode 2. Importantly the unified model also incorporates the functions of Bax and Bak in mitochondrial fission and fusion and postulates that only mode 2 repression affects this process. This model is therefore the first to explicitly link modes of MOMP regulation and mitochondrial dynamics.

The dual function assigned to anti-apoptotic proteins is thus shared by both embedded together and unified models. However in the former, the interplay between members of the Bcl-2 family are determined by competing equilibria therefore, the abundance of proteins and specific conditions of cell physiology including post-translational modifications will determine the prevailing interactions. As a result, the embedded together model differs from the unified model in that it predicts that either mode 1 or mode 2 can be dominant depending on circumstances such as particular form of stress and cell type. Further work to test the different predictions of the models with full-length wild-type proteins in different cells is required to resolve these issues.

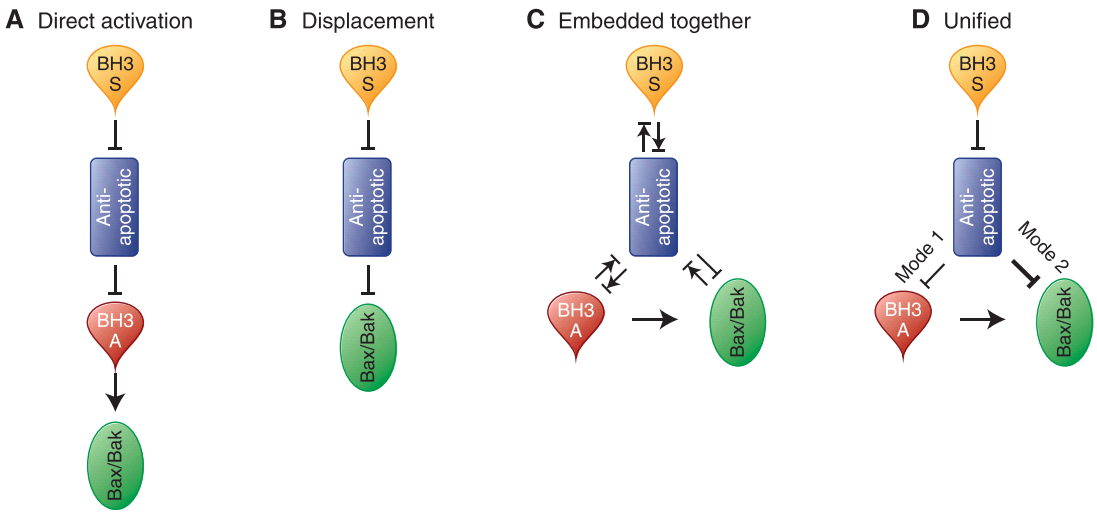

Figure 2.2 - Schematics of the core mechanisms proposed by various models for the regulation of MOMP by Bcl-2 proteins|

Arrows indicate activation, T's indicate inhibition, and T'd arrows indicate mutual recruitment/sequestration. Paired forward and reverse symbols indicate the model makes explicit reference to equilibria.

A. The direct activation model divides the different BH3 proteins by qualitative differences in function. The BH3 proteins with high-affinity for binding and activating Bax and Bak are termed as 'activators', whereas those that only bind the anti-apoptotic proteins are termed as 'sensitizers'. The activator BH3 proteins directly interact with and activate Bax and Bak to promote MOMP. The anti-apoptotic proteins inhibit MOMP by specifically sequestering the BH3 activators. The BH3 sensitizer proteins can compete for binding with the anti-apoptotic proteins, thus releasing the BH3 activator proteins to avidly promote MOMP through activation and oligomerization of Bax and Bak.

B. The displacement model categorizes the BH3 proteins solely based on their affinities of binding for the anti-apoptotic proteins (hence, does not recognize them as activators). In this model Bax and Bak are constitutively active and oligomerize and induce MOMP unless held in check by the anti-apoptotic proteins. Therefore, for a cell to undergo apoptosis, the correct combination of BH3 proteins must compete for binding for the different anti-apoptotic proteins to liberate Bax and Bak and for MOMP to ensue.

C. The embedded together model introduces an active role for the membrane and combines the major aspects of the previous models. The interactions between members of the Bcl-2 family are governed by equlibria, and therefore are contingent on the relative protein concentrations as well as their binding affinities. The latter are determined by post-translational modifications, fraction of protein bound to the membrane, and cellular physiology. At membranes, the activator BH3 proteins directly activate Bax and Bak that then oligomerize inducing MOMP. Both activator and sensitizer BH3 proteins can recruit and sequester anti-apoptotic proteins in the membrane. The anti-apoptotic proteins inhibit apoptosis by sequestering the BH3 proteins and Bax and Bak in the membrane or by preventing their binding to membranes. At different intracellular membranes, the local concentrations of specific subsets of Bcl-2

family members alter the binding of Bcl-2 proteins to the membrane and the binding equilibria between family members. As a result, Bcl-2 family proteins have distinct but overlapping functions at different cellular locations. **D.** The unified model builds upon the embedded together model by proposing that the anti-apoptotic proteins sequester the activator BH3 proteins (mode 1) and sequester Bax and Bak (mode 2). It differs in that in the unified model, inhibition of apoptosis through mode 1 is less efficient (smaller arrow in panel D) and therefore easier to overcome by sensitizer BH3 proteins. In addition, the unified model extends the role of Bcl-2 family proteins and the regulation of MOMP to mitochondria dynamics (not shown).

2.2.5. The models: who binds to whom?

One aspect of many of the models that is potentially confusing is that if an activator BH3 protein binds to an anti-apoptotic family member – which is being inhibited? Whether anti-apoptotic proteins sequester the BH3 proteins, or the BH3 proteins sequester the anti-apoptotic proteins becomes a semantic argument. A more productive way of characterizing the interaction is as a mutual sequestration that prevents their respective activation or inhibition effects on Bax and Bak. Therefore whether MOMP ensues is determined by the relative concentrations and affinities of the pro- and anti-apoptotic proteins at the membrane. This recasting of the players is reminiscent of the original rheostat model proposed by the Korsmeyer group (Oltvai et al. 1993), however it extends that model in ways not originally envisioned. For example, the rheostat model did not anticipate auto-activation. If there is sufficient cytosolic anti-apoptotic Bcl-XL, then those Bcl-XL molecules recruited to the membrane by a BH3 protein can recruit additional molecules of Bcl-XL to the membrane through ‘auto-activation’, a process also observed for Bax. Since BH3 protein binding is reversible, auto-activation ensures recruitment of sufficient Bcl-XL to provide efficient inhibition of the BH3 protein.

Another recently recognized aspect that determines the nature and fate of the binding interactions is composition of different membrane organelles. As mentioned above, the unified model provides a mechanistic link between MOMP regulation and mitochondrial fission and fusion. The importance of membranes in modifying conformations and binding partners as proposed by the embedded together model accounts for the overlapping but distinct function of the Bcl-2 family at the mitochondria and endoplasmic reticulum. It also explains how other membrane sites such as the Golgi can act as a reservoir for potentially activated Bax (Dumitru et al. 2012). Therefore, the roles of Bcl-2 family proteins in cell fate decisions and other processes

such as mitochondrial fusion and autophagy appear to be primarily governed by the relative concentrations and affinities of the different binding partners available in that specific subcellular membrane.

2.3. Multidomain pro-apoptotic members

Bax (Bcl-2 associated X protein), was identified by co-immunoprecipitation with Bcl-2 (Oltvai et al. 1993). Unlike Bcl-2, overexpression of Bax promoted cell death, and the opposing functions suggested a "rheostat" model whereby the relative concentrations of pro- and anti-apoptotic Bcl-2 family members determine cell fate. The discovery of Bcl-XL indicated that anti-apoptotic function could be mediated by more than Bcl-2; shortly thereafter Bak (Bcl-2 associated/killer) was cloned and recognized as the second pro-apoptotic protein functioning similar to Bax despite being more homologous to Bcl-2 than Bax (Chittenden et al. 1995; Farrow et al. 1995; Kiefer et al. 1995). Cells in which the gene encoding either Bax or Bak was knocked out were still susceptible to apoptosis. However $Bax^{-/-}$ /$Bak^{-/-}$ double knockout cells were resistant to almost all death stimuli (Wei et al. 2001). These seminal studies placed Bax and Bak in the same pro-death pathway and indicated significant functional redundancy. Furthermore, the demonstration that they are jointly necessary for almost all types of apoptotic cell death (except for death receptor pathways where effector caspases are directly activated by initiator caspases) provides the mechanism for integration of pro- and anti-apoptotic signals via the common mechanism of Bax- and Bak-mediated membrane permeabilization.

Both Bax and Bak mediate pro-death function at the MOM where they oligomerize and permeabilize the MOM resulting in the release of inter-membrane space (IMS) proteins such as cytochrome *c*, OMI/HTRA2, SMAC/DIABLO and Endonuclease G (Kuwana and Newmeyer 2003). The solution structures of Bax and Bak reveal that both proteins are composed of 9 alpha helices with a large hydrophobic pocket comprised of helices 2-4 (Suzuki et al. 2000; Moldoveanu et al. 2006). Both Bax and Bak contain a C-terminal transmembrane region, alpha helix 9, which targets the proteins to the MOM (See Table 2).

The differences between Bax and Bak are illuminating with respect to the common mechanism. While Bax has a high affinity for the anti-apoptotic proteins, Bcl-2 and Bcl-XL, Bak

has a high affinity for the anti-apoptotic proteins, Mcl-1 and Bcl-XL (Willis et al. 2005; Llambi et al. 2011). Another difference is that Bak is found constitutively bound to the MOM whereas Bax is primarily cytosolic but migrates to the MOM after apoptotic stimuli (Hsu et al. 1997; Wolter et al. 1997; Griffiths et al. 1999). The difference in localization of Bax and Bak in non-stressed cells is due to the position of helix 9. NMR studies indicate that in the initial step of activation helix 9 of Bax is bound to the hydrophobic pocket in "cis", preventing helix 9 from inserting into the MOM (Suzuki et al. 2000). Disruption of the interaction of helix 9 with the hydrophobic pocket causes constitutive Bax targeting to the mitochondria, thus recapitulating the intracellular location of Bak (Nechushtan et al. 1999; Brock et al. 2010). Conversely tethering helix 9 to the hydrophobic core of Bax abrogates Bax targeting to MOM and membrane permeabilization (Gavathiotis et al. 2010). Other portions of the protein involved in membrane binding (and MOMP) once helix 9 is displaced are described below. By contrast, it is presumed that helix 9 of Bak is positioned differently, since Bak bypasses the initial step of Bax activation and targets constitutively to mitochondrial membranes (Setoguchi et al. 2006).

2.3.1. Bax/Bak mediated MOMP

It was proposed that activated Bax would assemble a complex of proteins termed the permeability transition pore (PTP) to create an opening spanning through both membranes of the mitochondria, ultimately causing the MOM to rupture due to mitochondrial matrix swelling (Schwarz et al. 2007). The PTP is composed of the voltage-dependant anion channel (VDAC1) located within the MOM, adenine nucleotide translocase (ANT) located within the mitochondrial inner membrane (MIM) and Cyclophilin D located within the mitochondrial matrix (Brenner and Grimm 2006). Opening of the pore would ensue after activated Bax bound to VDAC1 causing a conformational change in this pre-existing channel, such that it is linked to ANT (Shimizu et al. 1999). However, by biochemical and gene knock-out studies, all three components of the PTP have been shown to be dispensable for Bax dependent MOMP (Tsujimoto and Shimizu 2007). Nevertheless, PTP formation by Bax/Bak independent mechanisms does have a role in cell death as it regulates necrosis in some circumstances (Nakagawa et al. 2005).

An alternative possibility is that activated Bax/Bak form pores directly in the MOM. Amphipathic alpha-helical peptides can porate membranes via two separate mechanisms termed

barrel-stave or toroidal leading to two distinct pores, proteinaceous or lipidic respectively (Yang et al. 2001). In both models, the helices line the pore, perpendicular to the membrane. The barrel-stave model creates a proteinaceous pore devoid of lipids. Conversely, a toroidal pore is composed of protein and lipid components. Bax inserts three amphipathic helices (5, 6 and 9) into the MOM prior to oligomerization and MOMP (Annis et al. 2005). Currently, there is evidence for Bax and Bak generating both proteinaceous and lipidic pores. Electro-physiologic studies using patch clamping identified a pore that was termed the mitochondrial apoptosis-induced channel (MAC) (Pavlov et al. 2001). The MAC contains oligomeric Bax or Bak, providing the first indication that these proteins can create a proteinaceous pore (Dejean et al. 2005). This complex is thought to be composed of nine Bax or Bak monomers yielding a pore diameter of ~5nm which should be sufficient to release cytochrome *c*, a 15 kDa protein. However, experiments investigating the core mechanism of Bax pore formation using liposomes or MOMs demonstrate that Bax can release high-molecular weight dextrans up to 2000 kDa (Kuwana et al. 2002) suggesting that the pore is likely larger *in vivo*. Furthermore, Bax can create pores ranging in size from 25-100 nm consistent with a lipidic pore, not a proteinaceous pore (Schafer et al. 2009). Additionally, peptides containing only helices 5 and 6 of Bax can cause pores to form in liposomes that resemble lipidic pores (Qian et al. 2008). Most of the evidence for proteinaceous pores has been observed with isolated mitochondria, whereas the evidence for lipidic pores is largely from experiments with liposomal-based systems. It is therefore conceivable that both mechanisms are operative at different steps *in vivo*: Bax or Bak may initially insert helices 5 and 6 (and 9) into the MOM forming small pores that resemble proteinaceous pores, and after further oligomerization, the pores increase in size and alter the lipid structure of the membrane facilitating the formation of a pore that can release larger IMS proteins such as OMI/HTRA2 (~49kDa) and SMAC/DIABLO (~27kDa).

2.3.2. Mechanism of Bax/Bak activation and pore formation

A conformational change in the N-terminal region of both Bax and Bak has been detected that correlates with activation (Hsu and Youle 1997; Griffiths et al. 1999; Dewson et al. 2009). When Bax interacts transiently with membranes, it exposes an N-terminal epitope that can be detected using the 6A7 monoclonal antibody (Hsu and Youle 1997; Yethon et al. 2003). After

interacting with BH3 proteins that cause membrane insertion of Bax, the epitope change detected by 6A7 is "locked in" i.e. it is no longer reversible. The exposure of the 6A7 epitope has been attributed to a conformational change in alpha helix 1 of Bax (Peyerl et al. 2007). The sequence of events is likely different for the N-terminal conformational change in Bak as the protein is constitutively membrane-bound.

After activation, the next step leading to oligomerization and pore formation is still under debate. Recently a second hydrophobic pocket of Bax was identified through binding with the BH3 peptide of Bim (Gavathiotis et al. 2008; Gavathiotis et al. 2010). This new binding surface termed the 'rear pocket' is composed of helices 1 and 6 and is located on the opposite side from the canonical 'front' BH3-binding pocket of Bax (composed of helices 2-4). In the cytoplasmic form of Bax, the rear pocket is masked by an unstructured loop between helices 1 and 2, much as the front pocket is masked by helix 9. If the helix 1-2 loop is tethered to the rear pocket, Bax cannot expose the 6A7 epitope or release helix 9 from the front pocket, rendering Bax inactive. This suggests that Bax needs to undergo multiple conformational changes in order to bind to membranes and oligomerize to form pores. Bax and Bak also contain two more putatively transmembrane regions located in helices 5 and 6. After activation, Bax inserts helices 5, 6 and 9 into the MOM (Annis et al. 2005). In contrast, helix 9 of Bak is constitutively transmembrane and Bak inserts (at least) α6 into the MOM after activation (Oh et al. 2010). Additionally, Bak lacking its C-terminal transmembrane domain is still able to insert into membranes and oligomerize causing pore formation after activation by BH3 proteins (Oh et al. 2010; Landeta et al. 2011). Thus, one or more domains of Bak in addition to helix 9 must be anchoring it within the membranes. Further studies are required to determine if Bak inserts both helices 5 and 6, as appears to be the case for Bax.

Whether it binds to the 'front' or the 'rear' pocket, the BH3 region located in alpha helix 2 of both Bax and Bak is essential for homo-dimerization (George et al. 2007; Dewson et al. 2008). Two models of how the pro-apoptotic pore forming proteins propagate the dimers into larger pore-forming oligomers have emerged. The asymmetric and symmetric dimer models both propose that Bax and Bak monomers interact via their BH3 regions and helix 6, however they differ in which pockets the proteins use to oligomerize beyond the dimer (Figure 3). The asymmetrical dimer model was proposed after the identification of the rear pocket (Gavathiotis

et al. 2008; Gavathiotis et al. 2010). In this model, activator BH3 proteins initiate the activation of Bax by binding to the rear pocket causing allosteric conformational changes that displace helix 9 allowing Bax to target to the MOM (Kim et al. 2009). Sequential oligomerization proceeds by the BH3 region of an activated Bax binding to the rear pocket of another Bax monomer thereby exposing its BH3 region to further propagate oligomerization.

The second model proposes that Bax forms symmetrical dimers whereby the BH3 regions of two Bax monomers reciprocally bind the front pockets of each other (Dewson et al. 2009; Bleicken et al. 2010; Oh et al. 2010; Zhang et al. 2010). This dimerization changes the conformation of Bax such that the rear pockets interact with each other to facilitate oligomerization.

These contrasting models postulate different "units" that are joined to form the oligomer. However, it is clear that in each model both hydrophobic pockets are important for the pro-apoptotic function of the proteins. Identification of the mechanism and dynamic binding surfaces that mediate oligomerization will be a great asset for assays testing small molecule modulators of Bax and Bak function to allow this rate-limiting step in apoptosis to be selectively activated or inhibited as dictated by clinical need.

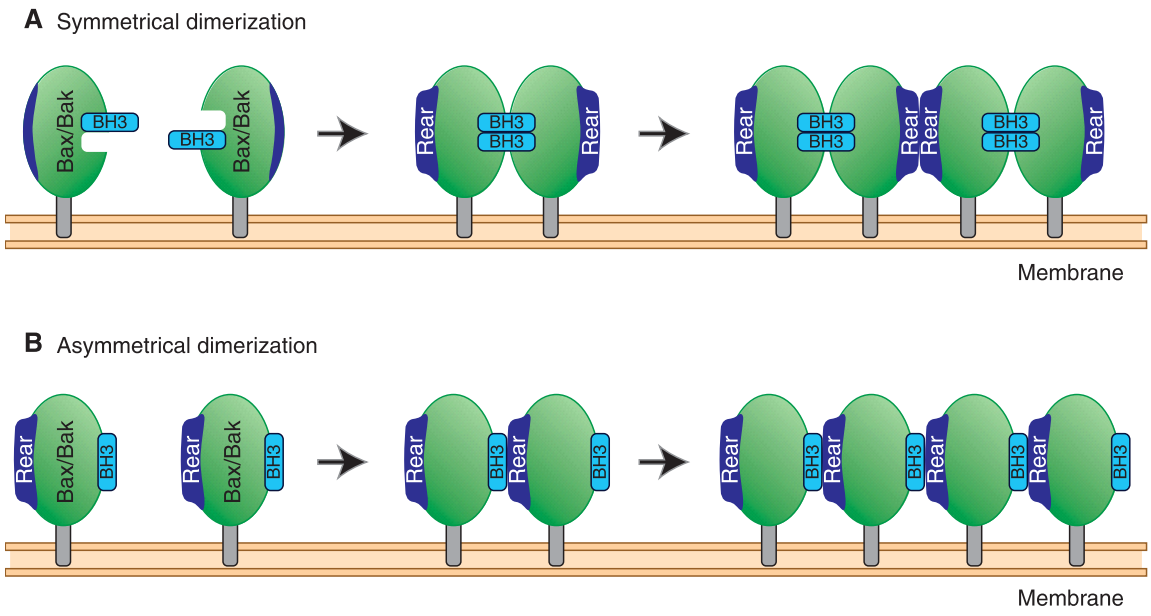

Figure 2.3 - Models of Bax and Bak dimer formation

A. Symmetrical dimers: Active Bax and Bak monomers with helices embedded within the MOM expose their BH3 regions which in turn bind to the 'front pocket' comprised of the hydrophobic BH1-3 groove of an adjacent monomer. This binding changes the conformation of the 'rear pocket' comprised of helices 1 and 6 allowing homodimers to form tetramers and further propagate oligomerization.

B. Asymmetrical dimers: Active Bax and Bak expose their BH3 regions which interact with the rear pocket on an adjacent monomer forming an oligomer through subsequent rear pocket:BH3 region interactions.

2.4. BH3 members

2.4.1. Evolution and structure of BH3 proteins

BH3 proteins interact with and regulate multi-region pro-apoptotic and anti-apoptotic Bcl-2 family members through the BH3 region, a shared homology region with other Bcl-2 family proteins. The specificity and affinity of the BH3 proteins for binding with their partners is determined by small differences in the amino acid sequence in the BH3 region (Table 1). Mutations in one or more of the key residues in the BH3 region of Bid and Bad can abolish binding with other Bcl-2 family proteins and impede their pro-apoptotic function (Wang et al. 1996; Zha et al. 1997).

The evolutionary relationship between multi-region Bcl-2 family members and BH3 proteins is distant, and BH3 proteins are thought to have originated after an expansion event during vertebrate evolution (Aouacheria et al. 2005). A subclass of BH3 proteins, Bnip proteins, has a different evolutionary history and likely originated independently. These Bnip proteins contain a less-well conserved BH3 region and may not require this to bind to other Bcl-2 family proteins (Chinnadurai et al. 2008).

NMR studies of Bim, Bad and Bmf, and *in silico* predictions for other BH3 proteins indicate that they are intrinsically unstructured proteins in the absence of binding partners, but undergo localized conformational changes in the BH3 region upon binding with anti-apoptotic proteins (Hinds et al. 2007). Bid is an exception to this observation, since it shares phylogenetic, structural and functional features with multi-region Bcl-2 family members (Billen et al. 2009). Bid was originally discovered through binding to both Bax and Bcl-2, and was classified as a pro-apoptotic 'BH3-only' protein since it contained only a BH3 region. However, Bid shares a high degree of similarity in the overall three-dimensional fold of the structure with other multi-region Bcl-2 family proteins (Chou et al. 1999; McDonnell et al. 1999). Furthermore, the presence of a newly identified BH4 region (Kvansakul et al. 2008), phylogenetic evidence and the mechanistic parallels between the activation of Bid and Bax suggest that Bid is more closely related to the multi-region family proteins than the BH3 proteins (Billen et al. 2009; Shamas-Din et al. 2010).

2.4.2. Structural plasticity and multiple members permits diversity in function

While there are five major anti-apoptotic and two main pro-apoptotic multi-region proteins, there are at least ten different BH3 proteins in the vertebrate genome (Aouacheria et al. 2005). The amplification of the BH3 protein subgroup allows the organism to induce apoptosis selectively by monitoring many different types of cell stress that may be restricted to certain subcellular sites, specific cell types or signalling pathways. Accordingly, there are many ways to turn on the different BH3 proteins, including transcriptional, translational, and post-translational mechanisms. Furthermore, the consequence of turning on specific BH3 proteins differs according to the binding specificity of the BH3 region for its "target" (Table 1). According to the

Direct Activation model, these quantitative differences in binding affinities lead to qualitative differences in function: only a restricted subclass (so far only tBid, Bim, and Puma) have high enough affinity for the multi-region pro-apoptotic proteins Bax and Bak to allow direct binding and activation as discussed in Section 2.3. These BH3 proteins are thus designated activators. By contrast, all other BH3 proteins have been proposed to act as "sensitizers" and displace activator BH3 proteins from binding to anti-apoptotic members. This frees the activator BH3 proteins to then bind to Bax/Bak. Sensitizer binding also prevents anti-apoptotic proteins binding activated Bax and Bak. Thus sensitizer BH3 proteins specifically bind to anti-apoptotic members, and do not bind to Bax/Bak directly. In subclassifying the BH3 proteins, the role of Puma remains somewhat controversial, as it has been shown to be either an activator (Cartron et al. 2004; Kim et al. 2006; Gallenne et al. 2009; Kim et al. 2009) or a sensitizer in different studies (Kuwana et al. 2005; Certo et al. 2006; Chipuk et al. 2008; Jabbour et al. 2009). This controversy may be caused by the fact that BH3 activators can also act as sensitizers via mutual sequestration of anti-apoptotic proteins (as discussed in section 2.2).

The inherent structural plasticity of most BH3 proteins also facilitates interactions with multiple binding partners including non-Bcl-2 proteins that govern their 'day jobs' (i.e. BH3 proteins in their non-activated state have roles independent of apoptosis). To further facilitate the 'day jobs', constitutively expressed BH3 proteins are located in parts of the cell distant from their apoptosis target membrane(s) where they participate in various non-apoptotic cellular processes (Table 2). Thus, to switch the function of BH3 proteins from the 'day jobs' to apoptosis, constitutively expressed proteins undergo post-translational modifications, such as phosphorylation, myristoylation, ubiquitination and proteolysis that restrict the proteins to one of the alternative functions (Kutuk and Letai 2008). In addition, the function of BH3 proteins such as Puma and Noxa are controlled at the transcriptional level, and are expressed only in the presence of death stimuli. Finally, the BH3 proteins can change their conformation at their target membrane(s) and upon binding to Bcl-2 family partner to change their function.

2.4.3. BH3 proteins binding to membranes as a critical step in regulating apoptosis

For the amplification of death signals, BH3 proteins translocate to MOM to activate Bax and Bak and promote MOMP. However, the exact mechanism by which different BH3 proteins migrate to, and insert into membranes varies. Mitochondrial-targeting and tail-anchor sequences are used to target several of the BH3 proteins to the MOM (Kuwana et al. 2002; Seo et al. 2003; Hekman et al. 2006; Lovell et al. 2008) (See Table 2). Moreover, the presence of specific lipids such as cardiolipin and cholesterol (Lutter et al. 2000; Hekman et al. 2006; Lucken-Ardjomande et al. 2008), and protein-receptors such as Mtch2 at the MOM have been shown to influence the targeting of other Bcl-2 family proteins to their target membranes (Zaltsman et al. 2010).

Once at the membrane, it is likely that BH3 proteins undergo extensive conformational changes that dictate their function. For example, after cleavage by activated caspase-8, initial association of cleaved Bid with the MOM causes separation of the two fragments, with subsequent insertion and structural rearrangement of the p15 fragment (tBid) that likely orients the BH3 region to bind to Bax or Bcl-XL. Furthermore, the other BH3 proteins that are intrinsically unstructured undergo localized conformational changes upon binding membranes and anti-apoptotic proteins.

Table 2.2 - Localization, targeting mechanism and non-apoptotic function of Bcl-2 family proteins

Bcl-2 protein	Targeting mechanism and location	Nonapoptotic function	References
Bax	Tail anchor Cystolic binds to MOM and ER membrane upon activation	Promotes mitochondria fusion in healthy cells and mitochondria fission in dying cells	Annis et al. 2005; Karbowski et al. 2006; Montessuit et al. 2010; Hoppins et al. 2011
Bak	Tail anchor Constitutively bound to MOM and ER membrane	Promotes mitochondria fusion in healthy cells, and mitochondria fission in dying cells	Griffiths et al. 1999; Karbowski et al. 2006; Brooks et al. 2007
Bid	Carboxy-terminal anchor? Helices 6 and 7 required for membrane binding Cytosolic and nuclear in healthy cells Localizes to MOM and ER upon cleavage by caspase-8 on the onset of apoptosis	Preserves genomic integrity and mediates intra-S-phase check point Interacts with and modulates NOD1 inflammatory response	Li et al. 1998; Luo et al. 1998; Hu et al. 2003; Kamer et al. 2005; Zinkel et al. 2005; Yeretssian et al. 2011
Bcl-2	Tail anchor Constitutively bound to MOM and/or ER membrane	Bcl-2 binds to the IP3 receptor at the ER, and inhibits the initiation phase of calcium-mediated apoptosis	Nguyen et al. 1993; Janiak et al. 1994; Hinds et al. 2003; Wilson-Annan et al. 2003; Chou et al. 2006; Dlugosz et al. 2006; Rong et al. 2009
Bcl-XL	Tail anchor Binds to MOM and ER membrane upon activation	Bcl-XL links apoptosis and metabolism via acetyl-CoA levels	Jeong et al. 2004; Brien et al. 2009; Yi et al. 2011
Mcl-1	Tail anchor Binds to MOM upon activation	Unknown Normally highly unstable protein	Zhong et al. 2005; Chou et al. 2006
Bcl-w	Noncanonical tail anchor Localization unknown	Unknown	Hinds et al. 2003; Wilson-Annan et al. 2003
A1/Bfl-1	Charged carboxyl terminus MOM (other membranes?) and perinuclear region	Unknown	Simmons et al. 2008
Bim	TOM complex-dependent carboxy-terminal hydrophobic segment—MOM	Associated with microtubules in healthy cells	O'Connor et al. 1998; Weber et al. 2007
Puma	Carboxy-terminal hydrophobic segment (?)—MOM	Unknown Transcriptionally regulated by p53	Nakano and Vousden 2001
Bad	Two lipid-binding domains at carboxyl terminus Cytosolic in healthy cells, mitochondrial in apoptotic cells	Regulation of glucose metabolism	Hekman et al. 2006; Danial 2008
Bik/Blk	Carboxy-terminal tail anchor Hydrophobic segment—ER	Unknown	Germain et al. 2002
Noxa	Targeting region at carboxyl terminus and via BH3 region mediated interactions with Mcl-1—MOM	Unknown	Oda et al. 2000; Ploner et al. 2008
Bmf	By binding to Bcl-2 family members? MOM during apoptosis	Binds myosin V motors by association with dynein light chain 2 in healthy cells Function unknown	Puthalakath et al. 2001
Hrk/DP5	Tail anchor MOM	Role in hearing loss in response to gentamycin suggests function in inner ear	Inohara et al. 1997; Kalinec et al. 2005
Beclin-1	Carboxy-terminal dependent? ER, MOM, *trans*-Golgi network	Regulates autophagy	Sinha and Levine 2008

?, inconclusive data.

Despite strong evidence for the functional interaction and activation of Bax and Bak by activator BH3 proteins, demonstration of binding of the full length protein (as opposed to peptides from the BH3 region) has only recently been reported: strong reversible binding of tBid to Bax was observed in liposomal MOM-like membranes (apparent K_d ~25 nM) (Lovell et al. 2008). Furthermore, when synthesized by *in vitro* translation, full-length BH3 proteins tBid, Bim and Puma induced Bax and Bak dependent MOMP and shifted monomeric Bax and Bak to higher-order complexes in mitochondria (Kim et al. 2006).

In vitro experiments clearly demonstrate that BH3 proteins recruit and sequester the anti-apoptotic Bcl-2 family proteins at the membrane. BH3 proteins bind the anti-apoptotic proteins by docking on the BH3 region in the hydrophobic groove made of BH1, BH2 and BH3 regions of the anti-apoptotic family proteins (Sattler et al. 1997; Liu et al. 2003; Czabotar et al. 2007). Similar to the differential binding to pro-apoptotic family members, experiments *in vitro* suggest that each BH3 protein selectively binds a defined range of anti-apoptotic proteins that is determined by differences in the structure and flexibility of the hydrophobic pocket of the anti-apoptotic proteins. Although to date, these interactions have been measured only with peptides from the different BH3 regions rather than the full-length proteins (See Table 1).

2.5. Anti-apoptotic members

2.5.1. Structure of family members alone and in complex with BH3 peptides

Early observations that specific mutations in Bcl-2 abrogated both anti-apoptotic function and binding to Bax, and the presence of BH3 regions in both classes of the pro-apoptotic Bcl-2 families that bind Bcl-2 as “ligands”, led to the concept of a receptor surface on Bcl-2. However, it was hard to confirm the details of this binding interaction using structural studies because of difficulties with purifying recombinant full-length Bcl-2. Initial success arose from NMR studies on Bcl-XL lacking its hydrophobic C-terminus (Muchmore et al. 1996), which similar to the structure obtained for Bax (Suzuki et al. 2000), was shown to contain two hydrophobic helices (5 and 6) forming a central hairpin structure surrounded by the remaining six amphipathic helices. Thereafter, co-crystals of “tail-less” Bcl-XL with BH3 peptides derived from Bak and Bim,

identified the BH3 binding surface as a hydrophobic cleft formed by non-contiguous residues in BH regions 1-3 (involving parts of helices 2, 7-8, and 4-6 respectively) (Sattler et al. 1997; Liu et al. 2003). These structural observations provided the platform for measurements of the many potential interactions between the binding pockets of different anti-apoptotic members and the BH3 regions of the pro-apoptotic family members. These differing binding affinities cluster into functional groupings (e.g. binding to multi-region vs. BH3 proteins, or activators vs. sensitizers) (Table 1) with functional consequences as elucidated below.

2.5.2. Multiple mechanisms of action of Bcl-XL: evidence of binding to both multi-region and BH3 members

Measurements of the affinity of binding between individual pairs of anti-apoptotic family members and BH3 peptides in solution provide valuable clues about functional relevance. However, in cells most of these interactions occur at or within intracellular membranes, and indeed the final commitment step in apoptosis being regulated is MOMP. Thus, experiments using recombinant full-length proteins or proteins synthesized *in vitro*, and isolated mitochondria or liposomes, have been critical in translating these interactions into testable models. For practical reasons such experiments are most feasible using recombinant Bcl-XL, as other anti-apoptotic proteins are much more difficult to purify in sufficient quantities due to problems with aggregation (e.g. Bcl-2) or marked protein instability (e.g. Mcl-1). Thus, details about the mechanism of action of Bcl-XL serve as a model for the other proteins, acknowledging that other members will differ in some aspects, as discussed below.

By examining membrane permeabilization in a system with recombinant Bcl-XL, Bax and tBid (both wild type and a mutant form that is unable to bind to Bcl-XL, but still activates Bax), it was shown that Bcl-XL inhibits MOMP not only directly by binding to tBid but also by binding to membrane-bound Bax (Billen et al. 2008). Thus, both of the major interactions postulated by the competing ‘direct activation’ and ‘displacement’ models contribute to inhibition of apoptosis. Furthermore, other mechanisms of action of Bcl-XL independent of these binding interactions were also identified including prevention of Bax insertion into membranes as perhaps the most potent mechanism. This initially contentious point has been recently supported by observations that Bax undergoes multiple conformational changes that ultimately

lead to oligomerization and MOMP, but the first of these steps is the exposure of the N-terminus at the membrane in a reversible equilibrium (Edlich et al. 2011). Bcl-XL changes this equilibrium such that Bax is shifted out of the conformation that binds it loosely to membranes. Moreover, consistent with the postulation that dynamic conformational changes are a feature of all three Bcl-2 families, these investigators observed that Bcl-XL also undergoes reversible conformational changes that allow it to come on and off the MOM without being inserted. The structural basis of this mechanism is unclear, although it is speculated that sequestering of the opposite partner's carboxy-terminal helix 9 in the BH3 binding groove may mediate this effect: in essence the helix 9 of the other protein acts as an (inactive) BH3 mimetic.

Taken together, these observations have identified multiple mechanisms that contribute to the ultimate function of Bcl-XL. Using defined amounts of proteins with an *in vitro* system allows measurement of the stoichiometry of inhibition and indicates that one Bcl-XL can inhibit ~ four Bax molecules. Therefore, as a conceptual overview, the functions of Bcl-XL can be most simply summarized as a dominant negative Bax, where it is able to undergo many of the binding interactions that Bax does, but does not make the final conformational change that allows it to bind to other Bcl-XL/Bax molecules and oligomerize to form a pore. In accordance with the postulated models of oligomerization discussed in Part II, this would imply that activated Bcl-XL cannot form a rear pocket in the analogous regions described for Bax/Bak.

2.5.3. Mediators of multiple mechanisms: membrane binding and conformational changes

Similar to Bax and Bak, there is evidence that the anti-apoptotic Bcl-2 family proteins adopt multiple conformations in associating with membranes. Bcl-2 initially inserts helix 9 in the membrane, but after binding to tBid or a BH3 peptide derived from Bim, helix 5 moves to a hydrophobic environment consistent with insertion in the membrane (Kim et al. 2004). Therefore it is plausible that Bcl-XL also adopts multiple conformations that are dictated by its interaction both with membranes and other Bcl-2 family members that shift the dynamic equilibrium between the different forms. Specifically, the data suggests that there is a form that is loosely bound to membranes (form 1), another in which helix 9 is inserted into membranes but not other helices (form 2) and finally a form in which helix 9 as well as helices 5 and 6 are inserted into

the membrane (form 3) (Figure 4). It is possible that these different conformations independently mediate the different mechanisms of action of Bcl-XL in inhibiting the final process of pore formation by activated Bax. Such a scheme is also compatible with observations that mutations that do not affect the BH3 binding pocket can still enhance anti-apoptotic function, either by forcing constitutive membrane insertion (into forms 2 or 3) by replacing the endogenous tail-anchor sequence (Fiebig et al. 2006), or by loosening intramolecular binding thereby "freeing" helices 5 and 6 to insert into membranes (form 3) (Asoh et al. 2000).

2.5.4. Comparison of different anti-apoptotic members

In simpler organisms such as *C. elegans* and Drosophila, there is only one inhibitory Bcl-2 family member while in vertebrates there are at least four. There are potentially multiple reasons for this redundancy: One that is firmly grounded on structural studies indicates that the different anti-apoptotic family members bind to (and sequester) the multiple BH3 members differentially, including the multi-domain pro-apoptotic members alluded to previously. Responding to multiple BH3 proteins allows fine-tuning of inhibitory responses in mammalian cells to different types of stress that "activate" specific BH3 proteins. Such a system provides multi-factorial responses much more diverse than those in simpler eukaryote cells. Characterization of the differences in binding has received much attention, and is conferred by the distinct sequence of each BH3 region that share a propensity to form an amphipathic helix containing four hydrophobic residues, and the topology of the BH3 binding groove on the anti-apoptotic "receptor". Peptides from certain BH3 regions like Bim, bind with high affinity to all the anti-apoptotic and apoptotic multi-region members, whereas others like Bad and Noxa are more selective (highly preferential binding to Bcl-2/Bcl-XL/Bcl-w, or Mcl-1/Bfl-1, respectively). Some of this specificity is explained by well-defined requirements e.g. any amino acid at the fourth hydrophobic position in the BH3 region will bind to Mcl-1 which has a shallow, open pocket for this residue, as opposed to Bcl-XL which does not accommodate charged or polar residues at this position (Lee et al. 2009; Fire et al. 2010). Other features also contribute: the higher global flexibility of Bcl-XL creates a pliable pocket for diverse BH3 mimetics compared to the deeper hydrophobic pocket with a rigid angle of entry in Mcl-1 that restricts binding to specific BH3 proteins (Lee et al. 2009).

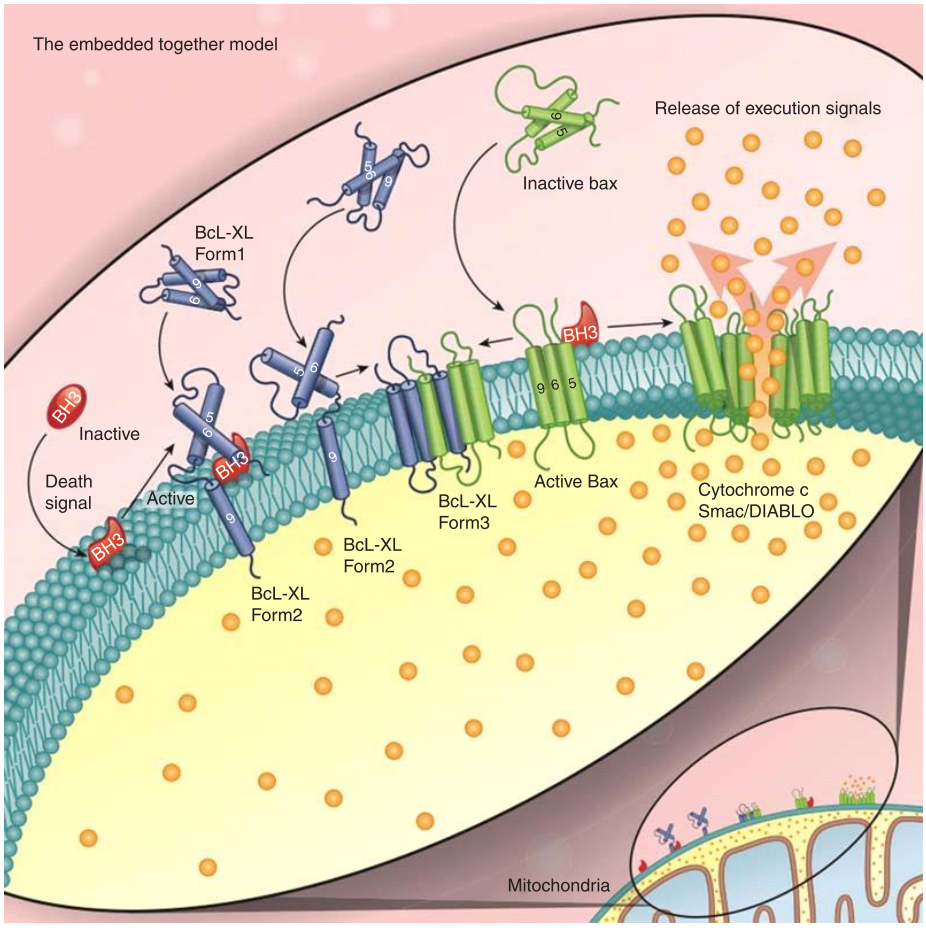

Figure 2.4 - Schematic overview of the Embedded Together Model

The role of the membrane is highlighted as the 'locus of action' where the effects of the interactions between the Bcl-2 family members are manifest. After the cell receives a death signal, an activator BH3 protein migrates to and inserts into the MOM, where it recruits cytoplasmic Bax. Bax undergoes conformational changes at membranes that allow it to respond to chemical changes in the cell such as the generation of reactive oxygen species, ion concentration and pH. Membrane-bound Bax or Bak change their conformation such that they oligomerize, leading to MOMP and/or recruit other cytoplasmic Bax. Both the activator and the sensitizer BH3 proteins sequester the anti-apoptotic proteins (such as Bcl-XL) by recruiting and strongly binding to them at MOM thereby preventing the inhibition of Bax and Bak. Bcl-XL changes its conformation depending on its binding partner: upon binding to a BH3 protein or Bax/Bak, Bcl-XL changes from form 1 (cytoplasmic or loosely attached to the MOM) to form 2 (helix 9 inserted in MOM) or to form 3 (helices 5, 6 and 9 bound to or inserted into MOM) respectively. It is likely that form 2 binds primarily BH3 proteins but also recruits additional Bcl-XL to the membrane while form 3 binds primarily Bax and Bak. No function has yet been ascribed to Bcl-XL form 1 although one is likely. Thus, by causing the proteins to adopt different conformations the membrane regulates their function in determining the fate of the cell. Unlike other models that propose uni-directional interactions, in this model all of the functional interactions are governed by dynamic equilibria of protein-membrane and protein-protein interactions.

As a consequence, no single anti-apoptotic member binds to all BH3 proteins *in vitro*, as assessed by biophysical measurements (See Table 1). These measurements have been largely (although not entirely) confirmed by experiments in transfected cell lines where over-expression of single anti-apoptotic proteins confers protection against apoptosis mediated by the BH3 binding partners identified *in vitro*. The discrepancy noted in a few experiments is likely due to the fact that in cells these interactions between full-length proteins occur on membranes rather than in the cytoplasm, and membrane binding may modify protein-protein interactions either allosterically or by post-translational modifications altering the binding surfaces (Feng et al. 2009) or affecting the orientation and proximity of the binding surfaces.

Multiple anti-apoptotic proteins also allow differential control of processes relevant to cell death independent of BH3 binding pocket interactions. The BH4 region of Bcl-2 binds to the regulatory and coupling domain of the inositol 1,4,5 triphosphate (IP3) receptor that controls calcium efflux from the ER, thereby inhibiting the initiation phase of calcium-mediated apoptosis (Rong et al. 2009). A residue critical for this binding interaction in Bcl-2 (Lys17) is not conserved in the BH4 domain of Bcl-XL (Asp11) rendering the latter ineffective at inhibiting IP3 mediated calcium release (Monaco et al. 2011).

Another reason for the diversity of anti-apoptotic proteins beyond specificity conferred by different binding partners is the control of sub-cellular localization. In particular cell types, there may be a benefit to having Bcl-2 family members constitutively present on membranes such as is the case with Bcl-2, as opposed to Bcl-XL, Mcl-1, Bfl-1 and Bcl-w all of which must undergo a conformational change before inserting into the membrane. In Bcl-2, it is presumed that the C-terminal region that is necessary and sufficient for membrane insertion (Janiak et al. 1994) is not bound to other hydrophobic regions of the protein once it is synthesized, and can therefore mediate direct membrane insertion. In the other anti-apoptotic proteins, the C-terminal tail is sequestered until the protein is activated. Even within this group, there are different strategies that control membrane localization. Unlike the other family members, Bfl-1 does not have a hydrophobic region at the C-terminus that mediates membrane insertion, but has an amphipathic helix (Brien et al. 2009). Bcl-XL is thought to exist as a homo-dimer in the cytoplasm, where the C-terminal tail is bound reciprocally to a hydrophobic groove in the dimer partner (Jeong et al. 2004). The longer C-terminal helix 8 of Bcl-w binds in its own BH3 binding

pocket, and can be displaced by BH3 peptides to allow membrane insertion (Hinds et al. 2003; Wilson-Annan et al. 2003) a mechanism reminiscent of Bax. Before apoptosis is elicited, Mcl-1 is constitutively loosely associated with mitochondria by an EELD motif in the amino-terminal portion, which can bind to the mitochondrial import receptor Tom70 (Chou et al. 2006). For all the anti-apoptotic proteins deletion of the C-terminal α helix decreases function, presumably by preventing assumption of forms 2 and 3 on the membrane where many of the relevant binding partners are localized. Furthermore, attachment of the inhibitor to the membrane increases the probability of interaction by increasing local concentration and the viscosity of the membranes restricting diffusion. A third justification for diversity of anti-apoptotic proteins is the benefit of varying regulation of protein abundance as a way of fine-tuning apoptosis. The *bcl-2* gene contains two estrogen response elements controlling expression in breast tissue. Bcl-2 is a long-lived protein whose expression does not change appreciably even during advanced stages of stress, partly due to presence of an internal ribosome entry site (IRES) in the 5' UTR that permits cap-independent translation (Willimott and Wagner 2010). The stability of the Bcl-2 transcript is positively regulated by the RNA binding protein nucleolin, and negatively regulated by the microRNAs mi-R15a and 16-1 (Willimott and Wagner 2010). Bcl-XL protein levels are more variable and increase acutely in response to internal stress and extracellular signals, mediated by the Jak-STAT and rel/NF-KB pathways (Grad et al. 2000). By contrast Mcl-1 is an extremely short-lived protein with rapid turnover tightly regulated by a complex cascade of phosphorylation-dependent de-ubiquitination by USPX9 (Schwickart et al. 2010) that reverses the ubiquitination and subsequent proteasomal degradation mediated by the BH3 protein E3 ubiquitin ligase MULE/ARF-BP1 (Zhong et al. 2005).

The consequences of these variations in the structure of binding pockets, control of subcellular localization and dynamic protein levels, is that despite sharing the core mechanism of inhibition, each anti-apoptotic protein has a distinct personality. This is evident in the specific profile of expression of the proteins in different cell types and organs in whole animals, with the result that each protein has different physiological roles that are apparent in the phenotypes of the knockout mice with different anti-apoptotic members.

2.6. Perspective and Future Prospects

This brief overview illustrates the enormous growth in our understanding of the mechanisms behind the pivotal role the Bcl-2 family plays in regulating apoptosis since the original identification of Bcl-2 as a chromosome translocation partner in human B-cell follicular lymphoma. We are now at stage where this understanding is yielding practical results, as several drugs mimicking BH3 regions that bind to Bcl-2 and Bcl-XL are in late stage clinical trials as cancer agents to elicit or enhance chemotherapy-induced apoptosis. The recognition that there are distinct binding profiles for each anti-apoptotic protein that arose from fundamental studies has now motivated the search for other small molecules to expand the therapeutic tool-kit (Stewart et al. 2010), so that in the future we will be able to target every anti-apoptotic protein.

To date, most attention has been paid to the role of the Bcl-2 family in regulating MOMP because of the well-characterized consequences of releasing IMS proteins in activating caspases. However, it is increasingly apparent that the ER is the site of many important processes that determine cell death and survival in which the Bcl-2 family is intimately involved. Aside from controlling calcium flux (Rong et al. 2009) and regulating the activity of Beclin-1 to initiate autophagy (see chapter 20 and 21), other death pathways are also inhibited by Bcl-2 at the ER (Germain et al. 2002). Beyond this, there is also evidence that a portion of the anti-apoptotic activity of Bcl-2/Bcl-XL does not depend on binding to and inhibiting the other two pro-apoptotic families (Minn et al. 1999). One recent suggestion suggests this mechanism involves regulation of cytoplasmic levels of acetyl-CoA as a substrate for protein-alpha acetylation (Yi et al. 2011). Elucidating potential binding partners that mediate this pathway is an important target of future research.

Our basic understanding of the core mechanism of the regulation of membrane permeabilization by Bcl-2 family members has passed from the stage of phenomenology to testable descriptions of mechanism. The next hurdle will be to extend quantitative measurements of the binding interactions that have been measured *in vitro* to what happens in organelles and in cells. This will allow further refinement and elaboration of exciting preliminary mathematical models of the control of apoptosis in whole cells (Spencer and Sorger 2011).

2.7. References

Annis MG, Soucie EL, Dlugosz PJ, Cruz-Aguado JA, Penn LZ, Leber B, Andrews DW. 2005. Bax forms multispanning monomers that oligomerize to permeabilize membranes during apoptosis. *The EMBO journal* **24**: 2096-2103.

Aouacheria A, Brunet F, Gouy M. 2005. Phylogenomics of life-or-death switches in multicellular animals: Bcl-2, BH3-Only, and BNip families of apoptotic regulators. *Molecular biology and evolution* **22**: 2395-2416.

Aranovich A, Liu Q, Collins T, Geng F, Dixit S, Leber B, Andrews DW. 2012. Differences in the mechanisms of proapoptotic BH3 proteins binding to Bcl-XL and Bcl-2 quantified in live MCF-7 cells. *Molecular cell* **45**: 754-763.

Asoh S, Ohtsu T, Ohta S. 2000. The super anti-apoptotic factor Bcl-xFNK constructed by disturbing intramolecular polar interactions in rat Bcl-xL. *The Journal of biological chemistry* **275**: 37240-37245.

Billen LP, Kokoski CL, Lovell JF, Leber B, Andrews DW. 2008. Bcl-XL Inhibits Membrane Permeabilization by Competing with Bax. *PLoS Biol* **6**: e147.

Billen LP, Shamas-Din A, Andrews DW. 2009. Bid: a Bax-like BH3 protein. *Oncogene* **27 Suppl 1**: S93-104.

Bleicken S, Classen M, Padmavathi PV, Ishikawa T, Zeth K, Steinhoff HJ, Bordignon E. 2010. Molecular details of Bax activation, oligomerization, and membrane insertion. *J Biol Chem* **285**: 6636-6647.

Brenner C, Grimm S. 2006. The permeability transition pore complex in cancer cell death. *Oncogene* **25**: 4744-4756.

Brien G, Debaud AL, Robert X, Oliver L, Trescol-Biemont MC, Cauquil N, Geneste O, Aghajari N, Vallette FM, Haser R et al. 2009. C-terminal residues regulate localization and function of the antiapoptotic protein Bfl-1. *The Journal of biological chemistry* **284**: 30257-30263.

Brock SE, Li C, Wattenberg BW. 2010. The Bax carboxy-terminal hydrophobic helix does not determine organelle-specific targeting but is essential for maintaining Bax in an inactive state and for stable mitochondrial membrane insertion. *Apoptosis* **15**: 14-27.

Brooks C, Wei Q, Feng L, Dong G, Tao Y, Mei L, Xie ZJ, Dong Z. 2007. Bak regulates mitochondrial morphology and pathology during apoptosis by interacting with mitofusins.

Proceedings of the National Academy of Sciences of the United States of America **104**: 11649-11654.

Cartron PF, Gallenne T, Bougras G, Gautier F, Manero F, Vusio P, Meflah K, Vallette FM, Juin P. 2004. The first alpha helix of Bax plays a necessary role in its ligand-induced activation by the BH3-only proteins Bid and PUMA. *Molecular cell* **16**: 807-818.

Certo M, Del Gaizo Moore V, Nishino M, Wei G, Korsmeyer S, Armstrong SA, Letai A. 2006. Mitochondria primed by death signals determine cellular addiction to antiapoptotic BCL-2 family members. *Cancer cell* **9**: 351-365.

Chen L, Willis SN, Wei A, Smith BJ, Fletcher JI, Hinds MG, Colman PM, Day CL, Adams JM, Huang DC. 2005. Differential targeting of prosurvival Bcl-2 proteins by their BH3-only ligands allows complementary apoptotic function. *Molecular cell* **17**: 393-403.

Chinnadurai G, Vijayalingam S, Gibson SB. 2008. BNIP3 subfamily BH3-only proteins: mitochondrial stress sensors in normal and pathological functions. *Oncogene* **27 Suppl 1**: S114-127.

Chipuk JE, Fisher JC, Dillon CP, Kriwacki RW, Kuwana T, Green DR. 2008. Mechanism of apoptosis induction by inhibition of the anti-apoptotic BCL-2 proteins. *Proceedings of the National Academy of Sciences of the United States of America* **105**: 20327-20332.

Chittenden T, Harrington EA, O'Connor R, Flemington C, Lutz RJ, Evan GI, Guild BC. 1995. Induction of apoptosis by the Bcl-2 homologue Bak. *Nature* **374**: 733-736.

Chou CH, Lee RS, Yang-Yen HF. 2006. An internal EELD domain facilitates mitochondrial targeting of Mcl-1 via a Tom70-dependent pathway. *Molecular biology of the cell* **17**: 3952-3963.

Chou JJ, Li H, Salvesen GS, Yuan J, Wagner G. 1999. Solution Structure of BID, an Intracellular Amplifier of Apoptotic Signaling. *Cell* **96**: 615-624.

Czabotar PE, Lee EF, van Delft MF, Day CL, Smith BJ, Huang DC, Fairlie WD, Hinds MG, Colman PM. 2007. Structural insights into the degradation of Mcl-1 induced by BH3 domains. *Proceedings of the National Academy of Sciences of the United States of America* **104**: 6217-6222.

Danial NN. 2008. BAD: undertaker by night, candyman by day. *Oncogene* **27 Suppl 1**: S53-70.

Dejean LM, Martinez-Caballero S, Guo L, Hughes C, Teijido O, Ducret T, Ichas F, Korsmeyer SJ, Antonsson B, Jonas EA et al. 2005. Oligomeric Bax is a component of the putative

cytochrome c release channel MAC, mitochondrial apoptosis-induced channel. *Mol Biol Cell* **16**: 2424-2432.

Dewson G, Kratina T, Czabotar P, Day CL, Adams JM, Kluck RM. 2009. Bak activation for apoptosis involves oligomerization of dimers via their alpha6 helices. *Molecular cell* **36**: 696-703.

Dewson G, Kratina T, Sim HW, Puthalakath H, Adams JM, Colman PM, Kluck RM. 2008. To trigger apoptosis, Bak exposes its BH3 domain and homodimerizes via BH3:groove interactions. *Molecular cell* **30**: 369-380.

Dlugosz PJ, Billen LP, Annis MG, Zhu W, Zhang Z, Lin J, Leber B, Andrews DW. 2006. Bcl-2 changes conformation to inhibit Bax oligomerization. *The EMBO journal* **25**: 2287-2296.

Dumitru R, Gama V, Fagan BM, Bower JJ, Swahari V, Pevny LH, Deshmukh M. 2012. Human embryonic stem cells have constitutively active Bax at the Golgi and are primed to undergo rapid apoptosis. *Molecular cell* **46**: 573-583.

Edlich F, Banerjee S, Suzuki M, Cleland MM, Arnoult D, Wang C, Neutzner A, Tjandra N, Youle RJ. 2011. Bcl-x(L) Retrotranslocates Bax from the Mitochondria into the Cytosol. *Cell* **145**: 104-116.

Farrow SN, White JH, Martinou I, Raven T, Pun KT, Grinham CJ, Martinou JC, Brown R. 1995. Cloning of a bcl-2 homologue by interaction with adenovirus E1B 19K. *Nature* **374**: 731-733.

Feng Y, Liu D, Shen X, Chen K, Jiang H. 2009. Structure assembly of Bcl-x(L) through alpha5-alpha5 and alpha6-alpha6 interhelix interactions in lipid membranes. *Biochimica et biophysica acta* **1788**: 2389-2395.

Fiebig AA, Zhu W, Hollerbach C, Leber B, Andrews DW. 2006. Bcl-XL is qualitatively different from and ten times more effective than Bcl-2 when expressed in a breast cancer cell line. *BMC cancer* **6**: 213.

Fire E, Gulla SV, Grant RA, Keating AE. 2010. Mcl-1-Bim complexes accommodate surprising point mutations via minor structural changes. *Protein Sci* **19**: 507-519.

Gallenne T, Gautier F, Oliver L, Hervouet E, Noel B, Hickman JA, Geneste O, Cartron PF, Vallette FM, Manon S et al. 2009. Bax activation by the BH3-only protein Puma promotes cell dependence on antiapoptotic Bcl-2 family members. *The Journal of cell biology* **185**: 279-290.

Garcia-Saez AJ, Ries J, Orzaez M, Perez-Paya E, Schwille P. 2009. Membrane promotes tBID interaction with BCL(XL). *Nature structural & molecular biology* **16**: 1178-1185.

Gavathiotis E, Reyna DE, Davis ML, Bird GH, Walensky LD. 2010. BH3-triggered structural reorganization drives the activation of proapoptotic BAX. *Mol Cell* **40**: 481-492.

Gavathiotis E, Suzuki M, Davis ML, Pitter K, Bird GH, Katz SG, Tu HC, Kim H, Cheng EH, Tjandra N et al. 2008. BAX activation is initiated at a novel interaction site. *Nature* **455**: 1076-1081.

George NM, Evans JJ, Luo X. 2007. A three-helix homo-oligomerization domain containing BH3 and BH1 is responsible for the apoptotic activity of Bax. *Genes & development* **21**: 1937-1948.

Germain M, Mathai JP, Shore GC. 2002. BH-3-only BIK functions at the endoplasmic reticulum to stimulate cytochrome c release from mitochondria. *J Biol Chem* **277**: 18053-18060.

Grad JM, Zeng XR, Boise LH. 2000. Regulation of Bcl-xL: a little bit of this and a little bit of STAT. *Curr Opin Oncol* **12**: 543-549.

Griffiths GJ, Dubrez L, Morgan CP, Jones NA, Whitehouse J, Corfe BM, Dive C, Hickman JA. 1999. Cell damage-induced conformational changes of the pro-apoptotic protein Bak in vivo precede the onset of apoptosis. *The Journal of cell biology* **144**: 903-914.

Hekman M, Albert S, Galmiche A, Rennefahrt UE, Fueller J, Fischer A, Puehringer D, Wiese S, Rapp UR. 2006. Reversible membrane interaction of BAD requires two C-terminal lipid binding domains in conjunction with 14-3-3 protein binding. *J Biol Chem* **281**: 17321-17336.

Hinds MG, Lackmann M, Skea GL, Harrison PJ, Huang DC, Day CL. 2003. The structure of Bcl-w reveals a role for the C-terminal residues in modulating biological activity. *The EMBO journal* **22**: 1497-1507.

Hinds MG, Smits C, Fredericks-Short R, Risk JM, Bailey M, Huang DC, Day CL. 2007. Bim, Bad and Bmf: intrinsically unstructured BH3-only proteins that undergo a localized conformational change upon binding to prosurvival Bcl-2 targets. *Cell death and differentiation* **14**: 128-136.

Hoppins S, Edlich F, Cleland MM, Banerjee S, McCaffery JM, Youle RJ, Nunnari J. 2011. The soluble form of Bax regulates mitochondrial fusion via MFN2 homotypic complexes. *Molecular cell* **41**: 150-160.

Hsu YT, Wolter KG, Youle RJ. 1997. Cytosol-to-membrane redistribution of Bax and Bcl-X(L) during apoptosis. *Proceedings of the National Academy of Sciences of the United States of America* **94**: 3668-3672.

Hsu YT, Youle RJ. 1997. Nonionic detergents induce dimerization among members of the Bcl-2 family. *J Biol Chem* **272**: 13829-13834.

Hu X, Han Z, Wyche JH, Hendrickson EA. 2003. Helix 6 of tBid is necessary but not sufficient for mitochondrial binding activity. *Apoptosis* **8**: 277-289.

Inohara N, Ding L, Chen S, Nunez G. 1997. harakiri, a novel regulator of cell death, encodes a protein that activates apoptosis and interacts selectively with survival-promoting proteins Bcl-2 and Bcl-X(L). *The EMBO journal* **16**: 1686-1694.

Jabbour AM, Heraud JE, Daunt CP, Kaufmann T, Sandow J, O'Reilly LA, Callus BA, Lopez A, Strasser A, Vaux DL et al. 2009. Puma indirectly activates Bax to cause apoptosis in the absence of Bid or Bim. *Cell death and differentiation* **16**: 555-563.

Janiak F, Leber B, Andrews DW. 1994. Assembly of Bcl-2 into Microsomal and Outer Mitochondrial Membranes. *J Biol Chem* **269**: 9842-9849.

Jeong SY, Gaume B, Lee YJ, Hsu YT, Ryu SW, Yoon SH, Youle RJ. 2004. Bcl-x(L) sequesters its C-terminal membrane anchor in soluble, cytosolic homodimers. *The EMBO journal* **23**: 2146-2155.

Kalinec GM, Fernandez-Zapico ME, Urrutia R, Esteban-Cruciani N, Chen S, Kalinec F. 2005. Pivotal role of Harakiri in the induction and prevention of gentamicin-induced hearing loss. *Proceedings of the National Academy of Sciences of the United States of America* **102**: 16019-16024.

Kamer I, Sarig R, Zaltsman Y, Niv H, Oberkovitz G, Regev L, Haimovich G, Lerenthal Y, Marcellus RC, Gross A. 2005. Proapoptotic BID is an ATM effector in the DNA-damage response. *Cell* **122**: 593-603.

Karbowski M, Norris KL, Cleland MM, Jeong SY, Youle RJ. 2006. Role of Bax and Bak in mitochondrial morphogenesis. *Nature* **443**: 658-662.

Kiefer MC, Brauer MJ, Powers VC, Wu JJ, Umansky SR, Tomei LD, Barr PJ. 1995. Modulation of apoptosis by the widely distributed Bcl-2 homologue Bak. *Nature* **374**: 736-739.

Kim H, Rafiuddin-Shah M, Tu HC, Jeffers JR, Zambetti GP, Hsieh JJ, Cheng EH. 2006. Hierarchical regulation of mitochondrion-dependent apoptosis by BCL-2 subfamilies. *Nature cell biology* **8**: 1348-1358.

Kim H, Tu HC, Ren D, Takeuchi O, Jeffers JR, Zambetti GP, Hsieh JJ, Cheng EH. 2009. Stepwise activation of BAX and BAK by tBID, BIM, and PUMA initiates mitochondrial apoptosis. *Molecular cell* **36**: 487-499.

Kim PK, Annis MG, Dlugosz PJ, Leber B, Andrews DW. 2004. During Apoptosis Bcl-2 Changes Membrane Topology at Both the Endoplasmic Reticulum and Mitochondria. *Molecular cell* **14**: 523-529.

Kutuk O, Letai A. 2008. Regulation of Bcl-2 Family Proteins by Posttranslational Modifications. *Current molecular medicine* **8**: 102-118.

Kuwana T, Bouchier-Hayes L, Chipuk JE, Bonzon C, Sullivan BA, Green DR, Newmeyer DD. 2005. BH3 domains of BH3-only proteins differentially regulate Bax-mediated mitochondrial membrane permeabilization both directly and indirectly. *Molecular cell* **17**: 525-535.

Kuwana T, Mackey MR, Perkins G, Ellisman MH, Latterich M, Schneiter R, Green DR, Newmeyer DD. 2002. Bid, Bax, and Lipids Cooperate to Form Supramolecular Openings in the Outer Mitochondrial Membrane. *Cell* **111**: 331-342.

Kuwana T, Newmeyer DD. 2003. Bcl-2-family proteins and the role of mitochondria in apoptosis. *Curr Opin Cell Biol* **15**: 691-699.

Kvansakul M, Yang H, Fairlie WD, Czabotar PE, Fischer SF, Perugini MA, Huang DC, Colman PM. 2008. Vaccinia virus anti-apoptotic F1L is a novel Bcl-2-like domain-swapped dimer that binds a highly selective subset of BH3-containing death ligands. *Cell death and differentiation* **15**: 1564-1571.

Landeta O, Landajuela A, Gil D, Taneva S, Diprimo C, Sot B, Valle M, Frolov V, Basanez G. 2011. Reconstitution of proapoptotic BAK function in liposomes reveals a dual role for mitochondrial lipids in the BAK-driven membrane permeabilization process. *J Biol Chem*.

Leber B, Lin J, Andrews DW. 2007. Embedded together: The life and death consequences of interaction of the Bcl-2 family with membranes. *Apoptosis* **12**: 897-911.

-. 2010. Still embedded together binding to membranes regulates Bcl-2 protein interactions. *Oncogene*.

Lee EF, Czabotar PE, Yang H, Sleebs BE, Lessene G, Colman PM, Smith BJ, Fairlie WD. 2009. Conformational changes in Bcl-2 pro-survival proteins determine their capacity to bind ligands. *J Biol Chem* **284**: 30508-30517.

Letai A, Bassik MC, Walensky LD, Sorcinelli MD, Weiler S, Korsmeyer SJ. 2002. Distinct BH3 domains either sensitize or activate mitochondrial apoptosis, serving as prototype cancer therapeutics. *Cancer cell* **2**: 183-192.

Li H, Zhu H, Xu CJ, Yuan J. 1998. Cleavage of BID by Caspase 8 Mediates the Mitochondrial Damage in the Fas Pathway of Apoptosis. *Cell* **94**: 491-501.

Liu X, Dai S, Zhu Y, Marrack P, Kappler JW. 2003. The structure of a Bcl-xL/Bim fragment complex: implications for Bim function. *Immunity* **19**: 341-352.

Llambi F, Moldoveanu T, Tait SW, Bouchier-Hayes L, Temirov J, McCormick LL, Dillon CP, Green DR. 2011. A unified model of mammalian BCL-2 protein family interactions at the mitochondria. *Molecular cell* **44**: 517-531.

Lovell JF, Billen LP, Bindner S, Shamas-Din A, Fradin C, Leber B, Andrews DW. 2008. Membrane binding by tBid initiates an ordered series of events culminating in membrane permeabilization by Bax. *Cell* **135**: 1074-1084.

Lucken-Ardjomande S, Montessuit S, Martinou JC. 2008. Bax activation and stress-induced apoptosis delayed by the accumulation of cholesterol in mitochondrial membranes. *Cell death and differentiation* **15**: 484-493.

Luo X, Budihardjo I, Zou H, Slaughter C, Wang X. 1998. Bid, a Bcl2 Interacting Protein, Mediates Cytochrome c Release from Mitochondria in Response to Activation of Cell Surface Death Receptors. *Cell* **94**: 481-490.

Lutter M, Fang M, Luo X, Nishijima M, Xie X, Wang X. 2000. Cardiolipin provides specificity for targeting of tBid to mitochondria. *Nature cell biology* **2**: 754-761.

McDonnell JM, Fushman D, Milliman CL, Korsmeyer SJ, Cowburn D. 1999. Solution Structure of the Proapoptotic Molecule BID: A Structural Basis for Apoptotic Agonists and Antagonists. *Cell* **96**: 625-634.

Minn AJ, Kettlun CS, Liang H, Kelekar A, Vander Heiden MG, Chang BS, Fesik SW, Fill M, Thompson CB. 1999. Bcl-xL regulates apoptosis by heterodimerization-dependent and -independent mechanisms. *The EMBO journal* **18**: 632-643.

Moldoveanu T, Liu Q, Tocilj A, Watson M, Shore G, Gehring K. 2006. The X-ray structure of a BAK homodimer reveals an inhibitory zinc binding site. *Molecular cell* **24**: 677-688.

Monaco G, Decrock E, Akl H, Ponsaerts R, Vervliet T, Luyten T, De Maeyer M, Missiaen L, Distelhorst CW, De Smedt H et al. 2011. Selective regulation of IP(3)-receptor-mediated Ca(2+) signaling and apoptosis by the BH4 domain of Bcl-2 versus Bcl-Xl. *Cell death and differentiation*.

Montessuit S, Somasekharan SP, Terrones O, Lucken-Ardjomande S, Herzig S, Schwarzenbacher R, Manstein DJ, Bossy-Wetzel E, Basanez G, Meda P et al. 2010. Membrane remodeling induced by the dynamin-related protein Drp1 stimulates Bax oligomerization. *Cell* **142**: 889-901.

Muchmore SW, Sattler M, Liang H, Meadows RP, Harlan JE, Yoon HS, Nettesheim D, Chang BS, Thompson CB, Wong SL et al. 1996. X-ray and NMR structure of human Bcl-xL, an inhibitor of programmed cell death. *Nature* **381**: 335-341.

Nakagawa T, Shimizu S, Watanabe T, Yamaguchi O, Otsu K, Yamagata H, Inohara H, Kubo T, Tsujimoto Y. 2005. Cyclophilin D-dependent mitochondrial permeability transition regulates some necrotic but not apoptotic cell death. *Nature* **434**: 652-658.

Nakano K, Vousden KH. 2001. PUMA, a novel proapoptotic gene, is induced by p53. *Molecular cell* **7**: 683-694.

Nechushtan A, Smith CL, Hsu YT, Youle RJ. 1999. Conformation of the Bax C-terminus regulates subcellular location and cell death. *The EMBO journal* **18**: 2330-2341.

Nguyen M, Millar DG, Yong VW, Korsmeyer SJ, Shore GC. 1993. Targeting of Bcl-2 to the mitochondrial outer membrane by a COOH-terminal signal anchor sequence. *The Journal of biological chemistry* **268**: 25265-25268.

O'Connor L, Strasser A, O'Reilly LA, Hausmann G, Adams JM, Cory S, Huang DC. 1998. Bim: a novel member of the Bcl-2 family that promotes apoptosis. *The EMBO journal* **17**: 384-395.

Oda E, Ohki R, Murasawa H, Nemoto J, Shibue T, Yamashita T, Tokino T, Taniguchi T, Tanaka N. 2000. Noxa, a BH3-only member of the Bcl-2 family and candidate mediator of p53-induced apoptosis. *Science (New York, NY* **288**: 1053-1058.

Oh KJ, Singh P, Lee K, Foss K, Lee S, Park M, Aluvila S, Kim RS, Symersky J, Walters DE. 2010. Conformational changes in BAK, a pore-forming proapoptotic Bcl-2 family member,

upon membrane insertion and direct evidence for the existence of BH3-BH3 contact interface in BAK homo-oligomers. *J Biol Chem* **285**: 28924-28937.

Oltvai ZN, Milliman CL, Korsmeyer SJ. 1993. Bcl-2 heterodimerizes in vivo with a conserved homolog, Bax, that accelerates programmed cell death. *Cell* **74**: 609-619.

Pavlov EV, Priault M, Pietkiewicz D, Cheng EH, Antonsson B, Manon S, Korsmeyer SJ, Mannella CA, Kinnally KW. 2001. A novel, high conductance channel of mitochondria linked to apoptosis in mammalian cells and Bax expression in yeast. *J Cell Biol* **155**: 725-731.

Peyerl FW, Dai S, Murphy GA, Crawford F, White J, Marrack P, Kappler JW. 2007. Elucidation of some Bax conformational changes through crystallization of an antibody-peptide complex. *Cell death and differentiation* **14**: 447-452.

Ploner C, Kofler R, Villunger A. 2008. Noxa: at the tip of the balance between life and death. *Oncogene* **27 Suppl 1**: S84-92.

Puthalakath H, Villunger A, O'Reilly LA, Beaumont JG, Coultas L, Cheney RE, Huang DC, Strasser A. 2001. Bmf: a proapoptotic BH3-only protein regulated by interaction with the myosin V actin motor complex, activated by anoikis. *Science (New York, NY* **293**: 1829-1832.

Qian S, Wang W, Yang L, Huang HW. 2008. Structure of transmembrane pore induced by Bax-derived peptide: evidence for lipidic pores. *Proceedings of the National Academy of Sciences of the United States of America* **105**: 17379-17383.

Rong YP, Bultynck G, Aromolaran AS, Zhong F, Parys JB, De Smedt H, Mignery GA, Roderick HL, Bootman MD, Distelhorst CW. 2009. The BH4 domain of Bcl-2 inhibits ER calcium release and apoptosis by binding the regulatory and coupling domain of the IP3 receptor. *Proceedings of the National Academy of Sciences of the United States of America* **106**: 14397-14402.

Sattler M, Liang H, Nettesheim D, Meadows RP, Harlan JE, Eberstadt M, Yoon HS, Shuker SB, Chang BS, Minn AJ et al. 1997. Structure of Bcl-xL-Bak peptide complex: recognition between regulators of apoptosis. *Science (New York, NY* **275**: 983-986.

Schafer B, Quispe J, Choudhary V, Chipuk JE, Ajero TG, Du H, Schneiter R, Kuwana T. 2009. Mitochondrial outer membrane proteins assist Bid in Bax-mediated lipidic pore formation. *Mol Biol Cell* **20**: 2276-2285.

Schwarz M, Andrade-Navarro MA, Gross A. 2007. Mitochondrial carriers and pores: key regulators of the mitochondrial apoptotic program? *Apoptosis* **12**: 869-876.

Schwickart M, Huang X, Lill JR, Liu J, Ferrando R, French DM, Maecker H, O'Rourke K, Bazan F, Eastham-Anderson J et al. 2010. Deubiquitinase USP9X stabilizes MCL1 and promotes tumour cell survival. *Nature* **463**: 103-107.

Seo YW, Shin JN, Ko KH, Cha JH, Park JY, Lee BR, Yun CW, Kim YM, Seol DW, Kim DW et al. 2003. The molecular mechanism of Noxa-induced mitochondrial dysfunction in p53-mediated cell death. *J Biol Chem* **278**: 48292-48299.

Setoguchi K, Otera H, Mihara K. 2006. Cytosolic factor- and TOM-independent import of C-tail-anchored mitochondrial outer membrane proteins. *The EMBO journal* **25**: 5635-5647.

Shamas-Din A, Brahmbhatt H, Leber B, Andrews DW. 2010. BH3-only proteins: Orchestrators of apoptosis. *Biochimica et biophysica acta*.

Shimizu S, Narita M, Tsujimoto Y. 1999. Bcl-2 family proteins regulate the release of apoptogenic cytochrome c by the mitochondrial channel VDAC. *Nature* **399**: 483-487.

Simmons MJ, Fan G, Zong WX, Degenhardt K, White E, Gelinas C. 2008. Bfl-1/A1 functions, similar to Mcl-1, as a selective tBid and Bak antagonist. *Oncogene* **27**: 1421-1428.

Sinha S, Levine B. 2008. The autophagy effector Beclin 1: a novel BH3-only protein. *Oncogene* **27 Suppl 1**: S137-148.

Spencer SL, Sorger PK. 2011. Measuring and modeling apoptosis in single cells. *Cell* **144**: 926-939.

Stewart ML, Fire E, Keating AE, Walensky LD. 2010. The MCL-1 BH3 helix is an exclusive MCL-1 inhibitor and apoptosis sensitizer. *Nature chemical biology* **6**: 595-601.

Suzuki M, Youle RJ, Tjandra N. 2000. Structure of Bax: Coregulation of Dimer Formation and Intracellular Localization. *Cell* **103**: 645-654.

Tsujimoto Y, Shimizu S. 2007. Role of the mitochondrial membrane permeability transition in cell death. *Apoptosis* **12**: 835-840.

Wang K, Yin XM, Chao DT, Milliman CL, Korsmeyer SJ. 1996. BID: a novel BH3 domain-only death agonist. *Genes & development* **10**: 2859-2869.

Weber A, Paschen SA, Heger K, Wilfling F, Frankenberg T, Bauerschmitt H, Seiffert BM, Kirschnek S, Wagner H, Hacker G. 2007. BimS-induced apoptosis requires mitochondrial

localization but not interaction with anti-apoptotic Bcl-2 proteins. *The Journal of cell biology* **177**: 625-636.

Wei MC, Zong WX, Cheng EH, Lindsten T, Panoutsakopoulou V, Ross AJ, Roth KA, MacGregor GR, Thompson CB, Korsmeyer SJ. 2001. Proapoptotic BAX and BAK: A Requisite Gateway to Mitochondrial Dysfunction and Death. *Science (New York, NY* **292**: 727-730.

Willimott S, Wagner SD. 2010. Post-transcriptional and post-translational regulation of Bcl2. *Biochemical Society transactions* **38**: 1571-1575.

Willis SN, Chen L, Dewson G, Wei A, Naik E, Fletcher JI, Adams JM, Huang DC. 2005. Proapoptotic Bak is sequestered by Mcl-1 and Bcl-xL, but not Bcl-2, until displaced by BH3-only proteins. *Genes & development* **19**: 1294-1305.

Wilson-Annan J, O'Reilly LA, Crawford SA, Hausmann G, Beaumont JG, Parma LP, Chen L, Lackmann M, Lithgow T, Hinds MG et al. 2003. Proapoptotic BH3-only proteins trigger membrane integration of prosurvival Bcl-w and neutralize its activity. *The Journal of cell biology* **162**: 877-887.

Wolter KG, Hsu YT, Smith CL, Nechushtan A, Xi XG, Youle RJ. 1997. Movement of Bax from the cytosol to mitochondria during apoptosis. *The Journal of cell biology* **139**: 1281-1292.

Yang L, Harroun TA, Weiss TM, Ding L, Huang HW. 2001. Barrel-stave model or toroidal model? A case study on melittin pores. *Biophys J* **81**: 1475-1485.

Yeretssian G, Correa RG, Doiron K, Fitzgerald P, Dillon CP, Green DR, Reed JC, Saleh M. 2011. Non-apoptotic role of BID in inflammation and innate immunity. *Nature* **474**: 96-99.

Yethon JA, Epand RF, Leber B, Epand RM, Andrews DW. 2003. Interaction with a Membrane Surface Triggers a Reversible Conformational Change in Bax Normally Associated with Induction of Apoptosis. *J Biol Chem* **278**: 48935-48941.

Yi CH, Pan H, Seebacher J, Jang IH, Hyberts SG, Heffron GJ, Vander Heiden MG, Yang R, Li F, Locasale JW et al. 2011. Metabolic Regulation of Protein N-Alpha-Acetylation by Bcl-xL Promotes Cell Survival. *Cell* **146**: 607-620.

Zaltsman Y, Shachnai L, Yivgi-Ohana N, Schwarz M, Maryanovich M, Houtkooper RH, Vaz FM, De Leonardis F, Fiermonte G, Palmieri F et al. 2010. MTCH2/MIMP is a major facilitator of tBID recruitment to mitochondria. *Nature cell biology*.

Zha J, Harada H, Osipov K, Jockel J, Waksman G, Korsmeyer SJ. 1997. BH3 domain of BAD is required for heterodimerization with BCL-XL and pro-apoptotic activity. *The Journal of biological chemistry* **272**: 24101-24104.

Zhang Z, Zhu W, Lapolla SM, Miao Y, Shao Y, Falcone M, Boreham D, McFarlane N, Ding J, Johnson AE et al. 2010. Bax forms an oligomer via separate, yet interdependent, surfaces. *J Biol Chem* **285**: 17614-17627.

Zhong Q, Gao W, Du F, Wang X. 2005. Mule/ARF-BP1, a BH3-only E3 ubiquitin ligase, catalyzes the polyubiquitination of Mcl-1 and regulates apoptosis. *Cell* **121**: 1085-1095.

Zinkel SS, Hurov KE, Ong C, Abtahi FM, Gross A, Korsmeyer SJ. 2005. A role for proapoptotic BID in the DNA-damage response. *Cell* **122**: 579-591.

3

Shedding light on apoptosis at subcellular membranes

3.1. Preface

This chapter has been previously published as a review in:

Kale, J., Liu, Q., Leber, B., and Andrews, D.W. (2012). Shedding light on apoptosis at subcellular membranes. Cell 151, 1179-1184.

The publisher has granted permission for the work to be reproduced here. The work presented has been edited for consistency and readability for this thesis. Specifically, paragraph 4 of the original publication was removed which pertained to Bcl-2 family member interactions already explained in previous chapters.

Author Contribution:

Kale, J wrote and prepared the entire review except for Figure 1C which was prepared by Liu, Q. Leber, B and Andrews, DW edited the manuscript and directed the layout of the book chapter.

Objective:

To provide a broad overview of how fluorescence techniques have enhanced our understanding of the regulation of apoptosis by the Bcl-2 family proteins. This chapter provides context as to why I used fluorescence techniques throughout the thesis.

Highlights:

- The Bcl-2 family proteins is a paradigm for complex protein-protein and protein-membrane systems
- The Bcl-2 family proteins requires the presence of membranes to function properly
    - This makes studying this protein system very difficult
- Fluorescence techniques have allowed researchers to elucidate the molecular mechanisms of the Bcl-2 family proteins *in vitro*, in live cells and *in vivo*

3.2. Apoptosis and membranes: the problem posed

Ironically the organelle that helps to provide cells with energy to live also serves as a platform to actively initiate cell death. Unlike forms of cell death triggered by mitochondrial dysfunction, during apoptosis the signals that regulate the fate of the cell are integrated at functioning mitochondria, and govern the irreversible step of mitochondrial outer membrane permeabilization (MOMP). Upon induction of apoptosis, the integrity of the mitochondrial outer membrane (MOM) is breached resulting in the release of cytochrome *c* and other intermembrane space proteins into the cytoplasm. The released proteins trigger the activation of multiple pathways that result in the demise of the cell. Thus a series of protein-protein and protein-membrane interactions control a process that is largely mechanical and that occurs in membranes.

The Bcl-2 family of proteins plays a major role in both sensing different types of cellular stress and regulating MOMP. To accomplish these tasks, different members of the Bcl-2 family are located in multiple parts of the cell and function as both cytoplasmic and membrane proteins by adopting distinct conformations that dictate their function (Figure 1A). Because of the distributed nature of this regulation and the involvement of complex membrane interactions this process deviates from the classical "lock-and-key" enzyme-substrate interactions fundamental to biochemistry and pharmacology. Moreover, even though apoptosis involves dramatic cell morphology changes, the techniques of observational molecular biology are not easily applicable to the analysis of apoptosis because it comprises a series of hierarchical stochastic events governed by complex reversible equilibria. Yet together, both approaches have led to tremendous insights (and blind alleys) in our quest to understand and therapeutically exploit apoptosis.

As Bcl-2 family proteins target to both the Endoplasmic Reticulum (ER) and the mitochondria, the cell fate decision is regulated by both complex binding equilibria between the proteins and the local concentration of active binding partners, which is very different at the two organelles (Figure 1A). Moreover, active Bax, a pro-apoptotic Bcl-2 family member, has also been found sequestered at the Golgi in embryonic stem cells providing a large pool of death effectors primed to cause MOMP upon the first indication of DNA damage. Therefore Golgi are another membrane system at which the Bcl-2 family proteins can interact, contributing further to

the complexity of regulating apoptosis (Dumitru et al., 2012). Thus, for the Bcl-2 family, the crucial role played by membranes makes the traditional approach of examining the underpinnings of particular cellular phenotypes with “grind and find” biochemistry problematic. To bridge this gap, several in vitro model systems of varying complexity have been exploited, and in this brief review we will highlight some of the insights gained by this approach with a focus on studies in which fluorescence techniques are being used to integrate observations from purified proteins with those from live cells and even animals. The ongoing theme is that molecular characterization of phenotypes observed at a cellular, tissue or organism level requires rigorous analysis with increasingly sophisticated model systems.

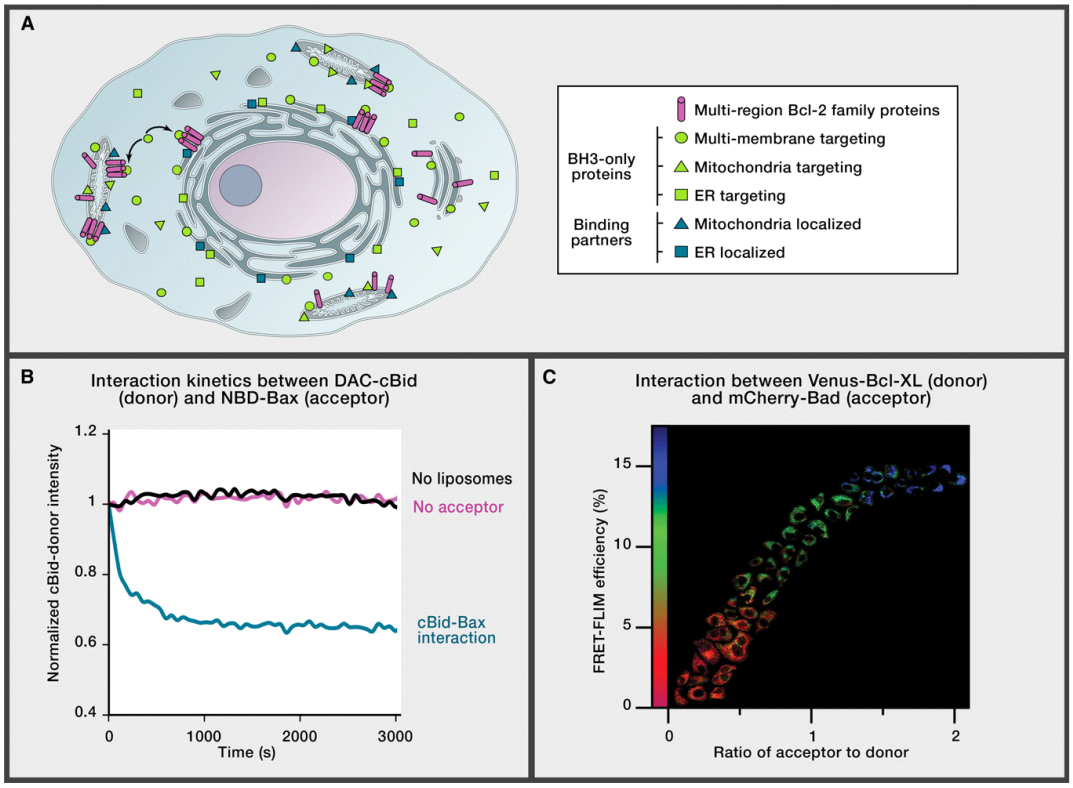

Figure 3.1 - The Bcl-2 family of proteins modulate apoptosis through a series of intricate protein-protein and protein-membrane interactions that exist in equilibrium

Fluorescence based assays uniquely permit quantitative analyses in *real-time* of interaction mechanisms that govern the biology of complex systems at membranes. A) Bcl-2 family proteins are located at multiple membranes within the cell and undergo a series of complex interactions that regulate apoptosis. Multi-region Bcl-2 family proteins (red cylinders) are found at ER and mitochondrial membranes with a small subset also at Golgi. BH3-only proteins (yellow) are found in many areas of the cell and are recruited to single (squares, ER; triangles, mitochondria) or multiple subcellular membranes (circles). The specific sets of binding partners are different at each subcellular membrane (blue squares, ER; blue triangles, mitochondria). The balance of interactions between all of these proteins governs the fate of the cell. B) Attaching fluorescent dyes to cBid (DAC; donor) and Bax (NBD; acceptor) and measuring FRET via a decrease in donor fluorescence in *real-time* reveals that a cBid-Bax interaction requires the presence of a membrane. Such measurements allow both affinities and the kinetics of the interaction to be quantified. C) Fluorescence techniques can be used to extend in vitro results to live cells by expressing Bcl-2 family proteins The observed FRET FLIM efficiency increases (according to the color scale) as the acceptor:donor ratio increases until the donors are saturated by bound acceptors generating a binding curve permitting the determination of binding constants.

3.3. In vitro models elucidate the core mechanisms

While studies using immunoprecipitation of whole cell lysates identified some of the potential interactions between Bcl-2 family proteins this method has limitations as non-ionic detergents such as Triton cause heterodimerization between Bax and Bcl-2 that does not occur constitutively in situ; conversely CHAPS dramatically decreases Bax binding to Bid. To circumvent these problems one can study interactions between purified proteins. However, many of these proteins have hydrophobic C-terminal tails which considerably complicates purification of full length and functional proteins, and in the case of some proteins which are constitutively localized to intracellular membranes (e.g. Bcl-2 and Bak), or are difficult to purify for various reasons (e.g. Mcl-1), this has not yet been accomplished. An approach to avoid problems encountered in purification was to use peptides and/or truncated versions of Bcl-2 family proteins lacking the C-terminal tail permitting the use of structural studies including NMR and crystallography. All of these approaches generated data indicating that Bcl-2 family proteins function as ligand-receptor pairs relying on the BH3 region of one protein binding to a hydrophobic groove termed the BH3 pocket, on the other member. Beyond this consensus, the limitations of the approaches resulted in both controversy and confusion in the field.

Many of these problems have been bypassed in an elegant series of studies (Kim et al., 2006; Kim et al., 2009) using a detergent-free system with full length proteins synthesized by in vitro translation that confirmed the hierarchical nature and presumed order of interactions as indicated above: these experiments also confirmed Bid, Bim and PUMA (the latter previously contentious) as activators of Bax or Bak, and demonstrated that anti-apoptotic proteins bound to all three activators, but differentially to sensitizer BH3-only proteins. For example, the sensitizer Bad displaced activator BH3-only proteins from Bcl-2 and Bcl-XL but not Mcl-1, whereas the sensitizer Noxa was effective against Mcl-1 but not Bcl-2/Bcl-XL.

However, it is not possible to study the kinetics of, or to measure the affinity of binding with such an approach. Therefore, we developed an in vitro system using liposomes of defined composition and included fluorescently labelled versions of the relevant recombinant full-length proteins. This system possesses several unique advantages. First, by using Förster Resonance Energy Transfer (FRET), the binding of the proteins to each other and to membranes could be

measured quantitatively at physiologic concentrations in an environment with liposomes that mimic the composition of the mitochondrial membrane (Figure 1B). Furthermore, by using combinations of fluorophores whose excitation/emission spectra allowed simultaneous analyses, the interactions could be ordered in *real-time*. Finally using fluorescent dyes for which the emission is sensitive to the presence of water allowed the insertion of these proteins into the hydrophobic environment of the membrane to be monitored (Lovell et al., 2008). The data indicated that the permeabilization of MOM by tBid activated Bax proceeds in a discrete series of steps: caspase mediated cleavage of the BH3-only protein Bid resulted in the cleaved protein cBid, containing a p7 and p15 fragment, binding rapidly to membranes. This binding causes the amino terminal p7 fragment to dissociate from the membrane bound form of the p15 fragment, tBid. Membrane bound tBid, which contains the BH3 region, then binds to Bax causing it to insert into the membrane. Studies of the binding between mutant proteins suggest that the basis of binding on the membrane likely involves structural changes in tBid and of the N-terminal helix of Bax that is required to stabilize the C-terminal transmembrane helix in the BH3 pocket, effectively masking this binding surface on Bax located in solution (Kim et al., 2009). After binding by tBid, this interaction in Bax is diminished allowing the transmembrane helix to disengage from the pocket and target Bax to membranes. Bax then oligomerizes in the MOM, permeabilizing it and releasing apoptogenic factors from the intermembrane space (e.g. cytochrome *c*, SMAC).

Using fluorescence to measure the rates of these individual interactions revealed that the insertion of Bax into the membrane was the rate-limiting step for MOMP (Lovell et al., 2008). The anti-apoptotic proteins interfere with this process at several steps. Similar to Bax, Bcl-XL is recruited to the membrane by tBid, and by binding to it at this location, Bcl-XL prevents tBid from interacting with Bax (Billen et al., 2008). However, Bad binding to Bcl-XL frees tBid to activate Bax (Lovell et al., 2008). This exchange of binding partners is governed by the affinities and therefore the relative abundance of the membrane-bound proteins, both factors that are hard to measure in cells. That the interacting partners are exchangeable and in equilibrium is the mechanistic basis for Bad functioning as a sensitizer.

Bcl-XL interacts with Bax in multiple ways. It binds directly to membrane inserted, activated Bax thereby preventing propagation of the oligomers required for MOMP. Perhaps

more importantly, Bcl-XL also causes the retro-translocation of Bax from the MOM to the cytoplasm before Bax attains the membrane inserted conformation competent for oligomerization (Edlich et al., 2011). In this way, Bcl-XL intercedes very early in the multi-step Bax activation sequence to shuttle peripherally bound Bax from the MOM to the cytoplasm, preventing incidental Bax activation in healthy cells due to Bax proximity to the membrane.

The above model of how the Bcl-2 family regulates MOMP is based on observations from a variety of cell free systems made by many laboratories. Collectively the results emphasize the importance of protein-protein and protein-membrane interactions. Binding to membranes shifts the equilibria between the conformations of Bcl-2 proteins, therefore the function of the proteins is markedly different in the cytoplasm and within the membrane. To reflect these observations the model has been named embedded together (Leber et al., 2010).

3.4. The next step: regulation of the core mechanism in cells

Because of the paramount importance of dysregulated apoptosis in many disease processes (too little in cancer, too much in neurodegenerative diseases and ischemia), understanding the core mechanism is critical for drug development. The Bcl-2 family is considered to be an excellent target for eliciting or enhancing an anti-cancer response because of a large body of cell based evidence indicating that cancer cells are "addicted'" to the presence of anti-apoptotic proteins (i.e. they are required for ongoing cellular survival; (Chonghaile and Letai, 2008). Based on structural studies, initial small molecule screens focussed on disrupting the interaction between peptides corresponding to BH3 regions and truncated versions of Bcl-2 family proteins. Because such assays only partially mimic the in vivo environment of these proteins, it is not surprising that few of the first generation of compounds actually hit their target in cells. In an elegant series of experiments testing these compounds using cell lines with both Bax and Bak knocked out as controls for cell death via non-apoptotic mechanisms, only ABT-737 (a peptidomimetic based on the Bad BH3 region) killed cells primarily by inducing apoptosis (Vogler et al., 2009). An orally available form of this drug (ABT-263, Navitoclax; (Tse et al., 2008) has rapidly moved into clinical trials for cancer, and consistent with the differential binding properties of Bad to anti-apoptotic proteins observed in vitro, the presence Mcl-1 in the tumour mediates resistance to the drug.

Recent sophisticated murine models of lymphoma addicted to specific anti-apoptotic Bcl-2 family members have suggested an additional Achilles' heel: ABT-737 was not able to kill tumours dependent on Bcl-XL inhibiting the BH3-only activator Bim (Merino et al., 2012). Current animal studies shed no light on molecular mechanisms and this feature of ABT-737 could not have been predicted from previous structural studies with peptides and protein fragments. However, the finding was independently predicted in a cellular model system using Fluorescence Lifetime Imaging Microscopy (FLIM) with fluorescent proteins functioning as FRET pairs fused to different Bcl-2 family members (Aranovich et al., 2012). By measuring the lifetime decrease of FRET donor Venus, in cells stably expressing Venus-Bcl-XL and expressing different (but measurable) amounts of mCherry acceptor (mCherry-Bad, -tBid, or -Bim), it was possible to generate a binding curve and thereby link biochemical observations with molecular mechanisms for proteins in live cells (Figure 1C). Relative Kd values can then be calculated in the presence or absence of a drug to test the effects of exogenous agents on the interaction. Using this approach it was shown that ABT-737 did not displace Bim from Bcl-XL but was effective at disrupting interactions with tBid and Bad. As an explanation for this difference, it was noted that mutations in the BH3 regions that disrupted the binding of tBid or Bad to Bcl-XL (and to Bcl-2), did not affect Bim binding to Bcl-XL. These results strongly suggest that in its physiologic membrane environment, Bim binds to Bcl-XL by a novel mechanism using other regions besides the traditional BH3 region, which confers its resistance to ABT-737 and ABT-263 (Aranovich et al., 2012; Liu et al., 2012). Moreover, this approach provides a means for identifying the residues required for protein-protein interactions in live cells, indicating that FRET based FLIM can effectively link studies using purified proteins and analyses in live cells to reveal novel insights in biochemistry and pharmacology.

Small molecules and fluorescence have been used to link cell free observations with the activity of proteins in cells. One example comes from studies of the novel binding site for a stapled Bim BH3 alpha helical peptide on purified Bax. The binding site identified, located opposite of the canonical BH3 pocket, is referred to as the rear pocket (Gavathiotis et al., 2008). Using a competitive fluorescence polarization assay and a library of small molecules predicted to dock to the rear pocket of Bax, a Bax-specific activator was identified that does not show appreciable affinity for the anti-apoptotic proteins or Bak. This activator can only cause

apoptosis in Bax containing cells illustrating how in vitro studies can be used to identify a specific protein mechanism(s), and thereby lead to the development of small molecules that can manipulate the core mechanism in live cells (Gavathiotis et al., 2012).

3.5. Cell death and survival beyond the core mechanism of MOMP

Beyond the canonical pathways of BH3-only proteins sensing different types of cell stress and then activating Bax/Bak at the MOM, other cellular processes regulated by the Bcl-2 family also prime the cell for death. Much attention has been paid to the ER as a source of these pathways (reviewed in (Heath-Engel et al., 2008).

The ER is the platform on which Bcl-2 regulates autophagy by interacting with Beclin 1, an autophagy promoter (Pattingre et al., 2005). The development of fluorescent protein fusions for the autophagy regulatory protein LC3 greatly facilitated the examination of autophagy at the molecular level in live cells, suggesting that this process is amenable to the precise ordering of regulatory events at membranes by using fluorescence techniques similar to the studies investigating MOMP described above. An obvious goal of these studies would be to reveal the molecular mechanisms that switch autophagy from a cell survival to a cell death process.

Calcium is one of the important mediators of intracellular signals, emanating from the ER that is modulated by the Bcl-2 family (He et al., 1997). Sudden changes in calcium concentrations within the cell can trigger apoptosis but it is unknown whether cell death is triggered via a sudden decrease or increase calcium levels within the ER or mitochondria respectively. Additionally, the calcium uniporter on the MOM has a low affinity for calcium, and it was unclear how it could respond to calcium leakage from the ER during signalling or stress, as the measured global increase in cytoplasmic calcium was not enough to allow calcium import into the mitochondria. Recently an important facet of this intra-organellar communication has been elucidated in live cells via fluorescence imaging measurements. Using a complex system with multiple fluorophores that allowed simultaneous measurements of the size of the ER-mitochondrial contacts and the local concentration of calcium at these points, experiments were conducted in cells that unequivocally demonstrated the existence of microdomains between these organelles (Csordas et al., 2010). Furthermore the high local concentration of calcium caused by

stimulation of IP3 receptors, which can be regulated by Bcl-2 at the ER, was enough to allow import of calcium into the mitochondrion. The stage is now set to precisely measure these changes, determine the magnitude of the response required to elicit mitochondrial dysfunction and cell death, and resolve how the Bcl-2 family can regulate this process.

Aside from interactions at different organelles, other mechanisms that modulate the core protein-protein interactions governing MOMP include post-translational modifications of the component proteins (reviewed in (Kutuk and Letai, 2008). Under normal cellular conditions Bim is located on microtubules. However, upon induction of apoptosis Bim is phosphorylated by JNK1 releasing it from microtubules whereupon it targets to the MOM and activates Bax and Bak leading to MOMP and apoptosis. Interestingly, phosphorylation of other Bcl-2 family members results in inhibition of apoptosis. Phosphorylation of Bad by AKT promotes Bad interaction with 14-3-3 proteins preventing the induction of apoptosis. AKT can also phosphorylate Bax resulting in its inhibition via an unknown mechanism. Although, functionally important post-translational modifications are generally identified using cells or tissues, determining how they affect the core molecular mechanisms of protein function requires the use of sophisticated cell free systems. Deciphering the molecular mechanism is particularly important for proteins like Bax that are potential therapeutic targets.

3.6. Future challenges: regulation of apoptosis in animals

With the emergence of new therapeutic agents that inhibit Bcl-2 protein interactions with the aim of regulating apoptosis in tumour development and resistance to chemotherapy, whole animal models would be an invaluable aid in determining the most rational way to combine these drugs with conventional cancer treatments. Because of the historic role of human B cell lymphoma in the discovery and identification of Bcl-2 as the first mammalian apoptotic regulator, it is perhaps fitting that the Bad BH3-mimetic drug Navitoclax may find its first use in this type of cancer. The murine lymphoma model alluded to previously (Merino et al., 2012) suggests its promise in this context. In the clinic, these cancers are traditionally treated with a complex schedule of multiple chemotherapy agents. Surprisingly, a recent analysis of the mechanism of action of two important drugs in the regime indicated that the simultaneous administration schedule used for the last 30 years actually leads to mutual antagonism of the Bcl-

2 dependent cytotoxic effect! (Ehrhardt et al., 2011). Using luminescence or fluorescence imaging of whole tumours in mice allows potential read-outs of "final" effects of anti-tumour treatment combinations. Although still not generally used, recent developments indicate that we may be able to be more precise and analytical with this approach. FRET probes have been developed with a caspase-3 cleavage site to monitor the activity of the final protease effector of apoptosis. This probe permits *real-time* monitoring of apoptosis in animals following anti-tumour therapy (Zhou et al., 2010). These studies report distinct time courses of apoptosis after different single agent anti-cancer treatments, underlining the importance of investigating these effects in the most natural context available. Therefore adding an inhibitor of Bcl-2 at an arbitrary time to this schedule may not be the most rational way to use this compound to modulate apoptosis. Monitoring apoptosis in animals using this technique is not without its limitations and is currently restricted to studying cancer cell lines and tumours at subcutaneous sites amenable to fluorescence measurements. Regardless, one can imagine extending this technique to look at protein-protein interactions between the Bcl-2 family of proteins within live animals in multiple tissues with and without chemotherapy treatment. Using FRET may permit observing not only binding between the proteins but provide binding dynamics as well. With the appropriate B cell lymphoma model such an approach would identify the best time to switch off Bcl-2 to maximize the pro-apoptotic effects of the other chemotherapy drugs.

Thus at all relevant levels of analysis in apoptosis research, from protein-protein interactions using increasingly sophisticated in vitro systems to investigation of whole animal models the application of novel fluorescence techniques suggests that the future is bright!

3.7. References

Aranovich, A., Liu, Q., Collins, T., Geng, F., Dixit, S., Leber, B., and Andrews, D.W. (2012). Differences in the mechanisms of proapoptotic BH3 proteins binding to Bcl-XL and Bcl-2 quantified in live MCF-7 cells. Molecular cell *45*, 754-763.

Billen, L.P., Kokoski, C.L., Lovell, J.F., Leber, B., and Andrews, D.W. (2008). Bcl-XL inhibits membrane permeabilization by competing with Bax. PLoS biology *6*, e147.

Chonghaile, T.N., and Letai, A. (2008). Mimicking the BH3 domain to kill cancer cells. Oncogene *27 Suppl 1*, S149-157.

Csordas, G., Varnai, P., Golenar, T., Roy, S., Purkins, G., Schneider, T.G., Balla, T., and Hajnoczky, G. (2010). Imaging interorganelle contacts and local calcium dynamics at the ER-mitochondrial interface. Molecular cell *39*, 121-132.

Dumitru, R., Gama, V., Fagan, B.M., Bower, J.J., Swahari, V., Pevny, L.H., and Deshmukh, M. (2012). Human embryonic stem cells have constitutively active Bax at the Golgi and are primed to undergo rapid apoptosis. Molecular cell *46*, 573-583.

Edlich, F., Banerjee, S., Suzuki, M., Cleland, M.M., Arnoult, D., Wang, C., Neutzner, A., Tjandra, N., and Youle, R.J. (2011). Bcl-x(L) retrotranslocates Bax from the mitochondria into the cytosol. Cell *145*, 104-116.

Ehrhardt, H., Schrembs, D., Moritz, C., Wachter, F., Haldar, S., Graubner, U., Nathrath, M., and Jeremias, I. (2011). Optimized anti-tumor effects of anthracyclines plus Vinca alkaloids using a novel, mechanism-based application schedule. Blood *118*, 6123-6131.

Gavathiotis, E., Reyna, D.E., Bellairs, J.A., Leshchiner, E.S., and Walensky, L.D. (2012). Direct and selective small-molecule activation of proapoptotic BAX. Nature chemical biology *8*, 639-645.

Gavathiotis, E., Suzuki, M., Davis, M.L., Pitter, K., Bird, G.H., Katz, S.G., Tu, H.C., Kim, H., Cheng, E.H., Tjandra, N., *et al.* (2008). BAX activation is initiated at a novel interaction site. Nature *455*, 1076-1081.

He, H., Lam, M., McCormick, T.S., and Distelhorst, C.W. (1997). Maintenance of calcium homeostasis in the endoplasmic reticulum by Bcl-2. The Journal of cell biology *138*, 1219-1228.

Heath-Engel, H.M., Chang, N.C., and Shore, G.C. (2008). The endoplasmic reticulum in apoptosis and autophagy: role of the BCL-2 protein family. Oncogene *27*, 6419-6433.

Kim, H., Rafiuddin-Shah, M., Tu, H.C., Jeffers, J.R., Zambetti, G.P., Hsieh, J.J., and Cheng, E.H. (2006). Hierarchical regulation of mitochondrion-dependent apoptosis by BCL-2 subfamilies. Nature cell biology *8*, 1348-1358.

Kim, H., Tu, H.C., Ren, D., Takeuchi, O., Jeffers, J.R., Zambetti, G.P., Hsieh, J.J., and Cheng, E.H. (2009). Stepwise activation of BAX and BAK by tBID, BIM, and PUMA initiates mitochondrial apoptosis. Molecular cell *36*, 487-499.

Kutuk, O., and Letai, A. (2008). Regulation of Bcl-2 family proteins by posttranslational modifications. Current molecular medicine *8*, 102-118.

Leber, B., Lin, J., and Andrews, D.W. (2010). Still embedded together binding to membranes regulates Bcl-2 protein interactions. Oncogene *29*, 5221-5230.

Liu, Q., Leber, B., and Andrews, D.W. (2012). Interactions of pro-apoptotic BH3 proteins with anti-apoptotic Bcl-2 family proteins measured in live MCF-7 cells using FLIM FRET. Cell Cycle *11*.

Lovell, J.F., Billen, L.P., Bindner, S., Shamas-Din, A., Fradin, C., Leber, B., and Andrews, D.W. (2008). Membrane binding by tBid initiates an ordered series of events culminating in membrane permeabilization by Bax. Cell *135*, 1074-1084.

Merino, D., Khaw, S.L., Glaser, S.P., Anderson, D.J., Belmont, L.D., Wong, C., Yue, P., Robati, M., Phipson, B., Fairlie, W.D., *et al.* (2012). Bcl-2, Bcl-x(L), and Bcl-w are not equivalent targets of ABT-737 and navitoclax (ABT-263) in lymphoid and leukemic cells. Blood *119*, 5807-5816.

Pattingre, S., Tassa, A., Qu, X., Garuti, R., Liang, X.H., Mizushima, N., Packer, M., Schneider, M.D., and Levine, B. (2005). Bcl-2 antiapoptotic proteins inhibit Beclin 1-dependent autophagy. Cell *122*, 927-939.

Tse, C., Shoemaker, A.R., Adickes, J., Anderson, M.G., Chen, J., Jin, S., Johnson, E.F., Marsh, K.C., Mitten, M.J., Nimmer, P., *et al.* (2008). ABT-263: a potent and orally bioavailable Bcl-2 family inhibitor. Cancer research *68*, 3421-3428.

Vogler, M., Weber, K., Dinsdale, D., Schmitz, I., Schulze-Osthoff, K., Dyer, M.J., and Cohen, G.M. (2009). Different forms of cell death induced by putative BCL2 inhibitors. Cell death and differentiation *16*, 1030-1039.

Zhou, F., Xing, D., Wu, S., and Chen, W.R. (2010). Intravital imaging of tumor apoptosis with FRET probes during tumor therapy. Molecular imaging and biology : MIB : the official publication of the Academy of Molecular Imaging *12*, 63-70.

4

Methods

4.1. Preface

This chapter has been previously published in:

Kale, J., Chi, X., Leber, B., and Andrews, D. (2014). Examining the molecular mechanism of Bcl-2 family proteins at membranes by fluorescence spectroscopy. Methods in enzymology 544, 1-23.

The publisher has granted permission for the work to be reproduced here. The work presented has been minimally edited for consistency and readability for this thesis. Specifically, paragraphs 1of both sections titled 'introduction' and 'an in vitro fluorescence-based liposome system' were removed which pertained to Bcl-2 family member interactions already explained in previous chapters.

Author Contribution:

Kale, J wrote the entire publication and prepared all of the figures and table with the exception that Chi, X wrote Section 3 "Membrane Permeabilization Assay" and prepared Figure 1. Leber, B and Andrews, DW edited the manuscript and directed the layout of the paper.

Objective:

To completely describe the fluorescence techniques used to investigate the precise molecular mechanisms of the Bcl-2 family proteins. This chapter describes in detail the main fluorescence methods used throughout this thesis.

Highlights:

- Using a highly defined liposome based system:
  - Expression, purification and site-specific fluorescent labeling of full-length Bax, Bcl-X_L and Bid
  - Production of mitochondria-like liposomes
- How to:
  - Measure membrane permeabilization
  - Study the interaction between two proteins using FRET
  - Track the conformation change of a protein using an environment sensitive dye
  - Determine the topology of proteins within membranes

4.2. Introduction

Significant research has been focused on determining the structure of Bcl-2 family proteins. X-ray crystallography and Nuclear Magnetic Resonance (NMR) spectroscopy have revealed that the Bcl-2 family proteins share a highly conserved core structure (Petros et al., 2004). These studies have provided insight into how the Bcl-2 family proteins bind to each other and suggest how they may interact with membranes. However, the current relatively static structures for the Bcl-2 family are for proteins without the lipid bilayer required for functional interactions of several of the Bcl-2 family proteins (Leber et al., 2007). Determining the structures of proteins within a membrane mimetic environment using X-ray crystallography and NMR spectroscopy is particularly difficult. These techniques require a large amount of protein in a sample environment that does not mimic that of the cell and typically includes detergents that can alter the functions of the Bcl-2 family proteins (Hsu and Youle, 1997). As an example, unlike native Bax, detergent treated Bax can cause permeabilization of the OMM when added to isolated mitochondria (Antonsson et al., 2000); can form oligomers that can be cross-linked in the absence of membranes (Zhang et al., 2010) and has undergone a conformational change that is a pre-requisite for Bax activation (Yethon et al., 2003). Additionally, the zwitterionic detergent CHAPS can prevent the authentic interaction of Bax and tBid (Lovell et al., 2008), further reinforcing the need to study the Bcl-2 family proteins in the absence of detergents.

Fluorescence based techniques are well suited to study protein dynamics at membranes under physiological conditions in the absence of detergents (Kale et al., 2012). Fluorescence spectroscopy allows observation of protein:protein and protein:membrane binding dynamics in real-time while gathering information about the kinetics and affinities of these interactions that cannot be measured using typical structural techniques due to complications from the membrane (Perez-Lara et al., 2012; Satsoura et al., 2012). Additionally, by using an environment sensitive probe such as NBD, it is possible to determine the environment of specific residues as they undergo conformational changes within membranes (Malhotra et al., 2013; Shamas-Din et al., 2013). Initial fluorescence based studies of the Bcl-2 family proteins have used a simple *in vitro* system to study the dynamic interactions that occur at, on and within membranes.

4.3. An *in vitro* Fluorescence-Based Liposome System

The molecular function of Bcl-2 family proteins is to permeabilize membranes. Therefore, to study the function of these proteins, a biochemical system is required that includes a phospholipid bilayer that separates two distinct aqueous compartments mimicking that of the cytoplasm and the interior of cellular organelles. We and others (Bleicken et al., 2010; Landeta et al., 2011; Ren et al., 2010; Shamas-Din et al., 2013) have used different variations of liposome or proteoliposome based systems to study the core mechanism of Bcl-2 family protein regulation of membrane permeabilization. All of these systems lack the detergents typically required for biochemical and structural studies of membrane proteins. For our studies fluorescently labeled purified full-length recombinant proteins and artificial membranes in the form of liposomes with a composition mimicking that of the OMM are used. This system is free of any other complicating factors such as unknown binding partners that may be present at the OMM or within the cytoplasm.

To use fluorescence to study proteins at membranes it is essential to make judicious choices of fluorophore, type of measurement and instrument. Fluorescence measurements require excitation of the fluorophore with a specific wavelength of light and then recording the emission from the fluorophore. Excitation of the fluorophore is accomplished by illuminating the sample with a set wavelength of light. The system must not contain components or contaminants that absorb light of the same wavelength as the fluorophore or they will absorb the excitation light. Upon excitation, after some period of time, termed the fluorescence lifetime (typically 1-10 nanoseconds), the fluorophore returns to the ground electronic state via emission of a photon at a lower energy, and thus longer wavelength, than the illuminating (excitation) light. Therefore, the system must also be free of molecules that absorb the emitted light because fluorescence is of much lower intensity than the excitation light. Molecules such as quenchers that provoke non-radiative decay of the fluorophore must also be avoided as they change the fluorescence properties of the dyes. If these conditions are met, changes in both fluorescence lifetime and emission intensity can provide specific information about the underlying biochemical properties of the protein the fluorophore is attached to (Lakowicz, 2006).

4.4. Site specific protein labeling

The fluorescence based techniques we use to study the Bcl-2 family proteins require purified recombinant proteins labeled with a fluorophore at a specific location. There are two main options for labeling proteins, thiol or primary amine labeling. Cysteine residues are less abundant than lysines in most protein sequences thus we most frequently create single cysteine mutants to label the protein as this approach minimizes the number of mutations in the protein. There is a full spectrum of fluorescent probes available for purchase, which have different spectral properties, that can be can be ordered with attached thiol reactive moieties such as iodoacetamide or maleimide derivatives. Dyes must be chosen that are compatible not only with your protein of choice but also with the system and equipment available.

In the methods reported below, the proteins were labeled with the low molecular weight fluorescent probes DAC (*N - (7 - Dimethylamino - 4 - methylcoumarin - 3 - yl) maleimide*) and NBD (N,N'-Dimethyl-N-(Iodoacetyl)-N'-(7-Nitrobenz-2-Oxa-1,3-Diazol-4-yl) Ethylenediamine). The small size of these dyes is a distinct advantage as they rarely perturb protein function however, measurements of NBD fluorescence require a sensitive instrument as the quantum yield (ratio of photons emitted to photons absorbed) is low. Moreover, excitation of DAC requires an ultraviolet light source and both the excitation and emission of this dye overlap endogenous fluorophores in cells typically limiting its use to liposome based systems. Many brighter (higher quantum yields and extinction coefficients) fluorescent dyes have molecular weights above 1kDa, and in our experience these larger dyes frequently change the function of the protein they are attached to.

Initially it is best to follow the labeling protocol included by the manufacturer when labeling your protein of interest, however it is often necessary to deviate from these conditions to get labeling that is both specific and efficient. Briefly, the protein and labeling reaction are both in a HEPES or PBS based buffer at pH 7.0-7.5. This pH range allows the cysteines to be most-reactive while decreasing the reactivity of primary amines. A 10-20x molar excess of dye is added to the sample tube and the labeling reaction is rotated at room temperature for approximately 2 hours in the dark. A reducing agent (5 mM DTT) is then added to quench the reaction and free dye is removed via gel filtration or affinity chromatography (providing the

recombinant protein contains an affinity tag). The protein is then dialyzed into a storage buffer to remove any remaining free dye and the protein is aliquoted and stored for later use. The efficiency of labeling is generally determined by absorbance spectroscopy as outlined in the protocol supplied by the manufacturer.

Single cysteine mutants of the purified recombinant protein need to be assayed functionally before and after labeling to determine if the mutation or the addition of the dye alters protein function. Ideally we begin using mutants where one of the endogenous cysteines is present to minimize the amount of mutations introduced into the protein. If the protein does not contain any cysteines, choosing which residue to mutate to cysteine for efficient labeling and proper protein function is largely serendipitous. Typically if the structure is known, one begins using solvent exposed residues, since those located in hydrophobic regions are difficult to label. Algorithms used to predict solvent exposure or antigenicity (antigenic sites tend to be both structured and solvent exposed) can often be useful in selecting a location if the structure of your protein is unknown.

4.5. Production of mitochondria-like liposomes

Large unilamellar vesicles (LUVs) are liposomes that have one lipid bilayer with a mean diameter of 120-140 nm (Hope et al., 1985). OMM-like LUVs have been established as a valid biochemical model for membrane permeablization by Bcl-2 family members (Kuwana et al., 2002). These liposomes are assembled from lipids in fixed molar ratio similar to that of the OMM, based upon lipid composition studies from solvent extracted Xenopus mitochondria (Kuwana et al., 2002). Such liposome-based systems allow the analysis of Bcl-2 family proteins in a simple context while preserving their authentic functions. It is possible to more directly explore Bcl-2 family function in this kind of system because the protein and lipid components are well defined and tractable, unlike isolated mitochondria or proteoliposomes prepared from membranes.

4.5.1. Preparing lipid films into liposomes

1. Chloroform solublized lipids are added to a glass test tube to make a lipid mixture of a defined composition (Table 1) to a total of 1 mg lipid mass. The chloroform is evaporated off with nitrogen gas while rotating the tube to ensure an even distribution of lipids on the wall and then put under vacuum for 2 hours at room temperature to remove any remaining chloroform. The dry lipid film is then either used immediately or can be stored for up to 2 weeks at -20°C. To reduce lipid oxidation by atmospheric oxygen during storage it is advisable to layer nitrogen or argon gas on top of the lipid film and seal the tube with parafilm.

2. The dry 1 mg lipid film is hydrated with 1 mL of assay buffer (10mM HEPES, 200mM KCl, 5mM $MgCl_2$, 0.2mM EDTA, pH7) . The lipids become suspended and spontaneously form lipid bilayer vesicles due to the association of the hydrophobic tails, forming the center of the bilayer, and the grouping of the hydrophilic heads of the phospholipids, forming the edges of the bilayer. However, these vesicles are multilamellar as they contain more than one lipid bilayer and their size distribution is not homogeneous. To generate unilamellar liposomes the lipid mixture is subjected to 8-10 freeze/thaw cycles by alternately placing the sample vial in liquid nitrogen and a warm water bath (Hope et al., 1985). The unilamellar liposomes are extruded eleven times through a filter with 0.1µm pore size to produce liposomes of a uniform size, at a final concentration of 1 mg/mL lipid.

Table 4.1 - Mitochondria-like lipid film composition

Name	Company	Catalog #	Molar (%)	Molecular weight (g/mol)	Amount needed for 1 mg lipid film (mg)
"PC": L-α-phosphatidylcholine (egg, chicken)	Avanti	840051C	48	770.123	0.4596
"PE": L-α-phosphatidylethanolamine (egg, chicken)	Avanti	841118C	28	726.076	0.2528
"PI": L-α-phosphatidylinositol (liver, bovine)	Avanti	840042C	10	902.133	0.1122
"DOPS": 1,2-dioleoyl-*sn*-glycero-3-phospho-L-serine	Avanti	840035C	10	810.025	0.1007
"TOCL": 1,1′,2,2′-tetra-(9Z-octadecenoyl) cardiolipin	Avanti	710335C	4	1501.959	0.0747

4.6. Membrane Permeabilization Assay

The Bcl-2 family proteins play a pivotal role in regulating apoptosis by controlling the permeabilization of the OMM through the activation of Bax/Bak. Thus a membrane permeablization assay is one crucial functional assay for the Bcl-2 family proteins. To assay liposome permeabilization the liposomes are encapsulated with a polyanionic fluorophore, 8-aminonaphthalene-1,3,6-trisulfonic acid (ANTS), and cationic quencher, p-xylene-bis-pyridinium bromide (DPX). Due to the high local concentration of DPX, ANTS fluorescence is quenched when liposomes are still intact. Recombinant Bax and/or other Bcl-2 family proteins and/or reagents are added to the system in order to assay permeabilization. As the liposomes permeabilize, ANTS and DPX are released from the liposomes, greatly decreasing the local concentration of the quencher resulting in a gain of ANTS fluorescence. The kinetics and extent of membrane permeabilization can reveal crucial information for studying relationships between Bcl-2 family members and how they regulate membrane permeabilization.

4.6.1. ANTS/DPX release assay

1. A dry 1 mg lipid film is hydrated with 1 mL of assay buffer with the addition of ANTS (12.5 mM) and DPX (45mM). The lipid suspension is vortexed until the ANTS and DPX dissolve, and liposomes are created as above via 10 freeze thaw cycles and extrusion through a 0.1µm pore size membrane

2. Excess ANTS and DPX are removed by applying the extruded liposomes onto a CL2B size-exclusion column (10 mL bed volume), that separate the ANTS/DPX encapsulated liposomes from the free ANTS/DPX in solution (Billen et al., 2008; Yethon et al., 2003). Fractions (1 mL each) are collected in glass tubes and the liposome containing fractions (typically fractions 3 and 4) are identified by an increase in cloudiness of the sample which occurs due to light scattering by the liposomes. The two liposome containing fractions are combined resulting in a final ANTS/DPX liposome concentration of approximately 0.5 mg/ mL lipid. These liposomes can now be used to test the regulation of membrane permeabilization by the Bcl-2 family proteins

3. The assay is set up in a low protein binding 96 well plate and in each well to be measured, 8 µL of ANTS/DPX liposomes are added to 92 µL of assay buffer. Background measurements (F_0) are recorded at 30°C using a fluorescence plate reader (Tecan M1000 pro) set to excite the sample at 355 nm (5 nm bandwidth) and collect emission at 520 nm (12 nm bandwidth).

4. Proteins are added to the desired concentrations and combinations in each well and fluorescence emission of ANTS (F) is recorded every minute for 3 hours at 30°C. Any increase in fluorescence emission is directly related to membrane permeabilization.

5. To normalize the data, 100% ANTS release is determined by the addition of Triton to each well at a final concentration of 0.2% (w/v) causing permeabilization of all liposomes and ANTS fluorescence is measured (F_{100}). This results in a slight over-estimation of the intensity of 100 percent release due to the dye becoming trapped in detergent micelles. Nevertheless, the release percentage generally does not take this into account and is calculated as follows:

$$\text{ANTS Release } (\%) = \frac{F - F_0}{F_{100} - F_0} \times 100\%$$

The ANTS/DPX release assay can be used to dissect exactly how the different classes of Bcl-2 family proteins affect permeabilization of the OMM. When cBid (20 nM), Bax (100 nM) or Bcl-X_L (40 nM) are added individually to liposomes they do not cause membrane permeabilization (Figure 1.1). Incubation of liposomes with cBid and Bax results in membrane permeabilization due to cBid binding to membranes causing separation of the two fragments of cBid and the larger of the two (tBid) activating Bax. Bcl-X_L inhibits this process by binding to and inhibiting both tBid and Bax (Billen et al., 2008; Lovell et al., 2008). Obviously, other techniques are needed to discern exactly how these interactions occur (see FRET section below), however this assay allows the functional consequence of the addition of any number of various combinations of Bcl-2 family members or small molecule effectors of the proteins to be determined. Furthermore, it provides information on how changes in relative concentrations between the proteins can change the extent of permeabilization or how alterations in the parameters of the assay affect membrane permeabilization. For example, it is possible quantify how changes in liposome composition affect Bcl-2 family proteins functions to permeabilize membranes or test specific mutations that may inhibit/activate the protein of interest. Additionally, the kinetics of pore formation can be studied allowing the comparison of kinetics for Bax mediated membrane permeabilization in response to various BH3-only activators (Figure 1.2).

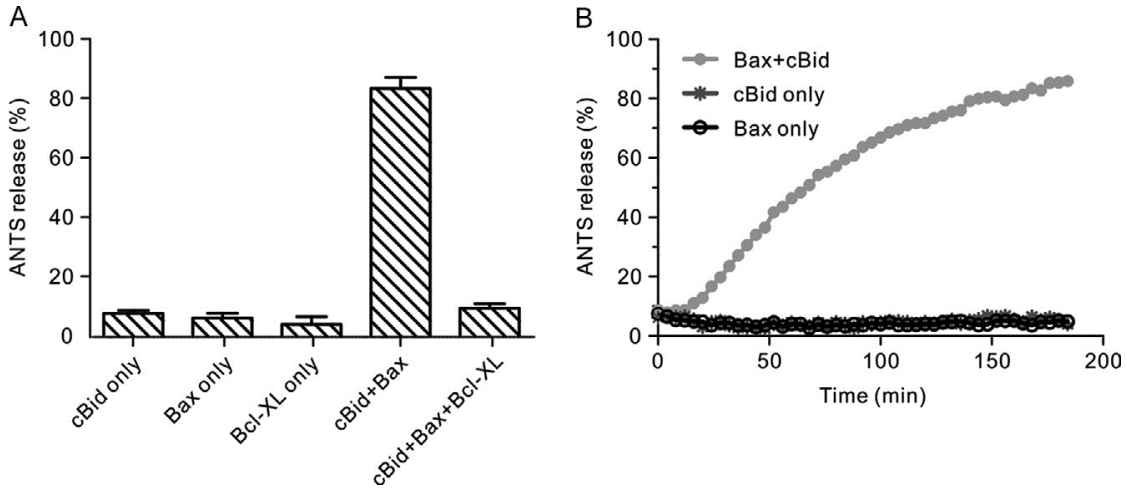

Figure 4.1 - ANTS/DPX release assay

A. Endpoint values of ANTS assay with 100 nM Bax, 20 nM cBid, 40nM Bcl-X_L or both, or with 100 nM Bax, 20 nM tBid, and 40nM Bcl-X_L. (n=3)

B. Liposomes encapsulated with ANTS and DPX were incubated with 100 nM Bax, 20 nM cBid, or both. Membrane permeabilization was assayed by an increase of ANTS fluorescence.

4.7. FLUORESCENCE RESONANCE ENERGY TRANSFER

Here Fluorescence Resonance Energy Transfer (FRET) will be used to detect binding between cBid and Bax, and Bax oligomerization. FRET is possible between fluorophores when the emission spectra of one fluorescent molecule, termed the donor, overlaps the excitation spectra of another fluorophore, the acceptor. When a donor fluorophore is excited by light, an electron moves to a higher energy state and, in the presence of an acceptor, the energy is transferred non-radiatively to the acceptor fluorophore via dipole-dipole interactions between the two probes. This transfer of energy results in a decrease of the donor emission, and it is the change in the light emitted by the donor that we will track to measure FRET between two proteins.

One of the main advantages of FRET is that it requires both the donor and acceptor fluorophores to be in close proximity for the required dipole coupling to occur. As a result FRET

efficiency decreases to the 6th power of distance according to the formula for FRET efficiency (E) at a fixed donor acceptor distance:

$$E = \frac{R_0^6}{R_0^6 + r^6}$$

Where R_0 is the Förster distance, the distance between a donor acceptor pair at which a 50% FRET efficiency is observed, and *r* is the distance between the donor and acceptor. The distance dependence of FRET is illustrated in Figure 2.1 where FRET efficiency is calculated for distances between a donor and acceptor pair with an R_0 of 50 Å (Lakowicz, 2006). For this dye pair, FRET will only be detected if the distance between the two fluorophores is 70Å or less. Typical R_0 values for a donor and acceptor pair are between 30-60Å, similar to the size of proteins, thus if FRET between donor and acceptor labeled proteins is detected then they are binding.

4.7.1. Detecting the interaction between two proteins using FRET

As mentioned in the introduction, the BH3-only protein cBid targets to, and embeds within the OMM where it recruits and activates cytosolic Bax (Leber et al., 2007; Lovell et al., 2008). Active membrane bound Bax oligomerizes within the OMM and resulting in membrane permeabilization. Here, we are using DAC and NBD as the donor and acceptor molecules respectively. We will be using FRET to detect 1) the binding between cBid and Bax and 2) the binding between Bax molecules during oligomerization.

1. Liposomes are made as above resulting in liposomes at a concentration of 1 mg/mL lipid

2. The fluorimeter (Photon Technology International) is set to record the fluorescence of DAC (380 nm excitation, 2nm slit width; 460 nm emission, 10 nm slit width) with stirring for 1 hour at 37°C. Either 200 μL of liposomes and 800 μL of assay buffer, or as a control, 1 mL of assay buffer is added to a quartz cuvette and the signal is read until it remains stable (approximately 5 minutes). Two reactions are required to detect FRET. One that contains both the donor and acceptor labeled proteins and a control that contains the donor labeled protein and unlabeled acceptor protein. This control accounts for any changes in the donor protein that occur due to

binding interactions, conformational changes or environment changes that may affect the spectral properties of the donor dye.

3. The donor labeled protein is added to the cuvette at a concentration of 20 nM and DAC fluorescence is read until the signal is stable. At this point the acceptor protein that is either labeled with NBD or unlabeled is added to the system at a concentration of 100 nM. It is important to keep the amount of acceptor higher (5-10 x) than that of the donor. This allows for the donor protein to be saturated by the acceptor ensuring that every donor dye has an acceptor for FRET to occur.

4. The DAC signal is recorded for 1 hour at 37°C. FRET efficiency (E) is measured by comparing the relative intensity of the donor in the presence of labeled (F_{DA}) and unlabeled (F_D) acceptor and is calculated by:

$$E = 1 - \frac{F_{DA}}{F_D}$$

Figure 2 illustrates two binding interactions between the Bcl-2 family proteins. Donor (DAC) labeled cBid (20 nM) is incubated with acceptor (NBD) labeled Bax (100 nM), and only in the presence of liposomes do the two proteins interact (Figure 2.2). This underlines the point that many functional interactions of the Bcl-2 family proteins only occur in the presence of a lipid bilayer. Additionally, the activator protein cBid is required for Bax to oligomerize, since FRET between donor (DAC) and acceptor (NBD) labeled Bax is only observed when cBid is added to the system (Figure 2.3). Since we can observe the interactions of two proteins in real-time, kinetics of the reactions can be determined. Indeed, it is clear from the data shown that the cBid-Bax interaction occurs faster than Bax oligomerization suggesting that cBid first binds to and activates Bax followed by Bax oligomerization. Additionally, it is possible to generate a binding curve where an affinity for the interaction can be determined as was done for the binding between cBid and Bax (Lovell, et al., 2008). To do this multiple FRET measurements are obtained by titrating the amount of acceptor while keeping the donor concentration fixed.

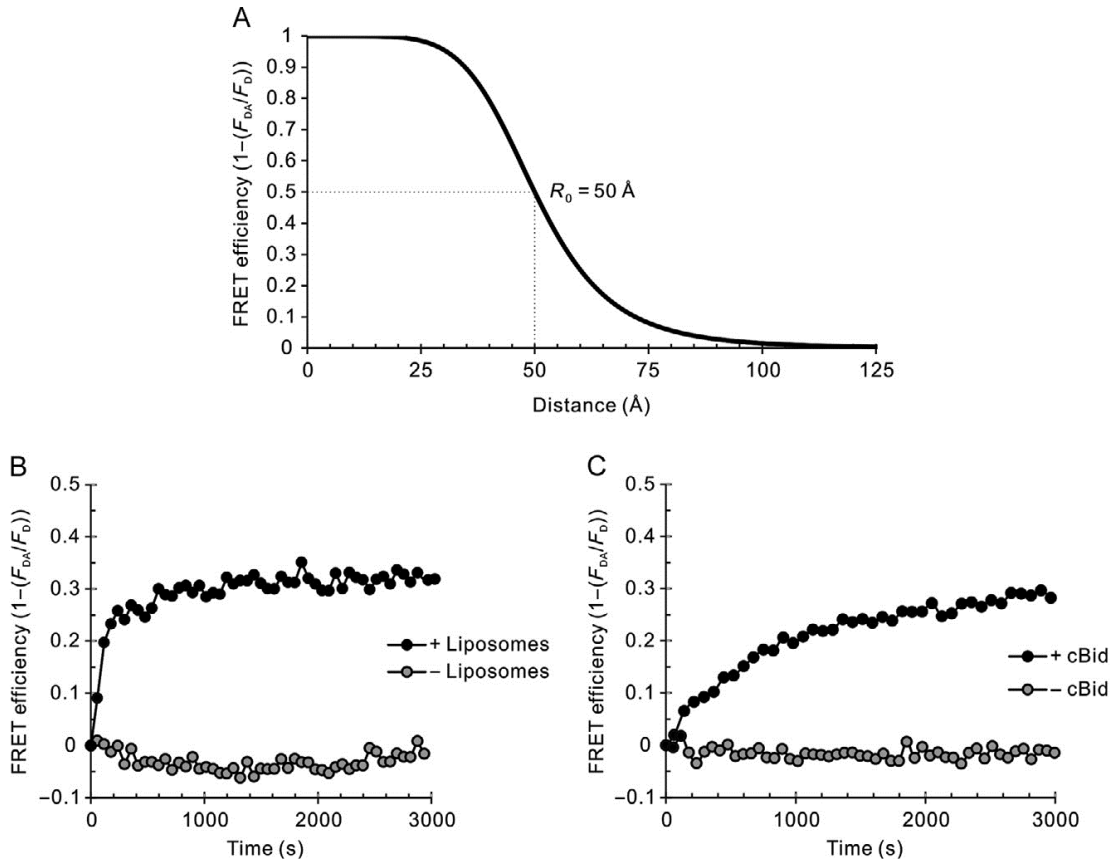

Figure 4.2 - Tracking protein:protein interactions via FRET

A. FRET efficiency as a function of distance between a dye pair with a theoretical Förster distance of 50 Å.

B. FRET between cBid-DAC (20 nM) and Bax-NBD (100 nM) in the presence (black circles) and absence (grey circles) of liposomes (0.2 mg/mL).

C. FRET between Bax-DAC (20 nM) and Bax-NBD (100 nM) in samples containing liposomes (0.2 mg/mL) with (black circles) or without (grey circles) 20 nM cBid

4.8. TRACKING THE CONFORMATION CHANGES OF A PROTEIN

NBD is an environment sensitive low-molecular weight fluorescent dye that has been used to track environment changes of specific residues of proteins (Dattelbaum et al., 2005; Lin et al., 2011b) . The emission intensity and fluorescence lifetime increases and the emission peak of NBD blueshifts from 570nm, in an aqueous environment, to 530 nm when it is in a

hydrophobic environment due to a decrease in fluorescence quenching by water (Crowley et al., 1993). The small size of NBD allows for the specific labeling of single cysteine mutants of proteins, with less potential perturbation of wild-type function. Importantly, NBD is uncharged but has sufficient polar characteristics that it remains stable in both polar and non-polar environments such that it is less likely than other environment sensitive dyes to change the membrane binding characteristics and/or conformation of the protein being studied (Shepard et al., 1998). These properties of NBD make it particularly useful to study membrane binding proteins such as Bax and cBid that transition from the aqueous environment and embed into a membrane bilayer (Lovell et al., 2008; Shamas-Din et al., 2013).

4.8.1. NBD-emission assay

Real-time changes in the fluorescence of NBD can be measured to determine whether and when specific regions of Bax (labeled with NBD) insert into the membrane during the activation of Bax. It is known from chemical labeling studies that Bax inserts helices 5, 6 and 9 into the membrane (Annis et al., 2005). By labeling Bax at residue 175 (helix 9) it is possible to track the conformational change of Bax as it transitions from a soluble monomer to membrane embedded oligomer.

1. The fluorimeter is set to record NBD fluorescence (475 nm excitation, 2nm slit width; 530 nm emission, 10 nm slit width) and, as in the FRET experiment above, 200 μL of 1 mg/mL liposomes are added to 800 μL of assay buffer in a quartz cuvette. Background signal (Bg) is recorded with stirring until stable at 37°C.

2. NBD labeled Bax (100 nM) is added to the cuvette. Since Bax does not insert into membranes in the absence of an activator (Hsu and Youle, 1998), Bax-NBD can be incubated with liposomes and an initial fluorescence value can be recorded (F_0) . Alternatively, the very first point upon addition of the protein can be used as the F_0 value if the protein insert into lipids too rapidly. This approach is useful for proteins that are unstable in the assay solution such as cBid which spontaneously targets to membranes (Shamas-Din et al., 2013). In the absence of membranes cBid has sufficient exposed hydrophobicity that it tends to aggregate and to stick to the walls of the cuvette.

3. In our example the change in emission over time (ΔF) of the dye labeled Bax is collected once an activator, cBid, is added. Fluorescence intensity plateaus after the protein comes to equilibrium (1 hour endpoint). By calculating the F/F_0 value one can track the relative change in emission intensity of the labeled residue in real-time:

$$\Delta F = \frac{F - Bg}{F_0 - Bg}$$

Both residues 3 and 175 of Bax transition to a more hydrophobic environment as indicated (Figure 3.1) by the relative change in emission (ΔF). Since the environment change of the residue can be tracked over time, kinetics of membrane binding can be measured. Tracking the kinetics of the environment changes of various residues as a protein undergoes a conformational change could be used to order specific structural changes of the protein (Shamas-Din et al., 2013). Here, the carboxyl terminus of Bax (residue 175) seems to have slower kinetics compared to that of the amino terminus of Bax (residue 3) suggesting that Bax undergoes a conformational change at residue 3 before that of 175. Additionally, residue 175 has a larger change in NBD emission suggesting that it is moving to a more hydrophobic environment. This paired with the quenching data discussed below, suggests that residue 175 of Bax inserts into the phospholipid bilayer. As this residue is part of a larger hydrophobic sequence believed to span the bilayer the kinetics for this residue likely represent insertion of the Bax carboxyl-terminal tail into membranes. This is in accordance with data that shows that residue 175C is embedded within the membrane (Annis et al., 2005). By using various activators of Bax or mutations known to perturb Bax function we could see if these changes affect the extent of or rate at which Bax helix 9 inserts into phospholipid bilayers.

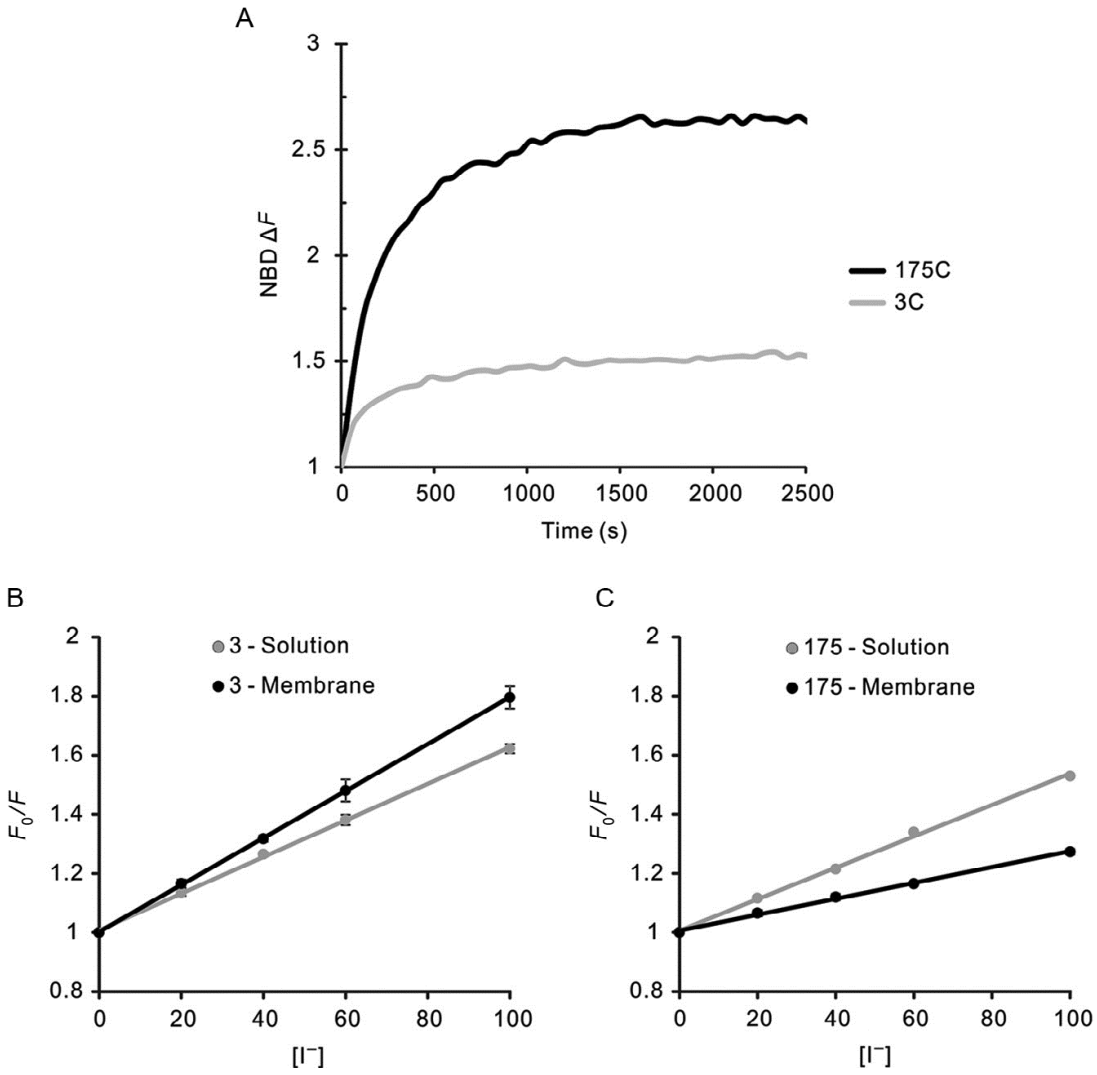

Figure 4.3 - Tracking the conformation change of proteins

A. NBD emission change for Bax 175C-NBD (100 nM) and Bax 3C-NBD (100 nM) upon addition of cBid (20 nM) in the presence of liposomes (0.2 mg/mL)

B. & C. Iodide quenching data of 100 nM Bax 3C-NBD (3.2) or 175C-NBD (3.3) in solution (black) or in the presence of liposomes (0.2 mg/mL) and cBid (20 nM) (grey)

4.9. Determining the topology of proteins within membranes

Fluorescence quenching by heavy atoms such as iodide can be used to determine how exposed a fluorescently tagged residue is to the solvent. This is due to collisional quenching that

occurs when I^- collides with an excited fluorophore, resulting in a loss of energy back to ground state without emission of a photon. Typically collisional quenching requires direct molecular interaction with the fluorophore such that the distance of quenching is <2Å giving a very high resolution to detect solvent accessibility (Lakowicz, 2006).

Since I^- quenches NBD fluorescence (Crowley et al., 1993; Lin et al., 2011a), this technique would be advantageous to look at the difference of residue solvent accessibility between soluble monomeric Bax, in the absence of activator, and membrane bound oligomeric Bax, in the presence of an activator.

4.9.1. Iodide quenching of NBD labeled Bax

1. As in the method for NBD emission change, the fluorimeter is set to record NBD fluorescence, and 200 µL of 1 mg/mL liposomes are added to 800 µL of assay buffer in a quartz cuvette. Background signal is read with stirring until stable at 37°C.

2. NBD labeled Bax (100 nM) and cBid (20 nM) are added to cuvettes containing either liposomes (200 µL liposomes, 800 µL assay buffer) for quenching of membrane bound Bax, or assay buffer only (1 mL assay buffer), for quenching of solution Bax. NBD emission (F_0) is recorded after incubation of the sample at 37°C for one hour.

3. Multiple quenching reactions are set up where aliquots of Potassium Iodide (2M, supplemented with 2 mM sodium thiosulfate to prevent oxidation) and Potassium Chloride (2M) stock solutions are added to each sample so that the total ion concentration, and thus ionic strength, in samples is the same (typically 100 mM) (Table 2). The NBD emission for each concentration of KI is determined (F) and collisional quenching is calculated by the Stern-Volmer equation:

$$\frac{F_0}{F} = 1 + K_{sv}[Q]$$

Where F_0 is the fluorescence intensity in the absence of quencher, F is the fluorescence intensity at a specific quencher concentration [Q] and K_{sv} is the Stern-Volmer quenching constant.

Table 4.2 - Iodide quenching values of NBD-labeled Bax

		3C[a]		175C[a]	
KI (m*M*)	KCl (m*M*)	Solution (F_0/F)	Membrane (F_0/F)	Solution (F_0/F)	Membrane (F_0/F)
0	100	1	1	1	1
20	80	1.1351 ± 0.0105	1.1657 ± 0.0136	1.1158 ± 0.0002	1.0650 ± 0.0134
40	60	1.2645 ± 0.0068	1.3176 ± 0.0101	1.2140 ± 0.0029	1.1110 ± 0.0112
60	40	1.3812 ± 0.0180	1.4807 ± 0.0373	1.3397 ± 0.0019	1.1647 ± 0.0020
100	0	1.6224 ± 0.0156	1.7954 ± 0.0376	1.5294 ± 0.0002	1.2730 ± 0.0093

As the concentration of I^- increases, so does the extent of quenching as determined by the Stern-Volmer equation, allowing the titration curve to be fit with a line where the slope is the Stern-Volmer constant (K_{sv}). The smaller the Stern-Volmer constant the more protected a residue is from the solvent. Quenching can then be used to compare the change in exposure of Bax residues to solvent upon the addition of an activator. Correlating with the NBD emission changes, residue 3 shows no change in protection from quenching upon the addition of cBid (Figure 3.2), whereas residue 175C of Bax becomes more protected from quenching, in agreement with this region of Bax inserting into the bilayer (Figure 3.3) (Annis et al., 2005).

4.10. Conclusion

Here, four techniques have been highlighted to show how membrane proteins can be studied by fluorescence spectroscopy. The high sensitivity of fluorescence based assays along with the ability to probe the dynamics of protein:protein and protein:membrane interactions in real-time lends itself well to study a complex regulatory system such as the Bcl-2 family of proteins. The techniques described here have been adapted to study many different aspects of apoptosis regulation in vitro and in live cells and can be applied to study other biological systems (Kale et al, 2012).

4.11. References

Annis, M.G., Soucie, E.L., Dlugosz, P.J., Cruz-Aguado, J.A., Penn, L.Z., Leber, B., and Andrews, D.W. (2005). Bax forms multispanning monomers that oligomerize to permeabilize membranes during apoptosis. EMBO J *24*, 2096-2103.

Antonsson, B., Montessuit, S., Lauper, S., Eskes, R., and Martinou, J.C. (2000). Bax oligomerization is required for channel-forming activity in liposomes and to trigger cytochrome c release from mitochondria. Biochem J *345 Pt 2*, 271-278.

Billen, L.P., Kokoski, C.L., Lovell, J.F., Leber, B., and Andrews, D.W. (2008). Bcl-XL inhibits membrane permeabilization by competing with Bax. PLoS biology *6*, e147.

Bleicken, S., Classen, M., Padmavathi, P.V., Ishikawa, T., Zeth, K., Steinhoff, H.J., and Bordignon, E. (2010). Molecular details of Bax activation, oligomerization, and membrane insertion. J Biol Chem *285*, 6636-6647.

Crowley, K.S., Reinhart, G.D., and Johnson, A.E. (1993). The signal sequence moves through a ribosomal tunnel into a noncytoplasmic aqueous environment at the ER membrane early in translocation. Cell *73*, 1101-1115.

Dattelbaum, J.D., Looger, L.L., Benson, D.E., Sali, K.M., Thompson, R.B., and Hellinga, H.W. (2005). Analysis of allosteric signal transduction mechanisms in an engineered fluorescent maltose biosensor. Protein Sci *14*, 284-291.

Hope, M.J., Bally, M.B., Webb, G., and Cullis, P.R. (1985). Production of large unilamellar vesicles by a rapid extrusion procedure: characterization of size distribution, trapped volume and ability to maintain a membrane potential. Biochimica et biophysica acta *812*, 55-65.

Hsu, Y.T., and Youle, R.J. (1997). Nonionic detergents induce dimerization among members of the Bcl-2 family. The Journal of biological chemistry *272*, 13829-13834.

Hsu, Y.T., and Youle, R.J. (1998). Bax in murine thymus is a soluble monomeric protein that displays differential detergent-induced conformations. The Journal of biological chemistry *273*, 10777-10783.

Kale, J., Liu, Q., Leber, B., and Andrews, D.W. (2012). Shedding light on apoptosis at subcellular membranes. Cell *151*, 1179-1184.

Kuwana, T., Mackey, M.R., Perkins, G., Ellisman, M.H., Latterich, M., Schneiter, R., Green, D.R., and Newmeyer, D.D. (2002). Bid, Bax, and lipids cooperate to form supramolecular openings in the outer mitochondrial membrane. Cell *111*, 331-342.

Lakowicz, J.R. (2006). Principles of fluorescence spectroscopy, 3rd edn (New York: Springer).

Landeta, O., Landajuela, A., Gil, D., Taneva, S., Diprimo, C., Sot, B., Valle, M., Frolov, V., and Basanez, G. (2011). Reconstitution of proapoptotic BAK function in liposomes reveals a

dual role for mitochondrial lipids in the BAK-driven membrane permeabilization process. J Biol Chem.

Leber, B., Lin, J., and Andrews, D.W. (2007). Embedded together: the life and death consequences of interaction of the Bcl-2 family with membranes. Apoptosis *12*, 897-911.

Lin, P.J., Jongsma, C.G., Liao, S., and Johnson, A.E. (2011a). Transmembrane segments of nascent polytopic membrane proteins control cytosol/ER targeting during membrane integration. J Cell Biol *195*, 41-54.

Lin, P.J., Jongsma, C.G., Pool, M.R., and Johnson, A.E. (2011b). Polytopic membrane protein folding at L17 in the ribosome tunnel initiates cyclical changes at the translocon. J Cell Biol *195*, 55-70.

Lovell, J.F., Billen, L.P., Bindner, S., Shamas-Din, A., Fradin, C., Leber, B., and Andrews, D.W. (2008). Membrane binding by tBid initiates an ordered series of events culminating in membrane permeabilization by Bax. Cell *135*, 1074-1084.

Malhotra, K., Sathappa, M., Landin, J.S., Johnson, A.E., and Alder, N.N. (2013). Structural changes in the mitochondrial Tim23 channel are coupled to the proton-motive force. Nat Struct Mol Biol *20*, 965-972.

Perez-Lara, A., Egea-Jimenez, A.L., Ausili, A., Corbalan-Garcia, S., and Gomez-Fernandez, J.C. (2012). The membrane binding kinetics of full-length PKCalpha is determined by membrane lipid composition. Biochim Biophys Acta *1821*, 1434-1442.

Petros, A.M., Olejniczak, E.T., and Fesik, S.W. (2004). Structural biology of the Bcl-2 family of proteins. Biochim Biophys Acta *1644*, 83-94.

Ren, D., Tu, H.C., Kim, H., Wang, G.X., Bean, G.R., Takeuchi, O., Jeffers, J.R., Zambetti, G.P., Hsieh, J.J., and Cheng, E.H. (2010). BID, BIM, and PUMA are essential for activation of the BAX- and BAK-dependent cell death program. Science *330*, 1390-1393.

Satsoura, D., Kucerka, N., Shivakumar, S., Pencer, J., Griffiths, C., Leber, B., Andrews, D.W., Katsaras, J., and Fradin, C. (2012). Interaction of the full-length Bax protein with biomimetic mitochondrial liposomes: a small-angle neutron scattering and fluorescence study. Biochimica et biophysica acta *1818*, 384-401.

Shamas-Din, A., Bindner, S., Zhu, W., Zaltsman, Y., Campbell, C., Gross, A., Leber, B., Andrews, D.W., and Fradin, C. (2013). tBid undergoes multiple conformational changes

at the membrane required for Bax activation. The Journal of biological chemistry *288*, 22111-22127.

Shepard, L.A., Heuck, A.P., Hamman, B.D., Rossjohn, J., Parker, M.W., Ryan, K.R., Johnson, A.E., and Tweten, R.K. (1998). Identification of a membrane-spanning domain of the thiol-activated pore-forming toxin Clostridium perfringens perfringolysin O: an alpha-helical to beta-sheet transition identified by fluorescence spectroscopy. Biochemistry *37*, 14563-14574.

Yethon, J.A., Epand, R.F., Leber, B., Epand, R.M., and Andrews, D.W. (2003). Interaction with a membrane surface triggers a reversible conformational change in Bax normally associated with induction of apoptosis. The Journal of biological chemistry *278*, 48935-48941.

Zhang, Z., Zhu, W., Lapolla, S.M., Miao, Y., Shao, Y., Falcone, M., Boreham, D., McFarlane, N., Ding, J., Johnson, A.E., *et al.* (2010). Bax forms an oligomer via separate, yet interdependent, surfaces. J Biol Chem *285*, 17614-17627.

5

Cancer-associated Bax point mutations block apoptotic pore formation at distinct conformations

5.1. Preface

The work presented here has been prepared for submission as a research article

Kale, J., Bachman, J.A., Sorger, P.K., Andrews D.W. (2016) Cancer-associated Bax point mutations block apoptotic pore formation at distinct conformations.

Author Contribution:

Kale, J and Bachman, JA wrote the entire publication. Kale, J performed all experiments and Bachman, JA did the modeling for the kinetic data. Sorger, PK and Andrews, DW edited the manuscript and directed the layout of the paper.

Objective:

To kinetically model the activation mechanism of Bax and to characterize the conformation changes of Bax as it transitions from a cytosolic monomer to a membrane embedded oligomer. This chapter addresses gaps in the field pertaining to the kinetics of Bax activation, how Bax is activated by activator BH3 proteins and specific conformations Bax adopts.

Highlights:

- Bax undergoes widespread conformation changes upon activation
- Kinetic modeling suggests:
    - Bax adopts 3 distinct conformations 1) solution Bax 2) an activator BH3-only-Bax intermediate and 3) Bax oligomer
    - Bax undergoes the same conformation changes irrespective of the activator used (cBid or Bim)
    - Transition into the intermediate is fast and is marked by a significant conformation change in the BH3 groove of Bax
    - After transitioning into the intermediate, Bax inserts helices 5, 6 and 9 into the membrane in concert.
- Specific point mutants block Bax in the intermediate conformation

5.2. Introduction

Apoptosis is a biochemically programmed cell death pathway that governs when and how cells die in response to internal or external stress stimuli. A key step in this process is mitochondrial outer membrane permeabilization, or MOMP, in which pores form in the mitochondrial outer membrane and release proapoptotic proteins, such as cytochrome *c* and Smac, into the cytosol (Tait and Green, 2010). The released proteins activate a family of proteases known as caspases that trigger the rapid degradation of cellular components. The processes downstream of MOMP are in general rapid and complete, making MOMP itself a key regulator of cell fate (Albeck et al., 2008; Goldstein et al., 2000; Rehm et al., 2002). Functional studies have shown that the tendency of mitochondria derived from cell lines and tumour cells to undergo MOMP correlates strongly with cell death in response to cytotoxic chemotherapy and ultimately, clinical outcomes (Ni Chonghaile et al., 2011; Vo et al., 2012).

MOMP is regulated by a set of evolutionarily related proteins known as the Bcl-2 family, which are responsible for activating, inhibiting, and permeabilizing the mitochondrial outer membrane (MOM) (Chipuk et al., 2010; Shamas-Din et al., 2013b; Youle and Strasser, 2008). The proapoptotic Bcl-2 family proteins, Bax and Bak are pore forming proteins and undergo conformational changes allowing them to oligomerize in the MOM resulting in MOMP (Kroemer et al., 2007). Furthermore, Bax and Bak are required for MOMP as Bax and Bak double knockout cells fail to undergo apoptosis whereas Bax or Bak knockout mouse embryonic fibroblasts respond to apoptotic signals (Wei et al., 2001). After insertion into the MOM, Bax oligomerizes resulting in MOMP at which point, the cell is committed to death (Annis et al., 2005; Er et al., 2006; Kroemer et al., 2007). Thus the activation status of Bax, whether it has formed pores or not, determines the fate of the cell.

The soluble form of Bax is a globular protein containing 9 α-helices, in which, the hydrophobic BH3-groove composed of the BH3-domain of Bax and surrounding residues (α helices 2-4), is occluded by the C-terminal α9 helix (Suzuki et al., 2000) (Figure 1A). Under normal circumstances Bax is predominately cytosolic with a small fraction binding transiently to membranes (Schellenberg et al., 2013; Yethon et al., 2003). Engagement of the BH3-domain of activator BH3 proteins such as tBid or Bim into the BH3-groove of Bax leads to displacement of

the C-terminal helix, exposure of both the N-terminus and the BH3-domain of Bax, the insertion of helices 5,6 and 9 into the membrane, and Bax oligomerization (Annis et al., 2005; Bleicken et al., 2014; Dewson et al., 2012; Gavathiotis et al., 2010; Kim et al., 2009; Lovell et al., 2008; Westphal et al., 2014a; Zhang et al., 2016b). The BH3-groove may not be the only activation site on Bax as binding of a stapled Bim BH3 peptides to full-length Bax protein analyzed by NMR revealed a novel binding pocket in Bax comprised of helix 1 and 6 termed the rear pocket (Gavathiotis et al., 2008). Binding of stapled Bim BH3 peptides to the rear pocket of Bax disengages an unstructured loop between α helices 1 and 2 which propagates a conformational change resulting in disengagement of α9 from the BH3 groove (Gavathiotis et al., 2010). Furthermore, helix 1 of Bax was shown to stabilize helix 9 in the hydrophobic cleft and upon direct interaction of helix 1 by Bid, Bim and Puma, helix 9 disengages allowing Bax to insert into the MOM (Kim et al., 2009). It remains to be conclusively shown whether or not there are differences in the activation site on Bax or in the conformational changes of Bax during activation by cBid or Bim.

Understanding the key regulatory steps in the activation mechanism of Bax is imperative for the development of drugs that can modulate apoptosis for therapeutic outcomes. Bax activation has been extensively studied yet the precise structure of active, membrane-bound and oligomerized Bax remains unknown. Multiple structural studies from different research groups have given a clearer picture on the arrangement of Bax molecules at the assembled pore (Bleicken et al., 2014; Czabotar et al., 2013; Zhang et al., 2016b). Although each study proposes different conformations of membrane-bound oligomerized Bax, all agree that Bax dimerization, initiated by interactions with activator BH3 proteins, involves symmetric binding via the BH3-domain (located in α2 of Bax) of one Bax and the hydrophobic groove (α2-4) of another. These studies also agree that the amphipathic α5 and α6 helices lie in-plane with the membrane and/or Bax pore and are not fully inserted within the bilayer whereas α9 fully inserts into the bilayer. However, these structures have been inferred from static structures in the absence of membranes, some of which appear to be off-pathway dead-end complexes. Therefore, the order of events remains highly speculative and whether each of these events constitutes a kinetically distinct step remains unknown.

It is clear that Bax has multiple distinct conformations that allow its targeting, insertion, oligomerization, and pore formation in the MOM. However, despite intensive research, a number of important questions regarding apoptotic pore formation remain. Existing studies based on static or equilibrium measurements offer insight into the structure of the assembled pore but less information about the nature of any intermediate conformations adopted by Bax or Bak. Conversely, kinetic studies have clarified aspects of the sequence of steps taken en route to pore formation, but lack structural information about the conformational states of Bax during this process (Kushnareva et al., 2012; Lovell et al., 2008; Saito et al., 2000). Moreover, the order of specific conformation changes and the kinetics of these changes in Bax remain elusive. In addition, because several of the existing structural studies have used a variety of methods for activating Bax (e.g., BH3 peptides vs. full-length BH3 proteins and liposomes vs. CHAPS detergent), it is unclear whether the particular rearrangements of Bax are contingent on the activator used. What is needed is a dynamic picture of the process by which Bax goes from the aqueous state to the assembled pore, using full-length proteins and membranes.

In this study we use we use fluorescence spectroscopy and kinetic modeling in an *in vitro* reconstituted system using liposomes and full-length recombinant proteins to order and define the conformational transitions that Bax undergoes as it transitions from a soluble monomer to a membrane embedded oligomer. We accomplish this by labeling the protein at 19 positions with an environmentally sensitive dye that reports on Bax insertion into membranes, complemented by intermolecular FRET to determine the timing of protein-protein interactions. We analyze approximately 400 experimental time courses using a set of kinetic models to identify the number and timing of conformational changes. We find that Bax transitions rapidly to an intermediate associated with binding of cBid or Bim, followed by a slower transition associated with Bax insertion into membranes, oligomerization and pore formation. Mutations found in cancer cells can trap Bax in this intermediate, preventing MOMP. The accompanying dataset, reporting dye release, Bax insertion, and FRET time courses between Bax and activators cBid and Bim, is provided in a variety of formats along with source code at (https://github.com/johnbachman/tbidbaxlipo). Plots of raw and processed data can be accessed in the Supplementary Online Material (SOM) at http://sorger.med.harvard.edu/data/bachman/kale/index.html.

5.3. Results

In order to elucidate how Bax unfolds into the membrane upon activation, 19 single cysteine Bax mutants were expressed, purified and labeled with the thiol-reactive fluorophore *NBD* as described (Kale et al., 2014; Lovell et al., 2008) (Figure 1B). We selected this dye because the fluorescence intensity of the emission peak of NBD depends on the hydrophobicity of the local environment of the dye. Therefore, if an NBD-labeled cysteine on Bax moves into a more hydrophobic environment (i.e. into the bilayer) the fluorescence intensity will increase and the opposite will happen if the dye labeled residue moves into a more hydrophilic environment. Moreover, due to the small size and limited hydrophobicity of NBD compared to other environment sensitive dyes, NBD has been used successfully for similar experiments for Bax and other proteins (Rojko et al., 2013; Shamas-Din et al., 2013a). Permeabilization of the bilayer was measured contemporaneously with Bax activation by encapsulating the fluorescent terbium-dipicolinic acid complex (Tb:DPA) inside liposomes and adding EDTA to the solution outside of the liposome. Upon membrane permeabilization by Bax, Tb:DPA is released from the liposomes and EDTA rapidly binds the Tb effectively quenching the fluorescence (Figure 1C) (Kale et al., 2014; Lovell et al., 2008). Measuring the changes in both NBD and Terbium fluorescence intensity enables characterization of Bax activation and pore formation in real time (Lovell et al., 2008).

Data from the fluorescence of the NBD dye at 19 different locations spanning the N-terminus, BH3-groove, pore-forming helices (α5 and α6), and C-terminus (α9) in Bax were compiled to track the changes in the environment of the nine different helices in Bax during pore formation (Figure 1A-B). Recent published data demonstrates that in liposomes Bim is faster than cBid at recruiting Bax to membranes because cBid must undergo a specific conformational change within the membrane before it can recruit Bax (Sarosiek et al., 2013; Shamas-Din et al., 2013a). Therefore, the activator proteins cBid and Bim were pre-incubated with liposomes for 5 minutes before the NBD labeled single cysteine mutants of Bax were added to ensure the conformational changes and membrane binding of the activators had come to equilibrium. This

allowed more precise ordering of Bax conformation changes because the kinetics of the activator BH3 proteins do not complicate the measured kinetics of Bax activation.

5.3.1. NBD-labeled mutants undergo distinct changes in hydrophobicity indicating widespread conformation changes in Bax during activation

The initial kinetic dataset (KD1) consisted of 40 different conditions (19 labeled Bax variants plus wild-type Bax, each incubated with one of two activator BH3 proteins) with three replicates each, for a total of 120 experiments (see SI Section 3.1). Our expectation, based on a previous analysis of Bax-C126-NBD (Lovell et al., 2008), was that each variant would exhibit roughly single-exponential membrane binding kinetics allowing differences in timescale to place each residue along a structural insertion "pathway". However, the results from our set of variants showed that NBD-Bax fluorescence trajectories were considerably more diverse and many were non-monotonic (Figure 2A).

The labeled proteins had distinct rates and dynamics of fluorescence changes, falling into two classes depending on the location of the label: 16 residues showed monotonic changes in fluorescence similar to what we had observed previously for Bax-C126-NBD. The rates of fluorescence change varied among these mutants, with some approaching their equilibrium value rapidly (e.g., Bax-3C-NBD) while others such as Bax-120C-NBD changed much more slowly (Figure 2A). The other class comprises four residues in the BH3-groove (54, 62, 68 and 79) that showed a kinetically fast increase in fluorescence, that for residues 54, 68 and 79 resulted in a transient peak in fluorescence intensity followed by a decline towards the equilibrium value. For residue 62 the initial increase was followed by a slow linear increase (Figure 2A and SI Section 3.1).

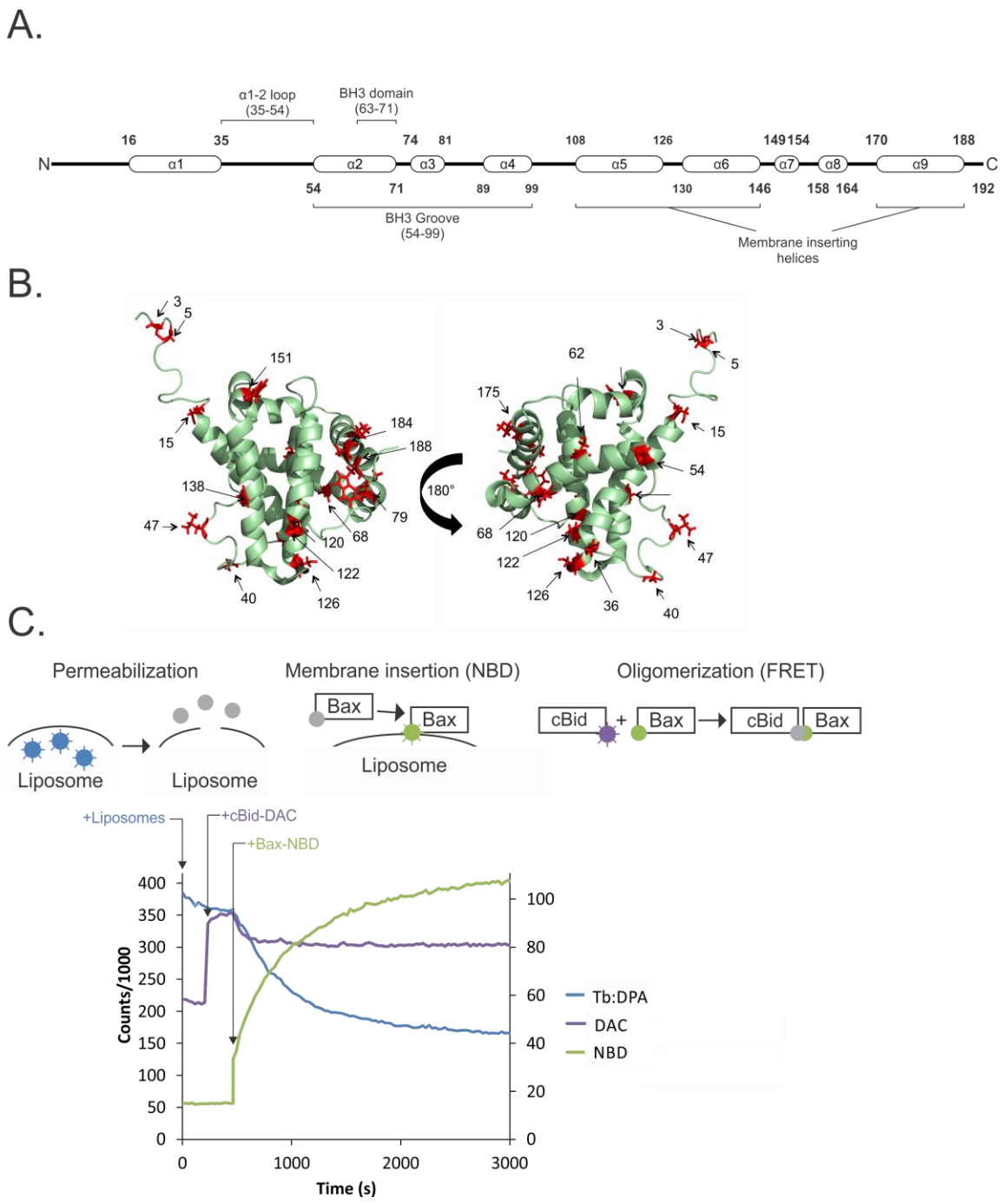

Figure 5.1 - Assaying dye release and conformational changes of labeled Bax mutants

A. Linear representation of Bax with BH3-groove and membrane inserting helices indicated.

B. Solution structure of Bax (PDB ID: 1F16) with positions of engineered cysteine mutations used for NBD labeling.

C. Design of multiplexed fluorescence spectroscopy assays. An activator BH3 protein, such as cBid (which in some experiments is labeled with the fluorescence donor DAC) is added to liposomes that contain the fluorescent complex

of Tb:DPA (terbium:dipicolinic acid) and allowed to equilibrate. NBD-labeled Bax mutants are then added and fluorescence time courses are recorded. Pore formation is measured as a decrease in Tb:DPAfluorescence as it is released into the solution, which contains EDTA that rapidly chelates Tb, thereby dismantling the Tb:DPA complex ; Bax conformational changes and membrane interactions are indicated by the fluorescence changes of NBD-Bax; and interactions between Bax and its activators are given by the decrease in fluorescence of the DAC-labeled BH3 protein due to FRET with NBD-Bax.

.

The *fold-change* in NBD fluorescence (F/F_0) upon Bax activation quantifies differences in the local environment of the residue between the aqueous and membrane-bound states (Figure 2B); a value greater than one indicates an increase in fluorescence, and thus hydrophobicity; a value less than one, a decrease. At a one hour end-point after addition of activator BH3 proteins 10 labeled residues had undergone a transition to a substantially more hydrophobic environment, 8 were relatively unchanged ($1<F/F_0<2$) and one residue (number 47), moved to a more hydrophilic environment (Fig. 2b). Residue 47 is located within the loop between helices 1 and 2, which is known to undergo a conformation change upon Bax activation, and both the magnitude and direction of the NBD fluorescence change suggests that this residue becomes more solvent exposed. Multiple residues outside of the pore-forming and C-terminal helices (e.g., residues 15, 62, 184, and 188) had relatively low absolute NBD fluorescence but large relative fluorescence changes, indicating that the rearrangements of Bax during pore formation encompass most regions of the protein, not only those known to insert in the membrane. Furthermore, the relative change in emission (F/F_0) indicates that irrespective of whether Bax was activated by cBid or Bim at end point the overall conformation of membrane-inserted oligomerized Bax was unaffected by which activator BH3 protein was used.

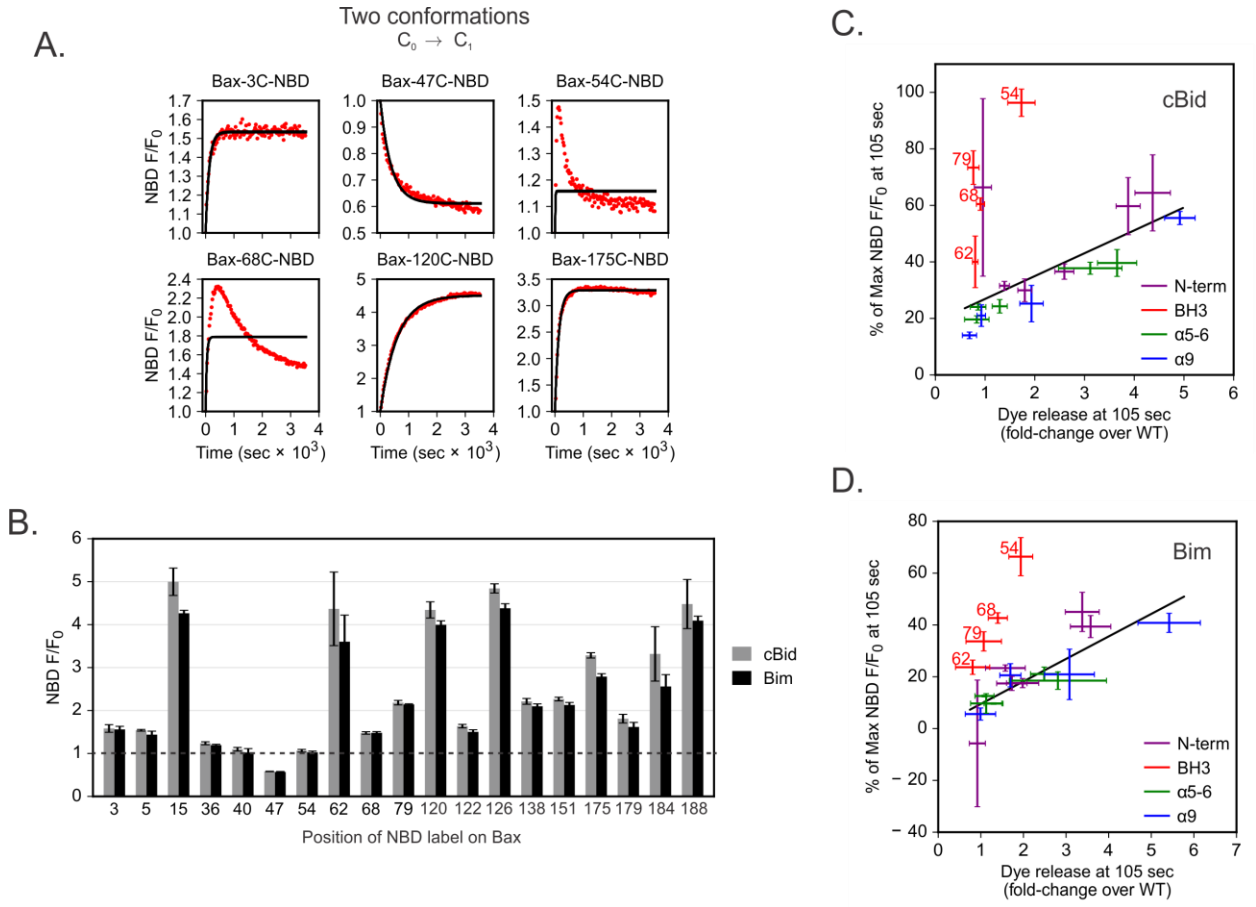

Figure 5.2 - Kinetics of NBD fluorescence changes

A. Example NBD-Bax fluorescence time courses, normalized to the initial fluorescence F_0 (red points). Each of the six time courses shown used cBid as the activator BH3 protein and is the first of three replicates. Black lines show fits of the two-conformation model.

B. One hour endpoint of the relative change of NBD emission at 530 nM after the addition of 20 nM cBid (grey) or Bim (black) in the presence of liposomes. Error bars represent +/- S.D. with n = 3.

C. Percentage of maximum NBD fluorescence reached at an early time point (105 sec), plotted against the amount of dye release relative to wild-type Bax, using cBid as the activator.

D. As for (**B**), but using Bim as the activator.

5.3.2. Most labeled Bax proteins can form pores but vary widely in permeabilization kinetics

Labeled single-cysteine Bax mutants have been used successfully in several previous equilibrium (Annis et al., 2005; Bleicken et al., 2014; Westphal et al., 2014a; Zhang et al., 2016b), and kinetic (Kushnareva et al., 2012; Lovell et al., 2008) structural studies of Bax. Consequently we expected that for most residues in Bax cysteine substitution and addition of the low-molecular-weight NBD would minimally affect the activity of the proteins. Measurements of membrane permeabilization confirmed this as at end-point two-thirds of the labeled proteins were 80-100% as active as unlabeled native protein, (SOM Section 1.1). However, mutants with NBD-labeled cysteine at positions 68, 79, 120 and 188 have attenuated pore-forming function but still permeabilized at least 40% of the liposomes in one hour, suggesting that the mechanism of permeabilization is unlikely to have been changed significantly. In contrast, most Bax mutants including those that had endpoint release activity similar to wild-type, showed an increased initial rate of dye release relative to the unlabeled native protein, suggesting that for many variants the addition of the NBD label preserved Bax pore formation activity but destabilized the protein by reducing energy barriers between its conformational states (SOM Section 1.1, 3.1).

The variation in the kinetics of pore formation activity prevented a straightforward comparison of NBD insertion timescales, even among those mutants with monotonic kinetics (e.g., by the comparison of reaction half-times). To assess the degree to which the observed variation in NBD fluorescence dynamics was attributable to differences in permeabilization activity, we plotted the percentage of NBD F/F0 change against dye release relative to WT Bax at a fixed early time point and again found that the residues fell into a set of two classes (Figures 2C & D). For residues outside the BH3-groove, faster rates of NBD fluorescence change corresponded to faster rates of dye release in a roughly linear pattern, suggesting that most of the differences in the initial rates of NBD fluorescence change can be explained by differences in overall activity attributable to the addition of the NBD label. However, residues in the BH3-groove (54, 62, 68, and 79) showed significant early NBD fluorescence changes that differed considerably from what would be expected due to pore formation activity differences alone. This suggests that the rapid increase in the fluorescence of these labeled residues is due to a structural rearrangement that precedes dye release.

5.3.3. Kinetic analysis of NBD fluorescence suggests three or four distinct conformational states

We sought to integrate the kinetic information from the entire set of Bax proteins into an overall picture of the conformation changes involved in Bax pore formation. We hypothesized that 1) pore formation requires a discrete series of conformational changes, and 2) the labeled variants differed in their transition rates between steps but not in the overall number of steps. To formalize this hypothesis, we considered a simple kinetic model involving linked equilibria between conformational states of Bax, each state having a different NBD fluorescence intensity for the labeled residue:

$$Bax_{F1} \leftrightarrow Bax_{F2} \leftrightarrow Bax_{F3} \leftrightarrow \ldots \leftrightarrow Bax_{Fn} \quad 1)$$

Because our data comprise bulk measurements of a reaction with individual Bax molecules distributed among different conformational states, the experimentally observed NBD fluorescence at any given time *t* is given by the summation over the concentrations of the different conformers:

$$NBD(t) = \sum_{i=1}^{n} C_i \, [Bax_{Fi}(t)], \quad 2)$$

Here the C_i are parameters denoting the NBD fluorescence of each of the *i* states of Bax. Though the generalized scheme in Eq. 1 incorporates both the forward and reverse reactions, in our analysis we considered models containing only irreversible forward reactions:

$$Bax_{F1} \xrightarrow[k_1]{} Bax_{F2} \xrightarrow[k_2]{} Bax_{F3} \xrightarrow[k_3]{} \ldots \xrightarrow[k_{n-1}]{} Bax_{Fn} \quad 3)$$

For experimental systems such as ours where only the aggregate fluorescence is measured, the reversible and irreversible formulations produce equivalent fits to the data and are indistinguishable in terms of their ability to identify the number of conformational states (Supplementary Information).

Qualitative inspection suggests that the kinetic curves for several of the NBD-labeled residues are reasonably well approximated by the two-state model, which takes the form of a single-exponential equation (Methods, Eq. 8;). This is particularly true for residues outside the BH3-groove (e.g., residues 3, 120, and 175 shown in Figure 2A; others in SOM Section 3.4). However, the non-monotone fluorescence curves of some BH3 region residues (62, 54, 68, 79) are very poorly fit by the single-exponential equation Eq. 8 (Figure 2A). Indeed, it can be proven that they cannot be fit by any two-conformation scheme in the form of Eq. 1 where the labeled residue undergoes a single fluorescence transition, due to the form of the mathematical formula describing such systems.

We therefore compared the performance of reaction schemes involving two to five conformational states by conditioning them on the NBD fluorescence data using Bayesian parameter estimation. An advantage of this approach is that, given a suitable error model (e.g., Gaussian-distributed error in the fluorescence time courses), the data can be used to estimate both the range of likely parameter values as well as the plausibility of models having different numbers of parameters (different numbers of conformations in this case)(Gelman, 2014). To limit the scope of our analysis to only conformation changes having an observable impact on our experimental data, we chose uniform prior distributions for the kinetic parameters bounded by the relevant timescales of the experiment (ranging from 10^{-1} to 10^{-6} sec^{-1}). We considered two prior probability distributions for the fluorescence scaling parameters based on the experimentally observed relative and absolute dynamic ranges for the dye NBD: one uniformly distributed over this range and the other Gaussian with greater probability assigned to smaller relative changes. As we discuss below, the results were similar for both fluorescence priors but we consider the latter assumption more realistic due to the observed data since none of the residues change more than 5-fold from their initial NBD fluorescence. Given the range of absolute fluorescence values we observe (~3000 counts for residue 184C at C0 to ~130,000 counts for residue 120 at C2) it is not equally probable that hydrophilic residues, like 184C,

would reach the highest fluorescent state of 130,000 counts (F/F0 of ~43) versus reaching a lower fluorescent state such as 9,000 counts (F/F0 of 3).

After calibrating the models we found that all labeled residues, not only those in the BH3 region, showed evidence of existing in at least three conformational states. This is illustrated by the dramatic improvement in the fits to data in going from two to three states (compare Figure 2A to 3A) and the corresponding improvement in model likelihood (Figure 3B). A handful of residues showed evidence of a fourth conformational state (Figure 3B and SOM Section 3.5). Notably, none of the residues showed evidence supporting five or more conformations (i.e., four or more fluorescence transitions). From these data we conclude that during the process of pore formation, Bax occupies at least three conformations: an initial one corresponding to the aqueous state, the final fully membrane-inserted state found at equilibrium and a transiently formed intermediate linking the two. Multiple residues throughout Bax change in hydrophobicity with each state transition.

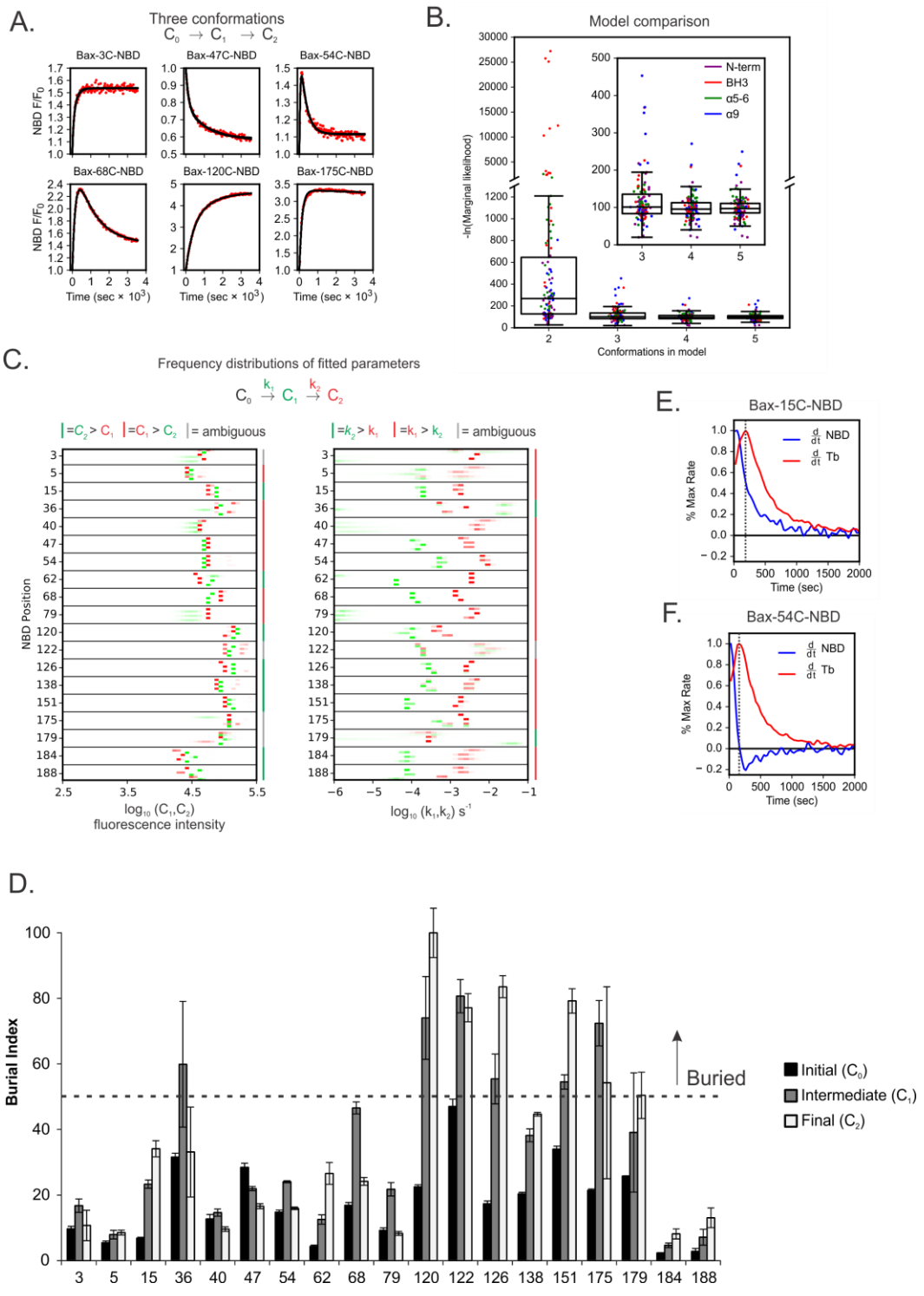

Figure 5.3 - Fits of kinetic models to NBD fluorescence time courses

A. Fits of the three-conformation model to the curves in Figure 2A.

B. Marginal likelihood values calculated for different models for all NBD time course replicates in the dataset by Markov chain Monte Carlo sampling. Each NBD time course replicate is colour coded based on where NBD is labeled on Bax (purple – N-terminus; red – BH3-groove; green – α5,α6; blue – α9). Inset shows differences between the three, four, and five conformation models on an increased scale. Boxes extend from the first to the third quartile of the data, with a horizontal line at the median; whiskers extend above and below to 1.5 × the interquartile range.
C. Marginal posterior distributions of the parameters of the three-conformation model using a Gaussian prior distribution for the fluorescence intensities of C_1 and C_2. The color intensities along each horizontal red and green band indicate the Markov chain Monte Carlo sample frequency at the corresponding interval of the parameter distribution. In the C_1/C_2 plot (left), frequencies for C_1 are indicated in red, C_2 in green; in the k_1/k_2 plot (right), frequencies for k_1 are indicated in red, k_2 in green. The section of the plot for a given residue contains three corresponding pairs of red and green bands; each pair is drawn from fits to a single experimental replicate.
D. Residue burial index calculated by normalizing the predicted absolute fluorescence values from Figure 3C for each residue to that of the predicted fluorescence value for Bax L120C-NBD in the final conformation (C_2). Error bars represent +/- S.D. with n = 3.
E. Derivatives of NBD and terbium release time courses for Bax-15C-NBD (first replicate, cBid as activator), normalized to the maximum rate of change. Derivatives were calculated numerically after processing the curves with a low-pass filter to reduce noise. The curves shown were for the first experimental replicate with cBid as the activator.
F. As for (**E**), but for Bax-54C-NBD (first replicate, cBid as activator). The vertical grey line is drawn at the peak rate of change of Tb:DPA release.

5.3.4. Fitted model parameters suggest a fast transition to an intermediate conformation with relatively higher hydrophobicity for the BH3 and surrounding regions

The estimated parameters for the three-conformation model comprise residue-by-residue rate constants for the first and second transitions (k_1 and k_2) as well as the fitted NBD fluorescence intensities of the intermediate and final conformations (C_1 and C_2; Figure 3C). For 16 of the 19 pairs of well-determined rate constants, (those that were uniquely identifiable with a Gaussian prior), k_1 was at least 6-fold faster than k_2. Three labeled residues in the N-terminus were mixed in their behavior (positions 3- $C_1>C_2$; 5-ambiguous; 15- $C_2>C_1$). Residues in the α1-2 loop (36, 40 and 47) were more hydrophobic in the intermediate state compared to the final state ($C_1>C_2$; Figure 3C). Moreover, with the exception of residue 62, residues in the BH3 groove (positions 54, 68 & 79) were also in a more hydrophobic environment in the intermediate

state than the final equilibrium state (C_1>C_2; Figure 3C). In contrast, residues in α5, α 6 and α9 (positions 120-188) were associated with lesser or equal hydrophobicity in the intermediate conformation (C_2>C_1; Figure 3C). From these data we conclude that a Bax intermediate conformation forms rapidly in the presence of activator BH3 proteins and then decays slowly to the equilibrium, pore-associated state. The environment of the BH3 groove and the α1-2 loop is more hydrophobic in the intermediate than the final conformation, whereas the membrane binding helices α5, α 6 and α9 are more hydrophobic in the final conformation compared to the intermediate.

5.3.5. Bax topology is consistent with insertion of helices 5, 6 and 9 and the BH3:in-groove dimer model

Due to the environment sensitivity of NBD, the fluorescence values generated by fitting the kinetic data (Figure 3C, left) are directly correlated with the hydrophobicity of the environment of that residue in each conformation state. Since, multiple studies have confirmed that residue L120 of Bax is embedded within the bilayer (Annis et al., 2005; Westphal et al., 2014a; Zhang et al., 2016b) we generated a burial index by normalizing all fitted fluorescence values (C_1 and C_2) to that of the fluorescence of L120C in the final (C_2) state (Figure 3D). Previous topological studies of Bax-membrane interactions have suggested that the α5, α6 and α9 helices are associated in-plane with or buried within the membrane at equilibrium (Annis et al., 2005; Westphal et al., 2014a; Zhang et al., 2016b). Figure 3D shows that residues 120, 122 and 126 in α5 all move to more hydrophobic environments consistent with embedding within the membrane, whereas residue 138 on α6 transitions from hydrophilic to a hydrophobicity between being fully exposed (e.g. residue 3) and fully embedded (e.g. residue 120). Residues in helix 9 (175, 179) are in environments consistent with being embedded within the membrane, whereas residues at the end of the helix (184 and 188) are in solution exposed environments (Figure 3D).

As reported above residues in the α1-2 loop (36, 40 & 47) and BH3 groove of Bax (54, 68 & 79) are in a markedly more hydrophobic environment in the intermediate (C_1) state compared to the initial (C_0) or final (C_2) states (Figure 3D). However, with the exception of C_1 for residue 36, all fluorescent states for residues 36-79 are consistent with a more hydrophilic environment suggesting that these residues are not embedded within the membrane. As

discussed above this increased fluorescence in the intermediate state is temporally similar to cBid and Bim binding to Bax. The temporary increase in the hydrophobicity of these residues upon binding cBid and Bim could be due both the formation of an activator:Bax binding interface as well as an increased proximity of Bax to the membrane. This region then transitions to a more hydrophilic environment when Bax is in a pore at equilibrium compared to α5-9 consistent with models where the BH3 groove (α2-4) is above the membrane or lining the pore (Bleicken et al., 2014; Czabotar et al., 2013).

5.3.6. The relative rates of NBD fluorescence change and dye release suggest that the intermediate conformational state precedes pore formation

A key question about the intermediate Bax conformation suggested by the NBD fluorescence data is whether it precedes or follows the formation of a pore. The date in Figure 2C and D suggested that for the BH3-groove residues (54, 62, 68, and 79) there was an initial increase in NBD fluorescence that preceded a proportional increase in dye release. To explore this relationship further, we calculated the time derivatives of both the NBD and dye release time courses (SOM Section 3.3). While the rate of change of NBD fluorescence is almost invariably fastest at the initial time points, the rate of change of dye release starts more slowly and reaches a maximum before declining to zero at equilibrium (shown for Bax-15C-NBD and Bax-54C-NBD in Figure 3C-D; other residues in SOM Section 3.3). This process is evident in the original dye release time courses as a slight lag phase at the earliest time points that is also present for wild-type Bax (SOM Section 3.1). The appearance of the lag phase in dye release was consistent for all mutants except a handful with low endpoint activity (68, 79, 179, and 188), though the duration of the lag between the labeled mutants varied depending on their release kinetics (mutants with accelerated release kinetics had a shorter lag phase). The time course derivatives indicate that even for the residues outside of the BH3-groove with monotonic kinetics, NBD fluorescence at the labeled residues undergoes an initial change that precedes pore formation.

5.3.7. Both cBid and Bim remain associated with Bax at equilibrium, but the cBid:Bax interaction peaks early

To order Bax conformational changes with respect to binding of activator BH3 proteins we measured Förster resonance energy transfer (FRET) between labeled Bax and cBid or Bim. Here, as above, Bax was labeled with NBD and Tb:DPA encapsulated liposomes were used. In addition, DAC labeled cBid and Bim were added to activate Bax. NBD is a good FRET acceptor for DAC, which allows the interaction between the activator BH3 protein and Bax to be measured via FRET in addition to simultaneously measuring Bax residue environment changes and pore formation (Figure 1C) (Kale et al., 2014; Lovell et al., 2008). For this analysis we chose 12 NBD-Bax derivatives with high levels of pore formation activity. Single cysteine mutants of cBid and Bim were created in which the cysteine was located 1 residue N-terminal of the H0 residue in the BH3-domain of cBid and Bim (residues 85 and 89 respectively) (Czabotar et al., 2013). This site was chosen because the BH3-domain of the activators is required for Bax activation and binds directly to Bax thus increasing the chance of a good FRET signal. Furthermore, the binding site and orientation for the BH3-groove is known in sufficient detail that as long as cBid and Bim bind to this same site on Bax the DAC donor dye on Bid and Bim will be located similar distances from the NBD dye on Bax.

For these experiments, FRET measurements were performed in triplicate for each of the 12 NBD-labeled Bax variants, incubated with either cBid-DAC or Bim-DAC, for a total of 72 assays (plots of raw data in SOM Section 5.1). Incubation of Bax with either DAC labeled cBid or Bim resulted in similar extents of pore formation confirming that the labeled proteins activated Bax equivalently (Figure S1a). Additionally, unlabeled and DAC labeled Bim and cBid proteins caused comparable changes in fluorescence emission of the NBD labeled Bax residues (Figure S1b). Accordingly, the DAC dye did not affect the Bax activation function of the BH3 proteins or the values measured for environment induced changes in NBD fluorescence, as expected (Lovell et al., 2008).

Changes in FRET occurred on a timescale similar to the initial environment changes in NBD fluorescence, reaching maximum levels in 1-15 minutes (Figure 4A and SOM Section 5.3). Endpoint %FRET between the activator BH3 proteins and Bax were variable for the different

sites on Bax, with the largest values for residues 36 and the α5 helix residues 122 and 126 for both cBid-DAC and Bim-DAC (Figure 4B). Strikingly, for several labeled Bax residues including 54C-NBD, the cBid-DAC FRET reached an early peak within 1-8 min and then declined, whereas for Bim, the FRET levels rose on the same timescale and were sustained (Figure 4A and SOM Section 5.1). These differences were quantified by comparing the maximal and endpoint FRET values using fitted curves to reduce experimental noise (Figure 4C). The differences in FRET dynamics between cBid-DAC and Bim-DAC suggest that in the later phases of activation, these proteins either adopt different bound states with Bax or have different affinities for Bax pre- or post-activation. Nevertheless, the fact that both activators have substantial FRET with at least a subset of Bax residues at the experimental endpoint indicates that they remain in an equilibrium binding state with Bax at a point when most Bax is in pores, consistent with our previous findings for tBid and Bax-C126-NBD (Lovell et al., 2008)

5.3.8. The initial conformational transition of Bax correlates with activator:Bax complex formation, the latter to Bax oligomerization

To compare the dynamics of cBid- and Bim-Bax FRET with changes in NBD-Bax fluorescence we fit the three-conformation model to the FRET and NBD time course data for two NBD-labeled Bax variants representing the BH3-groove and membrane-inserting regions (Figure 4D). For each variant we fit a single set of rate parameters and four fluorescence scaling parameters: two parameters for the NBD fluorescence of the intermediate and final states, and two parameters for the average Bax: BH3 protein FRET efficiencies associated with the two states. We found that the three-conformation model fit the data for Bax-54C-NBD and Bax-C126-NBD well with a single set of rate parameters, implying common underlying dynamics (Figure 4D). The marginal posterior distributions for the FRET efficiencies of the intermediate and final states indicated that, for both Bax-54C-NBD and Bax-C126-NBD, the maximal FRET efficiency occurred after the initial $Bax_{F1} \rightarrow Bax_{F2}$ transition, declining somewhat after the $Bax_{F2} \rightarrow Bax_{F3}$ transition. We therefore conclude that the initial hydrophobicity change of Bax occurs largely simultaneously with the formation of the Bax: BH3 protein complex.

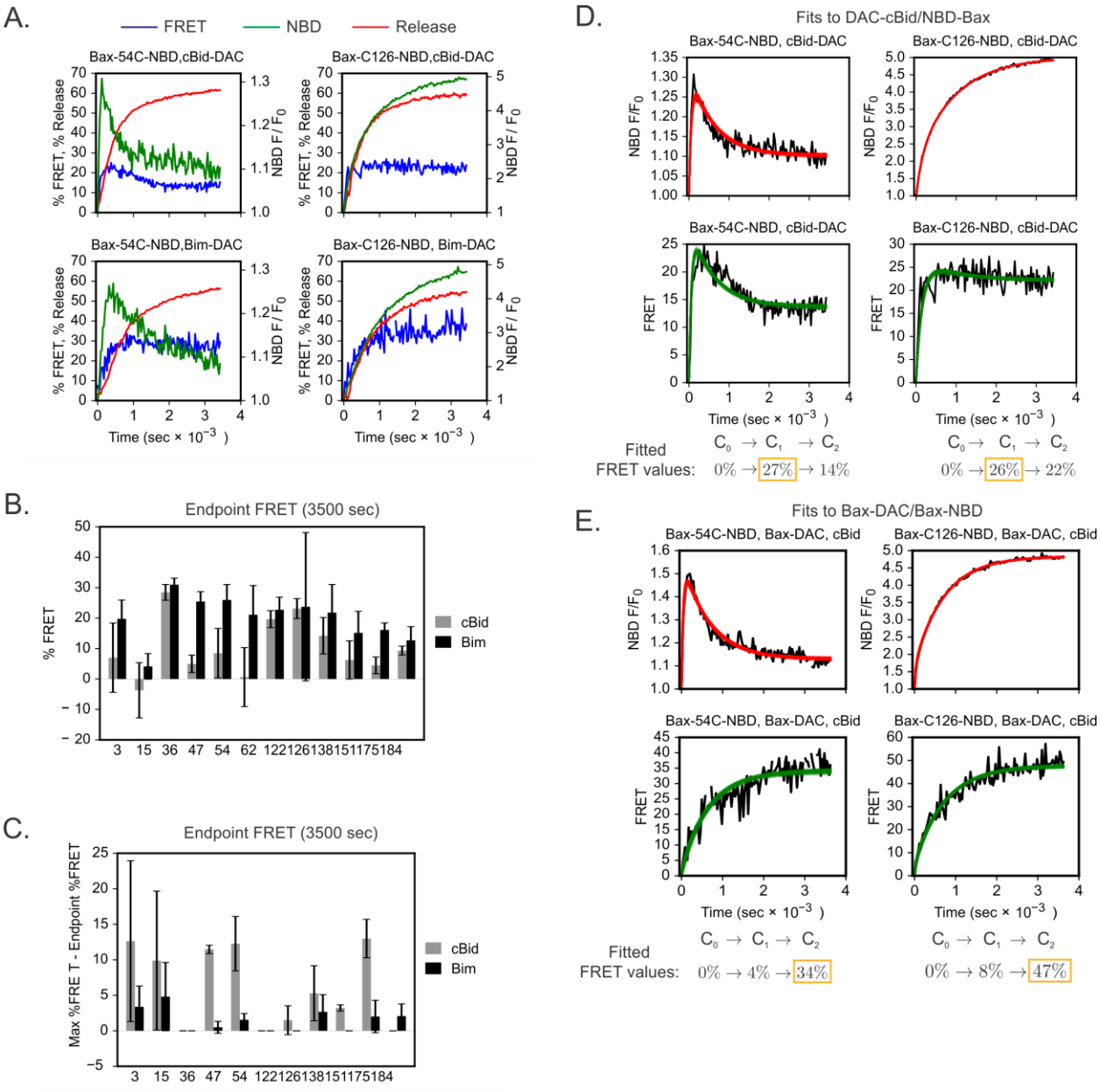

Figure 5.4 - FRET measurements of cBid-83C-DAC and Bim-L-89C-DAC with Bax

A. Simultaneous measurements of dye release, NBD-Bax fluorescence, and Bax:BH3 protein FRET for Bax-54C-NBD- and Bax-C126-NBD.

B. Endpoint FRET between activator BH3 proteins and labeled Bax mutants. Error bars represent +/- S.D. with n = 3

C. Difference between maximal and endpoint Bax: BH3 protein FRET. Error bars represent +/- S.D. with n = 3

D. Joint fits of three-conformation model to NBD fluorescence and cBid-DAC:Bax-NBD FRET time courses.

E.) Joint fits of three-conformation model to NBD fluorescence and Bax-DAC:Bax-NBD FRET time courses.

Bax oligomerization is a known requirement for pore formation (George et al., 2007). To determine the timing of Bax oligomerization relative to the conformation changes indicated by NBD fluorescence, we collected Bax:Bax FRET data using Bax-C126-DAC as the fluorescence donor (Kale et al., 2014; Lovell et al., 2008) (plots of raw data in SOM Section 6.1). Unlike FRET with cBid and Bim, Bax:Bax FRET increased late relative to the conformation changes of Bax. Using the same analysis as for the Bax:BH3 protein FRET data, we found that a three-conformation model with a single set of rate parameters could simultaneously fit both the NBD and Bax:Bax FRET data (Figure 4E). In addition, the parameter estimates indicated that Bax:Bax FRET increases monotonically, reaching a maximum in the final state. From this we conclude that the hydrophobicity changes associated with the final conformation of Bax correspond closely in time to the formation of Bax oligomers, and that a three-conformation model is sufficient to account for the dynamics of both protein-membrane and protein-protein interactions during Bax pore formation.

5.3.9. Cancer-associated Bax mutants have defects in specific conformational transitions required for pore formation

The development and validation of a 3 state kinetic model for Bax activation by BH3 proteins provides a quantitative framework to analyze the effect of mutations on Bax mediated pore formation. Therefore we used our kinetic model to reveal the specific molecular defect in mutants previously characterized to alter Bax function and to characterize new Bax point mutations found in human cancers. Point mutations known to abrogate Bax function include mutations found in cancer cell lines (G67R, G108V, G179E) (Fresquet et al., 2014; Meijerink et al., 1998), and mutations of S184, an AKT phosphorylation site (S184V, S184E)(Gardai et al., 2004; Nechushtan et al., 1999).

Bax acts as a tumour suppressor (Yin et al., 1997) thus mutations in Bax that disrupt pore formation are expected to reduce apoptosis, a necessary step in oncogenesis (Hanahan and Weinberg, 2011). We therefore postulated that a subset of the Bax mutations found in human cancers might inhibit Bax either by truncating the protein such that it is entirely non-functional or by blocking one or more of the structural transitions of Bax identified here. Increased

expression of multi-domain anti-apoptotic proteins is often seen in cancer therefore, we also expected that some cancers would be tolerant of mutations that increase the pore forming activity of Bax. Across all tumour types the most frequent Bax mutations recorded in cBioPortal (Cerami et al., 2012; Gao et al., 2013) were truncation mutations and of those the most frequent was a frameshift upstream of the BH3-domain (residue E41) that would abrogate all Bax function. However, we also identified multiple low-frequency missense mutations throughout the rest of the protein (Figure 5A).

We cloned and purified 19 Bax point mutants and analyzed their pore forming activity (Figure 5B). Activity was summarized as the concentration required for 50% dye release from liposomes over a 3 hour time course (i.e., the EC_{50} value). Six of the Bax point mutants (G67R, G108E, G108V, L113P, G179E, S184E) were 2- to 30-fold less active than wild type. The majority of these mutants have been previously characterized to abrogate Bax function *in vitro* or in cancer cell lines (G67R, G108E, G108V, G179E, S184E) (Fresquet et al., 2014; Kim et al., 2009; Meijerink et al., 1998; Nechushtan et al., 1999) however of these G67R, G108V and L113P were also found in humans cancers via cBioPortal (Cerami et al., 2012; Gao et al., 2013).

To identify the basis for the failure of pore formation in these six mutants, they were labeled with NBD at C126 and their interaction with cBid, insertion into membranes and pore formation were characterized (Figure 5C). Fluorescence of NBD at position C126 in the α6 helix reports primarily on the formation of the active conformation in which Bax has embedded in membranes (Kale et al., 2014; Lovell et al., 2008). We found that the L113P mutant showed little activity across all three fluorescence measures, very little FRET with cBid-DAC, and reduced 126C fluorescence relative to Bax-126C-NBD and minimal pore formation. The lack of activity in both upstream (FRET with cBid) and downstream (pore formation) measures suggests that this mutant does not bind cBid and is therefore blocked in the initial conformational transition. The cancer-cell line associated G179E (Goldstein et al., 2000) had a unique pattern of activity, with Bid-Bax FRET similar to WT, pore formation levels close to wild-type but relatively low α6-helix insertion consistent with a conformational defect in the membrane embedded oligomer (Figure 5C).

Finally, the G67R, G108V, G108E and S184E appear to represent a class of mutants blocked at the intermediate conformation. They exhibited high cBid-Bax FRET but low levels of α6-helix insertion and pore formation, consistent with failure of these mutants to complete the transition from intermediate to final conformation. From this data, we conclude that point mutations in Bax can affect the process of pore formation at all three steps, with some mutations preventing the initial transition to a required intermediate conformation, and others the transition from this intermediate to inserted in membranes and finally one mutant with a defect in pore formation.

5.4. Discussion

A key challenge in understanding the pore formation mechanism of Bax has been the difficulty in obtaining a dynamic picture of the full-length protein in membranes at high resolution. Most investigations of the activation of Bax used detergents known to change the conformation of Bax or truncated recombinant proteins (e.g. truncated Bax or BH3 peptides to activate Bax) or do not include a lipid bilayer. This is likely due to the difficulty in studying the Bcl-2 family proteins which require insertion into membranes to be fully functional and adopt their proper conformations (Leber et al., 2010). In this study we use a highly defined *in vitro* system free of detergents comprised of mitochondrial-like liposomes and fluorescently labeled full-length recombinant proteins. We combine an extensive dataset of kinetic measurements of fluorescently labeled Bax mutants with an analytical framework that allows us to integrate data from these mutants despite their differing activities. Taken together, our results indicate that Bax undergoes at least two significant structural rearrangements en route to dimerization and pore formation, passing through an intermediate state associated with activator BH3 protein binding that results in significant conformational changes across the entire protein (Figure 6). The transition from this intermediate to the final state is concomitant with Bax homo-oligomerization.

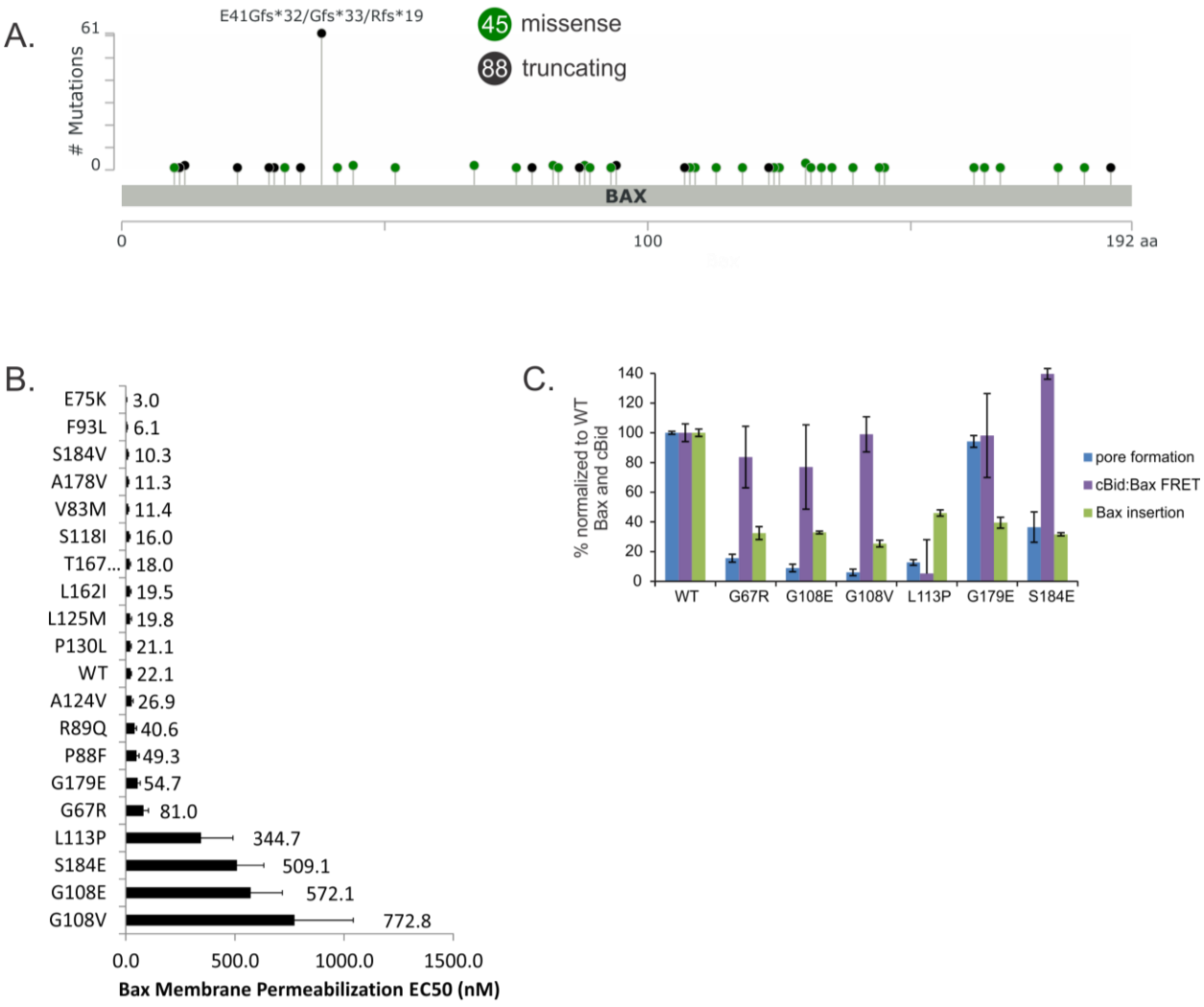

Figure 5.5 - Mechanistic characterization of Bax point mutations in cancer

A. cBioPortal generated figure of genomic alterations in Bax identified by cancer genome sequencing.

B. ANTS/DPX release activity of Bax point mutants represented by EC_{50}. Error bars represent +/- S.D. with n = 3.

C. Endpoint dye release, cBid-Bax FRET, and Bax-C126-NBD fluorescence normalized to the values of 'WT' Bax and cBid (Bax-C126-NBD + cBid-DAC) of labeled Bax point mutations

We identified the number of relevant conformation states by calibrating an ensemble of models to our experimental data. While the two-transition, three-conformation model captured the dynamics of virtually all of the labeled mutants we tested, data from several mutants suggested a high probability of a fourth conformation (third transition). Though Bayes factor calculations indicate that for some mutants the four conformation model is many times more likely than three, the size of the effect is likely to be small—that is, the additional conformation is either at relatively low concentration or involves only a very slight conformational change. One interpretation is that this fourth conformation involves subtle environmental changes that occur during large-scale oligomerization or pore enlargement (Gillies et al., 2015; Kuwana et al., 2016). Another possibility is that the apparent support for a fourth conformation is due to kinetic phenomena that are outside the scope of our class of simple models (saturation of activator BH3 proteins, bimolecular reactions, etc.). Proper attribution of this additional timescale evident in the Bax activation process will require additional modeling and experiments.

There have been a handful of previous studies aimed at understanding the Bax pore formation mechanism via kinetic modeling (Kushnareva et al., 2012; Saito et al., 2000). In one of the most recent, Kushnareva et al. identified a "lag phase" in pore formation that was apparent in dye release measurements using mitochondrial Outer Membrane Vesicles (OMVs) but not synthetic liposomes. Our results suggest that there is a lag phase in dye release for synthetic liposomes as well, though it is less pronounced than what is observed for OMVs, and that it is associated with the time required for Bax to pass through the intermediate conformation en route to forming a fully assembled pore.

Our kinetic analysis agrees with our previous data suggesting that Bax binding to activator BH3 proteins causes the insertion of Bax within the membrane rapidly followed by Bax oligomerization and pore-formation (Lovell et al., 2008). This can be clearly seen for the majority of residues of Bax particularly those in α5, α6 & α9 that insert into the lipid bilayer. However, the analysis of some individual residues suggests that the situation is somewhat more complex. There are clear changes in the environment of residues within the BH3-groove of Bax (54C, 62C, 68C and 79C) temporally similar to cBid binding and much faster than membrane permeabilization. These residues remain in relatively hydrophilic environments compared to the membrane embedded helices of Bax (Fig. 2C) suggesting that the changes in NBD fluorescence

are due to changes in the conformation of Bax that occur rapidly upon binding cBid or that bound cBid changes the environment of these residues directly (Figures 2 C-D, Figure 4A). Strikingly, for Bax-54C-NBD, a BH3-region mutant exhibiting both non-monotone kinetics and a measurable lag phase in dye release, the time point at which the maximum NBD fluorescence is reached (the zero of the NBD derivative) corresponds very closely to the time point at which dye release achieves its maximum rate (the peak in the dye release derivative; vertical line, Figure 3F). Taken together, the NBD and dye release kinetics indicate that many regions of Bax undergo a concerted transition to an intermediate state that precedes the formation of pore formation and dye release. In light of the three-conformation reaction scheme, one possible interpretation is that the *rate* of dye release is directly proportional to the *abundance* of the intermediate species associated with increased hydrophobicity at the Bax BH3-groove.

Engagement of the hydrophobic groove of Bax by cBid and Bim activates Bax, yet binding of this groove by the BH3-domain of another Bax molecule is necessary for pore formation (Czabotar et al., 2013; Dai et al., 2011; Dewson et al., 2012). The fact that the addition of excess activator BH3 protein does not appear to inhibit Bax suggests that the hydrophobic groove changes conformation in such a way as to allow Bax to discriminate between activator BH3 protein binding and dimerization. It is possible that this rearrangement of the BH3-groove is the basis of the intermediate conformation we identify in our study.

Unlike the predictions of most but not all models (Shamas-Din et al., 2013b) cBid and Bim remain bound to Bax at equilibrium. Our fluorescence based *in vitro* assay measures the fluorescent signal from the total population of labeled proteins, as such we cannot discriminate if cBid or Bim remain bound to Bax in a pore, or bound to a sub-population of Bax monomers. We hypothesize that both occur based on a recent study demonstrating that Bax, once activated, bound a Bim-BH3 peptide as an oligomer of Bax and as Bax monomers (Tsai et al., 2015).

Kinetic studies of the conformation changes of Bax during its transition from a soluble monomer to a membrane embedded oligomer provide an interpretive framework for data from studies that observe snap-shots of various conformations of Bax i.e. Bax membrane topology (Annis et al., 2005; Westphal et al., 2014a; Zhang et al., 2016b) or structural studies (Czabotar et al., 2013; Robin et al., 2015; Suzuki et al., 2000). Predicting the hydrophobicity of each residue

and comparing that to the hydrophobicity of a bona fide membrane embedded residue (L120) and modeling the kinetic data enabled the creation of a picture of the topology of Bax for all 3 of the conformation states identified (Figure 3D). This data supports a model in which the BH3-groove of Bax undergoes a significant conformation change to a more hydrophobic environment upon binding activator BH3 proteins. This initial change could result from the displacement of the Bax BH3-domain and thus changes in the BH3-groove structure by the BH3-domain of the activator protein that is required to form dimers (Dewson et al., 2008; Gavathiotis et al., 2010; Zhang et al., 2016b). Only after this initial conformation change occurs do helices 5, 6 and 9 insert into the membrane whereas the rest of the Bax (α1-4) remains in a more hydrophilic environment. This data is consistent with, but does not confirm, the BH3-domain:groove model of Bax activation whereby Bax forms dimers via reciprocal BH3-domain:groove interactions between two Bax monomers. Furthermore, considering that both helix 5 and 6 are amphipathic it is entirely possible that one side of both helix 5 and 6 is embedded within the bilayer while the other is exposed to solution, either lining the pore or on the surface of the membrane (Bleicken et al., 2014; Westphal et al., 2014a).

Quantitative assessment of a series of Bax point mutants derived from cancer genome sequencing studies or previously characterized cancer cell lines revealed that by far the most frequent genomic alteration of Bax in cancer is a frameshift deletion near the N-terminus, supporting the view that loss of Bax pore formation activity is in most cases tumour-enhancing. Nevertheless, some mutants appeared to have more pore formation activity than wild-type Bax, and others less. The majority of Bax missense mutations did not abrogate Bax function and are infrequent, suggesting that they were due to the genomic instability of cancers. Nevertheless, some point mutations did abrogate Bax function at discernable steps in the Bax activation pathway. These mutants could be used to further characterize the conformation of Bax when it is locked at a certain point in the pathway, potentially aiding the discovery of small-molecule modulators of Bax function.

Of the Bax mutants lacking membrane permeabilization function, Bax L113P could not bind cBid or insert into membranes. Thus Bax L113P could not transition to the intermediate conformation. The addition of a proline to the membrane embedding α5 helix of Bax is likely enough to abrogate all Bax function as Bax lacking helix 5 or with a proline substitution in helix

5 at a different position cannot oligomerize or form pores (George et al., 2007). It is noteworthy that the majority of mutants which inhibited Bax function were blocked in the intermediate conformation, one step upstream of insertion into the bilayer. As Bax insertion into membranes is the rate-limiting step in its activation mechanism (Lovell et al., 2008; Subburaj et al., 2015) this is where mutations would affect Bax function the most. While the functional role of the less common point mutations in altering tumour growth and survival is more difficult to interpret, it is important to point out that Bax conformations which are blocked at the intermediate conformation (e.g., G67R, G108V, and S184E) not only cannot form pores themselves but may also inhibit the activation of wild-type Bax and/or Bak by binding and sequestering activator BH3 proteins. Indeed, we recently discovered that Bax S184E acts as a dominant-negative Bax and prevents both liposome permeabilization and apoptosis in cells induced by a wide variety of apoptotic stimuli (manuscript in preparation).

Two point mutants from this dataset (G179E and S118I) did not abrogate Bax function as was previously reported (Fresquet et al., 2014; Zhang et al., 2016a). Fresquet et al. showed that Bax 179E was unable to target mitochondria in cells conferring resistance to the BH3 mimetic ABT-199. Bax G179E has half the activity as WT Bax (Figure 5B) but is still able to form pores (Figure 5C). In cells Bax is exists in an equilibrium between the cytosol and peripherally bound to the mitochondria where Bax is primarily cytosolic because the off-rate is faster than the on-rate (Schellenberg et al., 2013). Mutations to Bax C-terminus (S184V) can cause the on-rate to be faster than the off-rate resulting in Bax that is constitutively targeted to the mitochondrial outer membrane (Schellenberg et al., 2013; Todt et al., 2015). Perhaps for Bax 179E the off-rate is faster than the on-rate in cells thus allowing anti-apoptotic proteins to inhibit Bax activation and prevent MOMP. In our liposome assay only cBid and Bax are present but G179E is half as active as WT Bax. Given the lack of anti-apoptotic proteins in our system, G179E may be able to form pores albeit slower than WT Bax. Molecular dynamics simulations predicted that Bax S118I mutation would stabilize an off-pathway dimer thus preventing Bax pore formation (Zhang et al., 2016a) however we see that S118I is fully functional and is more active than WT Bax (Figure 5B). These discrepancies highlight the importance of using cell-free assays and purified proteins to characterize predicted deficiencies in the core-mechanisms of Bcl-2 family proteins free of potential confounding factors.

While this study accounts for the kinetics of the changes in Bax at a number of distinct locations along the protein, it does so primarily for a single set of concentrations of Bax, membranes, and activator. For a clearer picture of the dynamics of pore formation by Bax and the dependence of these dynamics on the balance of the various players, additional kinetic studies including titration of the various components will be needed.

There has been recent interest in developing inhibitors of Bax and Bak as a means to prevent pathologic cell death in clinical applications, especially as inhibition of executioner caspases alone has proven insufficient to halt death after MOMP (Galluzzi et al., 2015). The dual nature of the hydrophobic groove of Bax as both a site of activation and dimerization suggests that it may be difficult to identify ligands that are primarily inhibitors and not agonists. However, our results suggest that the hydrophobic groove of the conformational intermediate state may be a good target site for an inhibitor, as it could bind specifically to this partially-activated conformation to prevent Bax insertion into membranes, dimerization and pore formation.

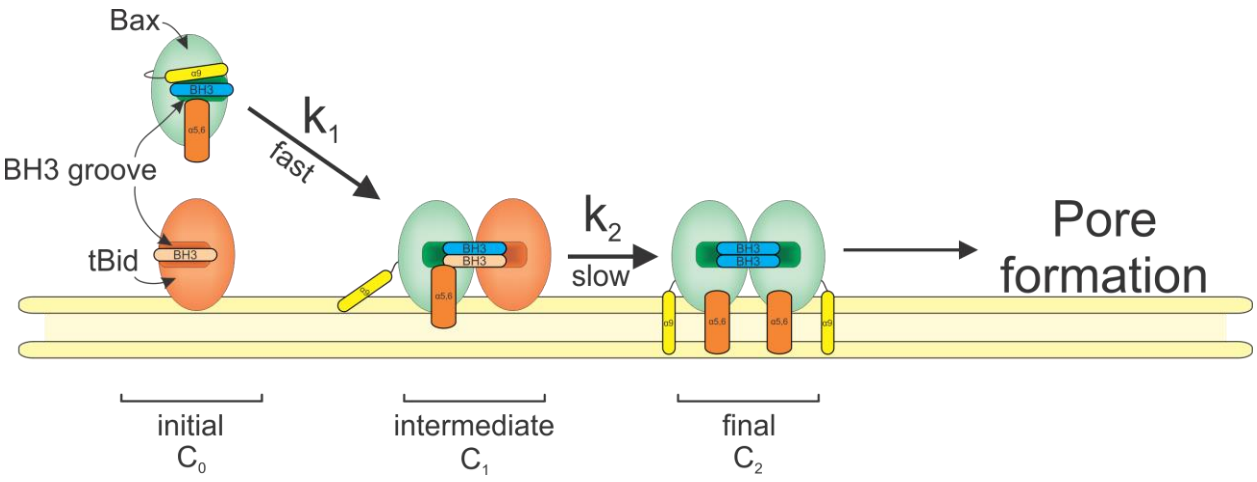

Figure 5.6 - A redefined Bax activation pathway

The current kinetic model of Bax activation suggests that Bax exists as a cytosolic monomer that reversibly tethers to the membrane via helix 9 (Czabotar et al., 2013; Garner et al., 2016; Luna-Vargas and Chipuk, 2016). Bax is then activated by a BH3 protein from the cytosol in a hit-and-run manner resulting in Bax insertion, oligomerization and pore formation. The extensive analysis of Bax conformation change kinetics upon activation by activator BH3-only proteins reported here does not support this model. We find that Bax exists in an inactive initial conformation (C_0) as a cytosolic monomer. Membrane embedded activator BH3 proteins, such as tBid, must be present at the

membrane in order to recruit and activate Bax. Activator BH3 binding to Bax, does not occur in a hit-and-run fashion and represents a time-resolved Bax:activator BH3 intermediate. This binding facilitates a rapid conformation change in the BH3-groove of Bax associated with an increase in hydrophobicity of this region. The intermediate conformation (C_1) of Bax is not fully inserted into the membrane with α-helices 5, 6 and 9 only having slight increases in hydrophobicity. Bax then transitions to a final membrane-embedded conformation (C_2) where helices 5, 6 and 9 insert simultaneously. Insertion of these helices does not appear to occur in a step-wise fashion and is the rate-limiting step in the Bax activation pathway. Upon insertion Bax rapidly oligomerizes forming pores in membranes. Furthermore our data suggests that all potential inserted forms of Bax (monomers, dimers, oligomers and pore-Bax) have similar conformations.

5.5. Methods

5.5.1. Mutagenesis, purification and labeling of recombinant proteins

Bax, cBid and Bim single cysteine mutants were created via site-directed mutagenesis. Purification and labeling of Bax, cBid and Bim single cysteine mutants was performed as in (Kale et al., 2014; Sarosiek et al., 2013). Site-specific labeling with a cysteine-reactive NBD was accomplished by mutating the two endogenous cysteines of Bax (C62 & C126) to alanine and then introducing single cysteine substitutions along the length of the protein. NBD labeling efficiency averaged ~75% with a range of 56 to 92% (SOM section 2).

5.5.2. Generation of liposomes

Mitochondria-like liposomes were generated as previously described (Kale et al., 2014). Briefly, 1 mg lipid film was hydrated with 1 ml assay buffer (200 mM KCl, 10 mM HEPES pH 7.0, 1 mM $MgCl_2$) supplemented with 1 mM $TbCl_3$ and 3 mM Dipicolinic acid. This lipid suspension was frozen and thawed 10 times, followed by 10 passes through a 100 nM pore-size membrane. The liposomes were then passed over a 10 mL CL2B gel-filtration column in order to remove unencapsulated Tb:DPA complex.

5.5.3. Fluorescence measurements

Fluorescence measurements were collected similar to that as previously described (Lovell et al., 2008). Fluorescence measurements were made in 1 mL total volume quartz cuvettes using a PTI (Photon Technologies International) fluorimeter. Samples were temperature controlled to 37°C and had constant stirring. The fluorimeter was set to read each fluorescence channel in succession using 5 nm excitation and emission bandwidths with a 1 s integration time. Channel reads were in the following order: 1) Tb:DPA fluorescence (290 excitation nm, 490 emission nm), 2) DAC Fluorescence (380 nm excitation, 460 nm emission) and 3) NBD fluorescence (475 nm excitation, 530 emission).

Background measurements were collected from sample cuvettes containing 250 ul of Tb:DPA encapsulated liposomes and 750 ul of Assay buffer supplemented with 5 mM EDTA in order to quench released Tb:DPA. Background was measured for 300s before the addition of 20 nM cBid or 20 nM Bim (labeled or unlabeled depending on the experiment). After reading for another 500s 100 nM of NBD labeled single cysteine mutants of Bax was added. Fluorescence was measured for another 3600 s before the addition of 0.5% w/v CHAPS to lyse the liposomes.

% Release was calculated as:

$$\%\ Release = 100 * (1 - \frac{F_f - F_{chaps}}{F_i - F_{chaps}})$$

Where F_i was the fluorescence before addition of 100 nM Bax, F_f was the fluorescence before the addition of CHAPS and F_{chaps} was the fluorescence after the addition of CHAPS

FRET efficiency was calculated as:

$$\%FRET\ Efficiency = 100 * (1 - \frac{F_{DA} - F_{bg}}{F_D - F_{bg}})$$

Where F_{DA} is the fluorescence DAC in a sample containing both the DAC labeled donor and NBD labeled acceptor, F_D is the fluorescence of DAC in a channel containing both the DAC labeled donor and an unlabeled acceptor, F_{bg} is the fluorescence before the addition of DAC

labeled protein. The DA and D only samples were measured in parallel using a turret which rotates samples into and out of the excitation light.

NBD F/F0 was calculated as:

$$\frac{F}{F_0} = \frac{F - F_{bg}}{F_0 - F_{bg}}$$

Where F is the fluorescence of the NBD channel after the addition of Bax, F_0 is the first fluorescent measurement upon the addition of NBD labeled protein and F_{bg} is the measurement of the NBD channel before NBD labeled protein was added to the sample. For several FRET experiments we observed transient but extreme fluorescence values; we believe these to be due to fluorescent debris in the solution and therefore removed them manually in a preprocessing step (SOM Section 5.2).

5.5.4. Kinetic modeling and simulation

Kinetic models were built programmatically using PySB (Lopez et al., 2013). The models were formulated as sets of ordinary differential equations and simulated either by 1) numerical integration using the VODE integrator (Brown et al., 1989) accessed via the Scipy library in Python (Oliphant, 2007) or 2) solved directly using a closed-form, analytical solution for the system.

The irreversible transition model with *n* states has *n-1* fluorescence transitions and *2n-2* free parameters: *n-1* transition rate parameters and *n-1* fluorescence scaling parameters; the fluorescence associated with the initial aqueous state of Bax, Bax_{F1}, can be calculated directly from the data.

In the simplest case, a labeled residue undergoes a single, irreversible environmental transition between two states with differential NBD fluorescence, denoted F_0 and F_1:

$$Bax_{F0} \underset{k}{\rightarrow} Bax_{F1} \quad (4)$$

In such a scheme, in which the transition between the collections of underlying chemical species associated with the fluorescent states F_0 and F_1 occurs by a single transition step, the change in the overall fluorescence is given by the following equation:

$$NBD(t) = C_0[Bax_{F0}(t)] + C_1[Bax_{F1}(t)] \quad 5)$$

where C_0 and C_1 are parameters indicating the NBD fluorescence of Bax_{F0} and Bax_{F1}, respectively. This equation has the solution:

$$NBD(t) = Bax_0[C_1 + (C_0 - C_1)e^{-kt}] \quad 6)$$

Since our data is normalized in terms of the fluorescence relative to the initial state Bax_{F0}, with the assumption that all Bax is in conformation Bax_{F0} at $t = 0$, (that is, $NBD(0) = Bax_0C_0$), we can also express this as a two-parameter, single exponential equation:

$$NBD_{norm}(t) = NBD(t)/(Bax_0C_0) \quad 7)$$

$$NBD_{norm}(t) = 1 + F_{max}(1 - e^{-kt}) \quad 8)$$

Where: $F_{max} = \frac{C_1}{C_0} - 1$.

5.5.5. Parameter estimation and model discrimination

Parameter estimation and model discrimination were performed using affine-invariant Markov chain Monte Carlo (MCMC) sampling implemented by the Python software package emcee (Foreman-Mackey et al., 2013) and based on the algorithm described by (Goodman and Weare, 2010). Parallel tempering was used to aid convergence and to calculate marginal likelihood values by thermodynamic integration (Geyer, 1991; Lartillot and Hervé, 2006). For each MCMC run, a ladder of 50 different temperatures was used, with 400 walkers at each temperature. Values for the reciprocal temperature, $\beta = 1/T$, were spaced logarithmically from 1 to a maximum temperature of $\beta = 10^{-6}$. Starting positions for the walkers were chosen randomly from the prior distributions for each parameter.

Convergence of the MCMC chains was assessed by several heuristics: 1) the log marginal likelihood (log(ML)) values were calculated by thermodynamic integration every 50 steps and assessed for asymptotic convergence by comparing log(ML) from the last 50 steps to the log(ML) value calculated from the previous 50 steps. If the difference in log(ML) was greater than an absolute threshold of 3, or greater than a relative threshold of 0.1 × err, where err was the error associated with the thermodynamic integration procedure itself, then the chain was considered to be non-convergent. 2) If the chain passed the test of convergence described in (1), the chains at each of the 50 temperatures were assessed for any trend towards increases in posterior probability over the 50-step convergence interval by performing linear regression on the posterior probability values associated with the sampled positions. If the trend for any of the 50 chains was positive with *p*-value less than 0.001, the chain ensemble was considered to be non-convergent. If a chain passed the programmatic heuristics in 1) and 2), the "burn-in" period was terminated and samples were recorded for an additional 100 steps, yielding 100 steps × 400 walkers = 40,000 samples for each parameter at each temperature. Chains were assessed for mixing by inspection of the posteriors associated with the positions of each walker across a subset of temperatures, which are plotted in SOM Section 3.4. The frequency of accepted temperature swaps was also inspected to ensure proper mixing between chains at different temperatures. Sampling runs were performed primarily on a computing cluster assembled from Amazon Elastic Compute Cloud (EC2) instances using the StarCluster software package (Fusaro

et al., 2011). All code necessary to reproduce the results of data analysis and model calibration is freely available on GitHub, at https://github.com/johnbachman/tBidBaxLipo.

5.5.6. Calculation of maximum Bax:BH3 protein FRET values

FRET time courses for Bid and Bim with Bax were fitted with the three-conformation, irreversible transition model to get a continuous curve approximating the fluorescence data. The maximum FRET value was then calculated from the fitted curve.

5.6. Supplementary Figures

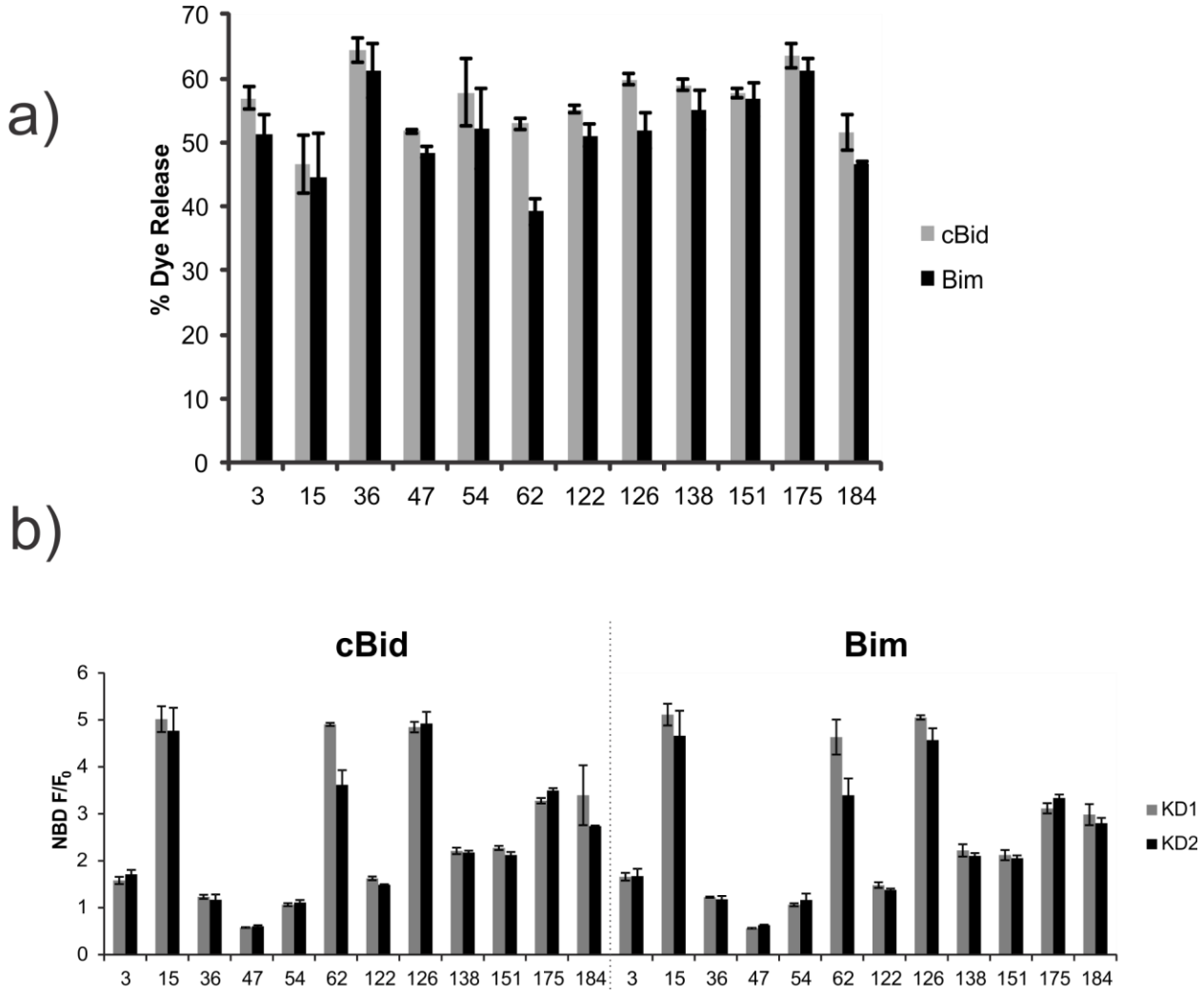

Supplementary Figure 5.1 – Labeling cBid or Bim does not affect Bax activation or conformation change

A. DAC Labeled cBid and Bim cause similar levels of Bax mediated membrane permeabilization. Percent Tb:DPA release of labeled Bax mutants relative to WT Bax. Tb:DPA encapsulated liposomes were incubated with 100 nM Labeled or WT Bax in the presence (Grey and Black) of 20 nM cBid-DAC or Bim-DAC respectively. Percent release was normalized to WT + cBid or Bim release set as 100%. Mean +/- STDEV n=3.

B. Unlabeled (Kinetic dataset 1, KD1) and DAC labeled (Kinetic dataset 2, KD2) cBid and Bim cause similar levels of NBD emission change when they activate Bax. One hour endpoint of the relative change of 100 nM Bax-NBD emission at 530 nM after the addition of 20 nM cBid (grey) or Bim (black) in the presence of liposomes.

5.7. References

Albeck, J.G., Burke, J.M., Spencer, S.L., Lauffenburger, D.A., and Sorger, P.K. (2008). Modeling a snap-action, variable-delay switch controlling extrinsic cell death. PLoS biology *6*, 2831-2852.

Annis, M.G., Soucie, E.L., Dlugosz, P.J., Cruz-Aguado, J.A., Penn, L.Z., Leber, B., and Andrews, D.W. (2005). Bax forms multispanning monomers that oligomerize to permeabilize membranes during apoptosis. EMBO Journal *24*, 2096-2103.

Bleicken, S., Jeschke, G., Stegmueller, C., Salvador-Gallego, R., Garcia-Saez, A.J., and Bordignon, E. (2014). Structural model of active Bax at the membrane. Molecular cell *56*, 496-505.

Brown, P.N., Byrne, G.D., and Hindmarsh, A.C. (1989). VODE, A variable coefficient ODE solver. SIAM J Sci Stat Comput *10*, 1038-1051.

Cerami, E., Gao, J., Dogrusoz, U., Gross, B.E., Sumer, S.O., Aksoy, B.A., Jacobsen, A., Byrne, C.J., Heuer, M.L., Larsson, E., *et al.* (2012). The cBio cancer genomics portal: an open platform for exploring multidimensional cancer genomics data. Cancer discovery *2*, 401-404.

Chipuk, J.E., Moldoveanu, T., Llambi, F., Parsons, M.J., and Green, D.R. (2010). The BCL-2 family reunion. Molecular cell *37*, 299-310.

Czabotar, P.E., Westphal, D., Dewson, G., Ma, S., Hockings, C., Fairlie, W.D., Lee, E.F., Yao, S., Robin, A.Y., Smith, B.J., *et al.* (2013). Bax crystal structures reveal how BH3 domains activate Bax and nucleate its oligomerization to induce apoptosis. Cell *152*, 519-531.

Dai, H., Smith, A., Meng, X.W., Schneider, P.A., Pang, Y.P., and Kaufmann, S.H. (2011). Transient binding of an activator BH3 domain to the Bak BH3-binding groove initiates Bak oligomerization. The Journal of cell biology *194*, 39-48.

Dewson, G., Kratina, T., Sim, H.W., Puthalakath, H., Adams, J.M., Colman, P.M., and Kluck, R.M. (2008). To trigger apoptosis, Bak exposes its BH3 domain and homodimerizes via BH3:groove interactions. Molecular cell *30*, 369-380.

Dewson, G., Ma, S., Frederick, P., Hockings, C., Tan, I., Kratina, T., and Kluck, R.M. (2012). Bax dimerizes via a symmetric BH3:groove interface during apoptosis. Cell death and differentiation *19*, 661-670.

Er, E., Oliver, L., Cartron, P.F., Juin, P., Manon, S., and Vallette, F.M. (2006). Mitochondria as the target of the pro-apoptotic protein Bax. Biochimica et biophysica acta *1757*, 1301-1311.

Foreman-Mackey, D., Hogg, D.W., Lang, D., and Goodman, J. (2013). emcee: The MCMC Hammer. Publications of the Astronomical Society of the Pacific *125*, 306-312.

Fresquet, V., Rieger, M., Carolis, C., Garcia-Barchino, M.J., and Martinez-Climent, J.A. (2014). Acquired mutations in BCL2 family proteins conferring resistance to the BH3 mimetic ABT-199 in lymphoma. Blood *123*, 4111-4119.

Fusaro, V.A., Patil, P., Gafni, E., Wall, D.P., and Tonellato, P.J. (2011). Biomedical cloud computing with Amazon Web Services. PLoS computational biology *7*, e1002147.

Galluzzi, L., Bravo-San Pedro, J.M., Vitale, I., Aaronson, S.A., Abrams, J.M., Adam, D., Alnemri, E.S., Altucci, L., Andrews, D., Annicchiarico-Petruzzelli, M., *et al.* (2015).

Essential versus accessory aspects of cell death: recommendations of the NCCD 2015. Cell death and differentiation *22*, 58-73.

Gao, J., Aksoy, B.A., Dogrusoz, U., Dresdner, G., Gross, B., Sumer, S.O., Sun, Y., Jacobsen, A., Sinha, R., Larsson, E., *et al.* (2013). Integrative analysis of complex cancer genomics and clinical profiles using the cBioPortal. Science signaling *6*, pl1.

Gardai, S.J., Hildeman, D.A., Frankel, S.K., Whitlock, B.B., Frasch, S.C., Borregaard, N., Marrack, P., Bratton, D.L., and Henson, P.M. (2004). Phosphorylation of Bax Ser(184) by Akt regulates its activity and apoptosis in neutrophils. Journal of Biological Chemistry *279*, 21085-21095.

Garner, T.P., Reyna, D.E., Priyadarshi, A., Chen, H.C., Li, S., Wu, Y., Ganesan, Y.T., Malashkevich, V.N., Almo, S.S., Cheng, E.H., *et al.* (2016). An Autoinhibited Dimeric Form of BAX Regulates the BAX Activation Pathway. Molecular cell *63*, 485-497.

Gavathiotis, E., Reyna, D.E., Davis, M.L., Bird, G.H., and Walensky, L.D. (2010). BH3-triggered structural reorganization drives the activation of proapoptotic BAX. Molecular cell *40*, 481-492.

Gavathiotis, E., Suzuki, M., Davis, M.L., Pitter, K., Bird, G.H., Katz, S.G., Tu, H.C., Kim, H., Cheng, E.H., Tjandra, N., *et al.* (2008). BAX activation is initiated at a novel interaction site. Nature *455*, 1076-1081.

Gelman, A. (2014). Bayesian data analysis. Chapman & Hall/CRC texts in statistical science, xiv, 661 pages.

George, N.M., Evans, J.J., and Luo, X. (2007). A three-helix homo-oligomerization domain containing BH3 and BH1 is responsible for the apoptotic activity of Bax. Genes & development *21*, 1937-1948.

Geyer, C.J. (1991). Markov chain Monte Carlo maximum likelihood. Computing Science and Statistics: Proc 23rd Symposium on the Interface, Interface Foundation, Fairfax Station, VA, 156-163.

Gillies, L.A., Du, H., Peters, B., Knudson, C.M., Newmeyer, D.D., and Kuwana, T. (2015). Visual and functional demonstration of growing Bax-induced pores in mitochondrial outer membranes. Molecular biology of the cell *26*, 339-349.

Goldstein, J.C., Waterhouse, N.J., Juin, P., Evan, G.I., and Green, D.R. (2000). The coordinate release of cytochrome c during apoptosis is rapid, complete and kinetically invariant. Nat Cell Biol *2*, 156-162.

Goodman, J., and Weare, J. (2010). Ensemble samplers with affine invariance. Communications in Applied Mathematics and Computational Science *5*, 65-80.

Hanahan, D., and Weinberg, R.A. (2011). Hallmarks of cancer: the next generation. Cell *144*, 646-674.

Kale, J., Chi, X., Leber, B., and Andrews, D. (2014). Examining the molecular mechanism of bcl-2 family proteins at membranes by fluorescence spectroscopy. Methods in enzymology *544*, 1-23.

Kim, H., Tu, H.C., Ren, D., Takeuchi, O., Jeffers, J.R., Zambetti, G.P., Hsieh, J.J., and Cheng, E.H. (2009). Stepwise activation of BAX and BAK by tBID, BIM, and PUMA initiates mitochondrial apoptosis. Molecular cell *36*, 487-499.

Kroemer, G., Galluzzi, L., and Brenner, C. (2007). Mitochondrial membrane permeabilization in cell death. Physiol Rev *87*, 99-163.

Kushnareva, Y., Andreyev, A.Y., Kuwana, T., and Newmeyer, D.D. (2012). Bax activation initiates the assembly of a multimeric catalyst that facilitates Bax pore formation in mitochondrial outer membranes. PLoS biology *10*, e1001394.

Kuwana, T., Olson, N.H., Kiosses, W.B., Peters, B., and Newmeyer, D.D. (2016). Pro-apoptotic Bax molecules densely populate the edges of membrane pores. Scientific reports *6*, 27299.

Lartillot, N., and Hervé, P. (2006). Computing Bayes factors using thermodynamic integration. Systematic Biology *55*, 195-207.

Leber, B., Lin, J., and Andrews, D.W. (2010). Still embedded together binding to membranes regulates Bcl-2 protein interactions. Oncogene *29*, 5221-5230.

Lopez, C.F., Muhlich, J.L., Bachman, J.A., and Sorger, P.K. (2013). Programming biological models in Python using PySB. Molecular systems biology *9*, 646.

Lovell, J.F., Billen, L.P., Bindner, S., Shamas-Din, A., Fradin, C., Leber, B., and Andrews, D.W. (2008). Membrane binding by tBid initiates an ordered series of events culminating in membrane permeabilization by Bax. Cell *135*, 1074-1084.

Luna-Vargas, M.P., and Chipuk, J.E. (2016). Physiological and Pharmacological Control of BAK, BAX, and Beyond. Trends in cell biology.

Meijerink, J.P., Mensink, E.J., Wang, K., Sedlak, T.W., Sloetjes, A.W., de Witte, T., Waksman, G., and Korsmeyer, S.J. (1998). Hematopoietic malignancies demonstrate loss-of-function mutations of BAX. Blood *91*, 2991-2997.

Nechushtan, A., Smith, C.L., Hsu, Y.T., and Youle, R.J. (1999). Conformation of the Bax C-terminus regulates subcellular location and cell death. EMBO Journal *18*, 2330-2341.

Ni Chonghaile, T., Sarosiek, K.A., Vo, T.T., Ryan, J.A., Tammareddi, A., Moore Vdel, G., Deng, J., Anderson, K.C., Richardson, P., Tai, Y.T., *et al.* (2011). Pretreatment mitochondrial priming correlates with clinical response to cytotoxic chemotherapy. Science *334*, 1129-1133.

Oliphant, T.E. (2007). Python for Scientific Computing. Computing in Science & Engineering *9*, 10-20.

Rehm, M., Dussmann, H., Janicke, R.U., Tavare, J.M., Kogel, D., and Prehn, J.H. (2002). Single-cell fluorescence resonance energy transfer analysis demonstrates that caspase activation during apoptosis is a rapid process. Role of caspase-3. The Journal of biological chemistry *277*, 24506-24514.

Robin, A.Y., Krishna Kumar, K., Westphal, D., Wardak, A.Z., Thompson, G.V., Dewson, G., Colman, P.M., and Czabotar, P.E. (2015). Crystal structure of Bax bound to the BH3 peptide of Bim identifies important contacts for interaction. Cell death & disease *6*, e1809.

Rojko, N., Kristan, K.C., Viero, G., Zerovnik, E., Macek, P., Dalla Serra, M., and Anderluh, G. (2013). Membrane damage by an alpha-helical pore-forming protein, Equinatoxin II, proceeds through a succession of ordered steps. The Journal of biological chemistry *288*, 23704-23715.

Saito, M., Korsmeyer, S.J., and Schlesinger, P.H. (2000). BAX-dependent transport of cytochrome c reconstituted in pure liposomes. Nat Cell Biol *2*, 553-555.

Sarosiek, K.A., Chi, X., Bachman, J.A., Sims, J.J., Montero, J., Patel, L., Flanagan, A., Andrews, D.W., Sorger, P., and Letai, A. (2013). BID preferentially activates BAK while BIM preferentially activates BAX, affecting chemotherapy response. Molecular cell *51*, 751-765.

Schellenberg, B., Wang, P., Keeble, J.A., Rodriguez-Enriquez, R., Walker, S., Owens, T.W., Foster, F., Tanianis-Hughes, J., Brennan, K., Streuli, C.H., *et al.* (2013). Bax exists in a dynamic equilibrium between the cytosol and mitochondria to control apoptotic priming. Molecular cell *49*, 959-971.

Shamas-Din, A., Bindner, S., Zhu, W., Zaltsman, Y., Campbell, C., Gross, A., Leber, B., Andrews, D.W., and Fradin, C. (2013a). tBid undergoes multiple conformational changes at the membrane required for Bax activation. The Journal of biological chemistry *288*, 22111-22127.

Shamas-Din, A., Kale, J., Leber, B., and Andrews, D.W. (2013b). Mechanisms of action of Bcl-2 family proteins. Cold Spring Harbor perspectives in biology *5*, a008714.

Subburaj, Y., Cosentino, K., Axmann, M., Pedrueza-Villalmanzo, E., Hermann, E., Bleicken, S., Spatz, J., and Garcia-Saez, A.J. (2015). Bax monomers form dimer units in the membrane that further self-assemble into multiple oligomeric species. Nature communications *6*, 8042.

Suzuki, M., Youle, R.J., and Tjandra, N. (2000). Structure of Bax: coregulation of dimer formation and intracellular localization. Cell *103*, 645-654.

Tait, S.W., and Green, D.R. (2010). Mitochondria and cell death: outer membrane permeabilization and beyond. Nature reviews Molecular cell biology *11*, 621-632.

Todt, F., Cakir, Z., Reichenbach, F., Emschermann, F., Lauterwasser, J., Kaiser, A., Ichim, G., Tait, S.W., Frank, S., Langer, H.F., *et al.* (2015). Differential retrotranslocation of mitochondrial Bax and Bak. The EMBO journal *34*, 67-80.

Tsai, C.J., Liu, S., Hung, C.L., Jhong, S.R., Sung, T.C., and Chiang, Y.W. (2015). BAX-induced apoptosis can be initiated through a conformational selection mechanism. Structure *23*, 139-148.

Vo, T.T., Ryan, J., Carrasco, R., Neuberg, D., Rossi, D.J., Stone, R.M., Deangelo, D.J., Frattini, M.G., and Letai, A. (2012). Relative mitochondrial priming of myeloblasts and normal HSCs determines chemotherapeutic success in AML. Cell *151*, 344-355.

Wei, M.C., Zong, W.X., Cheng, E.H., Lindsten, T., Panoutsakopoulou, V., Ross, A.J., Roth, K.A., MacGregor, G.R., Thompson, C.B., and Korsmeyer, S.J. (2001). Proapoptotic BAX and BAK: a requisite gateway to mitochondrial dysfunction and death. Science *292*, 727-730.

Westphal, D., Dewson, G., Menard, M., Frederick, P., Iyer, S., Bartolo, R., Gibson, L., Czabotar, P.E., Smith, B.J., Adams, J.M., *et al.* (2014a). Apoptotic pore formation is associated with in-plane insertion of Bak or Bax central helices into the mitochondrial outer membrane. Proc Natl Acad Sci U S A *111*, E4076-4085.

Yethon, J.A., Epand, R.F., Leber, B., Epand, R.M., and Andrews, D.W. (2003). Interaction with a membrane surface triggers a reversible conformational change in Bax normally associated with induction of apoptosis. The Journal of biological chemistry *278*, 48935-48941.

Yin, C., Knudson, C.M., Korsmeyer, S.J., and Van Dyke, T. (1997). Bax suppresses tumorigenesis and stimulates apoptosis in vivo. Nature *385*, 637-640.

Youle, R.J., and Strasser, A. (2008). The BCL-2 protein family: opposing activities that mediate cell death. Nature reviews Molecular cell biology *9*, 47-59.

Zhang, M., Zheng, J., Nussinov, R., and Ma, B. (2016a). Oncogenic Mutations Differentially Affect Bax Monomer, Dimer, and Oligomeric Pore Formation in the Membrane. Scientific reports *6*, 33340.

Zhang, Z., Subramaniam, S., Kale, J., Liao, C., Huang, B., Brahmbhatt, H., Condon, S.G., Lapolla, S.M., Hays, F.A., Ding, J., *et al.* (2016b). BH3-in-groove dimerization initiates and helix 9 dimerization expands Bax pore assembly in membranes. The EMBO journal *35*, 208-236.

6

Phosphorylation by Akt converts Bax into an anti-apoptotic protein promoting drug resistance

6.1. Preface

The work presented here has been prepared for submission as a research article to Molecular Cell

Kale, J., Kutuk, O., Brito, G., Andrews, T., Letai, T., Andrews D.W. (2016) Phosphorylation by Akt converts Bax into an anti-apoptotic protein promoting drug resistance

Author contribution:

The manuscript was written by Kale J with sections and figures adapted and edited from an early version of this manuscript written by Kutuk, O and Kale J. Editing of the manuscript was primarily performed by Andrews DW with additional edits by Kutuk, O and Letai, A. The experiments in Figures 1, 4 and S3 were performed by Ozgur K. The experiments in figures 2, 3, S1 and S2 were performed by Kale J. All figures and tables were put together by Kale J with some adapted from the previous manuscript mentioned above. The data in section 4.6.5 "Over-expression of Bax is countered by PI3K/AKT pathway activation in human cancer" was generated by Andrews, T and Brito, G. Andrews, DW and Letai, A directed the research.

Objectives:

To understand the pro-survival effects of AKT signaling in cancer cells and determine how AKT mediated phosphorylation affects the molecular mechanism of Bax. This chapter is related to chapter 5 by discovering a physiological relevance of the Bax intermediate conformation.

Highlights:

- Bax is phosphorylated in cell lines resistant to the BH3 mimetic ABT-737
- Phosphomimetic Bax can bind cBid, but does not insert into membranes thus pore formation is inhibited
- Phosphorylation on residue S184 converts Bax into an anti-apoptotic protein via sequestering activator BH3-only proteins
- Overexpression of Bax is positively correlated with PI3K/AKT pathway activation in human cancers suggesting a new mechanism for cancer cells to evade apoptosis

6.2. Introduction

Activation of the mitochondrial apoptosis pathway in cancer cells serves as an important route of cell death following treatment with chemotherapeutic agents. Alteration of this pathway can cause resistance to therapy in cancer cells. A decisive step for commitment to apoptosis is mitochondrial outer membrane permeabilization (MOMP) that releases intermembrane space proteins including cytochrome *c* into cytosol. This process is tightly controlled by the Bcl-2 family proteins (Brunelle and Letai, 2009; Shamas-Din et al., 2013b). Following a conformational change, Bax and Bak oligomerize to execute MOMP. This conformation change is provoked by activator proteins that include the BH3-only proteins Bim and Bid. Pro-survival Bcl-2 proteins (Bcl-2, Bcl-XL, Mcl-1, Bfl-1 and Bcl-W) inhibit MOMP either by sequestering activator BH3-only proteins or by directly binding Bax and Bak (Cheng et al., 2001; Willis et al., 2007). Other so-called "sensitizer" BH3-only proteins, including Bad, Noxa, and Bik, cannot activate Bax or Bak, but rather exert their pro-death function by competing for the BH3 binding sites of pro-survival proteins (Letai et al., 2002; Shamas-Din et al., 2013b). Differences in the affinities of the interactions, expression levels and post-translational modifications of these proteins together determine the fate of the cell.

Measurement of MOMP upon incubating BH3 domain-derived peptides with mitochondria and identifying differential response patterns was successfully translated into an assay called BH3 profiling (Certo et al., 2006; Ryan et al., 2010). By interpreting the pattern of mitochondrial sensitivity to BH3 peptides of different affinities for anti-apoptotic proteins, BH3 profiling can be used to identify dependence on individual anti-apoptotic Bcl-2 proteins for survival and sensitivity to inhibitors. Certain BH3 domain peptides, including Bid and Bim BH3, interact promiscuously with all known anti-apoptotic proteins. Mitochondrial sensitivity to these peptides can be interpreted as a measure of how close a cell is to the threshold of apoptosis, or how "primed" a cell is for death (Certo et al., 2006; Del Gaizo Moore et al., 2007). The degree of priming predicts how sensitive the cell will be to toxic insults, and correlates with clinical response to chemotherapy (Chonghaile et al., 2011).

In cancer, particularly in breast cancer, hyper-activation of the PI3K/Akt pathway is strongly associated with poor prognosis and resistance to therapy (Salmena et al., 2008). PTEN

(phosphatase and tensin homolog deleted on chromosome 10) functions as a lipid phosphatase to restrain PI3K/Akt pathway activation by diminishing the PIP_3 cellular pool through hydrolysis of 3-phosphate on PIP_3 to regenerate PIP_2. PI3Ks phosphorylate phosphatidylinositol-4,5-biphosphate (PIP_2) to generate phosphatidylinositol-3,4,5-biphosphate (PIP_3) promoting Akt recruitment to plasma membrane through binding its pleckstrin-homology (PH) domain. Following recruitment to the plasma membrane by PIP_3, Akt is phosphorylated by PDK1 at T308 and by mTORC2 at S473 which leads to its full activation (Manning and Cantley, 2007). Hence, inactivation or loss of PTEN results in increased accumulation of PIP_3 and constitutively active PI3K/Akt signaling. The PI3K/Akt pathway regulates fundamental processes in cells, including survival, cell cycle progression and metabolism. Deregulation of the PI3K/Akt signaling pathway is commonly detected in a wide spectrum of human cancers. Several mechanisms including genomic amplification of growth factor receptors, PTEN deletion or mutations, or activating mutations in pathway genes can activate Akt in cancer cells. Importantly, Akt distinctly blocks pro-death signaling upstream of MOMP (Kennedy et al., 1999). However, it is still unclear how pro-survival PI3K/Akt signaling makes the critical connection to the Bcl-2 family that controls the mitochondrial apoptosis pathway. Some suggest an indirect effect, for instance via transcriptional control of pro-apoptotic Bcl-2 family proteins via the FOXO family of transcriptional regulators (Manning and Cantley, 2007). Akt could play a more direct role since it can phosphorylate the pro-apoptotic BH3-only protein Bad. However, Bad is dispensable for apoptosis induced by several mechanisms (Ranger et al., 2003; Wang et al., 2005), suggesting that a more central Bcl-2 family protein might also be controlled by AKT such as Bax (Gardai et al., 2004; Xin and Deng, 2005). Exactly how phosphorylation inhibits Bax and the significance this has in determining cell fate remains to be understood.

Here we show that Akt localizes to mitochondria and directly phosphorylates Bax. Unexpectedly, phosphorylation of Bax converts its function from pro- to anti-apoptotic, thereby impeding mitochondrial priming for apoptosis. Furthermore we show that phosphorylated Bax is not only incompetent for the oligomerization that is essential for its membrane permeabilization function, but also acts as a dominant negative by competing with non-phosphorylated Bax for binding to activator BH3-only proteins. Additionally, we probed The Cancer Genome Atlas (TCGA) database and found that in cancers where Bax levels are increased, its expression is

positively associated with an increase in PI3K/AKT pathway genes. Taken together the data suggests that cancers with hyper-active PI3K/AKT pathway signalling select for increased levels of Bax as a potential mechanism to avoid apoptosis. Given the established role of Bax as a critical effector of MOMP downstream of many types of pro-apoptotic signalling, phosphorylation of Bax is likely a key mediator of the anti-apoptotic effect exerted by hyperactive Akt in cancer.

6.3. Results

6.3.1. Bax is phosphorylated in ABT-737 resistant cell lines

BH3 profiling with Bad can predict cellular sensitivity to Bcl-2 antagonism by ABT-737 (Certo et al., 2006; Del Gaizo Moore et al., 2007; Deng et al., 2007). To extend this observation we tested this correlation in a new cancer cell line panel. As shown in Figure 1A, we found that mitochondria from MDA-MB-435, MDA-MB-468, SF539 and 768-O cells were as or more sensitive to Bad than MCF-7, T47-D or ZR-75-1 cell lines. Surprisingly, only MDA-MB-435 cells were sensitive to ABT-737 (EC_{50}, 32 nM), and other cells were relatively insensitive to ABT-737 with EC50 values at micromolar levels (Figure 1B). Thus, MDA-MB-468, SF539 and 768-O cells were less sensitive to ABT-737 than predicted by mitochondrial BH3 profiling

One possible explanation for the deviation from sensitivity predicted by BH3 profiling is that post-translational modifications (PTMs) are present in cells that are not present in our in vitro system. Since Bax is required for MOMP, and it has been reported that Bax can be phosphorylated and inhibited (Gardai et al., 2004; Xin and Deng, 2005), we determined if resistant cells had phosphorylated Bax. We found that Bax is phosphorylated in ABT-737 resistant MDA-MB-468 cells, but not in ABT-737 sensitive MDA-MB-435 cells (Figure 1C). The difference between the BH3 profiling results and the cell data suggests that Bax is being dephosphorylated, potentially by mitochondria phosphatases, when mitochondria are isolated from cells.

While Bax is localized in both the cytosol and at mitochondria of many cells, translocation to the mitochondrion is essential for Bax pro-apoptotic function. As S184 at Bax C-

terminal domain (helix 9) was reported to be a target for the PI3K/Akt signaling pathway (Gardai et al., 2004; Wang et al., 2010; Xin and Deng, 2005; Yamaguchi and Wang, 2001), we created two mutants that either prevent (S184A) or mimic (S184E) phosphorylation. We evaluated the subcellular localization of GFP-tagged WT Bax, and the S184A and S184E mutants in ABT-737-resistant MDA-MB-468 cells. GFP-Bax was localized diffusely throughout cytoplasm with limited co-localization with mitochondria while the GFP-Bax S184A showed punctate, mostly mitochondrial localization (Figure 1D). In contrast, GFP-Bax S184E showed a diffuse and predominately cytoplasmic pattern of expression without mitochondrial localization. Moreover, mitochondria of cells expressing GFP-Bax S184E were less fragmented than mitochondria of cells expressing GFP-Bax and GFP Bax S184A. In transient transfection experiments, both GFP-Bax and GFP-Bax S184A were highly toxic to MDA-MB-468 cells. Spontaneous cell death was also increased in cells stably expressing these constructs (Figure 1D), whereas there was minimal basal cell death in GFP-Bax S184E expressing cells. Consistent with these results, GFP-Bax and GFP-Bax S184A-expressing MDA-MB-468 cells were also more sensitive to ABT-737 treatment. By contrast, cells expressing GFP-Bax S184E remained resistant to ABT-737 (Figure 1D). In ABT-737 resistant MDA-MB-468 cells GFP immunoprecipitation revealed that GFP-Bax was phosphorylated (Figure S1A). However, we could not detect serine phosphorylation on GFP-Bax S184A, supporting S184 as a primary phosphorylation site on Bax.

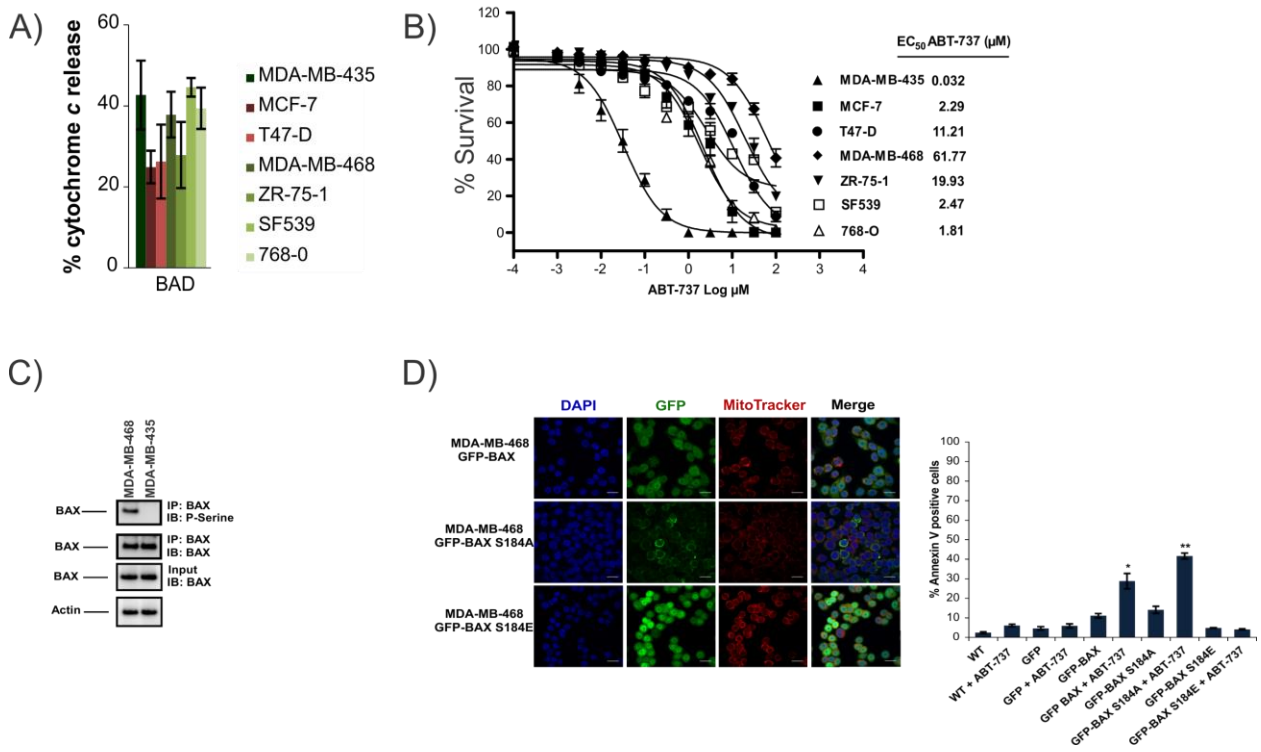

Figure 6.1 - Bax is phosphorylated in ABT-737 resistant cell lines

A) Mitochondria from the indicated cell lines were isolated, incubated with BAD peptide and MOMP was measured as cytochrome c release (mean±SEM, n=4)

B) ABT-737 EC_{50} values of cancer cell lines were determined by using MTT assay (mean±SEM, n=4)

C) Phosphorylation of BAX in MDA-MB-435, MDA-MB-468 cells

D) MDA-MB-468 cells were transfected with plasmids encoding GFP-BAX, GFP-BAX S184A and GFP-BAX S184E and the localization of BAX was evaluated by confocal microscopy. Cells were co-stained with MitoTracker Red CMXRos (mitochondria) and DAPI (nucleus). In addition, cells were treated with ABT-737 (100 nM, 48 hr) and apoptosis was evaluated by using Annexin V staining (mean±SEM, n=3, *P<0.05, **P<0.01).

See also Figure S1.

6.3.2. Phosphomimetic Bax can bind cBid, but does not insert helices 5 and 9 into the membrane thus pore formation is inhibited

We examined how Bax phosphorylation at S184 affects Bax-mediated membrane permeabilization using the phosphomimetic mutant of Bax (S184E) to ensure that all of the Bax functioned as a phosphorylated protein because *in vitro* Akt phosphorylation of recombinant Bax was incomplete (~50% - see fig S4D). When transitioning from a soluble monomer to a membrane embedded oligomer Bax undergoes sequential activation steps (Figure 2A) that can be examined using fluorescence spectroscopy and purified proteins (Kale et al., 2014; Lovell et al., 2008). The sequence begins with recruitment of Bax to the membrane by interaction with an activator BH3-only protein on the membrane surface. Bax then inserts helices 5, 6 and 9 into the membrane followed by oligomerization and membrane permeabilization (Figure 2A).

To assess how phosphorylation at S184 affects the first step, interaction between cBid and Bax, was measured using Fluorescence Resonance Energy Transfer (FRET) for the proteins labeled with the dyes DAC and NBD as the donor and acceptor (Lovell et al., 2008). As expected, WT Bax bound to cBid only in the presence of membranes (Figure 2B). Unexpectedly, Bax S184E bound to both cBid (Fig 2B) and Bim (Fig S2A) in the presence of membranes. Furthermore, WT Bax and Bax S184E bound cBid with similar affinities. (Fig 2B). Unlike WT Bax, Bax S184E bound cBid in solution.

As Bax S184E binds activator BH3-only proteins, we determined if it was impaired for insertion into the lipid bilayer. To examine the insertion into membranes of specific residues of Bax the residue to be probed was exchanged for a cysteine in an otherwise cysteine-less Bax and the mutant protein was labeled with an iodoacetamide-NBD dye. Positioning the environment sensitive NBD dye on cysteines located at either residue 126 in helix 5, or residue 175 in helix 9 enabled detection of the transition of the labeled region of the protein into the lipid bilayer by monitoring the resulting increase in NBD fluorescence. Upon activation of Bax by cBid residues 126 and 175 become protected from chemical labeling in cell lysates suggesting that in cells they insert into the mitochondrial outer membrane (Annis et al., 2005). In response to the addition of cBid to NBD-labeled WT Bax and liposomes the fluorescence of probes at either location increased confirming that these residues of helix 5 and 9 insert into membranes (Figure 2C). In

contrast, NBD labeled phosphomimetic Bax did not insert either residue into liposome membranes since the fluorescence emission from NBD-probes at 126C and 175C did not increase substantially. Thus insertion of phosphomimetic Bax into membranes is defective, consistent with this being the step inhibited by phosphorylation of Bax.

In the absence of Bax helix 5 and 9 insertion into membranes it is possible that Bax binds to cBid and oligomerizes on the surface of the liposome. Bax oligomerization can be measured by FRET, by mixing Bax molecules labeled with either the donor or acceptor dye and adding liposomes and cBid. As expected, FRET was detected between donor and acceptor labelled WT Bax proteins in this assay after incubation with cBid. However, FRET was not detected for Bax S184E or for mixtures of WT Bax and Bax S184E suggesting that phosphorylation prevents Bax-Bax binding and oligomerization (Figure 2D).

To corroborate our results suggesting that Bax S184E does not insert into membranes we assessed membrane permeabilization by Bax S184E compared to WT Bax. To test this final step in Bax activation (Figure 2A) we used a dye release assay in which permeabilization of liposomes releases both the entrapped dye ANTS and its quencher DPX. Release from liposomes dilutes both species resulting in a dramatic increase in the ANTS fluorescence. Compared to the wild-type protein, the phosphomimetic S184E mutation greatly attenuated ANTS release from liposomes in response to cBid (Figure 2E and S2B). This assay was also used in control experiments to confirm that neither labeling with the fluorescent dyes nor single cysteine mutations (required for NBD or DAC labeling) altered the membrane permeabilizing function of Bax.

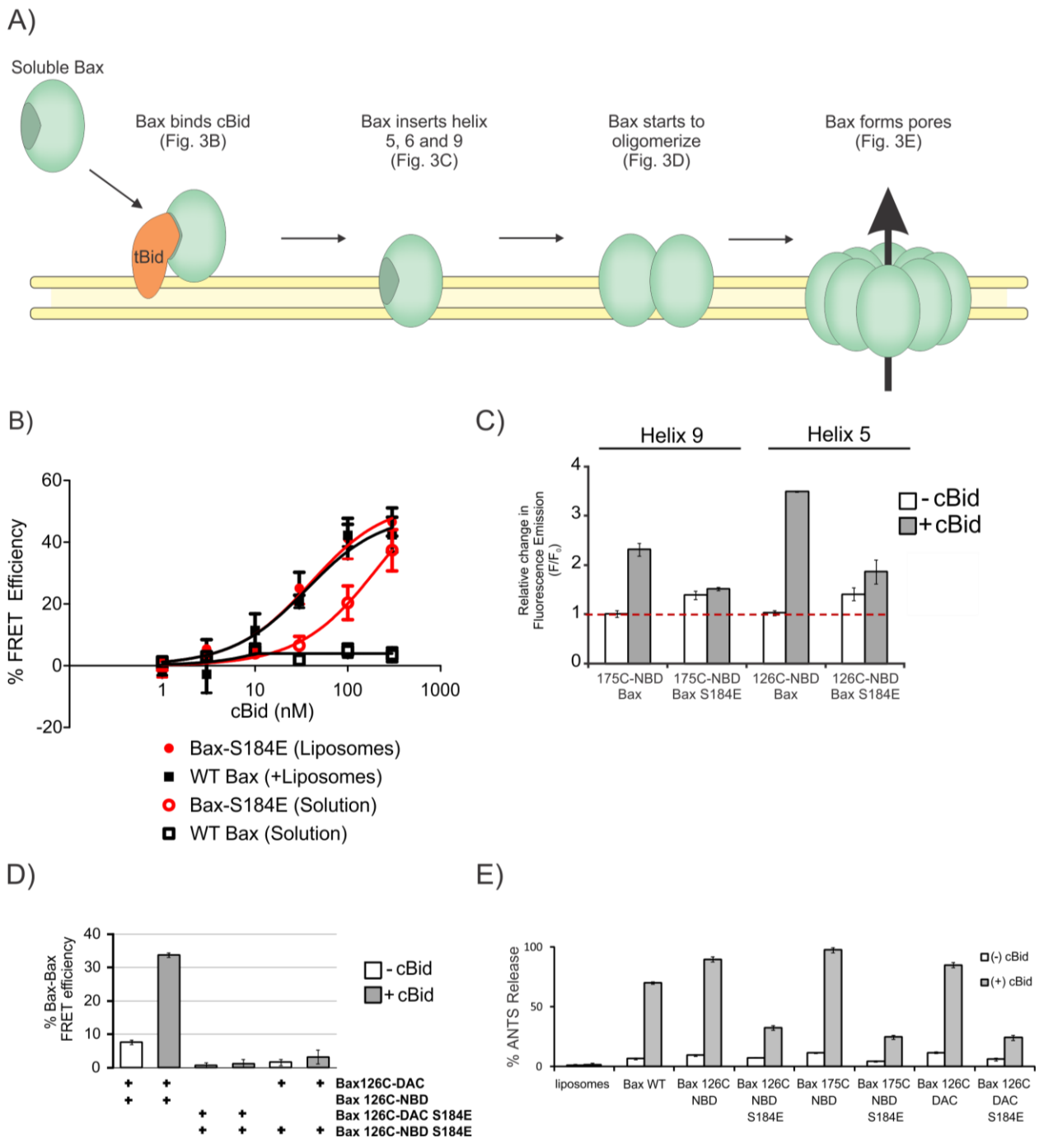

Figure 6.2 - Phosphomimetic Bax can bind cBid, but cannot insert helices 5 and 9 into the membrane abrogating pore formation

A) Schematic of the activation mechanism of Bax. Caspase 8 cleaved Bid (cBid) spontaneously targets to and embeds within the lipid bilayer. Here, the amino-terminal portion of cBid dissociates and the carboxy-terminal portion becomes tBid (truncated Bid) (Shamas-Din et al., 2013a). Soluble Bax interacts with tBid at the membrane. This interaction activates Bax and allows Bax to insert alpha-helices 5, 6 and 9 into the bilayer. Insertion of Bax within the lipid bilayer causes Bax to oligomerize and form pores within the membrane.

B) The apparent affinity between cBid and Bax (step 1) was measured using FRET. Samples containing liposomes were incubated with 20 nM cBid 126C-DAC and BAX-NBD was added as indicated. FRET efficiency was calculated as 1- (F_{DA}/F_D) at 2 hour endpoint (mean±STDEV, n>=3).

C) Insertion of alpha Helix 5 and 9 of Bax (step 2) was measured using the environment sensitive dye NBD covalently attached to the indicated residues on Bax. The relative change of NBD emission (F/F_0) at a one hour endpoint with or without the addition of 20 nM cBid in the presence of liposomes is shown (mean±STDEV, n>=3).

D) Bax oligomerization (step 3) was measured by FRET between Bax monomers. Samples containing liposomes were incubated with 10 nM DAC (donor) labeled WT or S184E BAX and 100 nM of NBD (acceptor) labeled WT of S184E BAX in the presence or absence of 20 nM cBid and liposomes. FRET efficiency was calculated as 1- (F_{DA}/F_D) at 2 hour endpoint (mean±STDEV, n>=3).

E) The liposome permeabilization activity of Bax was measured using the ANTS/DPX release assay. ANTS/DPX Liposomes were incubated with 100 nM of the indicated Bax in the absence or presence of 20 nM cBid (mean±STDEV, n≥3).

See also Figure S2.

6.3.3. Phosphorylation of Bax at residue 184 converts Bax into an anti-apoptotic protein.

Anti-apoptotic proteins like Bcl-XL inhibit MOMP by sequestering BH3-only proteins (mode 1) and activated Bax (mode 2). Bax S184E is blocked at insertion into membranes but can bind BH3 activator proteins suggesting that phosphomimetic Bax could inhibit MOMP by sequestering BH3-only proteins. Consistent with this hypothesis, phosphomimetic Bax reduced liposome permeabilization by WT Bax and cBid or Bim in a dose dependent manner as shown by a decrease in ANTS and DPX release (Figure 3A). Thus, contrary to expectation based on previous reports that suggest S184 phosphorylation activates Bax (Simonyan et al., 2016) or phosphomimetic Bax is completely non-functional (Gardai et al., 2004; Quast et al., 2013), by sequestering BH3-only proteins Bax S184E actually impaired liposome permeabilization.

If this activity of Bax S184E also occurs in cells it might be sufficient to protect cells from apoptotic stimuli. Bax S184E was expressed in cells with a fluorescence protein tag (mCer3) to enable monitoring expression of the mutant in cells expressing endogenous Bax. Consistent with Bax S184E functioning as an anti-apoptotic protein, stable expression in WT BMK cells inhibited apoptosis resulting from treatment of the cells with the pro-death cytokine TNF-α and cycloheximide, the pan-kinase inhibitor Staurosporine and the HDAC inhibitor

Panobinostat (Figure 3C, S3A). Cell death in response to these agonists was dependent on endogenous WT Bax and Bak since $Bax^{-/-}$ $Bak^{-/-}$ DKO BMK cells did not die after exposure to these agents. This result also suggests that sequestration of BH3 proteins by Bax S184E likely inhibits both Bax and Bak induced MOMP. Moreover, in these experiments exogenous Bax S184E protein levels were similar to that of endogenous Bax thus the decrease in apoptosis due to expression of Bax S184E was not due to decreased endogenous Bax or Bak compared to WT cells (Figure 3D). Thus, we suggest that phosphorylation of Bax at position 184 generates a protein that competes with WT Bax for binding to BH3-only proteins in a manner analogous to mode 1 inhibition of apoptosis by multidomain anti-apoptotic proteins like Bcl-XL (Billen et al., 2008).

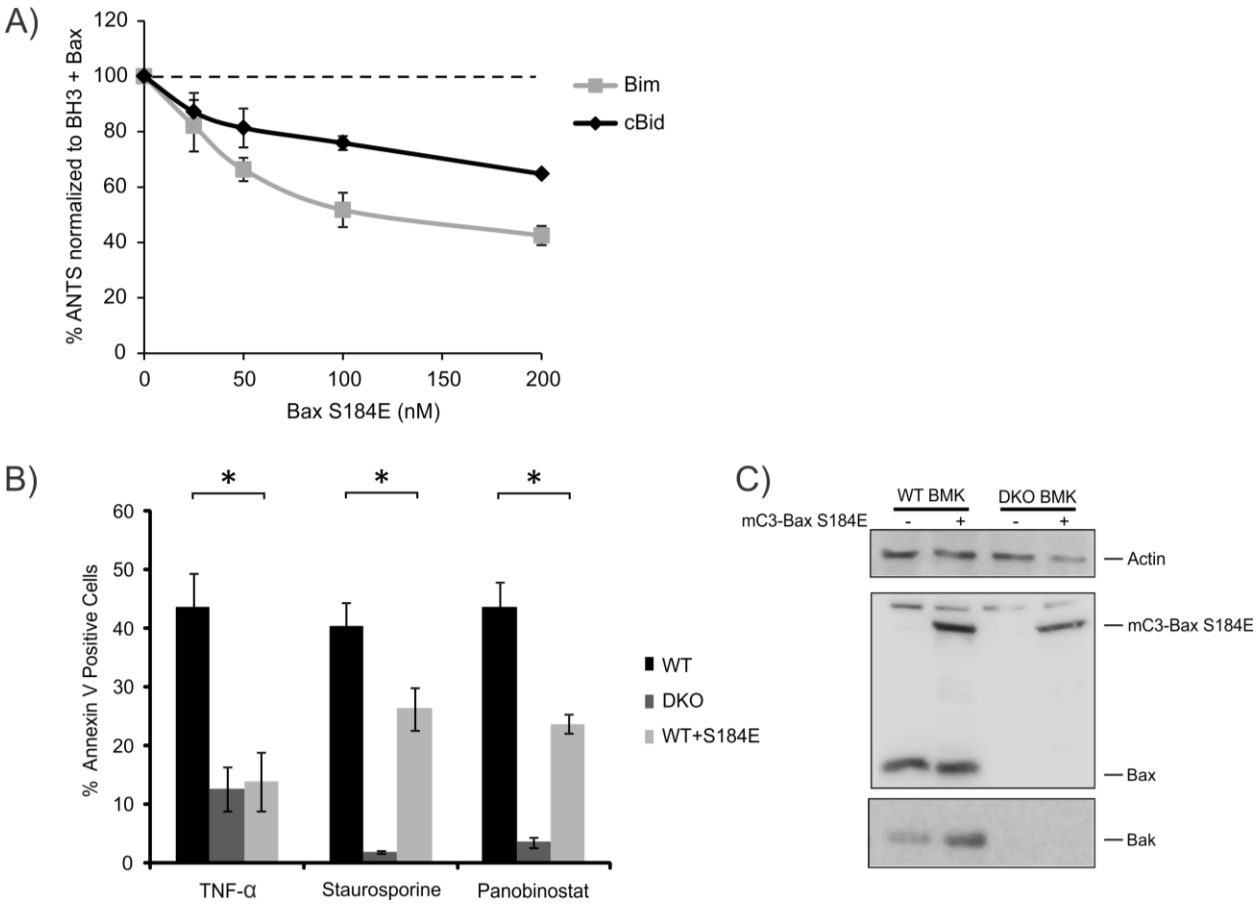

Figure 6.3 - Bax S184E protects from apoptotic stimuli

A) ANTS/DPX Liposomes were incubated with 50 nM WT Bax, 20 nM cBid or Bim and the indicated concentration of BAX 126C S184E (mean±STDEV, n≥3)

B) WT BMK, Bax/Bak DKO BMK and WT BMK cells stably expressing mCerulean Bax-S184E were treated with the indicated cell death stimuli for 24 hours and % annexin V positivity of cells was calculated (mean±SEM, n=3, *P<0.05).

C) Representative blot of cell lysates of WT, Bax/Bak DKO and WT BMK cells stably expressing mC3-Bax S184E were analyzed by gel electrophoresis followed by western blot using antibodies against Bax and Bak.

See also Figure S3.

6.3.4. Akt phosphorylates Bax in ABT-737 resistant cells

Since Bax can be phosphorylated at residue S184 by Akt, this pathway may mediate the resistance to ABT-737 we observed in cancer cells with active PI3K/Akt pro-survival signalling (Figure 1B). To test this hypothesis, we examined the effect of small molecule inhibitors of the PI3K/Akt pathway on mitochondrial priming. As predicted, treatment of ABT-737 resistant MDA-MB468 cells with PI3K/Akt inhibitors enhanced priming as shown by increased response to BH3 peptides (Figure 4A, left panel). However, these drugs did not cause a significant change in ABT-737 sensitive MDA-MB-435 cells (Figure 4A, right panel).

Thus we postulate that the phosphorylation of Bax by Akt affects the sensitivity of mitochondria to BH3-only protein dependent pro-apoptotic signalling. To test whether Akt directly alters mitochondrial priming, cytosolic (S100) fractions from ABT-737 resistant MDA-MB-468 cells were isolated and pre-incubated with mitochondria isolated from ABT-737 sensitive MDA-MB-435 cells before BH3 profiling experiments. This pre-incubation led to decreased priming of MDA-MB-435 mitochondria, with decreased cytochrome *c* release in response to Bid and other BH3 peptides (Figure 4B, S4A). Pre-treatment of ABT-737 resistant cells with PI3K/Akt inhibitors or immunodepletion of Akt from the S100 fraction abrogated inhibition of priming by the S100 fraction (Figure 4B). Using an active recombinant Akt in kinase assay buffer including ATP, we demonstrated that Akt by itself can unprime mitochondria from MDA-MB-435 cells (Figure 4C). Furthermore, Akt is localized both in cytosol and mitochondria in ABT-737 resistant MDA-MB-468 cells, but only in the cytosol of ABT-737 sensitive MDA-MB 435 cells (Figure S4B). Treatment with the inhibitors of PI3K/Akt signalling deguelin, LY294002 and MK-2206, prevented Akt from localizing to mitochondria of MDA-MB-468 cells but did not alter Akt localization in MDA-MB 435 cells. In contrast, A-443654, promoted Akt localization to mitochondria, however this drug is known to promote paradoxical Akt phosphorylation with concomitant Akt kinase inhibition (Luo et al., 2005). Taken together, our results indicate a potent direct effect of Akt to prevent priming of mitochondria, likely through the phosphorylation of Bax. As shown above (Figure 1C), Bax is phosphorylated in ABT-737 resistant MDA-MB-468 cells. Treatment of MDA-MB-468 cells with PI3K/Akt

inhibitors substantially inhibited Bax phosphorylation, confirming the role of Akt in Bax phosphorylation in ABT-737 resistant cells.

To test Akt-mediated Bax inhibition in a well-defined model system, we reconstituted Bax-regulated MOMP using mitochondria from Bax/Bak DKO MEFs, and recombinant tBid and Bax proteins. As expected, tBid and Bax combination treatment triggered cytochrome *c* release from mitochondria, although neither of the proteins led to substantial release when used alone (Figure 4D). Pre-incubating tBid and Bax with active Akt plus ATP before exposing them to mitochondria decreased cytochrome *c* release considerably. In this in vitro assay 53±4% (mean±SEM, n=3) of Bax was phosphorylated by Akt (Figure S4D). Adding MK-2206 to a kinase assay reaction composed of Akt, ATP, tBid and Bax attenuated the inhibitory effect of Akt on cytochrome *c* release confirming that Akt kinase activity was required for inhibition of tBid/Bax-mediated mitochondrial permeabilization. Consistent with this interpretation, excluding ATP from the reaction eliminated the protective effect of Akt (Figure S4E) while adding ATP alone to tBid/Bax did not have any impact on mitochondrial permeabilization.

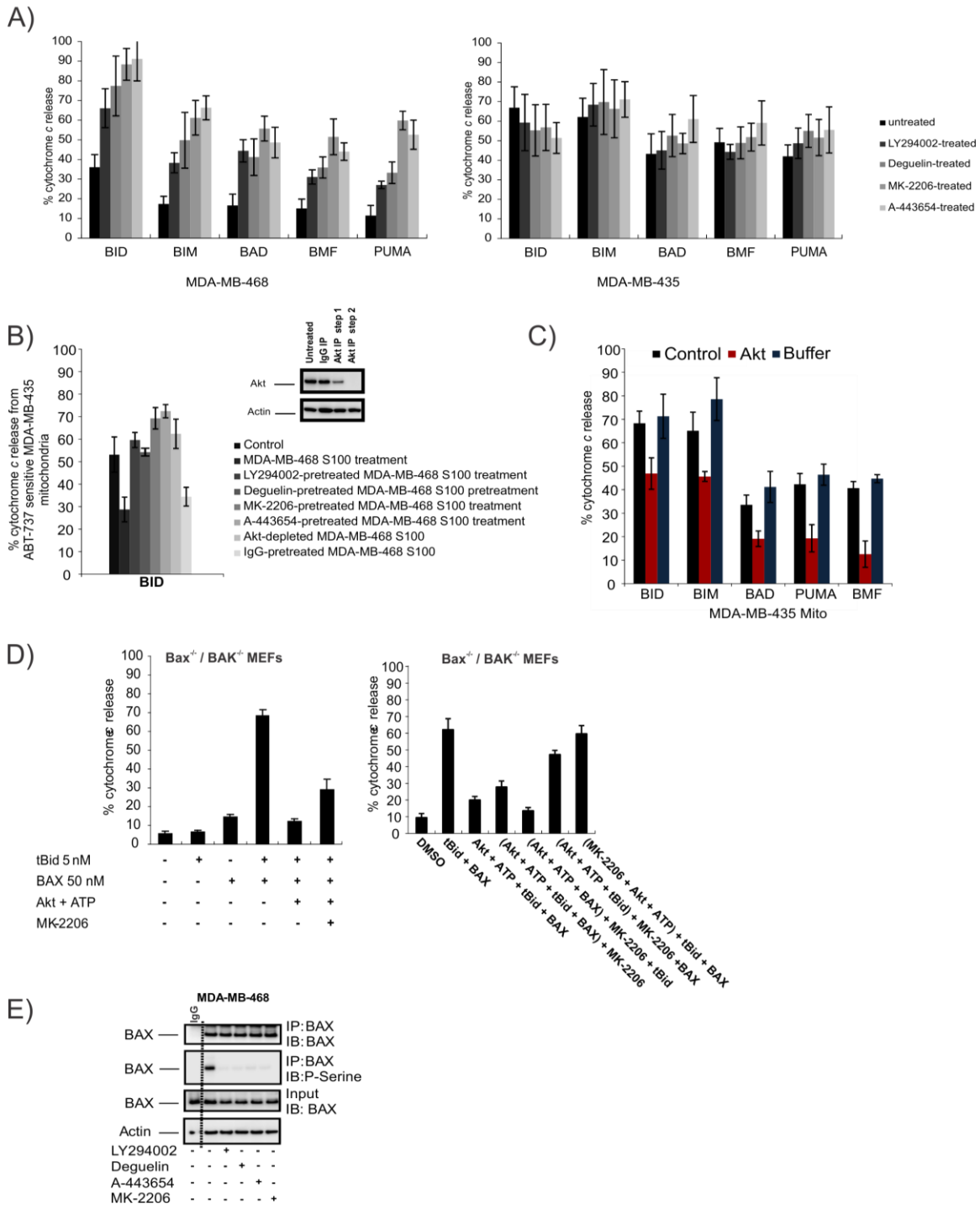

Figure 6.4 - AKT can render Bax phosphorylated and inhibited

A) Inhibiting PI3K/Akt pathway by small molecules led to increasing priming in PTEN-deficient cells. Cells were treated with specific Akt inhibitors (MK-2206 [1 μM], A-443654 [0.4 μM]) or PI3K/Akt inhibitors (LY294002 [25 μM], Deguelin [10 nM]) for 6 hr and BH3 profiles were analyzed (mean±SEM, n=3)

B) S100 fractions from untreated cells (MDA-MB-468) or from cells treated with Akt inhibitors (MK-2206, A-443654) or PI3K inhibitors (LY294002, Deguelin) were isolated. Akt was immunodepleted by sequential

immunoprecipitation in untreated S100 fractions and the efficiency of immunodepletion was tested by immunoblot analysis. IgG was used as a negative control for immunodepletion experiments. Indicated S100 fractions were incubated with MDA-MB-435 mitochondrial preparations and change in priming was assessed by using BH3 profiling on MDA-MB-435 mitochondria. Response to Bid BH3 peptide is shown (mean±SEM, n=3).
C) MDA-MB-435 mitochondria were incubated with recombinant active Akt in kinase assay buffer containing ATP and alteration of priming in MDA-MB-435 mitochondria was detected by using BH3 profiling.
D) tBid and BAX, with or without preincubation (2 hr) with active Akt plus ATP, were incubated with Mitochondria isolated from BAX/BAK DKO MEFs for 1 hr and mitochondrial cytochrome *c* release was analyzed by ELISA (mean±SEM, n=4). Akt inhibitor MK-2206 was used as a control for Akt activity.
E) Phosphorylation of BAX in MDA-MB-468 cells treated with MK-2206, A-443654, LY294002 and Deguelin. See also Figure S4.

6.3.5. Over-expression of Bax is countered by PI3K/AKT pathway activation in human cancer

The AKT pathway is frequently hyper-active in many cancers (Bellacosa et al., 2005) and we have shown that AKT phosphorylates Bax at position S184 converting Bax into an anti-apoptotic protein. Although Bax is generally considered an anti-oncogene and reduced expression is associated with poor prognosis (Krajewski et al., 1995; Schuyer et al., 2001) we hypothesized that certain cancers may be protected from apoptosis due to an increase in the amount of phosphorylated Bax. To address this hypothesis directly we tested commercially available antibodies for detection of phosphorylated Bax in patient samples. Unfortunately, no antibody recognized phosphorylated Bax on western blots of human cells or tissue and immunohistochemistry results were inconclusive. If, as our results suggest, AKT is a major enzyme responsible for phosphorylating Bax a prediction would be that in cancers overexpressing Bax the activity and/or amount of AKT would be increased. Therefore as an indirect assessment we examined gene copy number alterations (CNA) and mRNA expression data to determine if high Bax expression correlates with increased expression/activation of the PI3K/Akt pathway genes (*AKT1*, *AKT2*, *AKT3*, *PIK3CA*, *PIK3R1*) and the PI3K/Akt pathway inhibitor gene *PTEN*.

An initial examination of all available CNA data (16,557 samples) from cBioPortal revealed that *BAX* duplications were significantly associated with Akt pathway duplications ($p <$

10^{-10}) as 879/925 (95%) of patients with a *BAX* duplication also had at a duplication of at least one Akt pathway gene. In contrast, only 41% of all samples in the database had AKT duplications. In addition, 183/925 (20%) of patients with *BAX* duplications had duplications of three or more Akt pathways genes. Furthermore, there were deletions in the AKT negative regulator gene *PTEN* in 11% of patient samples with *BAX* duplications compared to *PTEN* deletions in 17% of all patient samples suggesting a slight but not statistically significant negative correlation. However, amongst the 46 patients with *BAX* duplications, but no AKT duplications, 13 (28%) had *PTEN* deletions ($p = 0.045$). This suggests cancers that have *BAX* amplifications tend to have hyper-active Akt either by PI3K/Akt pathway amplifications or *PTEN* deletions.

Amplification of the PI3K/Akt pathway may permit, but not directly result in, the overexpression of Bax. However, due to the anti-oncogenic nature of Bax, we hypothesize that overexpression of Bax in cancer requires hyper-activation of the PI3K/Akt pathway. Thus, we examined associations of both *BAX* CNA gain and *BAX* mRNA overexpression in relation to PI3K/Akt pathway genes from the TCGA database (Figure 5A). As expected from the results obtained with data from cBioportal, in pan-cancer patient samples *BAX* gain was associated with gain of *AKT1*, *AKT2* and *PIK3R1* and increased expression of *AKT1* and *AKT2* mRNA. Furthermore, high *BAX* mRNA expression is associated with an increase in *AKT1* and *AKT2* and a decrease in *PTEN* mRNA. This is consistent with the hypothesis that in cancers with high levels of Bax the protein is phosphorylated and anti-apoptotic. However, contrary to our hypothesis there was a significant association between either *BAX* gain or high *BAX* mRNA expression and decreased levels *PIK3CA* and *PIK3R1* mRNA. Akt directly targets Bax and thus the increased Akt levels make logical sense however we reason that low levels of PI3K activity due to lower expression of PI3K genes could be countered by the decreased expression of *PTEN* that we observe when *BAX* (CNA and mRNA) levels are high. To examine this further in a single cancer type we selected breast invasive carcinoma samples from TCGA datasets since five of the seven cell lines studied here are breast cancer cell lines (Figure 5A). In breast invasive carcinoma, we observe similar trends to that of the pan-cancer dataset, although fewer of the associations are statistically significant, a likely consequence of the smaller dataset.

Due to the positive associations between increased *BAX* levels and PI3K/Akt pathway genes we hypothesize a higher probability of PI3K/Akt pathway upregulation in patients with high *BAX* levels compared to that with low *BAX* levels (Figure 5B). Probing the TCGA database, 97.6% (200/205) of patients showing increase in *BAX* copy number also show up-regulation of PI3K/Akt pathway (defined here as an increases in *AKT1* OR *AKT2* OR *PIK3CA* OR decrease in *PTEN* copy number). This positive association is highly significant when compared to the whole population (p=7e-40). On the other hand, only 47% (93/198) of patients showing decrease in *BAX* copy number also show up-regulation of the PI3K/Akt pathway. When looking at breast invasive carcinoma, the association of *BAX* levels and PI3K/Akt pathway activation was similar to the pan cancer dataset. Thus, 97.5% (195/200) of breast cancer patients showing increase in *BAX* copy number also show up-regulation of PI3K/AKT pathway compared to 58% (291/502) of breast cancer patients with low BAX (p=2e-36). Taken together these results suggest that in tumors with elevated *BAX* the protein may be phosphorylated (due to an increase in the PI3K/Akt pathway) and therefore anti-apoptotic.

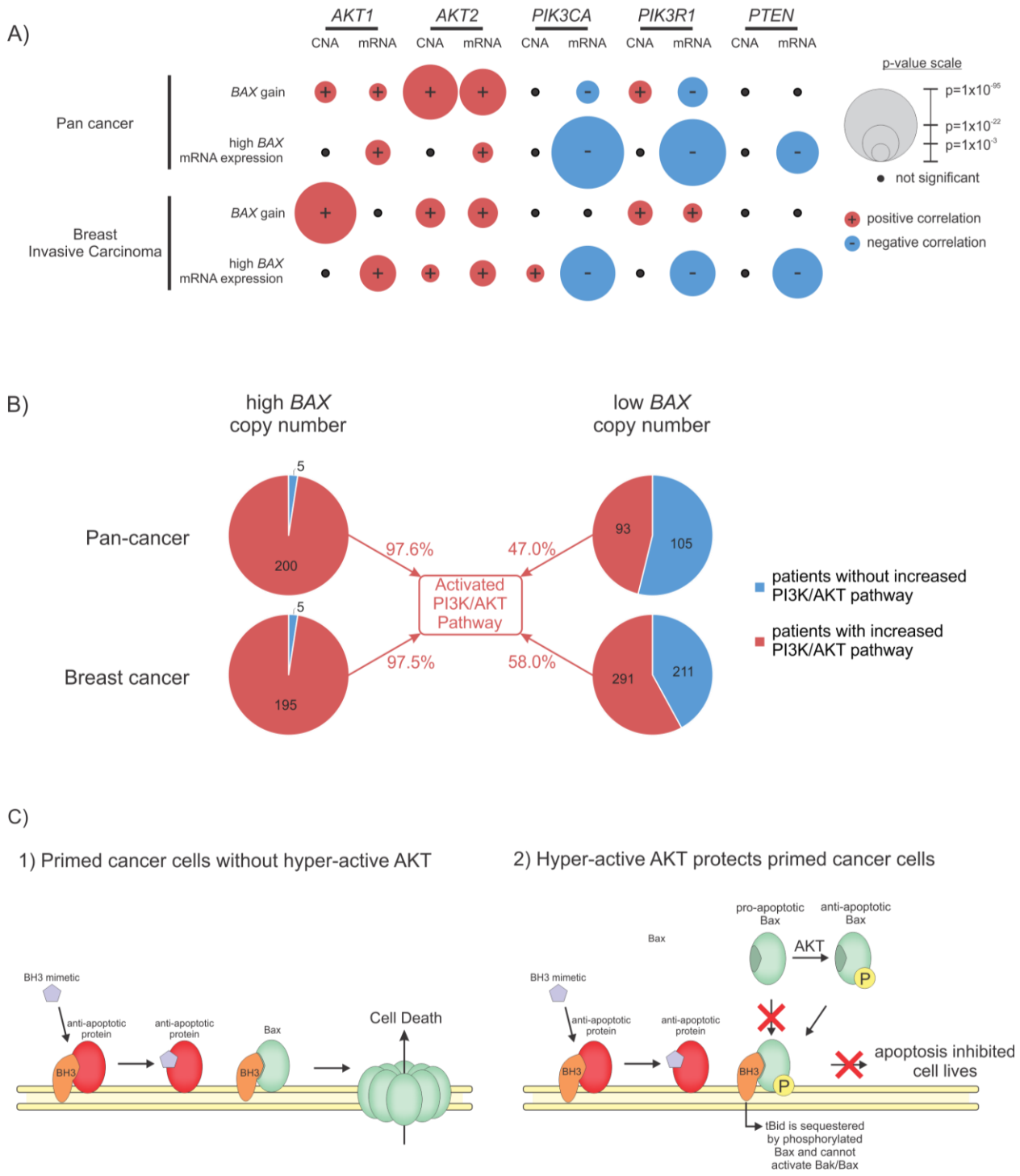

Figure 6.5 - Phosphorylated Bax protects cells from apoptosis

A) Copy number and mRNA for Bax is associated with increased expression of AKT1 and AKT2, and decreased expression of PTEN. TCGA database was probed for significant associations between the row heading (e.g BAX gain) and copy number (CNA) gain/loss (red[+]/blue[-]) or mRNA up/downregulation (red[+]/blue[-]) of the

indicated genes (*AKT1*, *AKT2*, *PIK3CA*, *PIK3R1* and *PTEN*). Association strength is proportional to –log(p-value), reflected in the radii of the circles. Black circles indicates non-significant association (p-value cutoff = 0.02).
B) Cancer patients with high *BAX* copy number tend to have activated PI3K/AKT pathway, compared to that with low *BAX* copy number. Each circle represents the total number of patients with either high Bax (left) or low Bax (right) copy number. Within each circle the proportion of patients with activated PI3K/AKT pathway (red) is compared to the proportion of patients without activated PI3K/AKT pathway (blue). Activated PI3K/AKT pathway is defined as an increase in *AKT1* or *AKT2* or *PIK3CA* or decrease in *PTEN* copy number.
C) Phosphorylation by Akt causes Bax to become an anti-apoptotic protein. 1) in cells sensitive to ABT-737, mitochondria are primed for death due to anti-apoptotic proteins binding activator BH3-only proteins at the mitochondrial outer membrane. Addition of a BH3 mimetic such as ABT-737, displaces tBid from Bcl-XL, where tBid activates Bax leading to MOMP and cell death. 2) In cells resistant to ABT-737 Bax is phosphorylated at position S184E by AKT. Phosphorylation at S184 prevents Bax inserting into the MOM while retaining cBid binding activity. This causes the cells to be resistant to ABT-737, because released activator BH3-only proteins are sequestered by phosphorylated Bax, preventing them from activating non-phosphorylated Bax and Bak.

6.4. Discussion

Residue S184 on Bax has been reported critical to control Bax activation because a series of point mutations at S184 were found to alter Bax pro-apoptotic function (Nechushtan et al., 1999). Akt has also been reported to phosphorylate Bax at S184 thereby inhibiting activation and mitochondrial localization in response to various perturbations in several normal tissues, including neutrophils and endothelial cells (Gardai et al., 2004; Kolliputi and Waxman, 2009; Wang et al., 2010). Activation of AKT and phosphorylation of Bax at S184 is induced by nicotine in lung cancer cell lines where it protects cells from cisplatin (Xin and Deng, 2005). However, a recent study also reported that either co-expression of Bax and AKT or expression of S184D phosphomimetic Bax in yeast results in the activation of Bax (Simonyan et al., 2016). Here we have confirmed that both Akt-mediated phosphorylation and a phosphomimetic Bax are defective in mediating membrane permeabilization in vitro**,** using a highly defined liposome based system (Figure 2), isolated mitochondria (Figure 4) and in mammalian cells (Figure 3), as has been previously reported (Gardai et al., 2004; Quast et al., 2013).

Although these studies correlated Bax inactivation and S184 phosphorylation the mechanism remained unclear. By assaying each step in the Bax activation pathway we identified

that insertion of Bax into membranes is inhibited by this post-translational modification. Subsequent steps including Bax homo-oligomerization and pore formation were also prevented suggesting the temporal order identified previously (Lovell et al., 2008) results from each step being dependent on successful completion of the one before it. Previous results were interpreted as suggesting that S184 phosphorylation of Bax abrogated all functions (Gardai et al., 2004; Wang et al., 2010; Xin and Deng, 2005)**.** However, since BH3-protein binding is a step before insertion of Bax into membranes we found that Bax S184E bound to activator BH3-only proteins on membranes and in solution (Figure 2B). BH3-only protein binding was unexpected in solution because when Bax is in solution the BH3 binding site is normally occluded by helix 9. Therefore, we speculate that the addition of a negative charge within the hydrophobic region of helix 9 by phosphorylation or mutation prevents helix 9 interaction with and thereby opens the BH3 binding site on Bax.

A phosphorylated Bax that does not permeabilize membranes yet binds activator BH3-only proteins inhibits MOMP by sequestering the BH3-protein similar to inhibition of BH3-proteins by anti-apoptotic Bcl-2 family proteins. As phosphomimetic Bax competitively sequesters activator BH3-only proteins, but does not bind WT Bax (Fig. 2D) it is expected to be less effective inhibiting apoptosis than anti-apoptotic Bcl-2 proteins. Nevertheless, phosphomimetic Bax acts in a dominant-negative fashion with a mechanism similar to mode 1, (but not mode 2) of Bcl-XL (Billen et al., 2008; Llambi et al., 2011). Thus, phosphorylation of Bax by Akt converts Bax from pro- to anti-apoptotic, resulting in a diminished sensitivity of mitochondria to apoptotic signalling by BH3-only proteins. As a consequence, cells are resistant to drugs that kill cells via the apoptotic pathway, including the Bcl-2/Bcl-XL/Bcl-w antagonist ABT-737 (Figure 1). Consistent with this conclusion expression of Bax S184E in cells with endogenous Bax and Bak, protected these cells from apoptotic stimuli (Figure 3B).

A predicted consequence of inhibition of apoptosis by phosphorylated Bax is that Bax phosphorylation in cells by hyperactive Akt likely provides a selective advantage for cancer cells that have increased levels of Bax. As a tumor suppressor Bax expression is usually decreased in cancer cells. Indeed overexpression of Bax sensitizes cancer cells to apoptosis induced by chemotherapy or radiation (Bargou et al., 1996; Lin et al., 2005; Sakakura et al., 1996; Sakakura et al., 1997; Xu et al., 2002) and is correlated with improved clinical outcomes in ovarian cancer

and gastric cancer (Pietrantonio et al., 2012; Tai et al., 1998). However, our analysis clearly demonstrates that when Bax copy number is increased, 97.6% of the patients also show up-regulation of the PI3K/Akt pathway (Fig. 5B). Phosphorylation by Akt provides an explanation for this observation as S184-phosphorylated Bax would allow cells to evade apoptosis by preventing BH3-proteins from binding to and activating WT Bax/Bak (Figure 5C). Thus increasing the expression of Bax in cells with hyper-active AKT represents an additional mechanism for cancer cells to prevent apoptosis.

Our findings are of clinical importance because activation of the PI3K/Akt pathway occurs often in cancer cells as a result of loss of PTEN, aberrant receptor tyrosine kinase activity or PIK3CA or AKT1 activating mutations. Because of this heterogeneity it has been difficult to establish predictive biomarkers. The important role of Bax phosphorylation in the anti-apoptotic effects of Akt elucidated here, suggests that phosphorylation of Bax at S184 is a potential predictive, and perhaps pharmacodynamic, biomarker for pharmacologic inhibitors of the PI3K/Akt pathway in cancer clinical trials. Thus the development of antibodies useful for immunohistochemistry is highly desirable. Moreover, considering the growing interest in BH3 mimetics as anti-cancer agents, and the ongoing development of PI3K/Akt inhibitors, we suggest that examination of possible combinatorial therapies for cancers with hyperactive Akt is warranted.

6.5. EXPERIMENTAL PROCEDURES

6.5.1. Antibodies, Reagents and Plasmids

Antibodies: Akt (#9272), Actin (#4967), GAPDH (#2118), GSK-3β(#9315), pGSK-3β (S9) (#9336) were from Cell Signaling, Beverly, MA, USA. cytochrome *c* (*7H8.2C12) were from* BD Biosciences, San Jose, CA, USA. phospho-Serine (4A9) were purchased from EMD Millipore, Billerica, MA, USA. MCL-1 (S-19), GFP (19F7) was from Memorial Sloan-Kettering Monoclonal Antibody Facility.

Reagents: ABT-737, negative control enantiomer and A-443654 were obtained from Abbott Laboratories. MK-2206 and LY294002 were purchased from *Selleck* Chemicals,

Houston, TX, USA. Deguelin was obtained from Tocris Bioscience Minneapolis, MN, USA. Recombinant Human Active Akt1 was obtained from R&D Systems, Minneapolis, MN, USA (1775-KS) and Sigma, St Louis, MO, USA (A8729).

Plasmids: GFP-Bax (hBax C3-EGFP, Addgene plasmid 19741), GFP-Bax S184A (hBax S184A C3-EGFP, Addgene plasmid 19742) and GFP-Bax S184E (hBax S184E C3-EGFP, Addgene plasmid 19743) were previously described (Nechushtan et al., 1999). GFP (PCDNA3-EGFP, Addgene plasmid 13031) was used as a control for transfections. Single cysteine Bax 126C (pMAC1731) and single cysteine cBid 126C (pMAC2118) were previously described (Lovell et al., 2008). The cDNA for single cysteine Bax 175C was transferred from the corresponding retro-viral vector (Annis et al., 2005) into the IMPACT expression system (New England Biolabs, Ipswich, MA, USA) generating pMAC 1739.

6.5.2. Cell Culture

MDA-MB-435, MCF-7, T47-D, MDA-MB-468, ZR-75-1, SF539 AND 768-O cells were grown in DMEM/F12 (Invitrogen, Carlsbad, CA, USA) and WT MEFs and Bax/Bak DKO MEFs were grown in DMEM (Invitrogen, Carlsbad, CA, USA) supplemented with 2 mM L-glutamine, 10% heat inactivated fetal bovine serum (Sigma, St Louis, MO, USA), 100 IU/mL penicillin, and 100 mg/mL streptomycin (Invitrogen) in a humidified incubator at 37°C and 5% CO_2. MDA-468TR-Vector and MDA-468TR-PTEN cells were grown as previously described (She et al., 2005). 24-well AlgiMatrix 3D cell culture system (Invitrogen, Carlsbad, CA, USA) was used to grow cells as spheroids using the same media for monolayer cultures as recommended by the manufacturer. MDA-MB-468 cells were stably transfected with vectors containing GFP, GFP-Bax, GFP-Bax S184A and GFP-Bax S184E plasmids using Fugene 6 (Roche, Indianapolis, IN, USA) and the clonal selection was carried out in the presence of G418 (1.2-1.6 mg/mL, Sigma, St Louis, MO, USA). Selected clones were maintained in growth medium containing 0.16 mg/mL G418.

6.5.3. Immunoblotting, Immunoprecipitation and Coimmunoprecipitation

Total cell lysates were prepared in 1% CHAPS buffer [5 mM MgCl2, 137 mM NaCl, 1 mM EDTA, 1 mM EGTA, 1% CHAPS, 20 mM Tris–HCl (pH 7.5), protease inhibitors (Complete, Roche, Indianapolis, IN, USA), and phosphatase inhibitors (PhosSTOP, Roche, Indianapolis, IN, USA)] as reported previously (Leu et al., 2004). AlgiMatrix dissolving buffer (Invitrogen, Carlsbad, CA, USA) was used to harvest spheroids before lysis in 1% CHAPS buffer. For coimmunoprecipitations, proteins (800 μg-10 mg) were immunoprecipitated with indicated antibodies at 4°C for 2 h or O/N and coimmunoprecipitates were captured by Dynabeads Protein G at 4°C for 2 h or O/N. Beads were recovered using DynaMag spin magnet and washed thrice in 1% Chaps buffer. To determine the activation of Bax and Bak, proteins (800 μg) were immunoprecipitated with anti-Bax (6A7) and anti-Bak (Ab-2) at 4°C for 2 h. Immunoprecipitates were captured by Dynabeads Protein G (Invitrogen, Carlsbad, CA, USA) at 4°C for 2 h. Immunoprecipitates were then recovered by DynaMag spin magnet and washed thrice in 1% Chaps buffer. For Bax immunoprecipitations aiming phosphorylation analysis, proteins were isolated in a modified RIPA buffer [50 mM Tris–HCl (pH 7.5), 150 mM NaCl, 1% NP-40, 0.5% Na-deoxycholate, 1 mM EDTA, 1 mM EGTA, 1 mM PMSF, protease inhibitors (Complete, Roche, Indianapolis, IN, USA), and phosphatase inhibitors (PhosSTOP, Roche, Indianapolis, IN, USA)] and immunoprecipitated with Bax Δ21 antibody. Immunoprecipitates, total cell extracts and subfractionation lysates were separated on NuPage 10% Bis-Tris gels. Following SDS-PAGE, proteins were transferred onto PVDF membranes (Immobilon, EMD Millipore, Billerica, MA, USA) and then blocked with 5% dried milk in PBS-Tween20. Membranes were incubated with primary and secondary antibodies (GE Healthcare Life Sciences, Pittsburgh, PA, USA) in a buffer containing 10% milk diluent blocking concentrate (KPL, Gaithersburg, MD, USA), and detected with SuperSignal West Pico Chemiluminescent Substrate (Thermo Fisher Scientific, Rockford, IL, USA). For phosphorylation blots, 4% BSA in TBS-Tween was used for blocking and antibody preparation and TBS-Tween was used for membrane washing steps. Blots were imaged with LAS4000 image analyzer (Fujifilm, Tokyo, Japan) on chemiluminescence mode. To detect interacting proteins in some coimmunoprecipitation experiments, protein A-horseradish peroxidase (GE Healthcare Life Sciences, Pittsburgh, PA, USA) was used as a secondary detection agent.

6.5.4. Peptide synthesis and protein purification

Peptides were synthesized by Tufts University Core Facility and purified by HPLC. Peptide identities were confirmed by mass spectrometry and stock solutions were prepared in DMSO. tBid generated from His-tagged human Bid cleaved with recombinant caspase-8 was a generous gift from Claudio Hetz (University of Chile, Santiago, Chile). The expression and purification of recombinant human Bax was done as previously reported (Suzuki et al., 2000).

6.5.5. Phosphoprotein gel staining

Protein samples after kinase reactions were separated on 10% Bis-Tris NuPAGE gels and stained with Pro-Q Diamond phosphoprotein gel stain and SYPRO Ruby total protein gel stain (Invitrogen, Carlsbad, CA, USA) according to manufacturer's protocol. Gels were imaged with LAS4000 image analyzer (Fujifilm, Tokyo, Japan), using the same exposure settings for different samples on green and blue fluorescence epi-illumination mode and the quantitation of bands was performed using ImageJ software (ImageJ, NIH, USA).

6.5.6. Protein Purification and Labeling, and Liposome Preparation

Single cysteine Bax mutants, 126C and 175C were expressed, purified and labeled with DAC or NBD, as previously described (Lovell et al., 2008). Bax S184E mutation was introduced into the Bax 126C and 175C plasmids via Quick-Change™ mutagenesis (Stratagene, La Jolla, CA, USA). Primers for S184E mutagenesis were 3'-GGAGTGCTCACCGCCGAACTCACCATCTGGAAG-5' (forward) and 3'-CTTCCAGATGGTGAGTTCGGCGGTGAGCACTCC-5' (reverse). Single cysteine His-Bid 126C was expressed, purified and labeled with DAC as previously described (Lovell et al., 2008). Liposomes were prepared as previously published (Lovell et al., 2008). Briefly, a 1 mg mitochondria-like lipid film (0.46 mg of egg phosphatidylcholine (PC), 0.25 mg of egg phosphatidylethanolamine (PE), 0.11 mg of bovine liver phosphatidylinositol (PI), 0.10 mg 18:1 dioleoyl phosphatidylserine (DOPS) and 0.08 mg tetraoleoyl cardiolipin (TOCL)) was hydrated 1 with mL of Assay Buffer (10 mM HEPES pH 7.2, 200 mM KCl, 1 mM $MgCl_2$)(All lipids were acquired from Avanti Polar Lipids, Alabaster, AL, USA). Hydrated lipid films underwent 10

freeze-thaw cycles and were extruded 11 times through a 100 nm pore size nucleopore track-etched polycarbonate membrane (Whatman, GE Healthcare Life Sciences, Pittsburgh, PA, USA).

6.5.7. Subcellular subfractionation

Subcellular fractionation was performed as reported before (Ruiz-Vela et al., 2005). Briefly, cells were harvested and washed in ice-cold PBS and then resuspended in an isotonic buffer [250mM sucrose, 20mM HEPES (pH 7.5), 10mM KCl, 1.5mM MgCl2, 1mM EDTA, 1mM EGTA, 1mM PMSF, and protease inhibitors (Complete, Roche)] on ice for 20 min. Phosphatase inhibitors (PhosSTOP, Roche, Indianapolis, IN, USA) were added as indicated. After incubation, cells were homogenized with Dounce homogenizer and centrifuged at 800 g for 10 min at 4°C. The remaining supernatant was centrifuged at 8000 g for 20 min at 4°C to obtain mitochondria-enriched HM pellet and cytosolic fractions. To obtain S-100 fractions, the remaining supernatant (cytosolic fraction) was further centrifuged at 100 000 g for 1 h at 4°C. The resulting pellet constituted LM and the supernatant was saved as S-100. Mitochondria-enriched pellets were lysed in 1% Chaps buffer for immunoblot analysis.

6.5.8. BH3 profiling

BH3 profiling assays and peptide sequences were previously reported (Certo et al., 2006; Deng et al., 2007). Briefly, 0.5 mg of protein/mL mitochondria were suspended in mitochondria buffer [125 mM KCl, 10 mM Tris-MOPS, pH 7.4, 5 mM glutamate, 2.5 mM malate, 1 mM KPO4, and 10 μM EGTA-Tris, pH 7.4)] and exposed to BH3 peptides (100 μM) for 40 minutes at room temperature. Phosphatase inhibitors (PhosSTOP, Roche, Indianapolis, IN, USA) were added as indicated to the mitochondria buffer. Cytochrome c release was determined by ELISA assay (R&D Systems, Minneapolis, MN, USA) and expressed as % of untreated control. For BH3 experiments using mitochondria treated with S100 fractions, S100 fractions were immunodepleted for Akt by sequential immunoprecipitations using anti-Akt antibody (Cell Signaling, #9272) and Dynabeads twice. IgG immunoprecipitations were done in parallel as a negative control. Mitochondria were incubated with immunodepleted S100 fractions for 1 hr at 30 °C, washed twice with mitochondria buffer containing PhosSTOP and incubated with BH3

peptides for 40 minutes at room temperature. Cytochrome c release was determined by ELISA assay. For BH3 experiments using mitochondria treated with recombinant active Akt, mitochondria (0.1 mg/mL) were incubated with recombinant active Akt (1 μg) and ATP (400 μM) for 1 hr in kinase assay buffer [25 mM Tris-HCl (pH 7.5), 5 mM beta-glycerophosphate, 2 mM dithiothreitol (DTT), 0.1 mM Na3VO4, 10 mM MgCl2] for 2 hr at 30 °C, washed twice with mitochondria buffer containing PhosSTOP and treated with BH3 peptides for 40 minutes at room temperature. Cytochrome c release was determined by ELISA assay.

6.5.9. Mitochondrial Permeabilization Assay

Mitochondria were purified from Bax/Bak DKO MEFs and resuspended in mitochondria buffer (0.5 mg of protein/mL mitochondria) and incubated with tBid and Bax for 1 hr at room temperature. tBid and Bax were preincubated with recombinant active Akt (400 ng) and ATP (200 μM) in kinase assay buffer for 2 hr at 30 °C in some experiments. Preincubation with 120 nM MK-2206 for 1 hr was used to block Akt kinase activity as indicated. Release of cytochrome c was determined by ELISA and expressed as % of untreated control (R&D Systems, Minneapolis, MN, USA).

6.5.10. Apoptosis and Cell Viability Assays

Cell proliferation kit (MTT) (Roche, Indianapolis, IN, USA) and alamar blue (Invitrogen, Carlsbad, CA, USA) were used to determine cell viability and survival of cells as described by the manufacturer. Apoptosis was evaluated by Annexin V-FITC and Annexin V-Cy3 (BioVision, Milpitas, CA, USA) staining using a FACSCanto (BD Biosciences, San Diego, CA, USA) flow cytometer and WinMDI 2.9 software (Scripps Institute, La Jolla, CA, USA). Results are expressed as mean±SEM.

6.5.11. Confocal Microscopy

GFP-tagged protein expressing cells were grown in Lab-Tek II chamber slides (Thermo Fisher Scientific, Rockford, IL, USA) and costained with MitoTracker Red CMXRos (Molecular Probes, Invitrogen, Carlsbad, CA, USA) before fixation in 4% PFA. Monolayer cells and

isolated spheroids fixed with 4% PFA were mounted with Vectashield mounting medium with DAPI (Vector Laboratories, Burlingame, CA, USA). Confocal images of cells and spheroids were captured on a spinning disk confocal microscope (Yokogawa) using an Andor iXon EM-CCD camera. Images were pseudocolored and analyzed by using ImageJ software (ImageJ, NIH, USA).

6.5.12. Bax Membrane Permeabilization: ANTS/DPX Release Assay

For membrane permeabilization assays, a mitochondria-like lipid film was hydrated with 1 mL of assay buffer supplemented with 12.5 mM of the fluorophore 8-Aminonaphthalene 1,3,6-trisulfonic acid (ANTS) and 45 mM of the quencher *p*-xylene-bis-pyridinium bromide (DPX) (Molecular Probes, Invitrogen, Carlsbad, CA, USA). Liposomes were prepared as above and after extrusion, unencapsulated ANTS and DPX were removed by passing the liposomes over a 10 mL CL2B gel-filtration column (GE Healthcare Life Sciences, Pittsburgh, PA, USA). ANTS/DPX release assay was performed as previously described (Billen et al., 2008; Lovell et al., 2008). Briefly, 8 μL of ANTS/DPX encapsulated liposomes were added to a reaction of 100 μL final volume in assay buffer. Fluorescence of ANTS (λ_{ex}=355 nm, λ_{em}=520 nm) was measured over the course of 2 hours at 37°C. Percent ANTS release was calculated as % release = $[(F_{final} – F_0)/(F_{100}-F_0)]*100$ where F_{final} is the fluorescence at a 2 hour endpoint, F_0 is the fluorescence in the absence of proteins and F_{100} is the fluorescence of liposomes permeabilized with 0.2% v/v Triton x-100.

6.5.13. Fluorescence Experiments: Measuring protein:protein and Bax helix insertion into membranes

NBD emission assays and FRET experiments were performed as previously described (Lovell et al., 2008). In a black 96 well half-area non-binding surface assay plate (Corning, NY, USA), 10 μL of 1 mg/mL mitochondria-like liposomes were added to a reaction of 100 μL final volume in assay buffer. Fluorescence emission of 100 nM Bax 175C-NBD and Bax 175C-NBD S184E (λ_{ex}=475 nm, λ_{em}=530 nm) incubated with or without 20 nM recombinant cBid was recorded using a Tecan Infinite M1000 plate reader (Tecan, Switzerland) at 2 hr end-point 37°C. Relative change in NBD emission was expressed as $F/F0=(F_{final} - F_{bckg})/(F_{initial} - F_{bckg})$ where

F_{bckg} is the fluorescence signal of liposomes and buffer, $F_{initial}$ is the fluorescence signal once NBD labeled protein was added to the well and F_{final} is the fluorescence signal at 1 hour endpoint. cBid-Bax FRET was similarly measured, however the emission of cBid 126C-DAC donor (λ_{ex}=380 nm, λ_{em}=460 nm) was recorded. FRET efficiency was calculated as % FRET efficiency=1 – [(F_{DA}-F_{bckg})/(F_D-F_{bckg})] where F_{DA} is the fluorescence emission of 20 nM cBid 126C-DAC donor in the presence of 100 nM Bax labeled NBD acceptor at 2 hour endpoint, F_D is the fluorescence emission of 20 nM cBid 126C-DAC donor alone in the presence of unlabeled Bax 126C at 2 hour endpoint and F_{bckg} is the fluorescence signal of liposomes and assay buffer alone. Bax-Bax FRET was measured as cBid-Bax FRET, however measurements were recorded in a PTI Quantamaster fluorometer (Photon Technology International, Birmingham, NJ, USA), using a 1 mL quartz cuvette containing 100 μL lipids in a final reaction volume of 1 mL in assay buffer at 37°C. FRET efficiency was calculated as above however F_{DA} is the fluorescence emission of 10 nM DAC labeled Bax donor in the presence of 100 nM NBD labeled Bax acceptor at 2 hour endpoint, and F_D is the fluorescence emission of 10 nM DAC labeled Bax donor in the presence of 100 nM unlabeled Bax acceptor.

6.5.14. Statistical Analysis

GraphPad Prism 5.0 software (GraphPad Software, San Diego, CA, USA) was used for data analysis and to determine the significance of statistical differences between data. Student's t-tail test was used for comparison of data and the significance was set at *P<0.05 and **P<0.01.

6.5.15. Bioinfomatics analysis:

CNA analysis - CNA data was obtained from the cBio database genomics (Cerami et al., 2012; Gao et al., 2013). Duplications and deletions were defined as log2CNA >0.5 or < -0.5 respectively. Association with the AKT pathway was evaluated using a Cochran-Armitage test for trend on the number of AKT pathway genes (AKT1, AKT2, AKT3, PIK3CA, PIK3R1) that were duplicated in patients carrying BAX of BAK duplications. Association with PTEN was evaluated using a Fisher exact test.

TCGA pan-cancer gene-level analysis – This analysis covered expression (n=9755), copy number (n=10843), and mutation data (n=6901) across 42 cancers. Data were obtained from the Cancer Browser (Cline et al., 2013). This database uses the software GISTIC2 (Mermel et al., 2011) to normalize copy number gain or copy number loss, which were defined in the present work as a GISTIC2 call ≥ 1 or ≤ 1, respectively. Gene expression association was evaluated by ranking expression values of the reference gene and applying a two-tailed unpaired Student's T-test to evaluate differential gene expression between 1st and 10th deciles across genes.

6.6. Supplementary Information

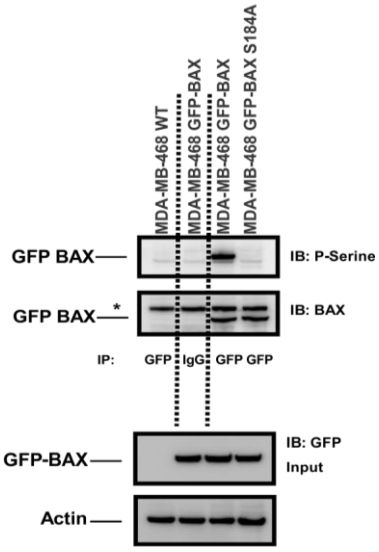

Supplementary Figure 6.1 - Related to Figure 1 - Phosphorylation of GFP-Bax in MDA-MB-468 cells.
Upper panels: Phosphorylation of BAX was evaluated using lysates from GFP-BAX and GFP-BAX S184A cells by blotting with the antibodies indicated at the left after precipitation with the antibodies indicate below the panels. Lysates from untransfected cells (MDA-MB-468 WT) and IgG IP are used as negative controls.
Lower panels: 5-10% of the total lysates were probed for GFP and actin as expression and loading controls, respectively.

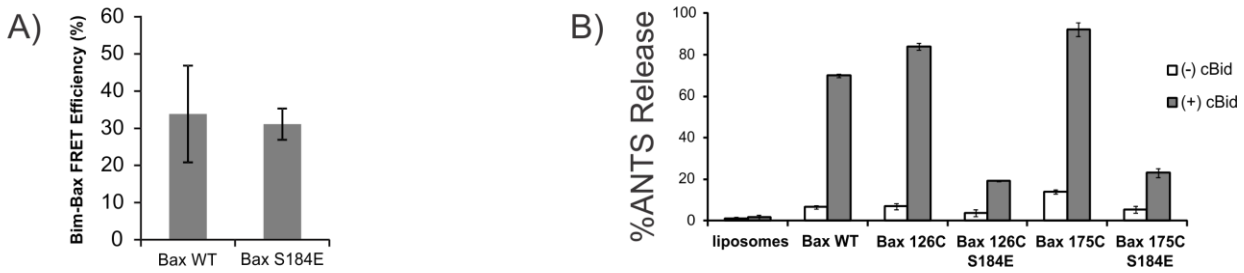

Supplementary Figure 6.2 – Related to Figure 2 - Bax S184E binds to Bid but membrane permeabilization is inhibited

A) the interaction between Bim and Bax was measured by FRET. Samples containing liposomes were incubated with 20 nM BIM 41C-DAC and BAX126C-NBD or Bax 126C-NBD S184E was titrated as indicated below. FRET efficiency was calculated as 1- (FDA/FD) at 2 hour endpoint (mean±STDEV, n≥3).

B) Permeabilization of liposomes by Bax and cBid was measured by release of ANTS/DPX. Liposomes encapsulating ANTS/DPX were incubated with 100 nM of the indicated Bax in the absence or presence of 20 nM cBid (mean±STDEV, n≥3).

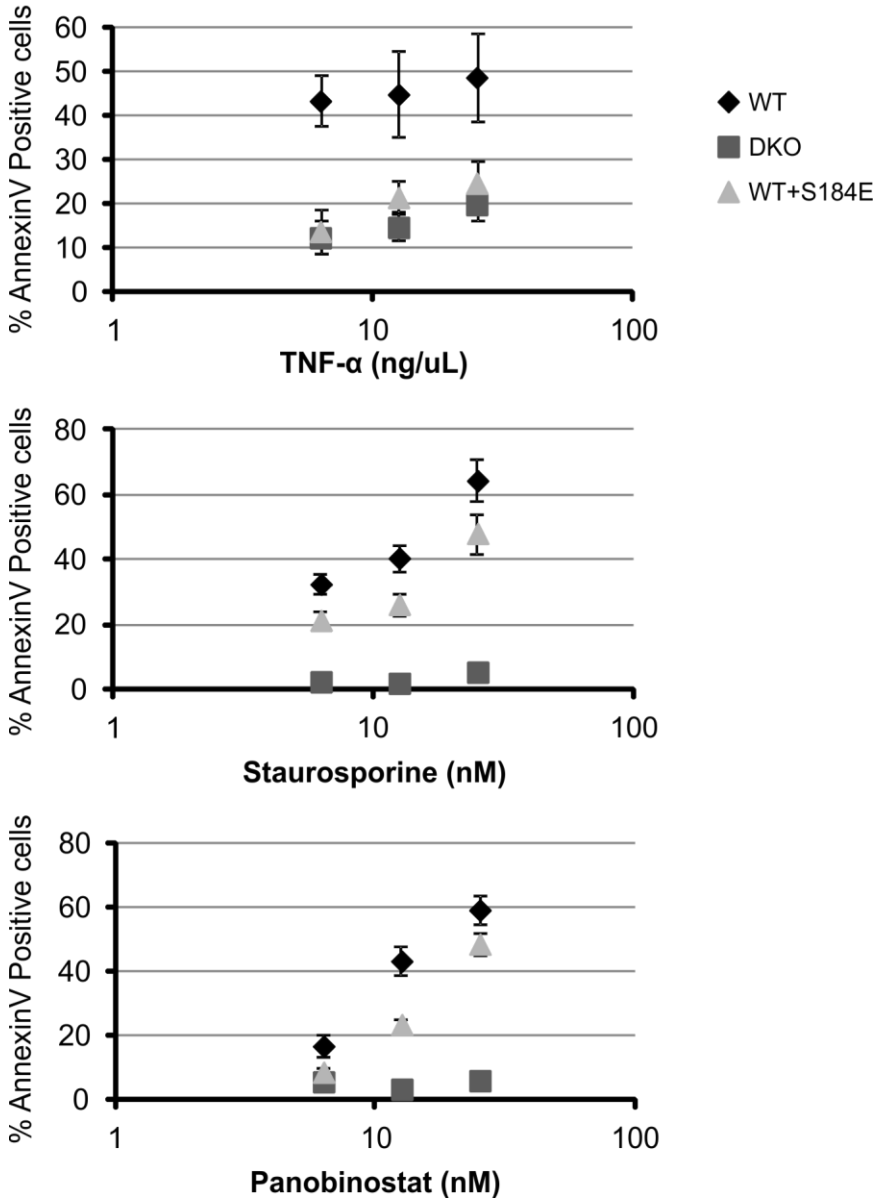

Supplementary Figure 6.3 – Related to Figure 3 - mCerulean Bax-S184E protects cells from apoptosis

WT BMK (WT), Bax/Bak DKO BMK (DKO) and WT BMK cells stably expressing mCerulean Bax-S184E (WT+S184E) were treated with the indicated cell death stimuli for 24 hours. Cells stained with Draq5 and Annexin V conjugated to Alexa 488 were imaged on an automated confocal microscope (>500 cells per data point). Draq5 staining was used to identify all cells and Annexin V-Alexa488 staining was used to identify dead cells. Annexin V-Alexa-488 positive cells were assigned based on a user defined threshold of a per cell Annexin V fluorescence that was greater than 2 standard deviations above the per cell Annexin V fluorescence of untreated DMSO controls. The % Annexin V positive cells was calculated from 3 independent experiments each with 2 technical replicates. Shown is mean±SEM, n=3.

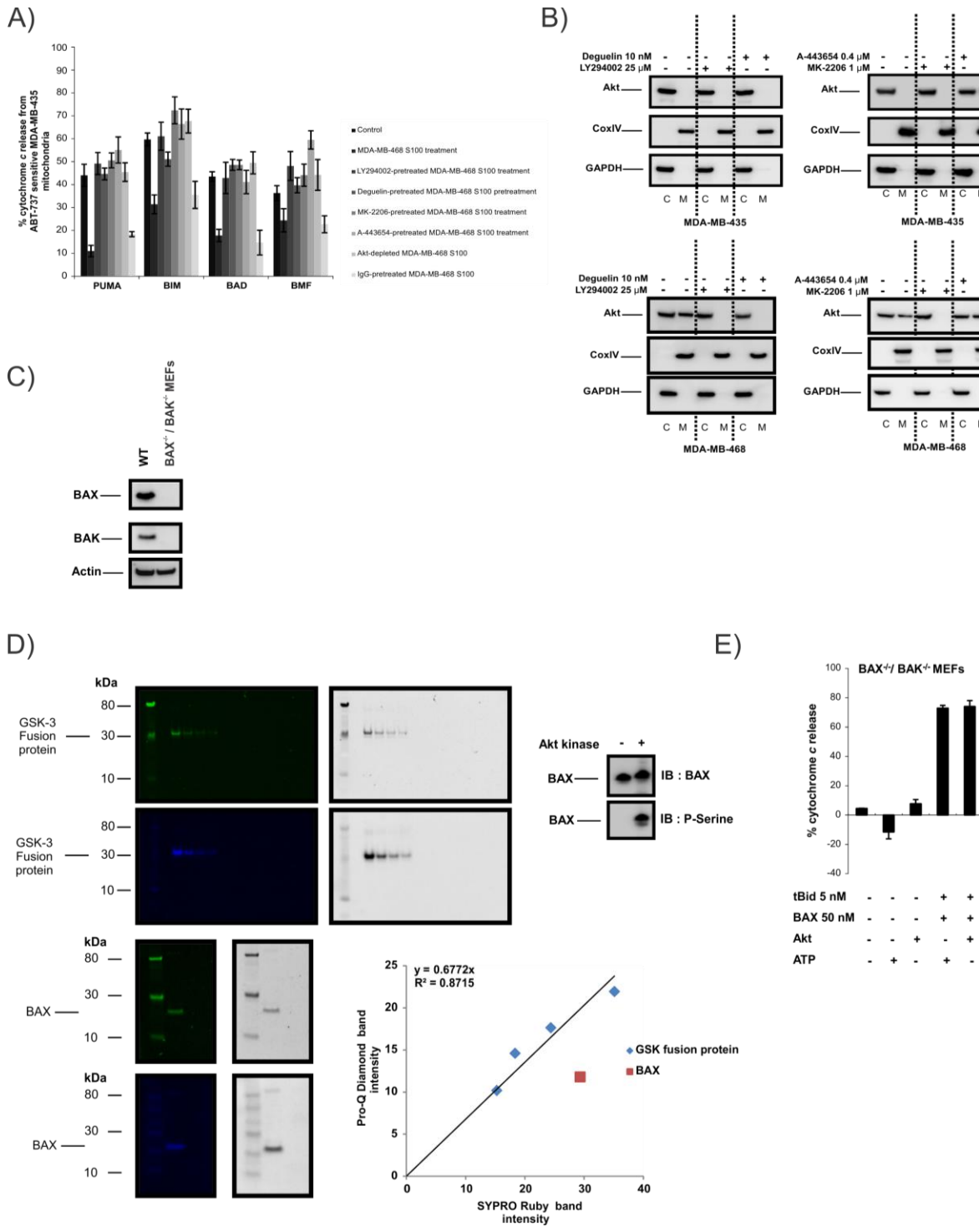

Supplementary Figure 6.4 – Related to Figure 4 - Akt and PI3K inhibitors change the localization of Akt and the primed state of mitochondria

A) S100 fractions from untreated cells (MDA-MB-468) or from cells treated with Akt inhibitors (MK-2206, A-443654) or PI3K inhibitors (LY294002, Deguelin) were isolated. Akt was immunodepleted by sequential immunoprecipitation in untreated S100 fractions and the efficiency of immunodepletion was tested by immunoblot

analysis. IgG was used as a negative control for immunodepletion experiments. Indicated S100 fractions were incubated with MDA-MB-435 mitochondrial preparations and change in priming was assessed by using BH3 profiling on MDA-MB-435 mitochondria. Responses to various BH3 peptides are shown (mean±SEM, n=3).
B) ABT-737 resistant MDA-MB-468 and ABT-737 sensitive MDA-MB-435 cells were treated with Akt inhibitors (MK-2206, A-443654) or PI3K inhibitors (LY294002, Deguelin) and mitochondrial and cytosolic fractions were immunoblotted for Akt. CoxIV was probed as the mitochondrial marker protein and GAPDH was used as the cytosolic marker protein (M: Mitochondrial fraction, C: Cytosolic fraction).
C) Lack of expression of BAX and BAK in DKO MEFs was detected by immunoblotting. Actin was probed as a loading control.
D) Phosphorylation of recombinant BAX following kinase reaction by Akt was evaluated by immunoblotting with phospho-Serine antibody. BAX was blotted as a loading control. Following kinase reaction with active Akt kinase, a standard curve of GSK-3 fusion protein was constructed after staining with Pro-Q Diamond phosphoprotein and SYPRO Ruby total protein dual staining assay. Band intensities were quantified by ImageJ software. Percent phosphorylation of BAX by active Akt after 2 hr of kinase reaction was derived from GSK-3 fusion protein standard curve after staining with Pro-Q Diamond/SYPRO Ruby dual staining. Representative gel images and standard curve graph are provided.
E) Akt or ATP did not alter cytochrome c release triggered by tBid/BAX treatment when used alone. Mitochondria from BAX BAK DKO MEFs were directly exposed to Akt or ATP or after incubated Akt or ATP with tBid and BAX as designated. Cytochrome *c* release from mitochondria was evaluated by ELISA (mean±SEM, n=3).

6.7. REFERENCES

Annis, M.G., Soucie, E.L., Dlugosz, P.J., Cruz-Aguado, J.A., Penn, L.Z., Leber, B., and Andrews, D.W. (2005). Bax forms multispanning monomers that oligomerize to permeabilize membranes during apoptosis. EMBO Journal *24*, 2096-2103.

Bargou, R.C., Wagener, C., Bommert, K., Mapara, M.Y., Daniel, P.T., Arnold, W., Dietel, M., Guski, H., Feller, A., Royer, H.D., *et al.* (1996). Overexpression of the death-promoting gene bax-alpha which is downregulated in breast cancer restores sensitivity to different apoptotic stimuli and reduces tumor growth in SCID mice. The Journal of clinical investigation *97*, 2651-2659.

Bellacosa, A., Kumar, C.C., Di Cristofano, A., and Testa, J.R. (2005). Activation of AKT kinases in cancer: implications for therapeutic targeting. Advances in cancer research *94*, 29-86.

Billen, L.P., Kokoski, C.L., Lovell, J.F., Leber, B., and Andrews, D.W. (2008). Bcl-XL inhibits membrane permeabilization by competing with Bax. PLoS biology *6*, e147.

Brunelle, J.K., and Letai, A. (2009). Control of mitochondrial apoptosis by the Bcl-2 family. J Cell Sci *122*, 437-441.

Cerami, E., Gao, J., Dogrusoz, U., Gross, B.E., Sumer, S.O., Aksoy, B.A., Jacobsen, A., Byrne, C.J., Heuer, M.L., Larsson, E., *et al.* (2012). The cBio cancer genomics portal: an open platform for exploring multidimensional cancer genomics data. Cancer discovery *2*, 401-404.

Certo, M., Moore, V.D., Nishino, M., Wei, G., Korsmeyer, S., Armstrong, S.A., and Letai, A. (2006). Mitochondria primed by death signals determine cellular addiction to antiapoptotic BCL-2 family members. Cancer Cell *9*, 351-365.

Cheng, E.H.Y.A., Wei, M.C., Weiler, S., Flavell, R.A., Mak, T.W., Lindsten, T., and Korsmeyer, S.J. (2001). BCL-2, BCL-X-L sequester BH3 domain-only molecules preventing BAX- and BAK-mediated mitochondrial apoptosis. Molecular cell *8*, 705-711.

Chonghaile, T.N., Sarosiek, K.A., Vo, T.T., Ryan, J.A., Tammareddi, A., Moore, V.D., Deng, J., Anderson, K.C., Richardson, P., Tai, Y.T., *et al.* (2011). Pretreatment Mitochondrial Priming Correlates with Clinical Response to Cytotoxic Chemotherapy. Science *334*, 1129-1133.

Cline, M.S., Craft, B., Swatloski, T., Goldman, M., Ma, S., Haussler, D., and Zhu, J. (2013). Exploring TCGA Pan-Cancer data at the UCSC Cancer Genomics Browser. Scientific reports *3*, 2652.

Del Gaizo Moore, V., Brown, J.R., Certo, M., Love, T.M., Novina, C.D., and Letai, A. (2007). Chronic lymphocytic leukemia requires BCL2 to sequester prodeath BIM, explaining sensitivity to BCL2 antagonist ABT-737. Journal of Clinical Investigation *117*, 112-121.

Deng, J., Carlson, N., Takeyama, K., Dal Cin, P., Shipp, M., and Letai, A. (2007). BH3 profiling identifies three distinct classes of apoptotic blocks to predict response to ABT-737 and conventional chemotherapeutic agents. Cancer Cell *12*, 171-185.

Gao, J., Aksoy, B.A., Dogrusoz, U., Dresdner, G., Gross, B., Sumer, S.O., Sun, Y., Jacobsen, A., Sinha, R., Larsson, E., *et al.* (2013). Integrative analysis of complex cancer genomics and clinical profiles using the cBioPortal. Science signaling *6*, pl1.

Gardai, S.J., Hildeman, D.A., Frankel, S.K., Whitlock, B.B., Frasch, S.C., Borregaard, N., Marrack, P., Bratton, D.L., and Henson, P.M. (2004). Phosphorylation of Bax Ser(184) by Akt regulates its activity and apoptosis in neutrophils. Journal of Biological Chemistry *279*, 21085-21095.

Kale, J., Chi, X., Leber, B., and Andrews, D. (2014). Examining the molecular mechanism of bcl-2 family proteins at membranes by fluorescence spectroscopy. Methods in enzymology *544*, 1-23.

Kennedy, S.G., Kandel, E.S., Cross, T.K., and Hay, N. (1999). Akt protein kinase B inhibits cell death by preventing the release of cytochrome c from mitochondria. Mol Cell Biol *19*, 5800-5810.

Kolliputi, N., and Waxman, A.B. (2009). IL-6 cytoprotection in hyperoxic acute lung injury occurs via PI3K/Akt-mediated Bax phosphorylation. Am J Physiol-Lung C *297*, L6-L16.

Krajewski, S., Blomqvist, C., Franssila, K., Krajewska, M., Wasenius, V.M., Niskanen, E., Nordling, S., and Reed, J.C. (1995). Reduced expression of proapoptotic gene BAX is associated with poor response rates to combination chemotherapy and shorter survival in women with metastatic breast adenocarcinoma. Cancer research *55*, 4471-4478.

Letai, A., Bassik, M.C., Walensky, L.D., Sorcinelli, M.D., Weiler, S., and Korsmeyer, S.J. (2002). Distinct BH3 domains either sensitize or activate mitochondrial apoptosis, serving as prototype cancer therapeutics. Cancer Cell *2*, 183-192.

Leu, J.I., Dumont, P., Hafey, M., Murphy, M.E., and George, D.L. (2004). Mitochondrial p53 activates Bak and causes disruption of a Bak-Mcl1 complex. Nat Cell Biol *6*, 443-450.

Lin, P.H., Pan, Z., Zheng, L., Li, N., Danielpour, D., and Ma, J.J. (2005). Overexpression of Bax sensitizes prostate cancer cells to TGF-beta induced apoptosis. Cell research *15*, 160-166.

Llambi, F., Moldoveanu, T., Tait, S.W., Bouchier-Hayes, L., Temirov, J., McCormick, L.L., Dillon, C.P., and Green, D.R. (2011). A unified model of mammalian BCL-2 protein family interactions at the mitochondria. Molecular cell *44*, 517-531.

Lovell, J.F., Billen, L.P., Bindner, S., Shamas-Din, A., Fradin, C., Leber, B., and Andrews, D.W. (2008). Membrane binding by tBid initiates an ordered series of events culminating in membrane permeabilization by Bax. Cell *135*, 1074-1084.

Manning, B.D., and Cantley, L.C. (2007). AKT/PKB signaling: Navigating downstream. Cell *129*, 1261-1274.

Mermel, C.H., Schumacher, S.E., Hill, B., Meyerson, M.L., Beroukhim, R., and Getz, G. (2011). GISTIC2.0 facilitates sensitive and confident localization of the targets of focal somatic copy-number alteration in human cancers. Genome biology *12*, R41.

Nechushtan, A., Smith, C.L., Hsu, Y.T., and Youle, R.J. (1999). Conformation of the Bax C-terminus regulates subcellular location and cell death. EMBO Journal *18*, 2330-2341.

Parshotam, G., Ashish, J., Justin, K., and Bruce, C. (2010). Congenital cervical bronchogenic cyst - A case report and review of literature. ANZ journal of surgery *80*, 945.

Pietrantonio, F., Biondani, P., de Braud, F., Pellegrinelli, A., Bianchini, G., Perrone, F., Formisano, B., and Di Bartolomeo, M. (2012). Bax expression is predictive of favorable clinical outcome in chemonaive advanced gastric cancer patients treated with capecitabine, oxaliplatin, and irinotecan regimen. Translational oncology *5*, 155-159.

Quast, S.A., Berger, A., and Eberle, J. (2013). ROS-dependent phosphorylation of Bax by wortmannin sensitizes melanoma cells for TRAIL-induced apoptosis. Cell death & disease *4*, e839.

Ranger, A.M., Zha, J., Harada, H., Datta, S.R., Danial, N.N., Gilmore, A.P., Kutok, J.L., Le Beau, M.M., Greenberg, M.E., and Korsmeyer, S.J. (2003). Bad-deficient mice develop diffuse large B cell lymphoma. P Natl Acad Sci USA *100*, 9324-9329.

Ruiz-Vela, A., Opferman, J.T., Cheng, E.H., and Korsmeyer, S.J. (2005). Proapoptotic BAX and BAK control multiple initiator caspases. EMBO Rep *6*, 379-385.

Ryan, J.A., Brunelle, J.K., and Letai, A. (2010). Heightened mitochondrial priming is the basis for apoptotic hypersensitivity of CD4(+) CD8(+) thymocytes. P Natl Acad Sci USA *107*, 12895-12900.

Sakakura, C., Sweeney, E.A., Shirahama, T., Igarashi, Y., Hakomori, S., Nakatani, H., Tsujimoto, H., Imanishi, T., Ohgaki, M., Ohyama, T., *et al.* (1996). Overexpression of bax sensitizes human breast cancer MCF-7 cells to radiation-induced apoptosis. International journal of cancer *67*, 101-105.

Sakakura, C., Sweeney, E.A., Shirahama, T., Igarashi, Y., Hakomori, S., Tsujimoto, H., Imanishi, T., Ogaki, M., Ohyama, T., Yamazaki, J., *et al.* (1997). Overexpression of bax sensitizes breast cancer MCF-7 cells to cisplatin and etoposide. Surgery today *27*, 676-679.

Salmena, L., Carracedo, A., and Pandolfi, P.P. (2008). Tenets of PTEN tumor suppression. Cell *133*, 403-414.

Schuyer, M., van der Burg, M.E., Henzen-Logmans, S.C., Fieret, J.H., Klijn, J.G., Look, M.P., Foekens, J.A., Stoter, G., and Berns, E.M. (2001). Reduced expression of BAX is associated with poor prognosis in patients with epithelial ovarian cancer: a multifactorial analysis of TP53, p21, BAX and BCL-2. British journal of cancer *85*, 1359-1367.

Shamas-Din, A., Bindner, S., Zhu, W., Zaltsman, Y., Campbell, C., Gross, A., Leber, B., Andrews, D.W., and Fradin, C. (2013a). tBid undergoes multiple conformational changes at the membrane required for Bax activation. The Journal of biological chemistry *288*, 22111-22127.

Shamas-Din, A., Kale, J., Leber, B., and Andrews, D.W. (2013b). Mechanisms of action of Bcl-2 family proteins. Cold Spring Harbor perspectives in biology *5*, a008714.

She, Q.B., Solit, D.B., Ye, Q., O'Reilly, K.E., Lobo, J., and Rosen, N. (2005). The BAD protein integrates survival signaling by EGFR/MAPK and PI3K/Akt kinase pathways in PTEN-deficient tumor cells. Cancer Cell *8*, 287-297.

Simonyan, L., Renault, T.T., da Costa Novais, M.J., Sousa, M.J., Corte-Real, M., Camougrand, N., Gonzalez, C., and Manon, S. (2016). Regulation of Bax/mitochondria interaction by AKT. FEBS letters *590*, 13-21.

Suzuki, M., Youle, R.J., and Tjandra, N. (2000). Structure of Bax: coregulation of dimer formation and intracellular localization. Cell *103*, 645-654.

Tai, Y.T., Lee, S., Niloff, E., Weisman, C., Strobel, T., and Cannistra, S.A. (1998). BAX protein expression and clinical outcome in epithelial ovarian cancer. Journal of clinical oncology : official journal of the American Society of Clinical Oncology *16*, 2583-2590.

Wang, Q.H., Sun, S.Y., Khuri, F., Curran, W.J., and Deng, X.M. (2010). Mono- or Double-Site Phosphorylation Distinctly Regulates the Proapoptotic Function of Bax. Plos One *5*.

Wang, S.W., Denny, T.A., Steinbrecher, U.P., and Duronio, V. (2005). Phosphorylation of Bad is not essential for PKB-mediated survival signaling in hemopoietic cells. Apoptosis *10*, 341-348.

Willis, S.N., Fletcher, J.I., Kaufmann, T., van Delft, M.F., Chen, L., Czabotar, P.E., Ierino, H., Lee, E.F., Fairlie, W.D., Bouillet, P., *et al.* (2007). Apoptosis initiated when BH3 ligands engage multiple Bcl-2 homologs, not Bax or Bak. Science *315*, 856-859.

Xin, M.G., and Deng, X.M. (2005). Nicotine inactivation of the proapoptotic function of Bax through phosphorylation. Journal of Biological Chemistry *280*, 10781-10789.

Xu, Z.W., Friess, H., Buchler, M.W., and Solioz, M. (2002). Overexpression of Bax sensitizes human pancreatic cancer cells to apoptosis induced by chemotherapeutic agents. Cancer chemotherapy and pharmacology *49*, 504-510.

Yamaguchi, H., and Wang, H.G. (2001). The protein kinase PKB/Akt regulates cell survival and apoptosis by inhibiting Bax conformational change. Oncogene *20*, 7779-7786.

7

Bad allosterically activates cBid through Bcl-XL homodimers

7.1. Preface

This article was written in manuscript format for molecular cell

Christian Bogner*, Justin Kale*, Xioake Chi, Aisha Shamas-Din, Cecile Fradin, Brian Leber and David W. Andrews. (2016) Bad allosterically activates cBid through Bcl-XL homodimers

*Authors contributed equally

Author Contribution:

This article was written by Kale, J and Leber, B. Figures were designed by Kale J. The experiments in Figures 1C, S1A, S1C, 2, S2, 3, S3 & S4 were performed by Bogner, C. The experiments in Figures 1B, S1B and 4 were performed by Kale, J. Experiments in Figure 1A were performed by Chi, X. Figure 5 was created by Kale, J and Chi, X. Table 1 was created by Bogner, C. Preliminary FCCS and Bid NBD experiments were performed by Shamas-Din, A. Editing was done by Bogner C, Fradin C and Andrews DW. Leber B and Andrews DW directed the research.

Objective:

To understand how the Bcl-2 family of proteins is regulated via Bcl-XL dimers. This chapter uncovers novel mechanisms for the regulation of apoptosis by the BH3 sensitizer Bad and Bcl-XL dimers. It is related to the rest of the thesis by deciphering how all of the Bcl-2 family proteins regulate the activation of Bax.

Highlights:

- Bcl-XL regulates MOMP as a homodimer during mode 1 of apoptosis inhibition but acts as a heterodimer with Bax during mode 2 of apoptosis inhibition
- Bcl-XL dimers contain two binding sites that can bind to cBid or Bad in a competitive fashion as part of a multiple partner complex

- When Bad binds a tBid:Bcl-XL dimer complex, tBid undergoes a conformation change that permits Bax activation while being bound to the Bcl-XL dimer complex
- Bad acts as a non-competitive inhibitor of Bcl-XL representing a novel mechanism that enhances the pro-apoptotic potency of Bad

7.2. Introduction

When a cell undergoes apoptosis, intermembrane space proteins such as cytochrome *c* and SMAC are released into the cytosol by mitochondrial outer membrane permeabilization (MOMP) - the commitment step in apoptosis that is regulated by the Bcl-2 Family of proteins (Tait and Green, 2010; van Delft et al., 2010). Current models of apoptosis regulation by the Bcl-2 family of proteins postulate that combinatorial interactions between family members in a ligand-receptor fashion determine cell fate, where the stoichiometry is assumed to be a dimer between different family members (Shamas-Din et al., 2013b). The sole exception is for Bax or Bak, where activation causes monomers to undergo conformational changes at the mitochondrial outer membrane (MOM) leading to the formation of large homo-oligomers that mediate MOMP. However, the activation of Bax/Bak occurs via a dimeric interaction with BH3 activators like tBid or Bim (Kim et al., 2009; Lovell et al., 2008). Furthermore the three different modes by which anti-apoptotic Bcl-2 family members like Bcl-XL prevent MOMP are also thought to be mediated by dimeric interactions (Llambi et al., 2011). In mode one, Bcl-XL sequesters BH3 activator proteins to prevent them from activating Bax. In mode two, Bcl-XL binds activated Bax to prevent the propagation of oligomers, and in mode zero, Bcl-XL prevents the peripheral binding of Bax to membranes, thus decreasing the available pool of Bax to be activated at the MOM (Edlich et al., 2011; Todt et al., 2013; Westphal et al., 2014b). Sensitizer BH3-only proteins like Bad function to inhibit Bcl-XL via heterodimeric interactions thus releasing active Bax, or releasing activator BH3-only proteins which then activate Bax leading to MOMP. These regulatory interactions between Bcl-2 family members that promote or inhibit apoptosis are postulated to be determined by binding between BH3 regions and BH3 binding pockets of the dimeric

partners. Therefore according to current models the outcome of apoptosis is dependent upon the relative abundance of Bcl-XL binding partners and their specific binding affinities (Chi et al., 2014; Volkmann et al., 2014).

The stoichiometry of Bcl-XL heterodimers controlling apoptosis has been assumed but never directly demonstrated. However the strict dependence of Bcl-2 family member binding on BH3 regions and BH3 binding pockets may not represent the only domains that mediate interactions as suggested by findings concerning the "rear" pocket of Bax and the recently described interaction between the BH4 region in Bcl-XL and Bax (Barclay et al., 2015; Ding et al., 2014; Gavathiotis et al., 2010). The existence of these other binding interfaces suggests that higher order complexes may regulate function.

We have examined this explicitly in a well-controlled in vitro system that recapitulates MOMP by using purified organelles and full-length recombinant proteins. Here we show that mode one of apoptosis inhibition is mediated by Bcl-XL dimers which serve as a scaffold for higher order complexes that regulate MOMP. Furthermore we have identified a new mechanism of apoptosis induction by the sensitizer BH3-only protein Bad. When tBid is inhibited by Bcl-XL dimers, Bad is able to bind the complex and allosterically activate tBid while it is bound to Bcl-XL thus allowing tBid to activate Bax leading to MOMP.

7.3. Results and Discussion

7.3.1. A Bcl-XL complex regulates MOMP

In Figure 1A we examine the interactions that occur during mode one of cell death inhibition by Bcl-XL. During apoptosis, the BH3 activator protein Bid is post-translationally cleaved by Caspase 8, denoted cBid (cleaved Bid) creating a p7 and p15 fragment that are bound together by strong hydrophobic interactions. After cBid binds to membranes the p15 fragment denoted tBid (truncated Bid), inserts into membranes after the p7 fragment dissociates from the complex. The membrane binding promotes a distinct

conformational change in tBid such that it can activate Bax, and this conformation change can be monitored by an increase in the hydrophobicity of the environment in residues in the fifth and sixth alpha helices of the protein (α5, 6) as tBid inserts into membranes (Shamas-Din et al., 2013a). The experiments in this paper have used cBid; however for simplicity we will denote it as tBid since this is the fragment that initiates apoptosis in the MOM. Thus in our system purified Bak-/- mitochondria are exposed to Bax and tBid in the presence of Bcl-XL, with increasing amounts of the BH3 sensitizer Bad. In the absence of Bad, MOMP is prevented, as no cytochrome c is released (Figure 1A - black triangles; arrow #1). In mode 1 we would expect inhibition to be caused by direct binding of Bcl-XL to tBid preventing the latter from activating Bax. We have characterized this interaction between tBid and Bcl-XL by fluorescence resonance energy transfer (FRET; Figure 1A – red circles; arrow #1). The detection of FRET is very sensitive to distance and occurs if the fluorescently labeled biomolecules are within 0-10 nm of each other. The closer the donor and acceptor labeled biomolecules are, the higher the FRET efficiency. As anticipated for a competitive interaction of tBid and Bad with Bcl-XL addition of increasing amounts of the sensitizer BH3-only protein Bad causes a decrease in FRET efficiency, indicating the displacement of tBid from Bcl-XL allowing free tBid to activate Bax causing MOMP (arrow #3). However, close inspection of the data in Figure 1A reveals that after adding 20 nM Bad (indicated by the red arrow #2) the majority of cytochrome c is released, whereas the binding between tBid and Bcl-XL remains unchanged from the baseline conditions where no cytochrome c is released (e.g. at 2.5 nM Bad).

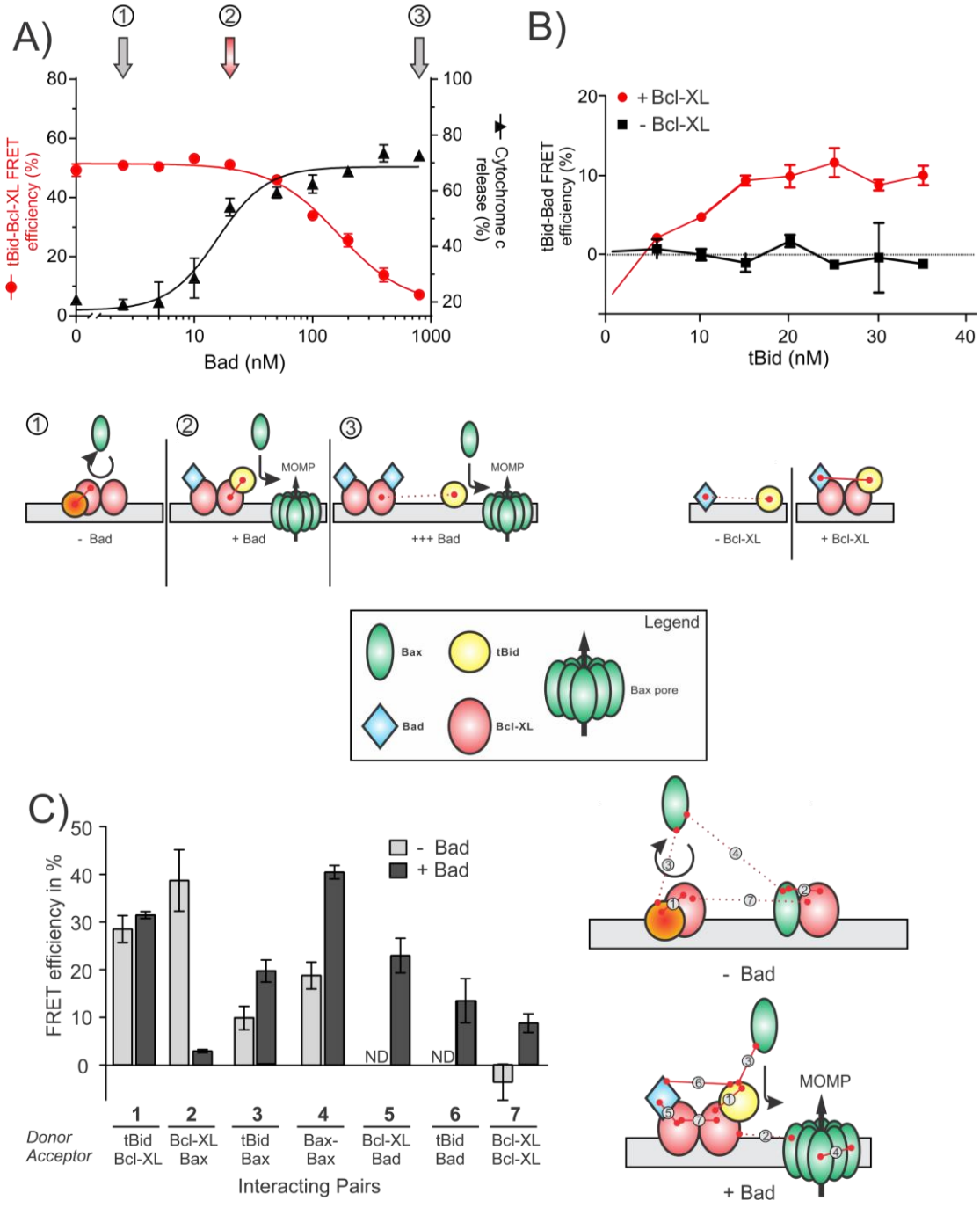

Figure 7.1 - Bcl-XL regulates mode 1 inhibition of MOMP via a multi-component complex

A. Isolated Bak -/- mouse liver mitochondria (MLM) were incubated with 4 nM donor labeled tBid (126C-Alexa 568) and 30 nM acceptor labeled Bcl-XL (152C-Alexa 647) with increasing concentrations of WT Bad. FRET efficiency (left axis, red circles) was calculated by the decrease in donor labeled tBid

fluorescence. Cytochrome c release (right axis, black triangles) was measured by separating each reaction into supernatant and pellet fractions, followed by SDS-PAGE and western blot against cytochrome c. The resulting blots were imaged and % cytochrome c was calculated by ratiometric analysis.
B. Isolated Bak -/- MLM were incubated with 20 nM donor labeled Bad (36C-Alexa 568) and increasing concentrations of acceptor labeled tBid (126C-Alexa 647) in the presence and absence of 20 nM WT Bcl-XL. FRET efficiency was measured by the decrease in donor labeled Bad fluorescence.
C. FRET efficiencies for acceptor and donor labeled pairs of Bcl-2 family members. For each reaction 0.25 mg/mL liposomes were incubated with 20 nM tBid, 50 nM Bcl-XL, 100 nM Bax (light bars), and 100 nM Bad where indicated (dark bars). Each lane contains the same concentrations of proteins but the acceptor and donor labeled proteins are changed, indicated below the graph. (A-C) Data shown are the average of 3 or more independent replicates with SEM.

The current model of hetero-dimers with displaceable partners postulates that Bad displaces tBid from Bcl-XL. If so, we would expect tBid and Bad to be mutually exclusively bound to Bcl-XL. By contrast, if these are components of a larger complex that contains both tBid and Bad as suggested by Fig. 1A we would expect these proteins to be in close proximity with each other. Indeed, when $Bak^{-/-}$ mouse liver mitochondria are incubated with donor labeled Bad and acceptor labeled tBid, we see an increase in FRET efficiency, but only when Bcl-XL is present and at tBid concentrations that are approximately equimolar with Bad (Figure 1B). Additionally, under these conditions this increase in proximity occurs at the mitochondrial membrane rather than in solution (Figure S1B), likely because both tBid and Bad cause Bcl-XL to bind to membranes (Billen et al., 2008; Jeong et al., 2004). Therefore these data suggest that Bcl-XL coordinates a multi-component complex whose composition determines if MOMP is initiated or prevented.

To precisely characterize this complex without the complication of endogenous mitochondrial proteins, we used a highly purified in vitro system containing liposomes that mimic the composition of the MOM and the same full-length recombinant proteins used with mitochondria (Kale et al., 2014). This in vitro system allows us to have full

control of all components and precisely modulate the players. Mode one Bcl-XL inhibition is shown in Figure S1A (left panel) where the addition of tBid and Bax causes marked permeabilization of liposomes (white) modeling MOMP as measured by the release of encapsulated fluorophore/quencher pair ANTS/DPX from the liposomes. With the addition of Bcl-XL, membrane permeabilization by Bax is inhibited (light grey) but regained with the addition of Bad (black). Furthermore binding between tBid and Bcl-XL is unchanged (Figure S1A; right panel) in the presence of Bax, Bad or both, thus recapitulating the results shown in Figure1A in a liposome based system. With the liposome system we can examine the individual pair-wise interactions between labeled proteins by FRET, in the presence or absence of Bad. In Figure 1C, the concentrations of the proteins remain constant, but the donor and acceptor labels are covalently attached to different Bcl-2 family proteins. Measurement of FRET between the donor and acceptor labeled proteins allows us to dissect the dynamic process of assembly and disassembly of the complex that mediates the outcomes seen in Figures 1A and S1A. In Figure 1C, lane 1, we observe that tBid remains bound to Bcl-XL even in the presence of Bad, replicating the core finding in mitochondria from Figure 1A. As expected by mode 2 inhibition, Bcl-XL is bound to Bax in the absence of a BH3-only activator, however with the initiation of MOMP by Bad, Bcl-XL is no longer bound to Bax (lane 2), whereas tBid activates Bax by binding to it (lane 3). As a consequence Bax binds to other Bax molecules thereby forming the oligomers that will mediate MOMP (lane 4). As anticipated from the complex inferred from Figures 1A and 1B, Bcl-XL mediates the close proximity of tBid and Bad (lane 6), by binding to Bad (lane 5) and tBid (lane 1) directly. These results demonstrate that Bcl-XL is binding to more than one partner, and imply that it is doing so "simultaneously" in a multiple partner complex rather than in separate heterodimers. Indeed we are able to detect Bcl-XL dimers by FRET (lane 7). When the same experiments are performed in the absence of Bax (Fig. S1C), we observe an increase in the FRET between each labeled partner compared to the FRET observed when Bax is present (Fig. 1C). This is consistent with mode 2 inhibition where Bcl-XL binds activated Bax, thus preventing Bcl-XL from binding either itself, Bad or tBid. Taken together these

data suggest that the control of apoptosis is coordinated by a complex containing Bcl-XL dimers with binding partners that are exchangeable.

7.3.2. Bcl-XL forms dimers with exchangeable binding partners

Critical to this notion of multiple partner formation is the presence of dimers (or a higher order complex) of Bcl-XL. Bcl-XL dimers have been observed after crosslinking both by incubating full-length purified Bcl-XL with isolated mitochondria (Ding et al., 2014) and from cell extracts (Jeong et al., 2004). The solution (Denisov et al., 2007) and crystal (O'Neill et al., 2006) structures of domain swapped Bcl-XL dimers have been solved. The dimers were able to bind BH3 peptides in a 2:1 ratio (Denisov et al., 2007) and bind membranes (O'Neill et al., 2006); however these studies did not use full-length protein as Bcl-XL had the amino-terminal unstructured loop and the carboxy-terminal membrane binding domain deleted. Recently the membrane bound structure of Bcl-XL (containing the carboxy-terminal tail but with the unstructured loop between α1 and α2 deleted) was solved using NMR spectroscopy by incubating Bcl-XL with lipid nanodiscs that support a lipid bilayer for Bcl-XL binding (Yao et al., 2015). They reported that Bcl-XL inserted its carboxy-terminal tail into the nanodisc as a monomer. However, the nanodiscs provide a small surface area for protein binding (average diameter of 9 nanometers). The membrane plays an integral role in stabilizing the conformation changes and the interactions between Bcl-2 family members, so it may be that dimers were not observed due to a lack of space within each nanodisc, or that the unstructured loop of Bcl-XL is required for dimerization.

Therefore we examined the dynamics and regulation of recombinant full length Bcl-XL dimer formation directly in a more simplified system in the presence or absence of individual binding partners, rather than with all of the proteins (Bax, tBid, Bcl-XL and Bad) present as is the case for the experiments shown in Figures 1C and S1C. Without other binding partners Bcl-XL forms dimers more readily, as the FRET efficiency is higher (compare Figure 2A with no interacting partners present to lane 7 in Figure 1C,

35% vs. 10% FRET efficiency respectively). This decreased dimer formation indicated by lower FRET efficiency in Figure 1C is due to the presence of activated Bax, as increasing concentrations of the latter causes the disassembly of Bcl-XL dimers (Fig 2A, triangles). The addition of Bad (circles) does not affect the formation of Bcl-XL dimers, and tBid (squares) does so only minimally. The presence of Bcl-XL dimers is also detectable by gel filtration chromatography of labeled proteins detected by fluorescence (*Fig S2C*), cross-linking and immunoblotting (*Fig S2D*), and FRET using other labeled residues (at amino acid 152 in the membrane binding region, Fig S5B). Dimer formation is dynamic, as the binding partners are exchangeable (Fig S2A). Furthermore, dimer formation is not dependent on liposomes as is it also detectable in solution, and similar to results obtained with membranes dimer formation is not prevented by other binding partners like tBid or Bad (*Figure S2B*), suggesting a different binding interface other than the "BH3 pocket".

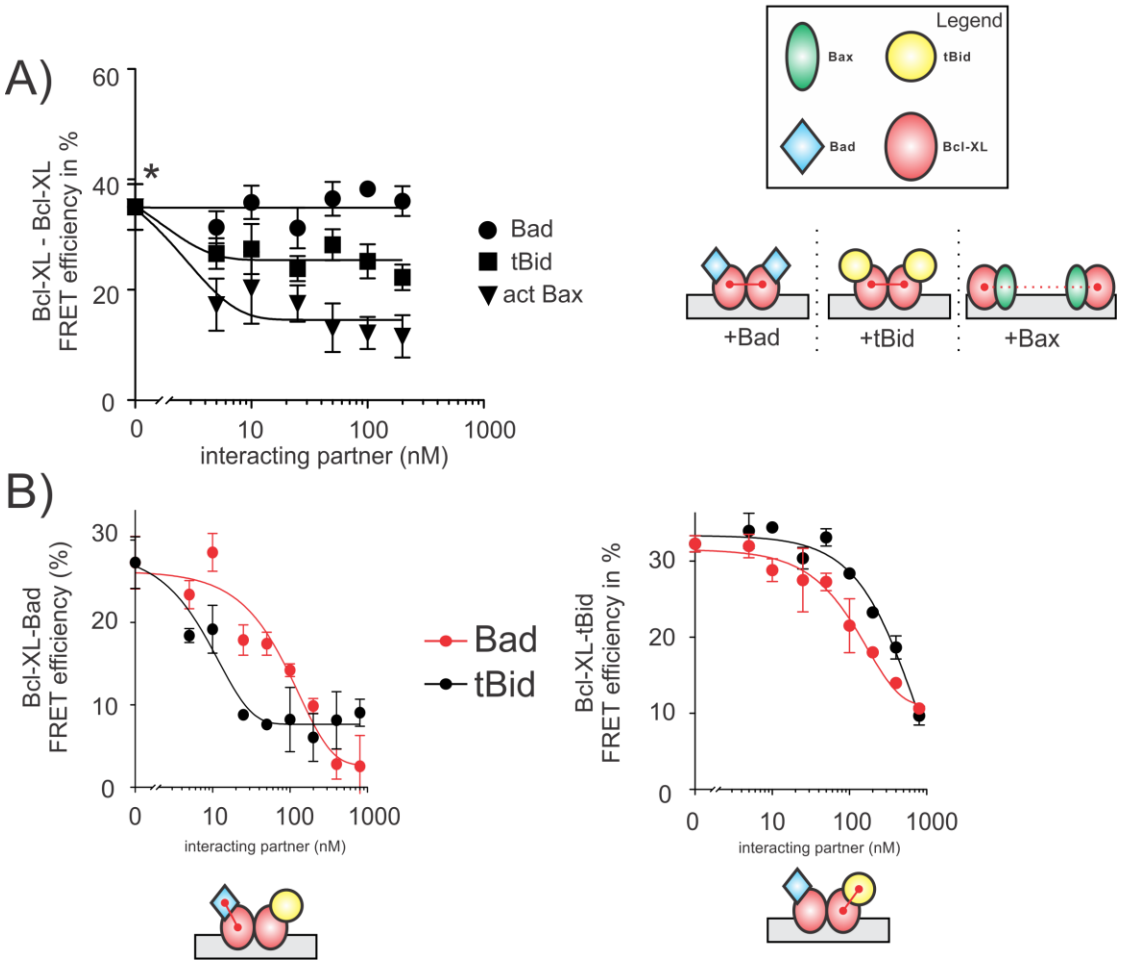

Figure 7.2 - The multi-component complex regulated by Bcl-XL dimers is dynamic

A. FRET efficiency of the interaction between 20 nM donor and 100 nM acceptor labeled Bcl-XL (219C-DAC, 219C-NBD respectively) incubated with 0.25 mg/mL liposomes and increasing concentrations of the indicated unlabelled Bcl-2 family proteins Bad (circles), tBid (squares) and activated Bax (triangles). For samples containing activated Bax, the Bax was first activated by incubating liposomes, Bax and 20 nM tBid mt1 (a mutant which only binds to Bax, and Bcl-XL). Shown are the average +- SEM results of three independent experiments.

B. FRET efficiency was measured between 20 nM donor labeled Bcl-XL (152C-DAC) and 100 nM acceptor labeled Bad (36C-NBD; left) or tBid (126C-NBD; right), in the presence of liposomes (0.25 mg/mL) and increasing concentrations of unlabelled Bad (red) or tBid (black). Shown are the average +- SEM results of three independent experiments.

Multiple experimental approaches thus confirm the spontaneous formation of Bcl-XL dimers that occur both in solution and on the membrane, and that can bind to different partners. Therefore we sought to determine the possible compositions of this complex, and specifically if the binding partners are exchangeable on the Bcl-XL dimer. If this is the case then there are 3 scenarios: 1) the Bcl-XL dimer has both a Bad and a tBid attached, 2) only Bad is bound, or 3) only tBid is bound. If binding partners are exchangeable, these scenarios are inter-convertible, depending on the concentrations and relative affinities of each partner for Bcl-XL. The data in Figure 2B demonstrate the existence of an interaction between fluorescently labeled Bcl-XL and fluorescently labeled Bad (left panel) or tBid (right panel), and further shows that an unlabeled partner (Bad or tBid) can displace the labeled partner from the complex. It indicates that this interaction is competitive, consistent with previous observations. The composition of the multi-molecular complex coordinated by Bcl-XL is governed by the concentrations of Bad and tBid as shown by the curves in Figure 2B and their absolute binding affinities with Bcl-XL, as measured in Fig S4 A-E and summarized in Table 1. Therefore, as a consequence of this mutually displaceable interaction either BH3 protein binds to the same dimeric complex.

Table 7.1 - Bcl-2 family dissociation constants

K_d in nM		Acceptor: Bax	Bcl-XL	tBid	Bad	
Donor	Bcl-XL	8+-2*	8+-3	3+-2	25+-9	+ liposomes
	Bax	25+-7*				
	tBid	18+-5				
	Bcl-XL	n/d*	56+-4	16+-5	13+-5	- liposomes

Summary of apparent dissociation constants (K_D; calculated from the binding curves in Fig. S4) in nM for Bcl-2 proteins interacting with each other in the presence or absence of liposomes (0.25 mg/mL), using FRET. The average +- SEM of three independent experiments is shown. When indicated (*) Bax was pre-activated with tBid mt1, a mutant of Bid that has impaired binding affinity towards Bcl-XL.

The data shown in Figure S4A-E indicates that Bcl-XL can bind itself, tBid and Bad in solution or on membranes. Therefore we would predict that higher order complexes coordinated by Bcl-XL would also form in the absence of membranes. Indeed FRET is observed in solution between two labeled tBid molecules (Figure 3A, left panel, Fig S3A) and two labeled Bad molecules (Figure 3A, right panel), but only in the presence of Bcl-XL. Furthermore, the addition of unlabeled Bad or cBid can displace the labeled cBid or Bad respectively from the complex, consistent with the binding sites being exchangeable. This confirms that the Bcl-XL dimer mediates the close proximity of

tBid or Bad molecules via binding to Bcl-XL, and that these interactions occur both in solution and on membranes (Figure 3A, S3A).

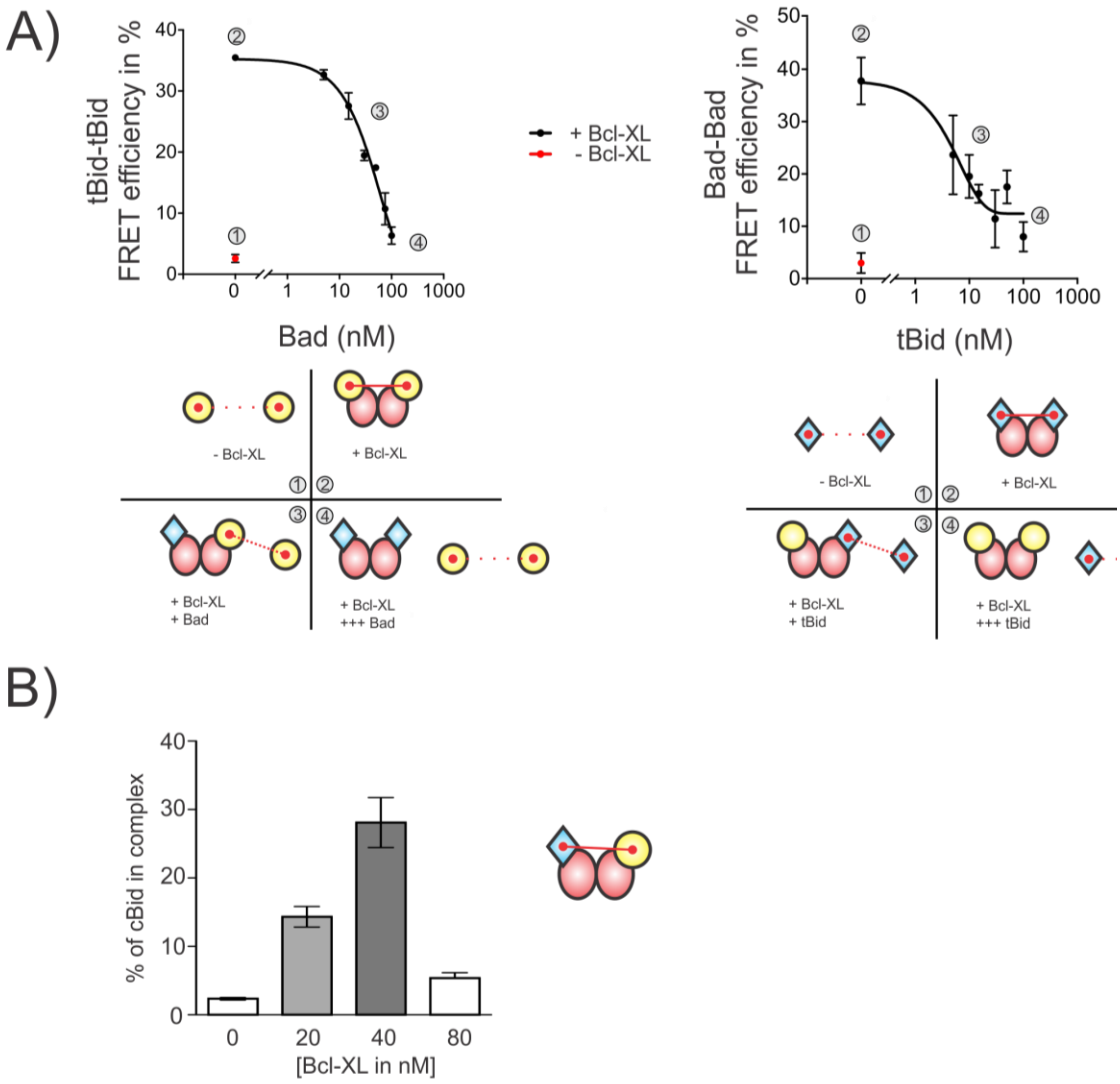

Figure 7.3 - tBid and Bad are in a complex together with Bcl-XL dimers

A. FRET efficiency between donor-acceptor pairs in solution was measured for left) 5nM donor labeled tBid (126C-DAC) and 20 nM acceptor labeled tBid (126C-NBD), and right) 5nM donor labeled Bad (36C-DAC) and 20 nM acceptor labeled Bad (36C-NBD) in the presence of 20 nM WT Bcl-XL and increasing concentrations of unlabeled WT Bad (left) or tBid (right). The gray bar indicates FRET efficiency in the absence of Bcl-XL. Shown are the average +- SEM results of three independent experiments.

B. The percent of tBid in a larger molecular weight complex in solution was calculated via FCCS (fluorescence cross-correlation spectroscopy).Fluorescently labeled 40 nM Bad (36C-Alexa 488) and 40

nM tBid (126C-Alexa 647) were incubated in the presence of increasing concentrations of WT Bcl-XL (0-80nM). Shown are the average +- SEM results of three independent experiments.

By using fluorescence cross-correlation spectroscopy (FCCS) we can further determine if Bad and tBid are part of the same complex. With this technique, as molecules move into and out of the confocal detection volume a signal is measured for each spectrally separated fluorophore. If the signal of the fluorophores correlates with each other then they are moving together as part of a larger complex. We fluorescently tagged tBid with Alexa 647 and Bad with Alexa 488 and measured the cross-correlation of tBid and Bad in solution and calculated the per cent of total tBid bound to the complex by FCCS. The data shown in Figure 3B clearly demonstrate that tBid and Bad are part of the same complex, but only in the presence of Bcl-XL in concentrations that are roughly equimolar with the two BH3 proteins. The data supports the existence of a multi-molecular complex mediated by Bcl-XL dimers as the hydrodynamic radius of this complex (14 nm, as inferred from the characteristic decay time of the cross-correlation function) is larger than what one would expect for a complex containing only one tBid molecule and one Bad molecule, with respective hydrodynamic radii (as also inferred from the correlation data) of 4.2 nm (consistent with the known protein structure) and 7.6 nm (in the correct range for an unfolded protein). Once Bcl-XL is at a high enough concentration, a cross-correlation is no longer present, presumably because tBid and Bad molecules now bind different Bcl-XL homodimers.

The FCCS data proves that tBid and Bad are part of the same multi-molecular complex, but on their own they cannot definitively tell us whether tBid and Bad are directly interacting or whether they are interacting via the Bcl-XL homodimers. However taken together with the FRET data, it is clear that Bcl-XL is absolutely required for this process. Since Bcl-XL forms dimers as we have demonstrated by multiple techniques, and the interactions are exchangeable, it is highly likely that tBid and Bad are not directly interacting but are in close proximity bound to different members of the Bcl-XL dimer.

However, what is remarkable is that the identity of the BH3 protein bound to the "other" Bcl-XL affects the nature of the binding interaction between Bcl-XL and tBid. Thus, when Bcl-XL binds to tBid the latter is sequestered from binding to and activating Bax, whereas when Bad "joins" the complex by binding the other Bcl-XL in the dimer, even though tBid is still bound to Bcl-XL the former can now activate Bax (Figure 1A). This suggests a conformational change that is allosterically mediated by Bad binding to the complex, such that tBid activates Bax while simultaneously being bound to Bcl-XL.

7.3.3. The Bcl-XL dimer complex mediates allosteric activation of tBid by Bad

To test this explicitly, we have exploited our previous observation that the conformational change in tBid that occurs after membrane binding can be monitored in real time by the change in the emission of tBid labelled at residue 163C in α6 with the environment sensitive fluorophore NBD (Shamas-Din et al, 2013). The emission of NBD is quenched by water, and is therefore increased in a hydrophobic environment. The emission of tBid (163C-NBD) does not change when tBid binds liposomes or binds Bax but increases ~3.5 fold when tBid binds Bcl-XL (as in mode 1 inhibition).

In the absence of Bad the addition of Bcl-XL increases the fluorescence of tBid (163C-NBD) indicating that it is in a more hydrophobic environment (Fig 4A; left panel). Subsequent addition of Bax does not result in a conformation change of tBid or membrane permeabilization (left and middle panels). Since tBid is in a more hydrophobic environment we speculate that Bcl-XL is "burying" tBid into the membrane, thus preventing tBid from activating Bax. If Bad does cause an allosteric change in, or displaces cBid we should observe a decrease in NBD emission and an increase in liposome permeabilization. Consistent with our hypothesis the addition of Bad to the tBid-Bcl-XL complex decreases the fluorescence of tBid (163C-NBD) in the presence or absence of Bax. Addition of Bax to the Bad-tBid-Bcl-XL complex results in the activation of Bax and subsequent membrane permeabilization. As a control we used the

Bad BH3 mimetic ABT-263 which mimics binding to the BH3 pocket of Bcl-XL and is able to displace tBid from Bcl-XL (Fig. S4A). The addition of ABT-263 decreases the fluorescence of tBid (163C-NBD). When Bax is added this causes Bax activation and membrane permeabilization, consistent with ABT-263 mediated displacement of tBid from the complex.

Both Bad and ABT-263 are able to displace tBid from Bcl-XL. However our data suggests that at lower concentrations of Bad, tBid is displaced minimally but retains almost full activity (Figure 1A, S1A). Thus, the decrease in emission of NBD labeled tBid due to the addition of Bad or ABT-263 could be explained by displacement of tBid, a tBid conformation change while being bound to Bcl-XL, or both. Regardless of the scenario the emission change is directly proportional to tBid activity (Figure 4A; right panel). Thus both displaced tBid and tBid in an active conformation while bound to Bcl-XL would have the same activity. To analyze this mechanism we need to calculate how much tBid is displaced from Bcl-XL at any concentration of Bad or ABT-263 and then compare this to the activity of tBid after the addition of Bad or ABT-263. If the activity of tBid is greater than what would be observed by the amount of tBid displaced, then the conformation change we measure is likely mediated by an allosteric change in tBid while still bound to the Bcl-XL dimer complex. This allosteric conformation change thus allows tBid to activate Bax while still bound to Bcl-XL.

To calculate how much tBid would be displaced by the addition of Bad or ABT-263, we fit the data from Figure 2B (right panel) and Figure S4B to a competitive inhibition model. At the beginning of the experiment the majority of tBid is bound to Bcl-XL. As the competitive inhibitor (Bad or ABT-263) is titrated into the reaction, there is loss in FRET indicating a displacement of tBid from Bcl-XL (Fig 4B). By fitting the data we can calculate the affinity for the competitive inhibitor to the tBid:Bcl-XL complex to obtain the K_I values for Bad and ABT-263 of 34.84 nM (28.49 – 41.2 nM 95% CI) and 527.2 nM (445.5 – 608.9 nM 95% CI) respectively. With these Ki values and the displacement of tBid from Bcl-XL modeled, we can calculate how much tBid is displaced

from Bcl-XL at each concentration of Bad and ABT-263. We can then re-plot the data shown in Figure 4A (middle panel) as a function of the concentration of displaced tBid (Figure 4C). This analysis indicates that the activity of tBid bound to the Bcl-XL dimer complex after the addition of Bad cannot be completely accounted for by displaced tBid. Taken together these data suggest a novel mechanism of apoptosis regulation by the sensitizer BH3-only protein Bad, where Bad binds the tBid-Bcl-XL complex eliciting the activation of tBid while the latter is still bound to Bcl-XL. By contrast the activity of tBid after the addition of ABT-263 can be directly related to the displacement of tBid. Thus the Bad BH3-mimetic ABT-263 does not provoke an allosteric change in tBid when it is bound to the Bcl-XL dimer complex, suggesting that a region outside of the Bad BH3 domain confers this novel function of Bad.

7.3.4. A new model for mode 1 inhibition of MOMP

The current model of mode 1 inhibition of MOMP by Bcl-XL posits that Bcl-XL and tBid are mutually sequestered and that Bad promotes apoptosis by displacing tBid from Bcl-XL, allowing tBid to activate Bax (Llambi et al., 2011; Shamas-Din et al., 2013b). In Figure 5 we propose a new model of mode 1 inhibition of MOMP by Bcl-XL based on our results and have summarized the differences between the models:

1) tBid is inhibited by binding to Bcl-XL dimers.
2) Bad binding to a tBid containing Bcl-XL dimer relieves Bcl-XL mediated inhibition of tBid function by effecting a conformational change in the latter; this allows tBid to activate Bax
3) Bcl-XL dimers bind to both tBid and Bad concurrently
4) tBid can activate Bax while it remains bound to Bcl-XL

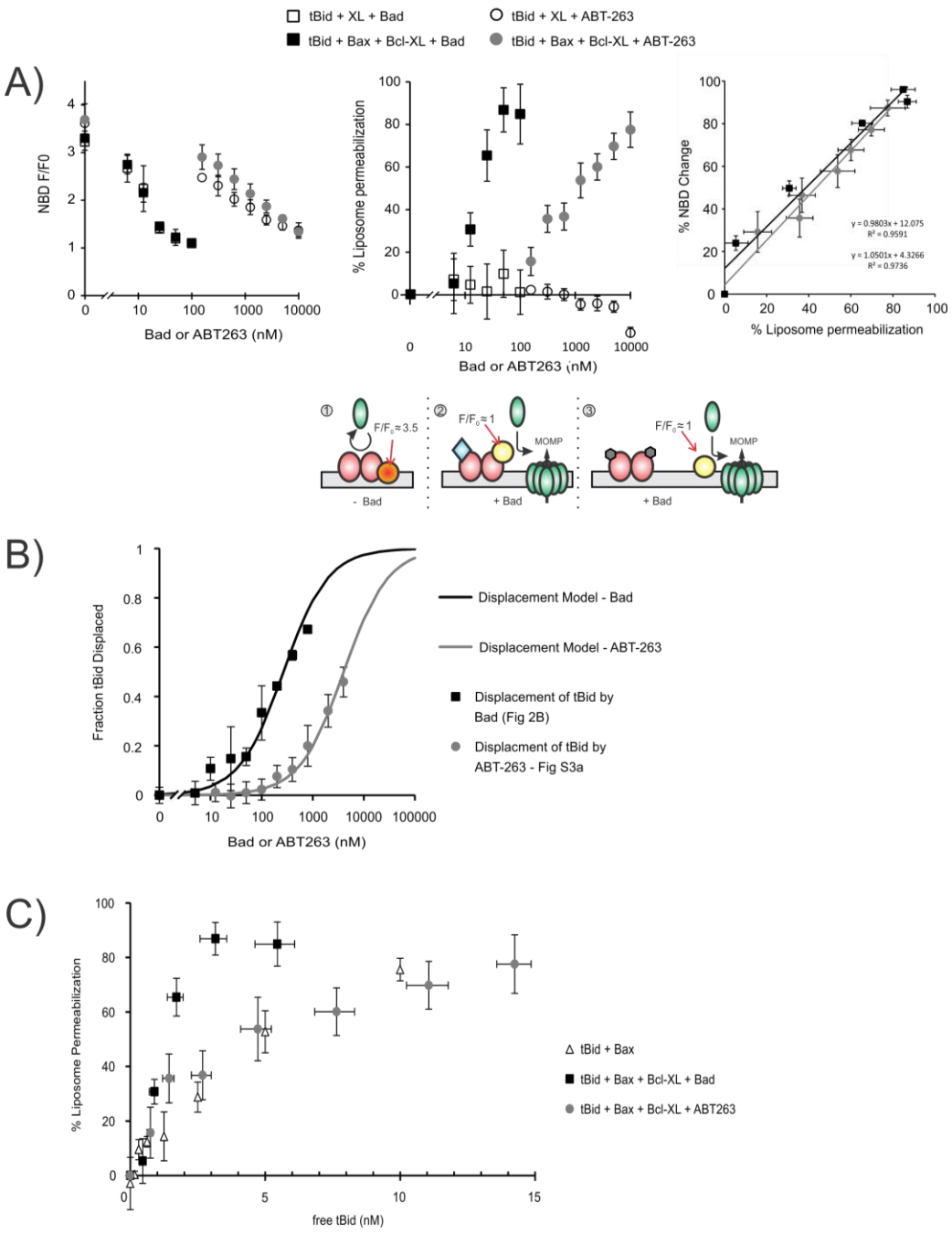

Figure 7.4 - Bad binds the XL dimer changing the conformation of tBid to an active state regulating pore formation

A. Liposomes (0.25 mg/mL) were incubated with 20 nM tBid (126C-NBD), 40 nM Bcl-XL and the indicated concentrations of Bad (squares) or ABT-263 (circles) in the absence (open symbols) or presence

(closed symbols) of 100 nM Bax for 2 hours. tBid environment change (left) and pore formation (middle) was measured simultaneously by tracking the fluorescence emission of NBD and decrease in fluorescence of Tb:DPA complex respectively. Right - NBD emission was scaled from 100% (tBid and Bcl-XL alone) to 0% (tBid alone) and plotted against the activity of tBid for each concentration of Bad (squares) or ABT-263 (circles). Data were plotted as with a straight line, where Bad was ($y=0.98x+12.08$; $R^2=0.96$) and ABT-263 was ($y=1.05x+4.33$; $R^2=0.97$). The averages +/- SEM results of three or more replicate experiments are shown.

B. Data from Fig 2B and Fig S4A were plotted as fraction cBid displaced, then fit to a competitive inhibitor model to determine the affinity (K_i) for Bad or ABT-263 to the tBid-Bcl-XL complex (see methods). The obtained values for the K_I for Bad were 34.84 nM (28.49 – 41.2 nM 95% CI) and 527.2 nM (445.5 – 608.9 nM 95% CI) for ABT-263. The model predicts how much tBid is displaced at any concentration of Bad (squares – experimental data; black line – model) or ABT-263 (circles – experimental data; grey line – model).

C. The activity of tBid in response to Bad (squares) or ABT-263 (circles) from Figure 4A (middle panel) is plotted with a transformed x-axis of "tBid displaced" calculated from the competitive inhibitor displacement model (Fig. 4B). This activity is then compared to a standard curve generated by incubating 100 nM Bax with varying concentrations of tBid. This standard curve yields the absolute activity of tBid at any concentration. The x-axis errors bars represent the 95% CI for displaced tBid. The y-axis represents averages (+/- SEM) of at least 3 replicate experiments.

We do not propose any changes to the model of Mode 2 or 0 inhibition of MOMP by Bcl-XL as our data indicates that it is controlled by Bcl-XL/Bax heterodimers. An important consequence of the regulation of Mode 1 by dimers that permit allosteric activation of tBid despite being bound to Bcl-XL is that it magnifies the effect of BH3 sensitizers like Bad. This occurs because sensitizers can directly displace BH3 activators from anti-apoptotic proteins to elicit MOMP, but can *also* do so by occupying the "empty" binding site on the other dimer partner and thereby function as both competitive and non-competitive inhibitors of the Bcl-XL/tBid interaction. Thus at the same concentrations and binding affinities for Bcl-XL, tBid and Bad our novel dimer regulation model predicts a 2-fold increase in Bad potency compared to the previous model (Figure 4C) .

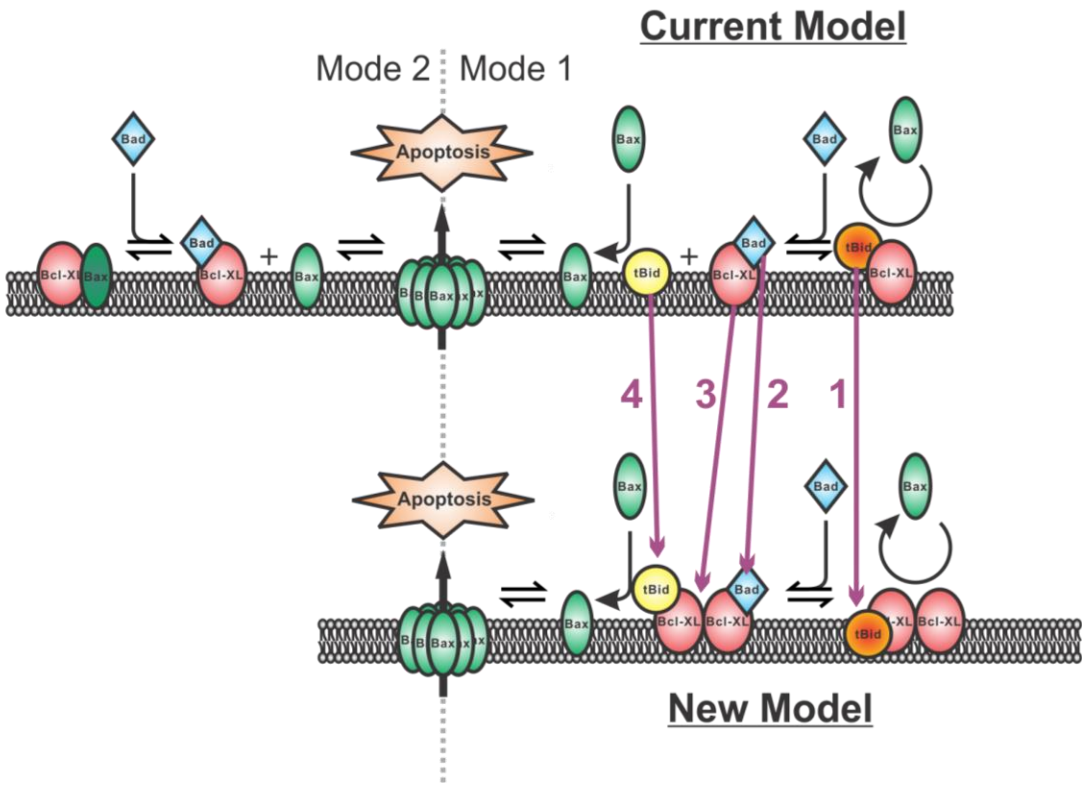

Figure 7.5 - A new model of mode 1 inhibition of MOMP regulated by a multi-molecular complex mediated by Bcl-XL dimers

The current model of MOMP regulation by the Bcl-2 family members suggests that Bcl-XL has two main modes of inhibiting MOMP via the formation of hetero-dimers with Bcl-2 family members. Bcl-XL can sequester activated Bax (mode 2) or sequester membrane bound tBid (mode 1), thus preventing pore formation by activated Bax. MOMP is initiated via BH3 sensitizers, such as Bad, that bind to Bcl-XL, displacing either activated Bax (mode 2), which can directly form pores, or displacing tBid from Bcl-XL resulting in MOMP via tBid mediated activation of Bax in solution. We propose that MOMP is regulated not by Bcl-XL monomers but by Bcl-XL dimers that coordinate a multi-molecular complex which regulates MOMP. The major changes from the current model are indicated in the scheme: 1) tBid activates Bax while bound to Bcl-XL, 2) Bcl-XL dimers bind tBid and Bad concurrently 3) Bad binding to a tBid containing Bcl-XL dimer relieves Bcl-XL mediated inhibition of tBid function, allowing the latter to activate Bax and 4) tBid is inhibited by binding to Bcl-XL dimers.

7.4. Materials and Methods

7.4.1. Measuring protein:protein interactions by fluorescence spectroscopy

To measure binding between specific Bcl-2 family members (Bcl-XL, tBid, Bax, and Bad) by Förster Resonance Energy Transfer (FRET), the proteins were labeled at cysteine residues listed in Supplemental Table XX with either DAC (7-diethylaminocoumarin-3-carbonyl) as the donor fluorophore or NBD (nitrobenzoxadiazole) as the acceptor fluorophore, as described previously (Lovell et al., 2008). Fluorescence was monitored in a PTI Quantamaster fluorometer, or for serial experiments in a TECAN Infinite® M1000 PRO plate reader (380 nm excitation and 460 nm emission, respectively). Background fluorescence for liposomes and/or assay buffer (F_{BG}) was subtracted from all measurements. The DAC-donor labeled Bcl-2 protein was incubated with liposomes (0.25 mg/mL lipid) in assay buffer, or in assay buffer alone to record the emission of the donor alone (F_D) after a stable signal was achieved. Parallel incubations containing DAC-donor labeled Bcl-2 protein and NBD-labeled acceptor Bcl-2 protein (Acceptor Labeled) were incubated for 1 hour in assay buffer (HEPES pH7.4, 100mM NaCl, 5mM $MgCl_2$, 5mM $CaCL_2$) before DAC fluorescence emission was measured (F_{D+AL}). To account for fluorescence changes of the DAC- labelled donor due to environmental changes of donor binding to acceptor parallel reactions were performed with equivalent unlabelled acceptor Bcl-2 protein (Acceptor Not Labeled) and DAC fluorescence emission was measured (F_{D+ANL}). The FRET efficiency, E, in % of Bcl-2 proteins interacting in complexes was then calculated as:

$$E = \left(1 - \frac{(F_{D+AL} - F_{BG})}{(F_{D+ANL} - F_{BG})}\right) \times 100$$

To acquire binding curves for Bcl-2 protein interactions and calculate dissociation constants (K_d) or changes in K_d with additional partners, FRET was measured using a

fixed concentration of DAC labelled donor protein and increasing concentrations of the NBD labelled acceptor. To measure subunit exchanges within a protein complex we measured the displacement of NBD labeled acceptor Bcl-2 proteins by an unlabeled equivalent protein for the DAC labeled donor such that the final concentration of acceptor (wild type and labeled) was constant. Where specified, Bax was pre-inserted into liposomes (0.25 mg/mL) by incubating either DAC-126-Bax or DAC-175-Bax (20 nM) with 20 nM tBid-G94E (tBidmt1- with impaired binding affinity for Bcl-XL) for 15 minutes at 37 °C. To examine changes in FRET efficiency and shifts of the Kd with additional binding partners we pre-incubated reactions with an unlabelled binding partner or added the unlabelled partner to a pre-existing complex. After one hour of co-incubation with DAC- and NBD-labelled partners, the emission of the DAC labelled donor was measured and FRET efficiency (*E*) and binding curves calculated from the average of triplicate experiments. Binding curves and K_d values were calculated as follows

$$y = F_{\max} \times \frac{(D + x + K_d - \sqrt{(D + x + K_d)^2 - (4 \times D \times x)})}{2 \times D}$$

in Prism 5 (GraphPad), where D= Donor concentration (usually 20nM), E_{max}= maximum FRET efficiency, K_d= dissociation constant. x= Acceptor concentration.

To measure interactions of BCl-2 proteins in complexes on mitochondria by FRET we used the fluorescent pairs Alexa568-36C-Bad/ Alexa647-126C-tBid and Alexa568-126-tBid/Alexa647-152-Bcl-XL to prevent interference by mitochondrial auto fluorescence. The proteins were incubated together with Bak -/- mitochondria (1 mg/mL) at 37^0C for one hour in regeneration buffer before measuring FRET on a TECAN Infinite® M1000 PRO plate reader (589 nm excitation; 602 nm emission). To distinguish membrane bound complexes from those in solution mitochondria were isolated by centrifugation and fluorescence emission at 602 nm measured in the supernatant and

pellet fractions. MOMP was measured by immunoblotting for cytochrome *c* in the supernatant and pelleted fractions.

7.4.2. Cross correlation spectroscopy

Cross correlation experiments were performed on an Alba FFS/FLIM Laser Scanning system interfaced with an Olympus epifluorescence microscope with water immersion objective and Picosecond Diode Laser (Becker&Hickl GmbH) to study complex formation between Alexa488-36-Bad and Alexa647-126-tBid in complex with Bcl-XL. ISS Vista Vision software was used for instrument control, data acquisition and data processing. After measuring the fluorescence background to obtain the brightness in the blue B_B and red B_R channel, calibrating the size of the detection volumes to obtain dye diffusion time (τ_D) and the detection volume aspect ratio *(S)* in the blue and red channels, we calculated the dimensions of the detection volume w_0 and z_0 in the blue and red channels. Calibration of the detection volumes overlap was performed with *DiD* (1,1-Dioctadecyl-3,3,3,3-tetramethylindodicarbocyanine) for the red channel and *DiO* (3,3-Dioctadecyloxacarbocyanine) for the blue channel to obtain the overlap correction factor (γ = 43%). Finally we measured the properties of the labelled binding partners Alexa488-36-Bad and Alexa647-126-tBid separately to obtain the fluorophore triplet state (τ_R) and the protein diffusion time (τ_D). From that we calculated the protein diffusion coefficient *D* and the hydrodynamic radius *R* as well as labelled protein specific brightness (η_R) and (η_B), absolute concentration and cross-talk from the blue to the red detection channel. We analyzed the auto-correlation function in the blue channel using a single species model with triplet state, where we fixed the value of the triplet state to that obtained in the calibration step. We recovered the average diffusion time of the blue species and the amplitude of the autocorrelation function, $G_B(0)$. The same was done for the red channel to get a diffusion time and an amplitude, $G_R(0)$, and for the cross-correlation function using a model with single species and no triplet state. We obtained a diffusion time, which allowed an estimate of the size of the complex (hydrodynamic radius) with an amplitude, $G_X(0)$.

The fraction of bound "red" protein is: $f_R = \frac{G_X(0)}{G_B(0)} \frac{(1-B_B/I_B)}{(1-B_R/I_R)} \frac{1}{L_B} \frac{1}{\gamma}$

The first correction is for background, the second for imperfect labeling efficiency and the third for imperfect volume overlap. Cross talk was found to be negligible and is therefore not accounted for in this formula. Note that although only the amplitude of the autocorrelation function in the blue channel appears in that formula, it is the fraction of bound red protein (tBid) which is obtained.

7.4.3. Protein Purification and Labeling

Wild type and single cysteine variants of Bax, Bcl-XL and Bid were purified as described previously (Billen et al., 2008; Kale et al., 2014; Satsoura et al., 2012; Shamas-Din et al., 2013a; Yethon et al., 2003) All of the Bad and Bid proteins used in our studies contain an N-terminal His tag and were purified using nickel-affinity chromatography (Qiagen). For clarity in the nomenclature, we have omitted the His prefix from the names of the proteins. Wild type and the 36C single cysteine variant of recombinant His_6-tagged full-length human Bad were obtained by site-directed mutagenesis (Stratagene). Wild-type (WT) Bad has no endogenous cysteine residues. All of the Bcl-XL and Bax proteins initially contain a chitin binding domain and an intein tag and were purified using chitin bead chromatography. The proteins were cleaved of the chitin beads using ß-mercaptoethanol or hydroxylamine.

Purified Bcl-XL, Bax, Bid and Bad mutants intended for labeling were dialyzed in storage buffer (20 mM TRIS, pH 8, 100 mM NaCl, 20% glycerol for Bcl-XL and Bad (+ 30mM imidazole for Bad), 10mM HEPES, pH 7.3, 100mM NaCl, 0.5mM EDTA, 10% glycerol for Bax and Bid). The proteins were labeled with the indicated dyes in the storage buffer in the presence of 0.5% CHAPS and up to 4M Urea for 2–3 h at room temperature on rotation. For labeling, a 10–15-fold molar excess of dye dissolved in

DMSO was added to the proteins slowly while ensuring that the final DMSO content of the reaction did not exceed 10%.

To remove the excess unreacted dye, Bid and Bad were subjected to nickel-affinity chromatography and washed with at least 25 mL of wash buffer (10 mM HEPES, pH 7.3, 300 mM NaCl, 0.5 mM EDTA, 10% glycerol and 0.5% CHAPS for Bid, 20mM TRIS, pH8, 100mM NaCl, 30 mM imidazole and 0,2% CHAPS for Bad). The labeled Bid and Bad was then eluted with elution buffer (wash buffer supplemented with 200 mM imidazole for Bid and 300 mM imidazole for Bad).

The labeling efficiency of Bid, Bad, Bcl-XL or Bax at a given residue was measured by dividing the dye concentration (measured by absorbance) by the protein concentration (measured by Bradford or BCA assay). Only if the labeling efficiency was ∼70% or higher was the protein used.

Purified unlabeled WT Bid or labeled Bid proteins were incubated with 500 units of Caspase 8 (Enzo Life Sciences) with a final concentration of 1 unit/µl for ∼40 h at room temperature to generate tBid. The cleavage efficiency was controlled by Coomassie Blue staining of an SDS-PAGE gel.

For our experiments we used tBid that became tBid (truncated Bid) (Oh et al., 2005) upon dissociation of the p7 fragment in the presence of membranes. For nomenclature reasons we use the term tBid in this script for interactions containing tBid in the absence or presence of membranes.

As Bax is not intrinsically active, we used tBid-mt1 (M97A/D98A) (Wang et al., 1996), a mutant of tBid with substitution of two residues within the BH3 region that does not bind stably to Bcl-XL, to activate Bax.

The proteins were dialyzed against dialysis buffer (10 mM TRIS pH8, 100mM NaCl and 20% glycerol for Bcl-XL and Bad, 20 mM HEPES pH7.3, 100mM NaCl, 0,5 mM EDTA and 10% glycerol for Bax and tBid) to remove the detergent CHAPS for Bad

and tBid, and to remove the excess unreacted dye and CHAPS for Bcl-XL and Bax. After measuring the final protein concentration and labeling efficiency using absorbance, Bradford or BCA assays, the proteins were stored at -80^0 C in dialysis buffer until further usage.

7.4.4. Liposome Preparation

Liposomes 100 nm in diameter with a lipid composition made up of phosphatidylcholine (48%), phosphatidylethanolamine (28%), phosphatidylinositol (10%), dioleoyl phosphatidylserine (10%), and tetraoleoyl cardiolipin (4%) (all from Avanti Polar Lipids) were prepared as described previously (Kale et al., 2014; Lovell et al., 2008). The liposome concentration was estimated as described (Satsoura et al., 2012) using the fact that there are ~84,000 lipids per liposome.

7.4.5. Mitochondria Preparation

Mitochondria were isolated from the livers of Bak$^{-/-}$ (Pogmore et al., 2016) mice and frozen in trehalose according to the literature (Yamaguchi et al., 2007). Briefly, mouse liver was prepared in AT buffer: 300 mM trehalose (Sigma), 10 mM HEPES-KOH, pH 7.5, 10 mM KCl, 1 mM EGTA, 1 mM EDTA, 0.1% (w/v) BSA (Bioshop). The isolated mitochondria were frozen at 50 mg/mL final protein concentration (Bradford assay) in 10µl aliquots and stored at −80 °C until use. When ready to use, mitochondria were rapidly thawed and washed in AT/KCl buffer at 1 mg/mL: 300 mM trehalose, 10 mM HEPES-KOH, pH 7.7, 80 mM KCl, 1 mM EGTA, 1 mM EDTA, 0.1% (w/v) BSA. The mitochondria were resuspended in regeneration buffer at 1 mg/mL final protein concentration (300 mM trehalose, 10 mM HEPES-KOH, pH 7.7, 80 mM KCl, 1 mM EGTA, 1 mM EDTA, 0.1% (w/v) BSA, 5 mM succinate, 2 mM ATP, 10 µM phosphocreatine, 10 µg/mL creatine kinase (added fresh) and used immediately.

7.4.6. Membrane Permeabilization Assays

Membrane permeabilization assays with liposomes encapsulating ANTS (8-aminonaphthalene-1,3,6-trisulfonic acid, disodium salt) and DPX (p-xylene-bis-pyridinium bromide) or encapsulated with Tb:DPA were carried out as described previously (Kale et al., 2014; Lovell et al., 2008).

Outer membrane permeabilization of mitochondria was assessed by measuring cytochrome c release after incubating the mitochondria with the proteins for 30 min to 1 hour at 37 °C. Mitochondria were isolated from the reaction by centrifugation, and cytochrome c was detected in the supernatant and pelleted fractions by immunoblotting. The cytochrome c polyclonal antibody was produced in our laboratory and was used at a dilution of 1:5000. The secondary antibody conjugated to horseradish peroxidase (Bio-Rad) was used at a dilution of 1:20,000. Immunoblots were analyzed using ImageJ. The curves were fit using Prism 5 (GraphPad).

7.4.7. Membrane Binding Assays

Experiments for Bcl-2 proteins spontaneously binding to mitochondrial like membranes, or after being targeted to membranes by other Bcl-2 proteins were performed as described previously (Billen et al., 2008).

7.5. Supplementary Figures

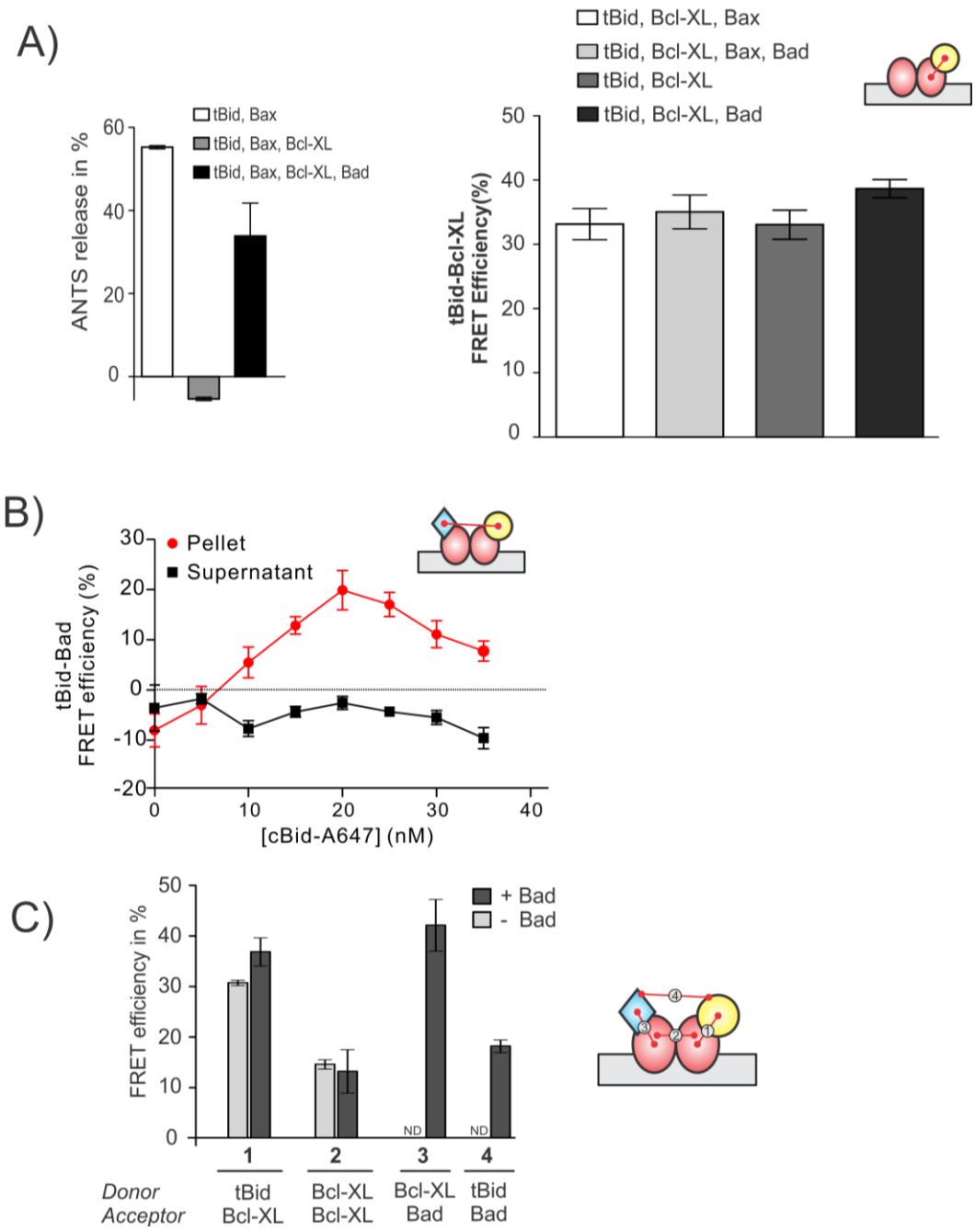

Supplementary Figure 7.1 - Related to Figure 1

A. - Supplemental to Figure 1a - ANTS release (left) and corresponding FRET efficiency (right) after one hour incubation of indicated recombinant proteins. Results are average +/- SEM of three independent

experiments. **Left:** ANTS release for liposomes (0.04 mg/mL) incubated with 20 nM donor labeled tBid (126C-DAC) with 50 nM WT Bax (white); in presence (gray) of 50 nM acceptor labeled BCL-XL (152C-NBD) and in the presence of both (black) 50 nM Bcl-XL (152C-NBD) and 100 nM WT Bad. **Right:** The interaction between tBid and Bcl-XL was measured by FRET. Liposomes (0.25 mg/mL) were incubated with 20 nM tBid (126C-DAC) and 50 nM Bcl-XL (152C-NBD) in the absence (dark gray) or presence of 100 nM WT Bad (black) or 50 nM WT Bax (white) or both (light gray).

B. Supplemental to Figure 1b - Isolated Bak -/- MLM were incubated with 20 nM donor labeled Bad (36C-Alexa 568) and increasing concentrations of acceptor labeled tBid (126C-Alexa 647) in the presence and absence of 20 nM WT Bcl-XL. Reactions were pelleted and separated into supernatant and pellet fractions. FRET efficiency was measured by the decrease in donor labeled Bad fluorescence, compared to an identical control containing unlabeled tBid (126C).

C. Supplemental to figure 1c – FRET efficiencies for acceptor and donor labeled pairs of Bcl-2 family members. Here 0.25 mg/mL liposomes were incubated with 20 nM tBid, 50 nM Bcl-XL (light bars) and 100 nM Bad where indicated (dark bars). Each lane contains the same concentrations of proteins but the acceptor and donor labeled proteins are changed, indicated below the graph. Data shown are the average of 3 or more independent replicates with SEM.

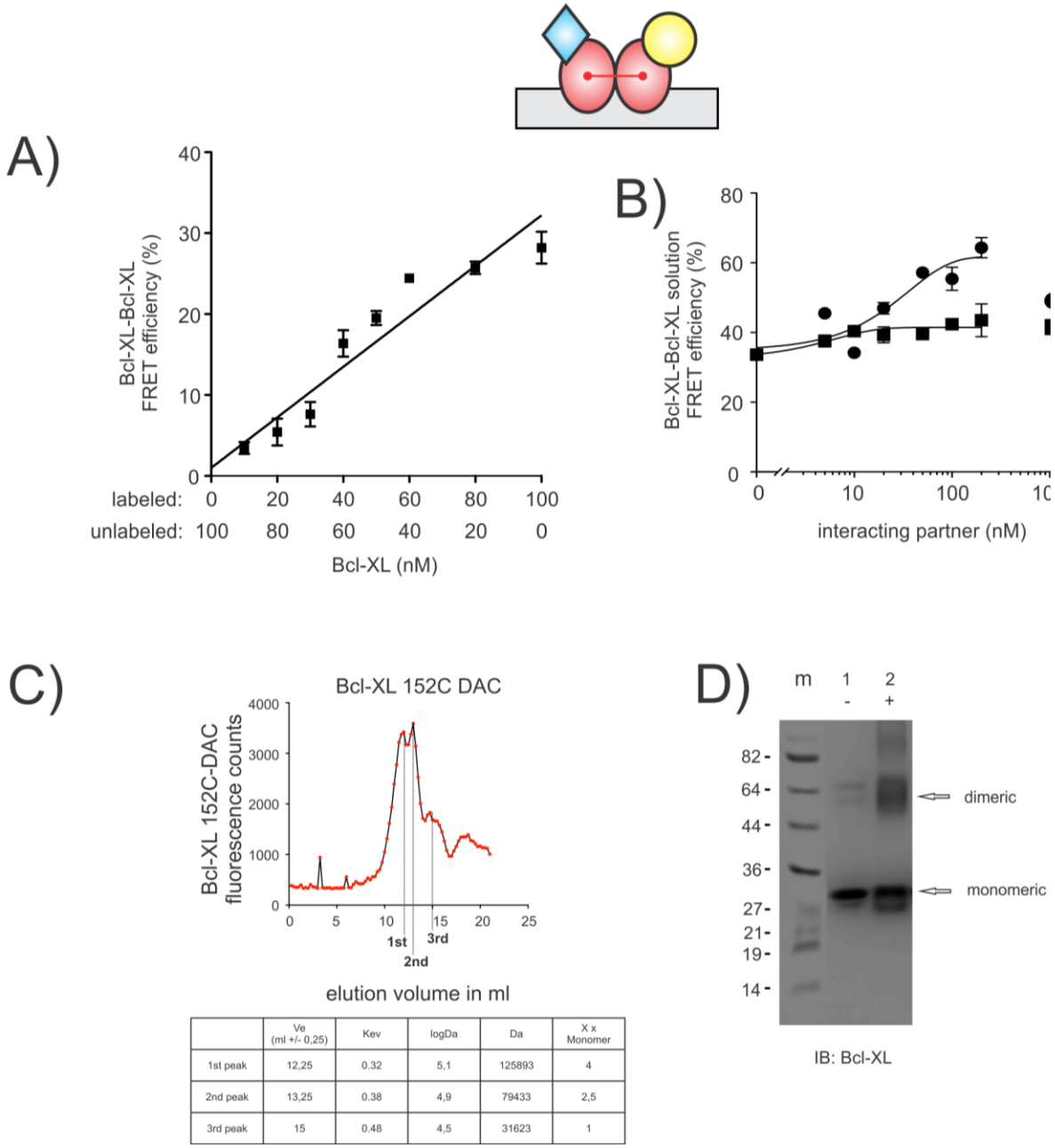

	Ve (ml +/- 0,25)	Kev	logDa	Da	X x Monomer
1st peak	12,25	0.32	5,1	125893	4
2nd peak	13,25	0.38	4,9	79433	2,5
3rd peak	15	0.48	4,5	31623	1

Supplementary Figure 7.2 – Related to figure 2

A. Supplementary to Figure 2a – **Left)** Subunit exchange in Bcl-XL dimers. Interactions between 20 nM Bcl-XL (219C-DAC) and indicated concentrations of Bcl-XL (219C-NBD) incubated with liposomes (0.25 mg/mL) were allowed to come to equilibrium (1 hour) and then unlabeled Bcl-XL was added to bring the final total concentration of Bcl-XL to 100 nM and FRET was measured after 1hr. The data was fit with a linear standard.

B. FRET efficiency of the interaction between 20 nM donor and 100 nM acceptor labeled Bcl-XL (219C-DAC, 219C-NBD respectively) incubated in assay buffer with increasing concentrations of the indicated unlabelled Bcl-2 family proteins Bad (circles) and tBid (squares). The average +/- SEM results of three independent experiments are shown.

C. Representative results of gel filtration chromatography of donor labeled BCL-XL (152C-DAC). The fluorescence intensity of each eluted fraction was measured at 380 nM excitation and 460 nM emission. The fluorescence emission directly correlates with the amount of labeled Bcl-XL present in each fraction. The molecular weight of Bcl-XL eluted in each fraction was determined by interpolation of a standard curve generated by running standardized proteins of known size over the column.

D. Representative immunoblot results of a cross linking experiment performed in the absence or presence of DSS, a crosslinker specific for primary amines. Shown are results +- DSS for 50 nM Bcl-XL in the presence of liposomes (0.25 mg/mL). The immunoblots were blotted against Bcl-XL.

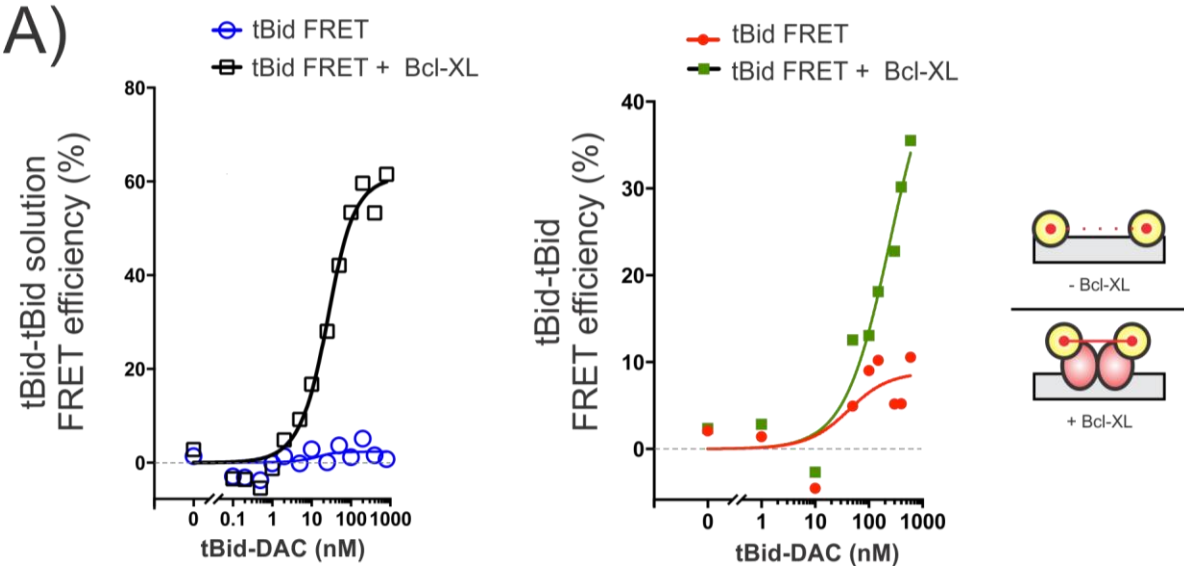

Supplementary Figure 7.3 – Related to Figure 3

A. Supplementary to figure 3a - Representative result of 20 nM tBid (126C-DAC) binding to an increasing amount of tBid (126C-NBD) in the presence (squares) or absence (circles) of Bcl-XL WT (100 nM), **left)** in the absence of liposomes or **right)** in the presence of liposomes (0.25 mg/mL).

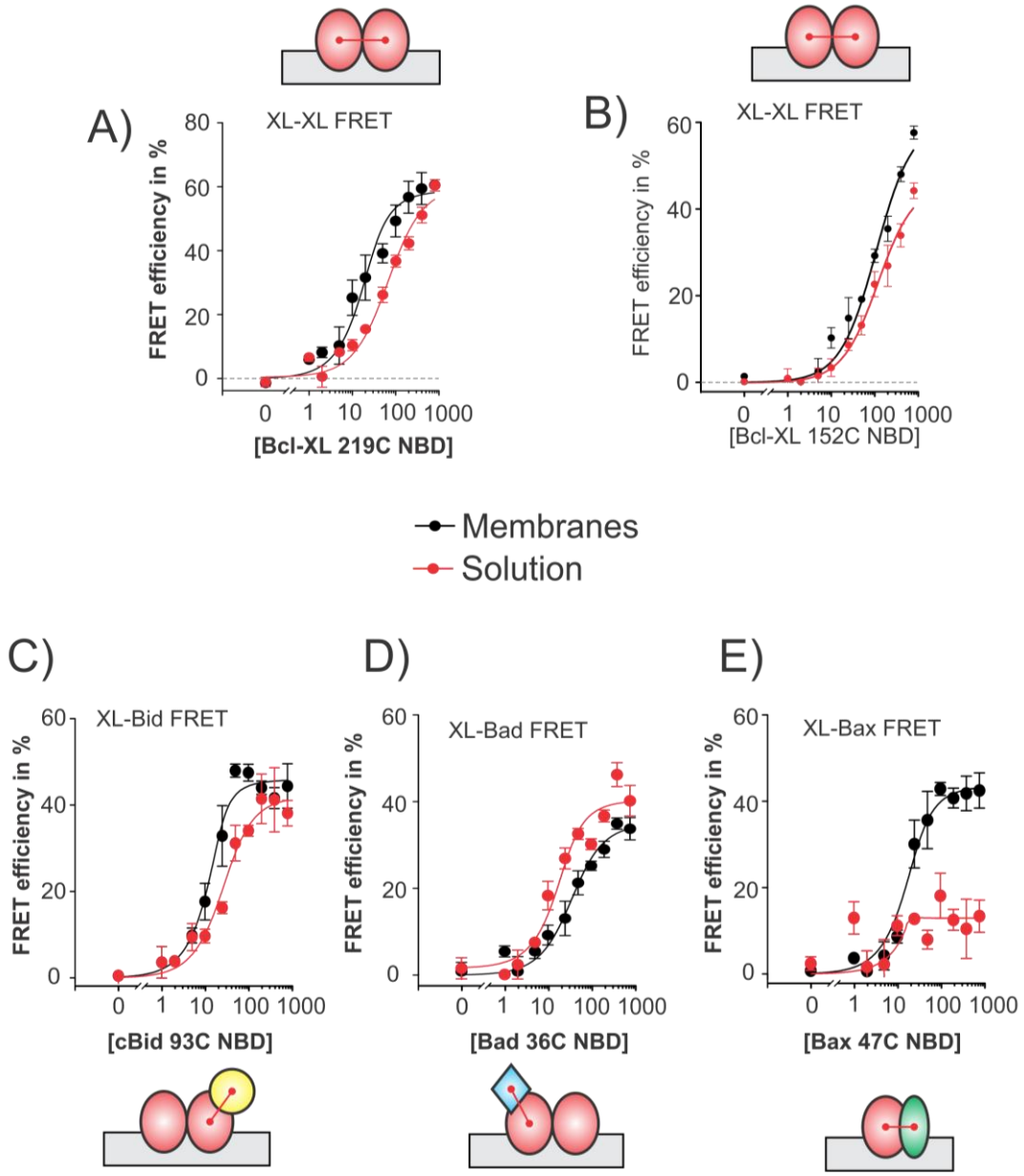

Supplementary Figure 7.4 – Related to Table 1

(A-E) Titration curves for Bcl-2 proteins interacting with each other in the presence (black) or absence (red) of liposomes (0.25 mg/ml), using FRET to determine binding. The "donor" was labeled with DAC (Em/Ex 380/460nm), the "acceptor" was labelled with NBD (Em/Ex 478/530nm). The concentration of the "donor" (DAC labeled Bcl-XL) was fixed to 20nM. The "acceptor" (indicated on each x-axis) was titrated to the donor from 0 to 800nM. Unlabeled acceptor proteins were included to the calculations to address for environmental changes. Dissociation constants (K_D) were calculated using best fit (see materials and methods). Shown is the average +- SEM of three independent experiments. In **(E)** Bax was pre-activated with tBid mt1, a mutant of Bid that has impaired binding affinity towards Bcl-XL.

7.6. References

Barclay, L.A., Wales, T.E., Garner, T.P., Wachter, F., Lee, S., Guerra, R.M., Stewart, M.L., Braun, C.R., Bird, G.H., Gavathiotis, E., *et al.* (2015). Inhibition of Pro-apoptotic BAX by a noncanonical interaction mechanism. Molecular cell *57*, 873-886.

Billen, L.P., Kokoski, C.L., Lovell, J.F., Leber, B., and Andrews, D.W. (2008). Bcl-XL inhibits membrane permeabilization by competing with Bax. PLoS biology *6*, e147.

Chi, X., Kale, J., Leber, B., and Andrews, D.W. (2014). Regulating cell death at, on, and in membranes. Biochimica et biophysica acta *1843*, 2100-2113.

Denisov, A.Y., Sprules, T., Fraser, J., Kozlov, G., and Gehring, K. (2007). Heat-induced dimerization of BCL-xL through alpha-helix swapping. Biochemistry *46*, 734-740.

Ding, J., Mooers, B.H., Zhang, Z., Kale, J., Falcone, D., McNichol, J., Huang, B., Zhang, X.C., Xing, C., Andrews, D.W., *et al.* (2014). After embedding in membranes antiapoptotic Bcl-XL protein binds both Bcl-2 homology region 3 and helix 1 of proapoptotic Bax protein to inhibit apoptotic mitochondrial permeabilization. The Journal of biological chemistry *289*, 11873-11896.

Edlich, F., Banerjee, S., Suzuki, M., Cleland, M.M., Arnoult, D., Wang, C., Neutzner, A., Tjandra, N., and Youle, R.J. (2011). Bcl-x(L) retrotranslocates Bax from the mitochondria into the cytosol. Cell *145*, 104-116.

Gavathiotis, E., Reyna, D.E., Davis, M.L., Bird, G.H., and Walensky, L.D. (2010). BH3-triggered structural reorganization drives the activation of proapoptotic BAX. Molecular cell *40*, 481-492.

Jeong, S.Y., Gaume, B., Lee, Y.J., Hsu, Y.T., Ryu, S.W., Yoon, S.H., and Youle, R.J. (2004). Bcl-x(L) sequesters its C-terminal membrane anchor in soluble, cytosolic homodimers. The EMBO journal *23*, 2146-2155.

Kale, J., Chi, X., Leber, B., and Andrews, D. (2014). Examining the molecular mechanism of bcl-2 family proteins at membranes by fluorescence spectroscopy. Methods in enzymology *544*, 1-23.

Kim, H., Tu, H.C., Ren, D., Takeuchi, O., Jeffers, J.R., Zambetti, G.P., Hsieh, J.J., and Cheng, E.H. (2009). Stepwise activation of BAX and BAK by tBID, BIM, and PUMA initiates mitochondrial apoptosis. Molecular cell *36*, 487-499.

Llambi, F., Moldoveanu, T., Tait, S.W., Bouchier-Hayes, L., Temirov, J., McCormick, L.L., Dillon, C.P., and Green, D.R. (2011). A unified model of mammalian BCL-2 protein family interactions at the mitochondria. Molecular cell *44*, 517-531.

Lovell, J.F., Billen, L.P., Bindner, S., Shamas-Din, A., Fradin, C., Leber, B., and Andrews, D.W. (2008). Membrane binding by tBid initiates an ordered series of events culminating in membrane permeabilization by Bax. Cell *135*, 1074-1084.

O'Neill, J.W., Manion, M.K., Maguire, B., and Hockenbery, D.M. (2006). BCL-XL dimerization by three-dimensional domain swapping. Journal of molecular biology *356*, 367-381.

Oh, K.J., Barbuto, S., Meyer, N., Kim, R.S., Collier, R.J., and Korsmeyer, S.J. (2005). Conformational changes in BID, a pro-apoptotic BCL-2 family member, upon membrane binding. A site-directed spin labeling study. The Journal of biological chemistry *280*, 753-767.

Pogmore, J.P., Pemberton, J.M., Chi, X., and Andrews, D.W. (2016). Using Forster-Resonance Energy Transfer to Measure Protein Interactions Between Bcl-2 Family Proteins on Mitochondrial Membranes. Methods in molecular biology *1419*, 197-212.

Satsoura, D., Kucerka, N., Shivakumar, S., Pencer, J., Griffiths, C., Leber, B., Andrews, D.W., Katsaras, J., and Fradin, C. (2012). Interaction of the full-length Bax protein with biomimetic mitochondrial liposomes: a small-angle neutron scattering and fluorescence study. Biochimica et biophysica acta *1818*, 384-401.

Shamas-Din, A., Bindner, S., Zhu, W., Zaltsman, Y., Campbell, C., Gross, A., Leber, B., Andrews, D.W., and Fradin, C. (2013a). tBid undergoes multiple conformational changes at the membrane required for Bax activation. The Journal of biological chemistry *288*, 22111-22127.

Shamas-Din, A., Kale, J., Leber, B., and Andrews, D.W. (2013b). Mechanisms of action of Bcl-2 family proteins. Cold Spring Harbor perspectives in biology *5*, a008714.

Tait, S.W., and Green, D.R. (2010). Mitochondria and cell death: outer membrane permeabilization and beyond. Nature reviews Molecular cell biology *11*, 621-632.

Todt, F., Cakir, Z., Reichenbach, F., Youle, R.J., and Edlich, F. (2013). The C-terminal helix of Bcl-x(L) mediates Bax retrotranslocation from the mitochondria. Cell death and differentiation *20*, 333-342.

van Delft, M.F., Smith, D.P., Lahoud, M.H., Huang, D.C., and Adams, J.M. (2010). Apoptosis and non-inflammatory phagocytosis can be induced by mitochondrial damage without caspases. Cell death and differentiation *17*, 821-832.

Volkmann, N., Marassi, F.M., Newmeyer, D.D., and Hanein, D. (2014). The rheostat in the membrane: BCL-2 family proteins and apoptosis. Cell death and differentiation *21*, 206-215.

Wang, K., Yin, X.M., Chao, D.T., Milliman, C.L., and Korsmeyer, S.J. (1996). BID: a novel BH3 domain-only death agonist. Genes & development *10*, 2859-2869.

Westphal, D., Kluck, R.M., and Dewson, G. (2014b). Building blocks of the apoptotic pore: how Bax and Bak are activated and oligomerize during apoptosis. Cell death and differentiation *21*, 196-205.

Yamaguchi, R., Andreyev, A., Murphy, A.N., Perkins, G.A., Ellisman, M.H., and Newmeyer, D.D. (2007). Mitochondria frozen with trehalose retain a number of biological functions and preserve outer membrane integrity. Cell death and differentiation *14*, 616-624.

Yao, Y., Fujimoto, L.M., Hirshman, N., Bobkov, A.A., Antignani, A., Youle, R.J., and Marassi, F.M. (2015). Conformation of BCL-XL upon Membrane Integration. Journal of molecular biology *427*, 2262-2270.

Yethon, J.A., Epand, R.F., Leber, B., Epand, R.M., and Andrews, D.W. (2003). Interaction with a membrane surface triggers a reversible conformational change in Bax normally associated with induction of apoptosis. The Journal of biological chemistry *278*, 48935-48941.

8

Concluding remarks

In 1993 Bax was identified via co-immunoprecipitation as the first binding partner for Bcl-2. In contrast to Bcl-2, overexpression of Bax resulted in cell death, and because the initial experiments demonstrated that Bax was constitutively bound to and inhibited by Bcl-2 (Oltvai et al., 1993), a rheostat model was proposed whereby the relative concentrations of pro- and anti-apoptotic members determined cell fate (Korsmeyer et al., 1993). Many subsequent experiments have demonstrated that in normal cells Bax exists as an inactive cytosolic monomer that requires activation in order to kill the cell. (Hsu and Youle, 1998; Letai et al., 2002; Shamas-Din et al., 2013b). The basis for the initial misconception of how Bax promotes apoptosis and how (and where) it binds to Bcl-2 was the use of detergents as it later became clear that non-ionic detergents such as the NP-40 used in the original experiment promote an artifactual interaction between Bax and antiapoptotic members by inducing an activated conformation of Bax (Hsu and Youle, 1997). Furthermore other detergents like the zwitterionic CHAPS do not activate Bax but by contrast disrupt the interaction between Bax and cBid (Lovell et al., 2008). Thus studying the authentic interactions between Bcl-2 family members (including Bax) is fraught with methodological problems: many biochemical and structure based techniques require the use of detergents which alter the conformations and interactions between the Bcl-2 family members, and the fact that Bcl-2 family proteins are membrane proteins with hydrophobic carboxy-terminal tails and highly flexible unstructured loops increases the propensity for these proteins to aggregate during purification. For these reasons most research on the Bcl-2 family proteins is performed with truncated versions of Bcl-XL and Bax, and peptides of the BH3 domains of the activator and sensitizer BH3-only proteins.

Determining the exact mechanisms of how Bax and Bak become activated has been termed the 'holy grail' of apoptosis research (Youle and Strasser, 2008). New techniques are required to circumvent these difficulties and our lab has been a leader in optimizing a highly defined in vitro liposome-based system free of detergents, using full-length recombinant Bcl-2 family proteins that reconstitute the process of MOMP *in vitro* (Bleicken et al., 2014; Kale et al., 2014; Kim et al., 2009; Landeta et al., 2011; Lovell et al., 2008; Satsoura et al., 2012; Shamas-Din et al., 2013a). The lipid composition of the these liposomes can be manipulated to investigate how these membrane components affect the binding of Bcl-2 family members, but for the studies described in this thesis we have used have a composition that mimics the OMM to recapitulate what occurs *in vivo*. This system has the advantage of being free of other factors which may complicate interpretation such as unknown binding partners that may be present at the OMM. This system is made even more powerful by using fluorescently labelled full-length recombinant Bcl-2 family proteins and analyzing the results by fluorescence spectroscopy, as described in detail in Chapter 4 of this thesis. Using these techniques we can observe protein:protein and protein:membrane binding dynamics in real-time, and simultaneously track conformation changes of the proteins using environment sensitive dyes. Integrating this information provides us with the unique opportunity to measure kinetics and binding affinities that regulate MOMP in a functionally relevant environment.

8.1. During activation Bax adopts at least 3 different conformations

Previous techniques could not obtain a dynamic picture of full-length Bax as it transitions from a soluble monomer to a membrane embedded oligomer. Modelling the kinetics of Bax conformation changes allows us to infer the hydrophobicity of each residue in each conformation

state, from which we can generate a dynamic topologic model of the protein. The overall interpretation of the hydrophobicity data suggests that helix 5, 6 and 9 of Bax are in environments consistent with being embedded in the bilayer, as discussed in Chapter 5. This does not necessarily rule out other models of Bax insertion into membranes, such as the "in-plane" model where helix 5 and 6 clamp the membrane (Bleicken et al., 2014; Westphal et al., 2014a). Furthermore it is possible that one side of both helices 5 and 6 are embedded within the bilayer whereas the other is exposed to solution, since both helices are amphipathic with charges residues located on one side and hydrophobic residues on the other. In this case the amphipathic residues of the respective helices may lie facing the pore or the surface of the membrane.

The current model for Bax activation posits that activator BH3-only proteins bind to and activate Bax in a hit-and-run fashion whereby Bax inserts helix 9 into the membrane first, followed by insertion the hairpin helices 5 and 6. (Garner et al., 2016; Kim et al., 2009; Luna-Vargas and Chipuk, 2016; Westphal et al., 2014a). However the data presented in Chapter 5 demonstrates that the interaction between Bax and activator BH3-only proteins is temporally distinct and precedes the formation of a separate conformation for Bax that inserts into and oligomerizes within the membrane. Furthermore Bax inserts helices 5, 6 and 9 in a concerted fashion, rather than inserting helix 9 first. Contrary to some other models of Bax activation, the mechanism is the same for both Bim and cBid suggesting that both bind to similar regions of Bax, presumably the BH3 groove (and not to a rear pocket) as only this region undergoes a conformation change that is temporally similar to BH3:Bax binding (Chi et al., 2014; Czabotar et al., 2013; Garner et al., 2016; Gavathiotis et al., 2008).

As an independent way to investigate the intermediate conformation of Bax as a physiologically relevant state, we searched for inhibitory Bax point mutations. We presumed that since cancer cells have blocks in apoptosis (Deng et al., 2007; Hanahan and Weinberg, 2011), some cancers may have point mutations which fully inactivate Bax, potentially at the intermediate state. Supporting this general hypothesis, the most frequent mutation of Bax found in human cancers by probing the TCGA database was a frameshift deletion near the N-terminus which would functionally inactivate Bax as the protein would lack helices 2, 4 and 5 required for Bax mediated MOMP (George et al., 2007). We investigated Bax missense mutations as probes for the intermediate state, but the majority did not affect the function of Bax in our assay, thus are likely passenger mutations to the *BAX* gene due to the genomic instability of cancer. Nevertheless, we did find some point mutations that block Bax at the intermediate conformation. Notably these point mutations prevented the insertion of Bax but did not prevent the binding of activator BH3-only proteins. This Bax is presumed to be interacting with the activator BH3-only proteins at the membrane since at the liposome concentration used >90% of the cBid is embedded in the bilayer (Shamas-Din et al., 2013a). Further experiments are needed to determine why these mutants are inactive. However, we can speculate that Bax S184E does not insert helix 9 into the bilayer due the negative charge from the glutamic acid. Indeed in Chapter 6 we used this mutant to characterize how phosphorylation of residue S184 affects the function of Bax. S184E Bax binds cBid with the same affinity to that of WT Bax, presumably via the BH3:groove interactions which may displace helix 9 (Kim et al., 2009). The other mutations (G67R, G108E, and G108V) are located in the BH3 groove of Bax and thus these mutants may not be able to oligomerize. Taken together the data from these functionally relevant mutations suggests that interaction with another Bax molecule is a prerequisite for insertion, such that

dimerization could precede or coincide with insertion into the bilayer followed by oligomerization. These results are consistent with recent research reporting that activated Bax forms dimer units in the membrane via BH3:groove interactions that further assemble into oligomers, possibly through α9:α9 interactions between Bax dimers (Subburaj et al., 2015; Zhang et al., 2016b).

8.2. Bax is converted into an antiapoptotic protein when phosphorylated by AKT

Our *in vitro* system has yielded important insights into the core mechanisms determining Bcl-2 family function. We have extended these studies to improve our understanding of how Bcl-2 family proteins control apoptosis in cells. Many post translational modifications have been identified that regulate the function of this family (Kutuk and Letai, 2008), and one of the most common is phosphorylation. Bax is phosphorylated at residues S163 (by GSK3β), T167 (by JNK) (Kim et al., 2006; Linseman et al., 2004). However, the most extensively studied site is S184; phosphorylation by AKT or mutations at this residue modulate Bax function (Gardai et al., 2004; Kim et al., 2009; Nechushtan et al., 1999; Wang et al., 2010; Xin and Deng, 2005). Phosphorylation of S184 or S184D/E mutations inhibit Bax function, and S184V or S184L mutations cause Bax to spontaneously target to membranes. However, the mechanistic basis for the inactivation of Bax by AKT-mediated phosphorylation of Bax S184 is unknown. Initially, the inhibition of apoptosis by AKT was thought to be mediated by phosphorylation of the sensitizer BH3-only protein Bad; however Bad is dispensable for apoptosis induced by several mechanism (Ranger et al., 2003; Wang et al., 2005). Thus, we speculated a more central player was involved. The studies presented in Chapter 7 show that phosphorylation of Bax not only inhibits the protein but converts Bax into an antiapoptotic protein capable of protecting the cell from

MOMP via sequestration of activator BH3-only proteins. This function was unexpected as S184 phosphorylated Bax or S184D/E mutated Bax was assumed to be completely inactive. After the identification of the Bax intermediate conformation as described in Chapter 5, it became clear how phosphorylation at S184 reverses Bax function. Bax S184E cannot insert helix 9 into the membrane (as discussed above) but can still bind to activator BH3-only proteins with a similar affinity to that of WT Bax. Thus phosphorylated Bax can bind to and sequester the BH3-only proteins because it is locked in the intermediate conformation. The studies presented in Chapter 5 and 6 provide physiological relevance for this intermediate conformation of Bax. Furthermore, in clinical samples from patients we find a positive association between the expression of Bax and genes in the AKT pathway suggesting that cancer cells with hyperactive AKT may selectively upregulate Bax as an additional means of evading apoptosis. Based on these observations Bax phosphorylation status in cells may be a potential prognostic biomarker. Furthermore it may be predictive of treatment outcome with certain drugs as our results indicate that the BH3 mimetic ABT-737 (Oltersdorf et al., 2005) fails to induce apoptosis in cells with phosphorylated Bax. However our analysis suggests a way to circumvent this resistance: PI3K/AKT pathway inhibitors may act synergistically with BH3-mimetics in cancer where this former pathway is over-active. Thus our results provide important clues in determining how the Bcl-2 family proteins are regulated in the cell via PTM and provide a template for the design of rational combination targeted therapeutics.

8.3. A new model for mode 1 inhibition of MOMP

To enrich our understanding about how the core mechanism of oligomer-mediated pore formation by Bax is regulated it is critical to determine how all of the partners (antiapoptotic,

sensitizer/ activator BH3-only proteins, and Bax/Bak) work together to regulate apoptosis. In Chapter 7 we uncover a new mechanism of regulation for mode 1 inhibition of apoptosis by Bcl-XL, as well as a new function for the sensitizer BH3-only protein Bad. Current models suggest that antiapoptotic proteins exert their inhibition by binding to and sequestering either Bax/Bak of BH3-only proteins via heterodimers (Llambi et al., 2011; Shamas-Din et al., 2013b). By contrast we demonstrated by multiple techniques that Bcl-XL exists as a dimer which acts as a scaffold for BH3-only proteins thereby creating a multimeric complex that regulates apoptosis. These novel finding underscore the importance of using full-length proteins at physiologic concentrations (in the low nanomolar range) (Polster et al., 2003). Specifically, the quantitative methods and varying concentrations of the Bcl-2 family members in each assay allowed us to observe this previously undescribed complex. For example, as a competitive inhibitor Bad will displace Bax/Bak or activator BH3-only proteins if bound to and sequestered by Bcl-XL. However, this function is observed at relatively high concentrations of Bad and is expected due to the differential binding affinities between tBid and Bad for Bcl-XL. The binding affinity between Bid and Bcl-XL is approximately 8-fold higher than that of Bad and Bcl-XL i.e. 3 nM vs. 25 nM. Therefore this model leaves unexplained low nanomolar concentrations of Bad in cells can exert its proapoptotic effect with such dramatic difference in affinities for tBid and Bad for Bcl-XL. Crucially, in our model systems we observe that Bad promotes MOMP at low nM concentrations where tBid would be minimally displaced by Bcl-XL. The basis of this activity at low concentrations (<50 nM) Bad is that it modulates the activity of tBid indirectly through Bcl-XL dimers. Bad bound to one side of a Bcl-XL dimer must propagate a series of conformation changes through the dimer structure such that tBid shifts from an inactive to an active state. This allows tBid to activate Bax while remaining bound to Bcl-XL. Thus, Bad binding acts as an

allosteric switch converting the antiapoptotic tBid:Bcl-XL dimer complex to a proapoptotic one. This novel function of Bad explains how Bad functions as such a potent sensitizer at low concentrations. Sensitizer BH3-only proteins can therefore function as both competitive and non-competitive inhibitors of the tBid:Bcl-XL complex.

Significantly the allosteric switch mechanism was not observed when the Bad BH3 mimetic ABT-263 was used in the same context. This suggests that the BH3 domain alone does not confer the allosteric switch activity to Bad; a region outside of the BH3 domain may be responsible. Work in our lab by Dr. Xiaoke Chi has shown that Bim lacking its carboxy-terminal membrane binding domain (MBD) acts as a sensitizer and cannot activate Bax. The data suggest that the MBD of Bim binds to Bcl-XL and prevents ABT-263 from displacing Bim from Bcl-XL in vitro and in cells. Therefore, the carboxy-terminal membrane binding domain of Bad would be a prime candidate to test if it confers the novel allosteric switch function to Bad and suggest experiments to test this proposal

Another outstanding question is how the Bcl-XL dimers are formed. Bcl-XL must have two separate binding sites, one to bind the other Bcl-XL monomer and another to bind BH3-only proteins. BH3-only proteins likely bind Bcl-XL via BH3:groove interactions as outlined in Chapter 2, thus a separate interface may mediate dimer formation. Interestingly, Bcl-XL does not function as a dimer during mode 2 inhibition of Bax as Bcl-XL dimers decrease in the presence of activated Bax. This implies that the binding interface between Bcl-XL dimers is similar to that of Bax and Bcl-XL heterodimers. Some evidence presented here suggests that the carboxy-terminal tail of Bcl-XL mediates dimerization. The FRET efficiency between labels in the carboxy-terminal tail of Bcl-XL is higher than that of labels on the membrane inserting α5 helix.

Therefore, the carboxy-terminal tails are in closer proximity to each other than the cores of the proteins. Furthermore, deletion of the c-terminal tail prevents Bcl-XL dimerization (unpublished results from our lab). Accordingly, Bcl-XL dimerization may be mediated by reciprocal binding between the carboxy-terminal tails of Bcl-XL monomers, or through a site similar to that of the rear pocket in Bax (Ding et al., 2014; Gavathiotis et al., 2008; Jeong et al., 2004)

As discussed throughout this thesis BH3-mimetics are being used as anti-cancer treatments. The new functions of both Bcl-XL dimerization and a Bad allosteric switch may represent a new therapeutic target. One can envision the development of new small molecules that 1) inhibit Bcl-XL dimerization, potentially mitigating the antiapoptotic activity of Bcl-XL or 2) elicit the allosteric changes in the tBid:Bcl-XL dimer complex promoting apoptosis.

8.4. Conclusion

The three main research chapters in this thesis (5, 6 & 7) have elucidated the regulation of MOMP, specifically focusing on the activation Bax. We were able to combine a highly defined liposome based-system with quantitative fluorescence techniques to gain deeper insight into the biochemical mechanisms regulating the Bcl-2 family of proteins. In order to control the fate of the cell for a wide range of positive therapeutic outcomes, we must fully understand how the Bcl-2 family proteins regulate MOMP *in vivo*. However, determining the precise mechanisms of the Bcl-2 family proteins *in vitro* has provided a good basis for developing small-molecules that translate into therapies as is the case for the BH3-mimetic venetoclax, which inhibits Bcl-2 and has been designated ‘breakthrough’ status by the FDA for treatment of CLL and AML. The research here uncovers new avenues for targeting the Bcl-2 family proteins whether it be the Bax

intermediate state, Bcl-XL dimers or synergistic combinations of AKT inhibitors and BH3-mimetics.

8.5. References

Bleicken, S., Jeschke, G., Stegmueller, C., Salvador-Gallego, R., Garcia-Saez, A.J., and Bordignon, E. (2014). Structural model of active Bax at the membrane. Molecular cell *56*, 496-505.

Chi, X., Kale, J., Leber, B., and Andrews, D.W. (2014). Regulating cell death at, on, and in membranes. Biochimica et biophysica acta *1843*, 2100-2113.

Czabotar, P.E., Westphal, D., Dewson, G., Ma, S., Hockings, C., Fairlie, W.D., Lee, E.F., Yao, S., Robin, A.Y., Smith, B.J., *et al.* (2013). Bax crystal structures reveal how BH3 domains activate Bax and nucleate its oligomerization to induce apoptosis. Cell *152*, 519-531.

Deng, J., Carlson, N., Takeyama, K., Dal Cin, P., Shipp, M., and Letai, A. (2007). BH3 profiling identifies three distinct classes of apoptotic blocks to predict response to ABT-737 and conventional chemotherapeutic agents. Cancer Cell *12*, 171-185.

Ding, J., Mooers, B.H., Zhang, Z., Kale, J., Falcone, D., McNichol, J., Huang, B., Zhang, X.C., Xing, C., Andrews, D.W., *et al.* (2014). After embedding in membranes antiapoptotic Bcl-XL protein binds both Bcl-2 homology region 3 and helix 1 of proapoptotic Bax protein to inhibit apoptotic mitochondrial permeabilization. The Journal of biological chemistry *289*, 11873-11896.

Gardai, S.J., Hildeman, D.A., Frankel, S.K., Whitlock, B.B., Frasch, S.C., Borregaard, N., Marrack, P., Bratton, D.L., and Henson, P.M. (2004). Phosphorylation of Bax Ser(184) by Akt regulates its activity and apoptosis in neutrophils. Journal of Biological Chemistry *279*, 21085-21095.

Garner, T.P., Reyna, D.E., Priyadarshi, A., Chen, H.C., Li, S., Wu, Y., Ganesan, Y.T., Malashkevich, V.N., Almo, S.S., Cheng, E.H., *et al.* (2016). An Autoinhibited Dimeric Form of BAX Regulates the BAX Activation Pathway. Molecular cell *63*, 485-497.

Gavathiotis, E., Suzuki, M., Davis, M.L., Pitter, K., Bird, G.H., Katz, S.G., Tu, H.C., Kim, H., Cheng, E.H., Tjandra, N., *et al.* (2008). BAX activation is initiated at a novel interaction site. Nature *455*, 1076-1081.

George, N.M., Evans, J.J., and Luo, X. (2007). A three-helix homo-oligomerization domain containing BH3 and BH1 is responsible for the apoptotic activity of Bax. Genes & development *21*, 1937-1948.

Hanahan, D., and Weinberg, R.A. (2011). Hallmarks of cancer: the next generation. Cell *144*, 646-674.

Hsu, Y.T., and Youle, R.J. (1997). Nonionic detergents induce dimerization among members of the Bcl-2 family. The Journal of biological chemistry *272*, 13829-13834.

Hsu, Y.T., and Youle, R.J. (1998). Bax in murine thymus is a soluble monomeric protein that displays differential detergent-induced conformations. The Journal of biological chemistry *273*, 10777-10783.

Jeong, S.Y., Gaume, B., Lee, Y.J., Hsu, Y.T., Ryu, S.W., Yoon, S.H., and Youle, R.J. (2004). Bcl-x(L) sequesters its C-terminal membrane anchor in soluble, cytosolic homodimers. The EMBO journal *23*, 2146-2155.

Kale, J., Chi, X., Leber, B., and Andrews, D. (2014). Examining the molecular mechanism of bcl-2 family proteins at membranes by fluorescence spectroscopy. Methods in enzymology *544*, 1-23.

Kim, B.J., Ryu, S.W., and Song, B.J. (2006). JNK- and p38 kinase-mediated phosphorylation of Bax leads to its activation and mitochondrial translocation and to apoptosis of human hepatoma HepG2 cells. The Journal of biological chemistry *281*, 21256-21265.

Kim, H., Tu, H.C., Ren, D., Takeuchi, O., Jeffers, J.R., Zambetti, G.P., Hsieh, J.J., and Cheng, E.H. (2009). Stepwise activation of BAX and BAK by tBID, BIM, and PUMA initiates mitochondrial apoptosis. Molecular cell *36*, 487-499.

Korsmeyer, S.J., Shutter, J.R., Veis, D.J., Merry, D.E., and Oltvai, Z.N. (1993). Bcl-2/Bax: a rheostat that regulates an anti-oxidant pathway and cell death. Seminars in cancer biology *4*, 327-332.

Kutuk, O., and Letai, A. (2008). Regulation of Bcl-2 family proteins by posttranslational modifications. Current molecular medicine *8*, 102-118.

Landeta, O., Landajuela, A., Gil, D., Taneva, S., Di Primo, C., Sot, B., Valle, M., Frolov, V.A., and Basanez, G. (2011). Reconstitution of proapoptotic BAK function in liposomes reveals a dual role for mitochondrial lipids in the BAK-driven membrane permeabilization process. The Journal of biological chemistry *286*, 8213-8230.

Letai, A., Bassik, M.C., Walensky, L.D., Sorcinelli, M.D., Weiler, S., and Korsmeyer, S.J. (2002). Distinct BH3 domains either sensitize or activate mitochondrial apoptosis, serving as prototype cancer therapeutics. Cancer Cell *2*, 183-192.

Linseman, D.A., Butts, B.D., Precht, T.A., Phelps, R.A., Le, S.S., Laessig, T.A., Bouchard, R.J., Florez-McClure, M.L., and Heidenreich, K.A. (2004). Glycogen synthase kinase-3beta phosphorylates Bax and promotes its mitochondrial localization during neuronal apoptosis. The Journal of neuroscience : the official journal of the Society for Neuroscience *24*, 9993-10002.

Llambi, F., Moldoveanu, T., Tait, S.W., Bouchier-Hayes, L., Temirov, J., McCormick, L.L., Dillon, C.P., and Green, D.R. (2011). A unified model of mammalian BCL-2 protein family interactions at the mitochondria. Molecular cell *44*, 517-531.

Lovell, J.F., Billen, L.P., Bindner, S., Shamas-Din, A., Fradin, C., Leber, B., and Andrews, D.W. (2008). Membrane binding by tBid initiates an ordered series of events culminating in membrane permeabilization by Bax. Cell *135*, 1074-1084.

Luna-Vargas, M.P., and Chipuk, J.E. (2016). Physiological and Pharmacological Control of BAK, BAX, and Beyond. Trends in cell biology.

Nechushtan, A., Smith, C.L., Hsu, Y.T., and Youle, R.J. (1999). Conformation of the Bax C-terminus regulates subcellular location and cell death. EMBO Journal *18*, 2330-2341.

Oltersdorf, T., Elmore, S.W., Shoemaker, A.R., Armstrong, R.C., Augeri, D.J., Belli, B.A., Bruncko, M., Deckwerth, T.L., Dinges, J., Hajduk, P.J., *et al.* (2005). An inhibitor of Bcl-2 family proteins induces regression of solid tumours. Nature *435*, 677-681.

Oltvai, Z.N., Milliman, C.L., and Korsmeyer, S.J. (1993). Bcl-2 heterodimerizes in vivo with a conserved homolog, Bax, that accelerates programmed cell death. Cell *74*, 609-619.

Polster, B.M., Basanez, G., Young, M., Suzuki, M., and Fiskum, G. (2003). Inhibition of Bax-induced cytochrome c release from neural cell and brain mitochondria by dibucaine and

propranolol. The Journal of neuroscience : the official journal of the Society for Neuroscience *23*, 2735-2743.

Ranger, A.M., Zha, J., Harada, H., Datta, S.R., Danial, N.N., Gilmore, A.P., Kutok, J.L., Le Beau, M.M., Greenberg, M.E., and Korsmeyer, S.J. (2003). Bad-deficient mice develop diffuse large B cell lymphoma. P Natl Acad Sci USA *100*, 9324-9329.

Satsoura, D., Kucerka, N., Shivakumar, S., Pencer, J., Griffiths, C., Leber, B., Andrews, D.W., Katsaras, J., and Fradin, C. (2012). Interaction of the full-length Bax protein with biomimetic mitochondrial liposomes: a small-angle neutron scattering and fluorescence study. Biochimica et biophysica acta *1818*, 384-401.

Shamas-Din, A., Bindner, S., Zhu, W., Zaltsman, Y., Campbell, C., Gross, A., Leber, B., Andrews, D.W., and Fradin, C. (2013a). tBid undergoes multiple conformational changes at the membrane required for Bax activation. The Journal of biological chemistry *288*, 22111-22127.

Shamas-Din, A., Kale, J., Leber, B., and Andrews, D.W. (2013b). Mechanisms of action of Bcl-2 family proteins. Cold Spring Harbor perspectives in biology *5*, a008714.

Subburaj, Y., Cosentino, K., Axmann, M., Pedrueza-Villalmanzo, E., Hermann, E., Bleicken, S., Spatz, J., and Garcia-Saez, A.J. (2015). Bax monomers form dimer units in the membrane that further self-assemble into multiple oligomeric species. Nature communications *6*, 8042.

Wang, Q.H., Sun, S.Y., Khuri, F., Curran, W.J., and Deng, X.M. (2010). Mono- or Double-Site Phosphorylation Distinctly Regulates the Proapoptotic Function of Bax. Plos One *5*.

Wang, S.W., Denny, T.A., Steinbrecher, U.P., and Duronio, V. (2005). Phosphorylation of Bad is not essential for PKB-mediated survival signaling in hemopoietic cells. Apoptosis *10*, 341-348.

Westphal, D., Dewson, G., Menard, M., Frederick, P., Iyer, S., Bartolo, R., Gibson, L., Czabotar, P.E., Smith, B.J., Adams, J.M., *et al.* (2014a). Apoptotic pore formation is associated with in-plane insertion of Bak or Bax central helices into the mitochondrial outer membrane. Proc Natl Acad Sci U S A *111*, E4076-4085.

Xin, M.G., and Deng, X.M. (2005). Nicotine inactivation of the proapoptotic function of Bax through phosphorylation. Journal of Biological Chemistry *280*, 10781-10789.

Youle, R.J., and Strasser, A. (2008). The BCL-2 protein family: opposing activities that mediate cell death. Nature reviews Molecular cell biology *9*, 47-59.

Zhang, Z., Subramaniam, S., Kale, J., Liao, C., Huang, B., Brahmbhatt, H., Condon, S.G., Lapolla, S.M., Hays, F.A., Ding, J., *et al.* (2016b). BH3-in-groove dimerization initiates and helix 9 dimerization expands Bax pore assembly in membranes. The EMBO journal *35*, 208-236.